Targeting Tissue-Specific Enzymatic Cascades of Local Angiotensin System in Human Atheroma

Ali Nehme

Université Libanaise
École Doctorale
Sciences et Technologies
Doyen

Université Claude Bernard Lyon 1

THESE EN COTUTELLE

Pour obtenir le grade de Docteur délivré par

L'Université Claude Bernard Lyon 1
Et
L'Université Libanaise
Ecole Doctorale des Sciences et Technologie

Spécialité: Pathophysiologie et Bioinformatique

Présentée et soutenue publiquement par

Ali Nehme

Le 25 Novembre, 2015

Ciblage Tissu-Specifique des Cascades Enzymatiques de l'Angiotensinogene dans l'Atherome Humain

Membres du Jury

Directeurs de thèse	**M. Giampiero Bricca**, *Université Claude Bernard Lyon 1*
	M. Kazem Zibara, *Université Libanaise*
Co -Encadreur de these	**Mme. Catherine Cerutti,** *Université Claude Bernard Lyon 1*
Rapporteurs	**M. Xavier Jeunemaitre,** *Université Paris Descartes*
	M. Wissam Faour, *Lebanese American University*
Examinateurs	**M. Pierre Lantelme,** *Université Claude Bernard Lyon 1*
	Mme. Eva Hamade, PU, *Université Libanaise*

UNIVERSITE CLAUDE BERNARD - LYON 1

Président de l'Université	**M. François-Noël GILLY**
Vice-président du Conseil d'Administration	M. le Professeur Hamda BEN HADID
Vice-président du Conseil des Etudes et de la Vie Universitaire	M. le Professeur Philippe LALLE
Vice-président du Conseil Scientifique	M. le Professeur Germain GILLET
Directeur Général des Services	M. Alain HELLEU

COMPOSANTES SANTE

Faculté de Médecine Lyon Est – Claude Bernard	Directeur : M. le Professeur J. ETIENNE
Faculté de Médecine et de Maïeutique Lyon Sud – Charles Mérieux	Directeur : Mme la Professeure C. BURILLON
Faculté d'Odontologie	Directeur : M. le Professeur D. BOURGEOIS
Institut des Sciences Pharmaceutiques et Biologiques	Directeur : Mme la Professeure C. VINCIGUERRA
Institut des Sciences et Techniques de la Réadaptation	Directeur : M. le Professeur Y. MATILLON
Département de formation et Centre de Recherche en Biologie Humaine	Directeur : Mme. la Professeure A-M. SCHOTT

COMPOSANTES ET DEPARTEMENTS DE SCIENCES ET TECHNOLOGIE

Faculté des Sciences et Technologies	Directeur : M. F. DE MARCHI
Département Biologie	Directeur : M. le Professeur F. FLEURY
Département Chimie Biochimie	Directeur : Mme Caroline FELIX
Département GEP	Directeur : M. Hassan HAMMOURI
Département Informatique	Directeur : M. le Professeur S. AKKOUCHE
Département Mathématiques	Directeur : M. le Professeur Georges TOMANOV
Département Mécanique	Directeur : M. le Professeur H. BEN HADID
Département Physique	Directeur : M. Jean-Claude PLENET
UFR Sciences et Techniques des Activités Physiques et Sportives	Directeur : M. Y.VANPOULLE
Observatoire des Sciences de l'Univers de Lyon	Directeur : M. B. GUIDERDONI
Polytech Lyon	Directeur : M. P. FOURNIER
Ecole Supérieure de Chimie Physique Electronique	Directeur : M. G. PIGNAULT
Institut Universitaire de Technologie de Lyon 1	Directeur : M. le Professeur C. VITON
Ecole Supérieure du Professorat et de l'Education	Directeur : M. le Professeur A. MOUGNIOTTE
Institut de Science Financière et d'Assurances	Directeur : M. N. LEBOISNE

ACKNOWLEDGEMENTS

Though only my name appears on the cover of this dissertation, a great many people have contributed to its production. I owe my gratitude to all those people who have made this dissertation possible and because of whom my graduate experience has been one that I will cherish forever.

First and foremost, I would like to express my sincere gratitude to my advisors Prof. Giampiero Bricca and Prof. Kazem Zibara who have supported me thoughout my thesis with their patience and knowledge whilst allowing me the room to explore on my own, and at the same time the guidance to recover when my steps faded. Their guidance helped me in all the time of research and writing of this thesis. They taught me how to question thoughts and express ideas. I could not have imagined having a better advisor and mentor for my Ph.D study. One simply could not wish for better or friendlier supervisors.

My deep gratitude is to my co-advisor Mme. Catherine Cerutti without whom this work wouldn't have been done. Thank you for the advice, patience, caring and always being next to me.

Beside my advisors, I would like to thank the rest of my thesis committee: Prof. Xavier Jeunemaitre, Prof. Wissam Faour, Prof. Pierre Lantelme and Prof. Eva Hamade for for their kind acceptance to be evaluators for this work. Thanks for their insightful comments and encouragement, but also for the hard questions which incented me to widen my research from various perspectives.

I thank my fellow labmates in for the stimulating discussions and for all the time we have had in the last four years. Special thanks go to my friends Mohammed bou Mhaiza and Nedra Dhaouadi for the great times we spend together, for the guidance and always standing next to me whenever needed.

Last but not the least, my deepest gratitude to my parents who have supported me throughout my studies. Also to my brothers and sister for supporting me spiritually throughout writing this thesis and my whole life in general. I wouldn't have reached this level and wrote this thesis without the support of this great familly.

DEDICATION

"If I have seen further than others, it is by standing upon the shoulders of giants". *Isaac Newton*

This dissertation is dedicated to the soul of my director, Pr. Giampiero, who passed away on 18 October, 2015, one month before my thesis defense. It was an honor for me to work with such a great scientific person. Pr. BRICCA was a lovely, gentle, caring, enthusiastic and humanitarian person. I learned too many things from him, especially how to be a scientific person that care about doing science for the sake of humanity.

This work is also dedicated to all the reasearchers who studied the renin-angiotesnin-aldosterone system and atherosclerosis, thus guiding us to our hypothesis and the experimental approaches that we followed in our project.

Pr. Giampiero Bricca (1957-2015)

TABLE OF CONTENTS

LIST OF ABBREVIATIONS

Abbreviation	Description
11β-HSD2	11-β-dehydrogenase isozyme 2
AAA	Abdominal aortic aneurysms
ABCA1	ATP-binding cassette transporter, member 1
ACE	Angiotensin converting enzyme
ACE2	Angiotensin I converting enzyme 2
ACEi	Angiotensin converting enzyme inhibitor
ACTH	Adrenocorticotropic hormone
AGE	Advanced glycation end-product
AGT	Angiotensinogen
AL	Atherosclerotic lesion
Ang-(1-12)	Angiotensin-(1-12)
Ang-(1-5)	Angiotensin-(1-5)
Ang-(1-7)	Angiotensin-(1-7)
Ang-A	Angiotensin-A
Ang-I	Angiotensin-I
Ang-II	Angiotensin-II
Ang-III	Angiotensin-III
Ang-IV	Angiotensin-IV
ApoA	Apolipoprotein isoform A1
ApoB	Apolipoprotein isoform B
ApoE	Apolipoprotein isoform E
ARB	Angiotensin type 1 receptor blocker
aSMA	Alpha smooth muscle actin
AT1R	Angiotensin-II type 1 receptor
AT2R	Angiotensin-II type 2 receptor
CPA3	Carboxypeptidase A3
CTSA	Cathepsin A
CTSG	Cathepsin G
CX3CL1	Rhemokine (C-X3-C motif) ligand 1
DC	Dendritic cell
DNA	Deoxy-nucleic acid
EC	Endothelial cell
ECM	Extracellular matrix

ERK	Extracellular signal-regulated kinases
ExtRAAS	Extended renin-angiotensin-aldosterone system
GEO	Gene expression Omnibus
GP	Glycoprotein
GPER	G protein-coupled estrogen receptor
GR	Glucocorticoid receptor
HDL	High density lipoprotein
ICAM-1	Intercellular adhesion molecule 1
IFN-g	Interferon gamma
IGFII	Insulin-like growth factor II
IL	Interleukin
IPA	Intimal physiological adaptations
JAM	Junctional adhesion molecule
JG	Juxtaglomerular cell
LDL	Low density lipoprotein
LOX-1	Lectin-like oxidized low-density lipoprotein receptor-1
M6P	Mannose 6-phosphate
MAPK	Mitogen-activated protein kinase cascade
MasR	Mas receptor
MCP-1	Monocyte chemoattractant protein 1
MCSF	Macrophage colony-stimulating factor
MFC	Macrophage-derived foam cell
MHC	Myosin heavy chain
MIT	Macroscopically intact arterial tissue
MLC	Macrophage-like cell
MME	Neprilysin/metallo-endopeptidase/neutral endopeptidase
MMP	Matrix metalloproteinase
MR	Mineralocorticoid receptor
NADPH	Nicotinamide adenine dinucleotide phosphate
NFKB	Nuclear factor-kappa b
NLN	Neurolysin
NO	Nitric oxide
nTS	Nucleus of the solitary tract
OxLDL	Oxidized-LDL
PBS	Phosphate-buffered saline
PBS-	PBS without calcium and magnesium

PDGF	Platelet-derived growth factor
PECAM-1	Platelet endothelial cell adhesion molecule (*PECAM-1*)
PG	Proteoglycan
PGL-1	P granule component 1
PI3K	Phosphatidylinositol 3-kinase
PRCP	Prolylcarboxipeptidase
PREP	Prolylendopeptidase
R/PR	Renin/prorenin receptor
RAAS	Renin-angiotensin-aldosterone system
RER	Rough endoplasmic reticulum
RNA	Ribo-nucleic acid
RnBP	Renin-binding protein
ROS	Reactive oxygen species
RUNX2	Runt-related transcription factor 2
siRNA	Small interefering RNA
SLC	SMC like cell
SMC	Smooth muscle cell
SMCFC	SMC-derived foam cells
SR	Scavenger receptor
StAR	Steroidogenic acute regulatory protein
T2D	Type 2 diabetes
TF	Transcription factor
TGF-b	Transforming gowth factor beta
THOP1	Thimet oligopeptidase 1
TLR	Toll-like receptor
TNFα	Tumor necrosis factor alpha
tPA	Tissue plasminogen activator
VCAM-1	Vascular cell adhesion molecule 1
vLDL	Very low density lipoprotein
VSMC	Vascular smooth muscle cell
WHO	World health organization

LIST OF FIGURES

LIST OF TABLES

ABSTRACT

Atherosclerosis remains and continues to be the leading cause of death and disability in the world. The implication of Renin-angiotensin-aldosterone system (RAAS) in the development of the disease is well experimentally and clinically documented. However, due to the complexity of the system, these studies remain dispersed and give no clear global view of the association between the system and the disease. In this regard, we studied the functional organization of a set of 37 genes encoding classical and newly discovered RAAS participants, including substrate, enzymes and receptors. This set was called extended RAAS (extRAAS). Using statistical analysis of human carotid atheroma transcriptome involving gene clustering, we revealed special features of extRAAS expression associated with atheromatous remodeling. An important feature of this pattern was the coordination of 2 clusters of genes that are known to favor atheroma formation. The first cluster constitutes genes that encode for angiotensin peptidases, including ACE, CTSG, CTSD and RNPEP. Whereas the second encode for receptors (AGTR1, MR, GR and LNPEP). We hypothesized that the local pattern of extRAAS gene expression plays a key role in the development of atherosclerosis by orienting the metabolism of active peptides.

However several important questions remain to be answered about the determinants and the biological importance of these co-expression patterns in atheroma development. Thus the aim of our project is to unmask the answers by investigating:

1. Whether the organization we have obtained from carotid atherosclerotic lesion is reproducible in other types of atheroma (coronary, renal, peripheral) and if it is specific for atheroma. To prove that this organization is atheroma specific, we compared it to the organization of extRAAS in 23 normal human tissues (no normal artery) in addition to atherosclerotic and control aortas from Apo E -/- mice.
2. Whether coordination of gene expression is a tissue or a cell property. This was addressed using primary vascular smooth muscle cells (VSMCs) in culture adopting different phenotypes related to atheroma (contractile, lipid storing and osteoblastic). The transcriptome of these cells will be analyzed in order to define extRAAS co-expression patterns related to these phenotypes. The results will compared to atheroma data to check whether either type of these cells is responsible for the co-expression pattern observed in atheroma.

3. What are the transcriptional mechanisms behind the organization obtained? Using bioinformatics tools and statistics we proposed candidate transcription factors that may play a role in the regulation of extRAAS gene expression.
4. Whether and how the transcript clusters translate into protein and signaling peptide production? This question will be answered by tracking the enzymatic cleavage of Angiotensin-I in carotid atheroma tissue in vitro. The results will answer whether the transcribed extRAAS model observed in atheroma is translated into a biologically active model at the protein level.

This study will pave the way to a better understanding of the biological significance and therapeutic regulation of a highly complex system locally in atheroma in a tissue- or process-specific manner.

RESUME

L'Athérosclérose est la principale cause de décès et d'invalidité dans le monde. L'implication du système rénine-angiotensine-aldostérone (RAAS) dans le développement de la maladie est expérimentalement et cliniquement bien documentée. Toutefois, en raison de la complexité du système, ces études ne donnent pas de vision claire sur l'association entre le système et la maladie. À cet égard, nous avons étudié l'organisation fonctionnelle d'un ensemble de 37 gènes codant pour les composants classiques et nouvellement découverts du RAAS, y compris les substrats, les enzymes et les récepteurs. Cet ensemble a été appelé RAAS étendu (extRAAS). En utilisant une analyse statistique des données du transcriptome de l'athérome carotidien humain, nous avons révélé des caractéristiques spéciales de l'expression de l'extRAAS associées au remodelage athéromateux. Une caractéristique importante de ce modèle est la coordination de 2 groupes de gènes qui sont connus pour favoriser la formation de l'athérome. Le premier groupe est constitué de gènes codant pour les peptidases de l'angiotensine, y compris ACE, CTSG, CTSD et RNPEP. Le deuxième groupe est constitué des gènes codant pour les récepteurs AGTR1, MR, GR et LNPEP.

On suppose que la structure locale de l'expression génique d'extRAAS joue un rôle important dans le développement de l'athérosclérose en orientant le métabolisme des peptides actifs. Ainsi, le but de notre projet est de comprendre :

1. Si l'organisation que nous avons obtenue dans l'athérosclérose carotidienne est reproductible dans d'autres types d'athérome (coronaire, rénal, périphérique) et si elle est spécifique de l'athérome. Pour prouver la spécificité de cette organisation, nous l'avons comparée à l'organisation de extRAAS dans 23 tissus humains normaux, en plus des aortes athérosclérotiques de souris Apo E - / - et de souris contrôles.
2. Si la coordination de l'expression des gènes est la propriété du tissu ou des cellules. Cela a été traitée en utilisant des cultures primaires de cellules musculaires lisses vasculaires humaines (CMLVh) et en leur faisant adopter différents phénotypes liés à l'athérome (contractile, adipocytique et ostéoblastique). Le transcriptome de ces cellules sera analysé afin de définir des motifs de co-expression du extRAAS en relation avec ces phénotypes. Les résultats seront comparés aux données d'athérome pour vérifier si le phénotype de ces cellules est responsable de l'organisation des transcrits observée dans l'athérome.
3. Quels sont les mécanismes de transcription responsables de l'organisation obtenue? En utilisant des outils bioinformatiques et statistiques, nous avons proposé des facteurs de

transcription candidats qui peuvent jouer un rôle dans la régulation de l'expression génique de l'extRAAS.

4. Comment la structure de l'expression transcriptomique se traduit en protéines et en production de peptides de signalisation? Cette question sera traitée par le suivi du clivage enzymatique de l'angiotensine-I dans le tissu de l'athérome carotidien in vitro. Les résultats montreront si le modèle d'organisation des transcrits d'extRAAS observé dans l'athérome est traduit en un modèle biologiquement actif au niveau protéique. Ces travaux devraient ouvrir la voie à une meilleure compréhension de la signification biologique et de la régulation transcriptionnelle d'un système complexe fonctionnant localement dans l'athérome, d'une manière spécifique au tissu vasculaire ou au processus athéromateux.

Cette étude ouvre la voie à une meilleure compréhension de la signification biologique et de la régulation thérapeutique, d'une manière spécifique aux tissus ou au processus d'un système très complexe localisé dans l'athérome.

I. INTRODUCTION

I.1 THE BLOOD VESSEL WALL

The blood vessels are the part of the circulatory system that transports blood throughout the human body. They are made up of a lumen, through which blood flows, surrounded by the vessel wall. There are three major types of blood vessels[1]: the arteries, which carry the blood away from the heart; the capillaries, which enable the actual exchange of water and chemicals between blood and tissues; and the veins, which carry blood from the capillaries back toward the heart. Different types of vessels are discriminated by their vessel wall thickness and components.

I.1.1 Layers of the vessel wall

The vessel wall of arteries and veins consists of three main layers that differ in their cellular and extracellular matrix (ECM) constituents: the *Intima*, the *Media* and the *Externa*[1] (Figure I.1).

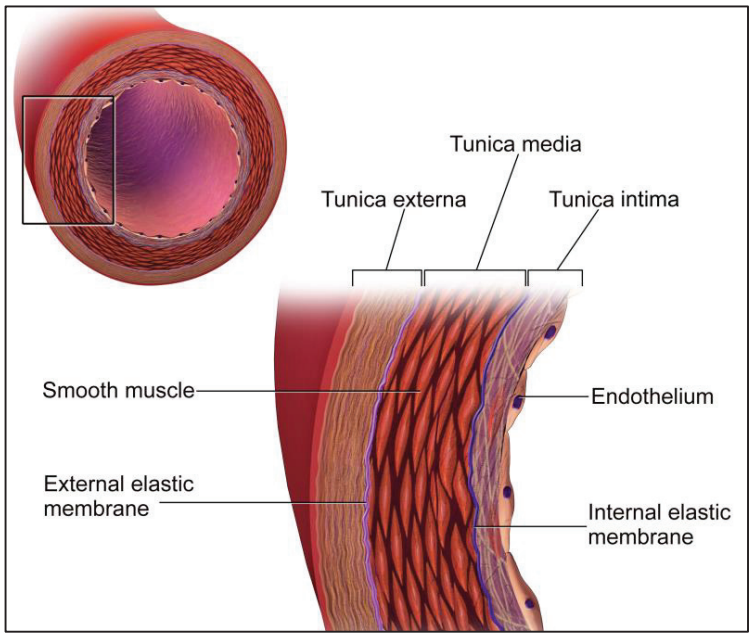

Figure I.1: the artery wall structure (DOI:10.15347/wjm/2014.010).

I.1.1.1 *Tunica intima*

The tunica intima is the innermost layer of the vessel wall facing the lumen[1,2]. It is composed of endothelium and sub-endothelial connective tissue. The endothelium is composed of a continuous monolayer of endothelial cells (ECs), a specialized type of epithelial cells[3], that rest on their own basement membrane[4]. The sub-endothelial layer consists of a delicate connective tissue with scattered macrophages, vascular smooth muscle cells (VSMCs) and

mast cells, which are known to be present in the normal intima since fetal life[2]. Capillaries consist only of a layer of endothelium and occasional connective tissue to facilitate exchange.

I.1.1.2 *Tunica Media*

The tunica media is the middle layer that provides structural support, vaso-reactivity and elasticity and is the thickest layer in arteries[1]. The tunica media is principally made of VSMCs that are embedded in their own basement membrane that is made of types I and III collagen and proteoglycans (PGs), in addition to a complex mixture of elastic fibers that are arranged into distinct layers[4]. The intima is separated from the media by a dense elastic membrane called the internal elastic lamina, which is considered a part of the media and consists of a network of elastic fibers, having principally a longitudinal direction[1]. Vasoconstriction or relax vasodilatation is controlled in VSMCs by autonomic nerves (*nervi vasorum*) and local metabolic factors that are mainly produced by ECs[1]. The media is separated from the adventitia by a dense elastic membrane called the external elastic lamina. Elastic fibers allow the vessel to expand with systole and contract with diastole, thereby propelling blood forward[5].

I.1.1.3 *Tunica Externa*

The *Tunica Externa*, also called *Tunica adventitia,* is the outermost layer and is almost entirely made of connective tissue with scattered fibroblasts[1,5]. It also contains nerves that supply the vessel as well as nutrient capillaries (vasa vasorum) in the larger blood vessels.

I.1.2 Major Components of the vessel wall

The normal vascular tissue is a diverse population of cell types, including ECs, VSMCs, fibroblasts and other connective tissue cell types, all embedded in a complex ECM.

I.1.2.1 *Endothelial cells (ECs):*

ECs are simple squamous cells that line the interior surface of blood vessels and form a barrier between the blood in the lumen and the subsequent layers of the vascular wall[6]. They are the cells in charge of synthesizing and secreting their ECM and basal membrane components, such as fibronectin, laminins, PGs and collagen (mainly types I, III and V)[2]. ECs are joined by tight junctions, which prevent the passage of molecules between them from the blood into the vessel wall. However, ECs are permeable to almost all plasma proteins which pass into the vessel wall through transcytosis and intercellular junctions in the EC membrane, which allows a strict regulation of molecular transport from the circulation[7]. The

cell wall of ECs contains receptors for several ligands, including low density lipoprotein (LDL), insulin and histamine[2]. The cytoskeleton of ECs is made up mainly of microfilaments rich in F-actin and myosin, in addition to intermediate filaments and microtubules[6]. A special characteristic of ECs is the Weibel-palade bodies, which are storage granules that store and release two principal molecules, von Willebrand factor, involved in blood coagulation, and P-selectin, involved in leukocytes recruitment and attachment to ECs, thus playing a dual role in hemostasis and inflammation[6]. Since they are the cells in contact with the circulating blood and reacting with physical and chemical stimuli, ECs have a major role in regulating hemostasis, vasomotor tone, and immune and inflammatory responses[8]. In addition, the endothelial cells are pivotal in angiogenesis and vasculogenesis[6]. ECs are a permeability barrier, but also form a multifunctional paracrine and endocrine organ. They are involved in the immune response, coagulation, growth regulation, production of extracellular matrix components, and are a modulator of blood flow and blood vessel tone[6]. In fact, endothelial injury, activation or dysfunction, loss of semi-permeable membrane function, and thrombosis[6] are hallmarks of many pathologic states including atherosclerosis,.

I.1.2.2 *Vascular smooth muscle cells (VSMCs):*

VSMCs are the particular type of smooth muscle found within and composing the majority of the wall of blood vessels[1]. They are mainly present in the tunica media of vessel wall, with only few scattered cells present in the intima[2]. VSMCs are the cellular component of the normal blood vessel wall that provides structural integrity and regulates the diameter by contracting and relaxing dynamically in response to vasoactive stimuli[9]. Two major phenotypic forms of VSMCs are present in normal vessels: Contractile and synthetic[2]. The two forms are characterized by different morphology, expression levels of SMC marker genes, proliferative potential and migration properties. Contractile VSMCs are elongated, spindle-shaped cells, with low protein synthesis activity, manifested by the little rough endoplasmic reticulum (RER) and golgi apparatus[2,10]. These cells contain large amounts of connected contractile filaments rich in α-actin. On the other hand, synthetic SMCs are less elongated and have a cobblestone morphology which is referred to as epithelioid or rhomboid[2,10]. As their name indicates, synthetic SMCs contain a high number of organelles involved in protein synthesis[2]. Moreover, synthetic and contractile SMCs have different proliferative and migratory characteristics. Generally, synthetic SMCs exhibit higher growth rates and higher migratory activity than contractile SMCs[10]. Phenotypic modulation of VSMCs, which is the ability to switch between different phenotypes, gives them the ability to

accurately adapt to external stimuli, either on the short-term by regulation of the vessel diameter, or on the long-term via structural remodeling by changing cell number and connective tissue composition[10].

I.1.2.3 *Fibroblasts:*

A fibroblast is a type of cell that functions mainly in ECM synthesis. Fibroblasts are the most common cells in connective tissue and are present in low numbers in the three layers of the vascular wall[2].

I.1.2.4 *The Extracellular matrix (ECM):*

ECM occupies a large proportion in the vessel wall, accounting for about 50% of the large vessel weight[11]. The elimination of VSMCs from large aortas does not alter the static mechanical properties of mature aortas, suggesting that ECM account for most of the mechanical characteristics of the vessel wall. The ECM of the vessel wall is produced by resident cells of the wall, mainly VSMCs and ECs[12]. Under normal conditions, ECM contain mostly collagen (mainly types I, III, IV, V, and VI), elastic fibers (elastin and fibrillin), fibulins, in addition to a complex set of PGs and glycoproteins (GPs)[13]. ECM plays a key role in vascular wall homeostasis by controlling tensile strength and vasoelasticity, nutrients transport, accumulation of products and metabolites, cellular phenotypes and attachment and migration of cells[13]. The ECM can adapt by changing quantity and quality under pathological conditions, such as age and atherosclerosis[14].

I.2 ATHEROSCLEROSIS

I.2.1 Definition

The most accepted definition of atherosclerosis is the one set by the world health organization (WHO) in 1958 as “a variable combination of changes in the intima of arteries (as distinguished from arterioles) consisting of focal accumulation of lipids, complex carbohydrates, blood and blood products, fibrous tissue and calcium deposits, and associated with medial changes”[15]. Indeed, this definition holds true until now as defined by the American heart association in 2014[16]. These accumulations will lead with time to the formation of an “atherosclerotic plaque” that will continue to grow, thus narrowing the artery lumen and leading to cardiovascular complications (Figure I.2).

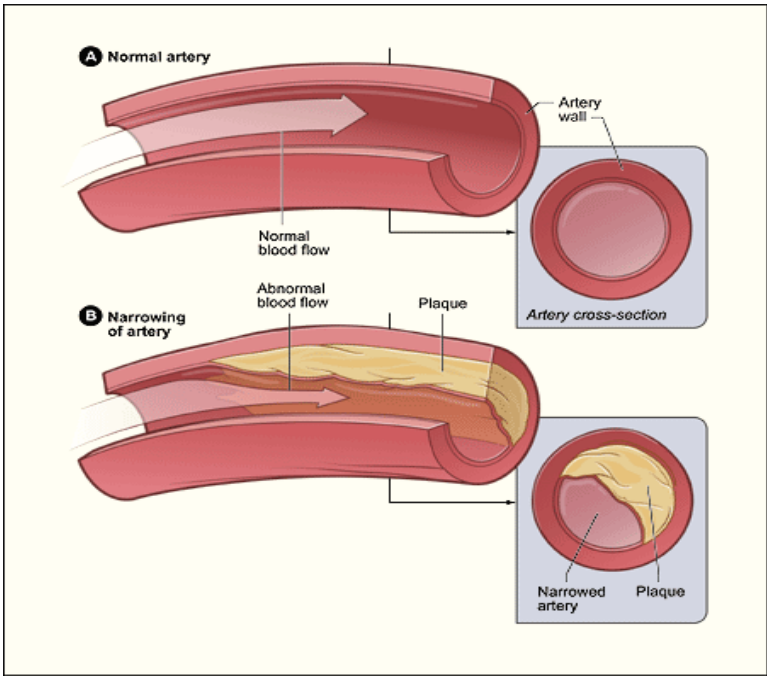

Figure I.2: normal versus atherosclerotic wall. Normal wall maintain normal blood flow; whereas atherosclerotic wall contains a plaque lipids, complex carbohydrates, blood and blood products, in addition to fibrous tissue and calcium deposits. This plaque will narrow the lumen and may lead to cardiovascular events. (Source: http://lafeber.com/vet/omega-3-fatty-acids-and-atherosclerosis-in-birds/).

I.2.2 Symptoms, diagnosis and treatment

Atherosclerosis is usually not associated with signs and symptoms until it severely narrows or totally blocks an artery. The complications that are associated with atherosclerosis depend on the artery bed in which the plaque is formed and the downstream organs that are affected by the reduced oxygen and nutrition as a result of insufficient blood flow[17]. The arteries mainly associated with atheroma formation are the coronary arteries, carotid arteries, renal arteries and peripheral arteries (i.e. legs, arms and pelvis). Since coronary arteries supply the heart with oxygen and nutrients, a plaque that form in such arteries may lead to angina in the chest, shoulders, arms, neck, jaw, or back, in addition to shortness of breath and arrhythmias. As the plaque continues to grow, the shear force of the blood flow increases, which may eventually lead to plaque rupture, resulting in the formation of thrombus that plug the artery completely that will eventually lead to heart attack[18]. On the other hand, if the carotid artery is affected, this will lead to reduced blood flow into the brain, associated with headache, weakness, paralysis, loss of consciousness, dizziness, confusion and troubles in speech, even may lead to death by stroke in case of thrombus formation[17]. In the case of affected renal artery, an atherosclerotic plaque may lead to chronic kidney disease, characterized by tiredness, changes in frequency of urination, loss of appetite, nausea, swelling in the hands or feet,

itchiness or numbness, and trouble concentrating. Finally, if the atheroma plaque forms in a major peripheral artery, it may lead to numbness and pain in the affected organ[17].

A combination of several tests may be required to diagnose atherosclerotic patients to define the type and level of severity of the disease[17]. The doctor may first ask about family history, life style and associated symptoms in order to define the possible atherosclerosis type. After this, several tests should be done in order to define the type of lesion and its severity, including stethoscope examination, physical test, blood test, electrocardiogram (EKG), chest X-ray, echocardiography, Computed Tomography (CT) Scan, angiography, and ankle/brachial Index. In addition the doctor may ask for magnetic resonance imaging (MRI) and positron emission tomography (PET) to better view plaque buildup in the arteries.

Based on the International Atherosclerosis Society Panel recommendations[19], primary prevention of atherosclerosis involve lifestyle therapies to reduce atherogenic lipo-proteins by adhering to a heart-healthy diet, regular exercise habits, avoidance of tobacco products, and maintenance of a healthy weight etc. Secondary prevention emphasizes use of cholesterol-lowering drugs to attain optimal levels of atherogenic lipoproteins. The Doctor may also prescribe certain drugs to manage other risk factors of atherosclerosis such as b-blockers or RAAS blockers to manage blood pressure[19]. However, drug therapy is only recommended for subjects at greater risk. Finally, if the patient has severe atherosclerosis, the doctor may recommend a medical procedure or surgery[17]. The latter includes percutaneous coronary intervention (PCI, or coronary angioplasty) to open blocked or narrowed coronary arteries (heart), coronary artery bypass grafting (CABG), which can also be used for peripheral atherosclerosis, or carotid endarterectomy to remove plaque buildup from the carotid arteries in the neck[17].

I.2.3 Epidemiology and risk factors

Atherosclerosis remains and continues to be the main cause of death and morbidity in the world, mainly in developed countries[20,21]. Indeed, Ischemic heart disease and stroke, both mainly caused by atherosclerosis, have remained the top major causes of death during the past decade, each killing 48.6% and 13.2%, respectively[22]. Together they killed more than 14 million individual in 2012, which is greater than the number of deaths caused by the 7 subsequent leading causes of death in the same year. However, the burden of the disease has been decreasing during the last decade[22] as a result of the better understanding of the disease and its treatment. Indeed, the identification and understanding of new atherosclerosis risk

factors, along with the classic risk factors, improve our ability to predict future risks and thus a better prevention of the disease[23]. Indeed, over 300 risk factors have been associated with atherosclerosis and its major complications, coronary heart disease and stroke[21]. Atherosclerosis develops over the course of years of an individual as a result of the combining effects of several intrinsic and extrinsic risk factors, including family history, hypertension, diabetes and insulin resistance, metabolic syndrome, hyperlipidemia, hypercholesterolemia, smoking, sedentary life, infection, in addition to several other factors[21].

I.2.4 Atheroma plaque initiation

Although the histologic features of the different stages of atheroma plaque had been well described[18,24], the mechanisms of initiation of plaque formation are not well understood. Indeed, the mechanism of atheroma plaque formation, mainly during the initial stages, has been the subject of debate for a long time and several hypotheses have emerged to explain the initial steps in atheroma development. This can be mainly due to the species- and spatial-specificity of the mechanisms by which atheroma plaque develops[25,26]. The difficulty of obtaining early stage plaques from humans, obliged researchers to rely on animal studies for the study of atherosclerosis[25]. In fact, the recent advances in molecular biology improved our understanding of atherosclerosis and atheroma plaque development using special genetic animal models. However, mouse models may develop atherosclerosis to varying extents, in a time and diet dependent manner[25]. The choice of a mouse model should be based on the investigator's specific needs as it relates to their hypothesis being tested. Although several hypotheses described the initial steps in atheroma plaque development[27–30], here we discuss only two of them.

In the "response-to-retention" hypothesis, atheroma plaque initiation is thought to rely mainly on lipid retention in the arterial wall[30]. This view relied on several *in vivo* and *in vitro* observations, which showed that lipid accumulation was the earliest step observed after LDL infusion into animal models[31], even before vascular cell adhesion molecule 1 (VCAM-1) expression by ECs[32–34] and macrophages accumulation in the sub-endothelial space[35,36]. In this hypothesis, macrophages are the principle cells that are involved in the initiation process, which are recruited by the modified (mainly by oxidization and esterification) LDL trapped in intima by matrix components[24,30]. Although lipid accumulation occurs in normal arteries, this may not initiate atheroma plaque formation unless reaching certain threshold that can

stimulate macrophages recruitment and expression of inflammatory markers[2]. The "response-to-retention" hypothesis was originally the most accepted hypothesis describing atheroma plaque formation; however, recent advances in molecular biology shifted the view toward the "response-to-injury" hypothesis.

In the "response-to-injury" hypothesis, atherosclerosis is defined as a non-resolving inflammatory condition, where inflammation is the key contributor to all stages of the disease, from initial lesions to plaque rupture[37,38]. The inflammatory reaction is initiated by vascular wall injury, mainly endothelial dysfunction[39]. Injury may be caused by hyperglycemia[40,41], hypertension[42], modified LDL[33,43], inflammation and infection[38], regardless of dyslipidemia[44]. One of the main supports for this hypothesis is that most mammals do not develop a prominent intimal physiological adaptations like humans, including mice, rats and rabbits[44]. In this hypothesis, VSMCs and macrophages contribute equally in the initial steps, and even VSMCs are thought to be activated before macrophages recruitment[38]. Indeed, ICAM-1, a macrophage adhesion molecule, was shown to be expressed on VSMCs in human atheroma-prone regions before monocytes infiltration[45].

I.2.4.1 *Intimal physiological adaptations of the vascular wall:*

Intimal physiological adaptation (IPA) is a small thickness in the intima of the vessel wall that doesn't obstruct the vascular lumen and has no clinical significance and is present in fetuses and infants[36]. IPA is usually formed as an adaptation to mechanical stress or wall tension as a result of increased tensile stress, or decreased wall shear[2]. IPA is composed of two layers: the upper layer is called the proteoglycan layer due to its rich ECM components with abundant PGs; and the lower layer is called the musculo-elastic layer because of the abundance of VSMCs and elastic fibers[2,36]. IPA is characterized by an increased turnover of ECs and low proliferative activity of VSMCs with anti-apoptotic phenotype[46]. In addition, IPA is characterized by a greater flow of LDL and plasma components, with greater amounts of macrophages and VSMCs[2]. The latter are most of the contractile phenotype that are present in the lower musculo-elastic intima near the media. Under mechanical stress, these VSMCs may migrate toward the upper layers of the intima and shift their form to become synthetic VSMCs characterized by RER-rich cytoplasm[2]. VSMCs are thought to play a major role in the stabilization of the IPA through the production of collagen and other ECM components, in addition to growth factors (GFs) that regulate cellular migration and proliferation. Moreover, these cells express thrombomodulin, which may contribute in

maintaining an anti-thrombotic effect in IPA[26]. In fact, there is a debate about the origin of VSMCs found in the IPA that can be summarized by 2 major hypotheses which were both tested and validated *in vivo* and *in vitro*: the first hypothesis claims that these VSMCs originate from the proliferation of precursor VSMCs that are known to be present in the normal intima in very low numbers since fetal life or that may originate from blood[2,47]. The second hypothesis propose that they originate from VSMCs of the media that migrate to and proliferate in the intima under stress conditions[48].

There are two types of IPA, diffuse and eccentric, which are usually contiguous and run into one another[2]. The eccentric thickening is usually associated to special geometric regions of the vascular system where mechanical stress is not uniformly distributed, usually at branches and orifices. This type of thickening is normally present in the arteries of babies since the first week of life[2]. On the other hand, the diffuse thickening is not associated with geometric regions of the arteries, with less thickening than eccentric thickenings[2]. Eccentric IPA is assumed to be as a precursor of atheroma plaques due to its association with atheroma prone regions that are characterized by an increased mechanical stress and LDL accumulation. Using human autopsy subjects who died between 36 weeks of gestation and 30 years of age, Nakashima *et al.* examined the distribution of IPA in systemic arteries and found that IPA was specifically present in atherosclerotic-prone arteries but not in the resistant arteries[49].

I.2.5 Atheroma plaque development

The processes involved in atheroma initiation and progression are summarized in figure I.3.

I.2.5.1 *Endothelial dysfunction and LDL accumulation*

Vascular net activity depends in large part on the operation of endothelial cells[50]. In its physiological normal state, the endothelium balances the vasomotor activity of the vessel wall by secreting equal amounts of vasodilators and vasoconstrictors[51]. In addition, it protects against the infiltration of monocytes and LDL into the sub-endothelium which are known to be major drivers of atheroma formation[8]. Moreover, the normal endothelium creates a thrombo-resistant environment[52] in the vessel wall through the production of anti-thrombotic molecules such as thrombomodulin, plasminogen activator and prostacyclin, in addition to the degradation of platelet aggregating agents, such as serotonin and prostaglandin F1[53]. Endothelial dysfunction, also called endothelial injury or endothelial activation, is defined as new structural and functional properties in endothelial cells[44]. One of the main features of

endothelial dysfunction is an imbalance in production of vasoactive substances by the endothelium, characterized by an increase in the vasoconstrictors to vasodilators ratio[51]. This is accompanied with a decrease in nitric oxide (NO) production which may lead to vascular damage. The phenotypic switch of ECs into a secretory phenotype, manifested by increased RER and Golgi network, leads to the production of a multilayered basal lamina[44] that entraps modified LDL and disrupts EC-EC tight junctions and EC-VSMCs gap junctions[54]. Activated ECs also express and secrete von Willebrand factor, which recruit platelets and initiate their adherence to ECs[55,56]. Activated platelets then start to secrete proinflammatory cytokines and chemoattractants (P-selectin, soluble CD-40 ligand and MMPs), leading to platelets-monocytes interaction (P-selectin with PGL-1) and promotes the binding of monocytes to ECs via VCAM-1[49].

The change in EC features is usually accompanied with increased permeability to lipoproteins and other plasma molecules[44,57]. One of these molecules is LDL, which is known to be a major player in atheroma lesion initiation and progression. In the subendothelial space, LDL accumulates and attach to ECM components through ionic interactions[24]. The accumulating LDL is then subjected to modifications in its protein component, mainly by oxidation. However, LDL modification may also occur in the plasma or when crossing the endothelium[44]. Although LDL oxidation is a passive process, it was shown that it is promoted *in vitro* in the presence of macrophages, ECs, VSMCs and PGs, which are major components in atheroma lesions[39]. The produced oxidized-LDL (oxLDL) induces expression of LOX-1 scavenger receptor expression and EC apoptosis, which may favor endothelial dysfunction[58]. In addition, oxLDL induces proatherogenic gene expression, such as adhesion molecules[59], inflammatory cytokines and MMPs[60]. Moreover, oxLDL is a potent chemoattractant for monocytes[61], VSMCs[62], T-lymphocytes[63] and dendritic cells (DCs)[64].

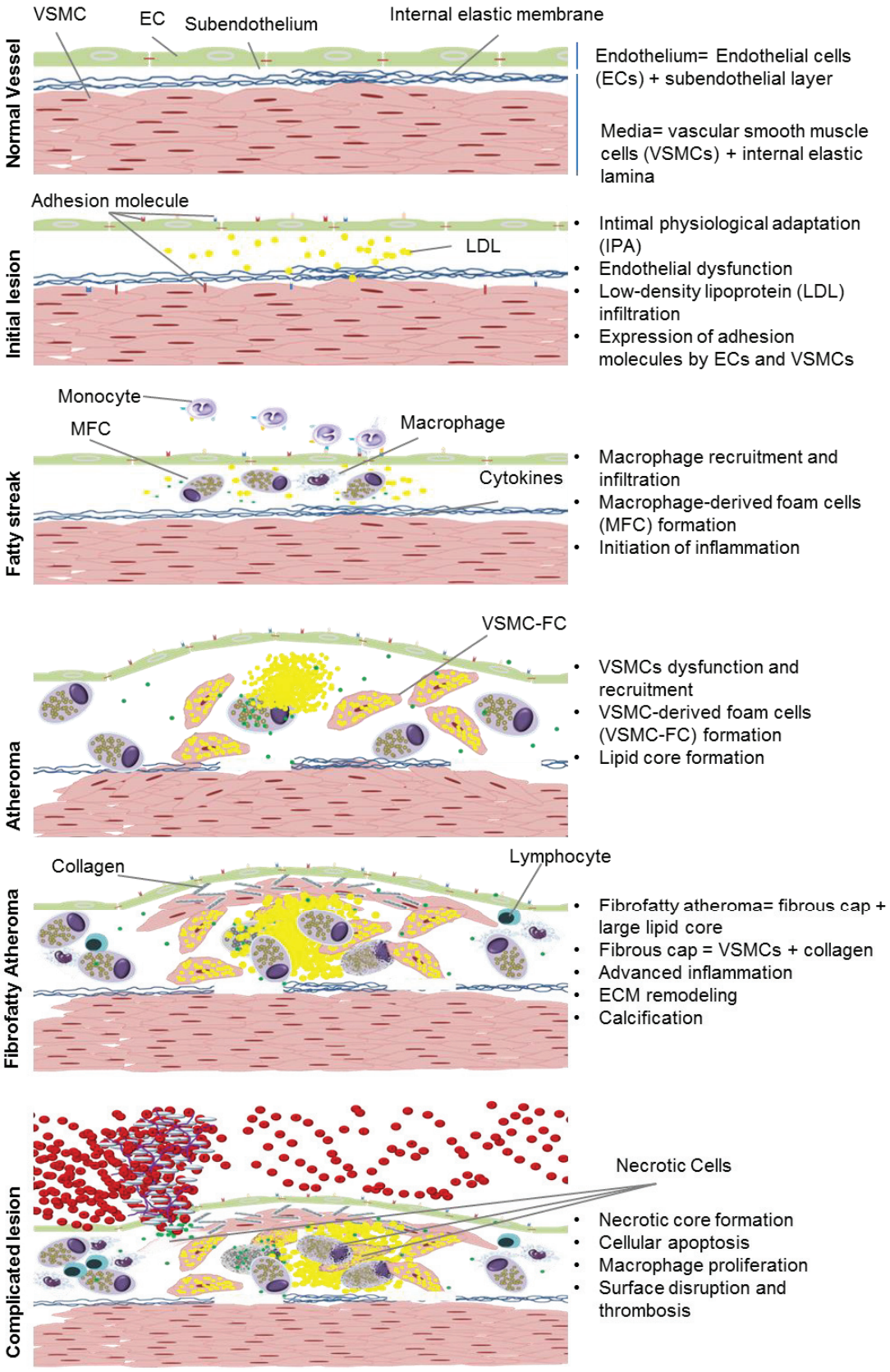

Figure I.3: atheroma stages and processes involved in atheroma development.

I.2.5.2 *Monocytes infiltration and differentiation into macrophages*

ECs do not support leukocytes adherence under normal physiological conditions[55]. However, upon stimulation by certain factors such as asymmetric wall tension, LDL, interleukin-1 (IL-1) and tumor necrosis factor (TNF), ECs start to express adhesion molecules, such as selectins, VCAM-1, intercellular adhesion molecule1 (ICAM-1), Platelet endothelial cell adhesion molecule (PECAM-1) and junctional adhesion molecules (JAMs)[44], leading to capture, rolling, adhesion and diapedesis of monocytes into the intima. The expression of these adhesion molecules by ECs can be upregulated by various factors including oxLDL, smoking, hypertension, diabetes and mechanical stress[65,66]. In addition to adhesion molecules, ECs were shown to express monocytes chemoattractants MCP-1, IL-8[67], also T-lymphocytes and mast cells chemokines[68]. The recruitment of macrophages is a key step in atheroma plaque initiation and progression as been shown in ApoE-/- mice, where ICAM-1 or P-selectin knockout offered resistance to atherosclerosis[69].

After entering the sub-endothelium, monocytes differentiate to macrophages in the presence of macrophage colony-stimulating factor (MCSF)[70] and other factors, including oxLDL, advanced glycation end-products (AGEs), Angiotensin-II (Ang-II) and endothelin[71].

Studies have pointed toward the presence of two different phenotypes of macrophages in atherosclerosis[70]: pro-inflammatory (M1) phenotype and anti-inflammatory (M2) phenotype. The M1 phenotype can be activated by lipopolysaccharide and IFN-γ, leading to the production of high levels of IL-2, IL-23, IL-6, IL-1 & TNFα[70]. This type is also involved in foam cells formation[72]. On the other hand, the anti-inflammatory (M2) phenotype may differentiate in the presence of IL-4, IL-13 and IL-1, and produce large amounts of IL-10[73]. Like M1 macrophages, M2 macrophages express SRs and exhibit Scavenger activity and are thus involved in foam cells formation[73]. In fact, it was shown that M1/M2 balance of plaque macrophages reflects the pro-/anti- atherosclerotic conditions *in vitro*[72]; however, this needs to be also validated *in vivo*.

I.2.5.3 *VSMCs recruitment and phenotypic switching*

Macrophages in the plaque exert several effects on VSMCs in the vessel wall. Macrophages can induce VSMCs proliferation through platelet-derived growth factor (PDGF) secretion[74]. In addition, IL-6 and tumor necrosis factor alpha (TNFα) secreted by macrophages induce VSMCs to produce MMP-1, which may facilitate the degradation of VSMCs basal lamina

and thus enhance their migration[75]. Moreover, macrophages were shown to trigger VSMCs apoptosis by secreting TNFα and NO[76].

VSMCs in the intima of atheroma plaque can originate from bone marrow precursor cells, medial cells and resident VSMCs, and the latter is thought to be the main source of these cells[44,77]. Recent studies have shown that ICAM-1 and VCAM-1 were expressed on VSMCs in atheroma-prone regions before monocytes infiltration in both human[45] and mouse[78]. In fact, VSMCs and macrophages can interact directly through ICAM-1 and VCAM-1 and chemokine (C-X3-C motif) ligand 1 (CX3CL1)[78,79], which were shown to be expressed on VSMCs in different atheroma types (coronary, carotid and aorta), in both human and mice, but not in healthy medial VSMCs[79]. In addition, there is high association between VCAM-1 expression on VSMCs and intimal macrophages number[80]. All these point toward the involvement of VSMCs in, not only progression of the atherosclerotic lesion, but also in its initiation through recruitment of macrophages.

A prominent feature of VSMCs in atheroma is the phenotypic switch from the "quiescent" contractile phenotype to a proinflammatory synthetic phenotype[81], which can be stimulated by several atherogenic stimuli including shear stress, ECM components (fibronectin, laminin and collagen IV)[82,83], cytokines (PDGF and transforming gowth factor beta (TGF-b))[84–86], reactive oxygen species (ROS)[87] and lipids[88]. In their steady state, mature VSMCs[4,81,89] are quiescent and proliferate at a very low rate and exhibit a low synthetic activity with high expression of contractile marker genes, ACTA1, SM22a, MHC, H1 calponin and smoothelin[81,89]. Mature VSMCs perform several functions including vaso-modulation, ECM synthesis, GFs production and injury repair (migration, proliferation and ECM production)[77]. Phenotypic switching is thought to be a normal response for injury repair, however, exaggerated in atherosclerosis due to continuous inflammation[81,90].

In addition to "intracellular" phenotypic switching, recent studies are showing that an "inter-cellular" switch between VSMCs and macrophages could also occur. Indeed, this was validated both *in vivo* and *in vitro*[91–93]. Allahverdian et al. recently showed that cells expressing both CD68 and smooth muscle markers in lipid rich regions of atherosclerosis were identified both in grossly normal aortic areas and in atherosclerotic lesions (fatty streaks and atherosclerotic plaques)[92]. They also showed that more than 50% of the intimal cells in atherosclerotic lesions are lipid engorged and express alpha smooth muscle actin (aSMA). The incubation of VSMCs in cholesterol *in vitro* induced them to form macrophage-like cells

(MLCs) that express macrophage-specific markers and induced phagocytic and antigen-presenting activity[91]. In addition, MLCs expressed high levels of proteolytic enzymes, suggesting a role for these cells in plaque instability. Similarly, the other way of trans-differentiation was shown to be also true. Indeed, several groups identified SMC like cells (SLC) of monocytes origin[94,95]. In vitro studies have shown that some CD14/CD105 positive peripheral mononuclear cells can differentiate into aSMA positive cells[93]. In addition, cultured macrophages express of aSMA in the presence TGF-b and thrombin (Martin et al. 2009; stewart et al. 2009). However, it is well accepted that most SMCs in the atherosclerotic plaque are of local origins and not hematopoietic origin[96]. Indeed, Allahverdian et al. 2014 showed *in vivo* that 40% of CD68+ cells in atheroma are also CD45+[92]. However, these studies still have certain limitations. For instance, there is still no rigorous methods for the identification of cells of VSMCs origin after selective-marker genes go into undetectable levels[89]. In addition, several cell types of non-SMC origin, such as skeletal muscle cells, cardiomyocytes and fibroblasts, may also express VSMC marker genes like aSMA under certain conditions such as during development or wound repair[97,98].

I.2.5.4 *Inflammation*

Activated macrophages in the lesion secrete multiple factors that may contribute to further plaque inflammation and growth[99], including inflammatory cytokines (TNFα IL-1, MCP-1, MCSF), GFs for VSMCs and ECs (PDGF), chemotactic factors for VSMCs (Ang-II), Angiogenic factors and ROS through Nicotinamide adenine dinucleotide phosphate (NADPH) oxidase (Nox).

Pro-inflammatory synthetic VSMCs are characterized by a marked decrease in contractile marker genes and increased proliferation, migration and production of ROS, ECM, proteases, GFs and cytokines[77,81,100,101]. Pro-inflammatory VSMCs express inflammatory genes, such as PDGF, Interferon gamma (IFN-g), TGFb, MCP-1[77,81]. In addition, they can produce cytokines that attract and activate leukocytes, induce VSMCs proliferation, promote endothelial dysfunction and stimulate VSMCs components.

An important mediator of the inflammatory reactions in atherosclerosis is ROS, which can be produced by VSMCs, macrophages, ECs and fibroblasts, mainly through NADPH oxidase[77]. Indeed, ApoE-/- deficient in NADPH-p47phox subunit showed decreased atherosclerotic lesions progression compared to control apoE-/- mice[102]. ROS is the major driver of LDL oxidation. Oxidized LDL (oxLDL)[30] is a major driver of atheroma progression by promoting

several cellular mechanisms in atheroma lesions (see also part II.5.a). Indeed, oxLDL promotes inflammatory responses, induces macrophages and VSMCs growth, promote ECs apoptosis and enhance thrombosis. In addition, oxLDL interact with and damage DNA and proteins[103] in the cell, leading to the formation of a necrotic core, which destabilizes the lesion and make it more susceptible for rupture[60]. Moreover, ROS interact with NO to produce peroxynitrite (a potent oxidant)[104], which scavenges NO, leading to increased inflammation, platelet activation and vasoconstriction[77].

In addition to macrophages and VSMCs, other inflammatory cells are recruited to the atheroma lesion, which augment local inflammatory reactions and help in atheroma progression. Indeed, advanced lesions may contain T-lymphocytes, dendritic cells (DCs), neutrophils, mast cells and platelets[105]. T-helper and T-killer cells, in addition to antigen presenting dendritic cells were detected in pre-lesional stages of plaque formation[44]. In fact, various antigens in the plaque induce T-cells proliferation, including modified LDL[105]. Indeed, human atherosclerotic lesions contain both T-helper and T-killer cells that recognize oxLDL as an antigen[106]. T-helper cells are thought to play a key role in the progression of atheroma lesions by the secretion of several cytokines and cell-surface molecules that activate macrophages and potentiate local inflammation[44], in addition to other effects, such as angiogenesis and the expression of adhesion molecules, chemokine and tissue factors[39].

Dendritic cells (DCs) are antigen presenting cells required for T-cells activation[107]. DCs are present in all stages of lesion development, particularly in the advanced lesion shoulders[107]. DCs are recruited to the lesion by binding to ECs under various atherogenic stimuli, including oxLDL and TNFα[64]. In addition to presenting antigens and activating macrophages, DCs were also shown to proliferate and form foam cells in the atherosclerotic lesions[108].

Neutrophils are also present in atherosclerotic lesions and there is a correlation between the number of neutrophils in blood and their presence in the vascular wall in coronary artery disease[44]. Activated neutrophils secrete superoxide and pro-inflammatory mediators, which aid in EC dysfunction and monocytes activation[44]. Neutrophils are thought to play a role in plaque destabilization by releasing a wide variety of mediators, most of which can contribute to lesion formation and progression, extracellular matrix degradation, and plaque erosion[109].

Mast cells are mainly present in advanced lesions of atherosclerosis[18]. It was shown *in vitro* that mast cells can be induced by oxLDL-IgG complexes to release contents of their cytoplasmic granules, including neutral proteases, GFs and pro-inflammatory cytokines

(TNFα, IL-8 and MCP-1) that will act on ECM and lesion cells[44] leading to lesion progression.

I.2.5.5 *Foam cells formation*

Foam cells formation is a prominent feature in early and advanced atheroma plaques. Foam cells can be formed by the different cell types present in the plaque[24] and play a major role in the formation of the necrotic core in advanced atheroma plaques[18].

Macrophages are believed to be the major source of foam cells in atheroma lesions[18,44]. Macrophages preferentially take up oxLDL by recognizing the modified apoB part[44]. Macrophages express SRs for acetylated and oxLDL, such as LOX-1[110], SR-AI, SR-AII and SR-B (CD36)[44], which are involved in the uptake of oxLDL, AGEs, anionic phospholipids and apoptotic cells[44]. oxLDL uptaken by macrophages through SR is then hydrolyzed into free cholesterol and fatty acids in the endosomes[44]. Hydrolyzed cholesteryl esters and free cholesterol are then released from endosomes and transported outside the cells to apoA1 and HDL via ATP-binding cassette transporter (ABC) A1 (ABCA1) and ABCG1 or through passive diffusion into cholesterol-poor HDL[44]. Excess cholesterol in the cells will be esterified by ACAT and accumulate in the cytosol, leading to foam cells formation[44]. Free cholesterol accumulation in the plasma and endosomal compartment may enhance inflammatory signaling in macrophages, mainly through TLRs[111], which upon activation leads to the production of inflammatory cytokines and NO and induction of DC maturation[112]. In addition, MFCs secrete cytokines, GFs, tissue factor, IFN-g, MMPs and ROS[44], which contribute to plaque growth and destabilization. Macrophage-derived foam cells can also proliferate in the presence of MCP1 and MCSF[29].

The second source of foam cells in atheroma lesion is VSCMs. VSMCs express LOX-1[110], SR type I and type II[113], LDL receptor[114], VLDL receptor[115], CD36[116] and CXCL16/SR-PSOX[117]. This combination permits the uptake of unmodified and modified LDL in addition to other forms of cholesterol[79]. Lipid receptors can be induced by atherogenic cytokines[57,114] and LDL uptake[118,119]. Initial cholesterol loading by VSMCs is associated with upregulation of ABCA1 and ABCG1 and down-regulation of SMC marker genes. However, continued lipid uptake is associated with down- regulation of ABC transporters, which favors foam cell formation[72,75].

In addition to macrophages and VSMCs, ECs may also contribute to foam cells formation by expressing scavenger receptors, mainly LOX-1[120]. LOX-1 can be induced by a variety of proinflammatory factors, including lipoplysaccharide, TNFα, IL-1b, INF-g, oxLDL and shear stress[81]. EC derived foam cells (EFCs) usually occur in advanced lesions and are fragile and susceptible to erosion[44].

Lipid uptake by cells is considered beneficial during early lesions, where it may exert a protective role by clearance of oxLDL[112]. However, since lipid uptake is not inhibited by cellular cholesterol content[44], it will exert pro-atherosclerotic role in advanced lesions by inducing apoptosis due to the toxic accumulations of free cholesterol[121].

I.2.5.6 *Apoptosis*

At this stage, macrophages perform a double effect; a negative one through apoptosis and a positive one through efferocytosis. Macrophages apoptosis can be triggered by RER stress[122], GFs deprivation, oxidative stress and death receptor activation, in addition to NFKB, IFN and TLR2/4 inhibition[123]. However, macrophages are not totally harmful. Indeed, one of the major roles of macrophages in stabilizing the atheroma plaque is efferocytosis[122]. In fact, plaque necrosis is defined by the balance between apoptosis and efferocytosis. Efferocytosis is the action of removing apoptotic bodies before their decomposition and release of toxic molecules[122]. This will trigger an IL-10 and TGFb-mediated anti-inflammatory response in efferocytes, which promotes cell survival of efferocytes with robust esterification and efflux of cholesterol and oxLDL[122].

In vitro studies have shown that macrophages and VSMCs co-culture prevents apoptosis[124] of macrophages and enhances IL-6 and MCP-1 production compared to single cultures of either cell type[125]. This can be a mechanism contributing to inflammation, foam cells formation and atheroma growth and progression. On the contrary, it was also shown that macrophage-derived NO upregulates Fas expression by VSMCs & Fas-L by macrophages, which may enhance VSMCs apoptosis[71]. This was supported by the fact that blockade of either NO or Fas abrogated VSMCs apoptosis. This interaction between VSMCs and macrophages could be a mechanism by which monocytes can be retained and survive in the intima[124], thus augmenting inflammation, foam cells formation and atheroma growth and progression.

I.2.5.7 *ECM remodeling*

ECM constitutes 60% of intima volume and plays an important role in maintaining cell-tissue structure and directing cell functions by binding to special receptors on cell membrane that induce specific signaling cascades within the cell[126]. Thus, a change in the ECM components will lead not only to structural changes in the acellular part of the wall, but also to critical changes at the cellular level. ECM remodeling in atherosclerosis is done both at the synthesis and degradation levels.

In atherosclerosis, PGs of the ECM were shown to change and play different roles during atheroma development. One of the main roles of PGs in atherosclerosis is LDL trapping in the intima through ionic interactions between sulfated groups of PGs and the apoB component of LDL particles[127]. In addition to LDL trapping, sulfated PGs interact with LDL in the intima and favor their modification (oxidization and esterification)[128] and internalization by macrophages[129] and VSMCs[130]. In addition, sulfated PGs, cytokines and oxLDL were shown to induce VSMCs to produce sulfated PGs[131], and thus providing a positive loop over LDL trapping, modification and internalization, which will favor atheroma plaque progression[127]. Dermatan sulfate was shown to have a high affinity to LDL under physiological conditions[132] and to be positively correlated to apoB accumulation[36]. On the other hand, heparan sulfate, which is known to regulate cell proliferation, decrease with lesion severity, which can be a way of loss of control on cellular proliferation[2]. In advanced lesions, ECM of the intima changes from being mostly of collagen types I and III to become PG-rich with scattered collagen type I and fibronectin[79]. This is thought to be a molecular mechanism to stabilize the plaque by conferring tensile strength and vasoelasticity[133]. In addition, VSMCs basal lamina, which maintain their contractile phenotype and prevent their dedifferentiation, growth and proliferation, changes its composition during atheroma progression, with an increase in PGs, osteopontin and fibronectin[134]. The latter two are known to induce proinflammatory cascades in VSMCs through NF-KB and AP-1[135,136]. PGs induce proliferation by downregulation of cdk2 inhibitors (Doran et al. 2008). VSMCs proliferation under these ECM conditions may induce a positive loop by further degrading collagen and producing PGs and fibronectin[79].

In addition to the synthetic level, cells of the atherosclerotic lesion contribute to the changes in ECM by degrading its components. Macrophages contribute to ECM degradation by secreting MMPs, collagenases, elastases and PG degrading enzymes, which degrade the

fibrous cap connective tissue, leading to unstable plaque formation[57]. Collagen I polymers, which are known to inhibit VSMCs proliferation and migration[137], are degraded by MMPs that are produced by several cell types under inflammatory conditions[138], thus leading to VSMCs proliferation. In addition, the produced collagen monomers activate expression of VCAM-1 in VSMCs[139] and induce their migration[140]. Moreover, Elastin products produced upon cleavage by macrophage- and VSMC-derived elastases are known to be highly chemotactic for macrophages. It was shown that synthetic VSMCs secrete 25 to 46 times more collagen than contractile VSMCs and exhibit higher lipid uptake with higher expression of LDL and scavenger receptors[48,79]. In fact, VSMCs secrete most of the ECM in complex atherosclerotic lesions[24]. The number of RER-rich synthetic VSMCs with dense basement membrane is associated with lesion severity and is found in advanced but not early lesions . Synthetic VSMCs are more frequent in the cap region of advanced lesions between the lipid core and the vascular lumen, where they are thought to provide a mechanical support to the lesion surface[18].

I.2.5.8 *Calcification*

Calcification is a prominent feature in advanced stages of atheroma that favor plaque instability and subsequent rupture. Indeed, calcification serves as a surrogate marker for the disease, and predicts a higher risk of myocardial infarction and death[141]. Several hypotheses were proposed to explain atherosclerotic calcification[142]. However, the most supported hypothesis of calcification in atherosclerotic lesions is that VSMC are stimulated to adopt an osteogenic phenotype and become calcifying vascular cells[142], which involve the normal process of biomineralization. Indeed, the chemical composition of calcified sites was identical to hydroxyapatite, the major inorganic component of bone[143]. Atherosclerotic aortas from post-mortem tissues showed a higher expression of biomineralization markers, such as osteopontin, BMP2, Osteonectin, osteocalcin and S100A9[144]. At the same time, these aortas possessed lower expression of calcification inhibitors, including osteoprotegerin, fetuin-A and matrix Gla protein. In addition, it was shown that senescent VSMCs can be induced to express Runt-related transcription factor 2 (RUNX2)[144], an osteoblast master transcription factor, by oxLDL[145], ROS[146], b-glycerophosphate[145] (Bear et al. 2008), FGF-2[147]. RUNX2 induce BMP2 expression, which in turn can induce the expression of Pit-1, a type III sodium-dependent P(i) cotransporter, and down-regulation of SMC markers[148]. Another cellular calcification marker, alkaline phosphatase (ALP), was shown to be induced *in vitro* in VSMCs incubated in macrophage-conditioned media[149].

I.2.6 Stages of the atheroma plaque

After describing the different processes involved in atherosclerotic lesion development, we are going to describe the different types (stages) of atherosclerotic lesions with their prominent features. Based on the American heart association (AHA) classification, atherosclerotic lesion formation could be divided into 8 stages that are discriminated by certain histologic and molecular characteristics and are usually correlated to the age of patients[24]. Types I and II lesions are the only types of lesions that can be found in children. Type III is an intermediate type between early and advanced lesions that usually evolve soon after puberty. Type IV lesion is considered the first advanced lesion type, it usually appear during the third decade of life and is usually not associated with clinical events[18]. Types V and VI are the advanced lesions associated with clinical events that occur in advanced ages and/or advanced patients after the 4th decade of life. The features of the different stages[2,18,24,44,141] are represented in Figure I.4.

I.2.7 The vulnerable plaque characteristics

Plaque stability depends on several factors including plaque size, cellular composition, cellular mechanisms, ECM composition and inflammatory reactions[18,44,150]. Vulnerable plaques are advanced plaques (stages V, VI, VII or VIII) that are susceptible for erosion and/or rupture, thus leading to thrombus formation[18]. The large size thrombus with the plaque may locally block the lumen of the artery or detach, migrate and occlude a smaller artery downstream leading to acute cardiovascular syndromes and death. Vulnerable plaques are characterized by a large plaque and thin cap. The cap region provides a mechanical support to the plaque to prevent it from rupture, and the composition of the cap region is a major determinant in plaque vulnerability[151]. Indeed, thrombogenic potential does not depend on the stage of the lesion but rather on the composition of the lesion, since more advanced lesions are usually stabilized by the fibrous cap of collagen and VSMCs, while less advanced lesions (type IV and V) are more prone for destruction[18]. Increased macrophage to VSMC ratio in the cap region is associated with increased ECM degradation/synthesis ration, and thus weakness of the cap region[44,151].

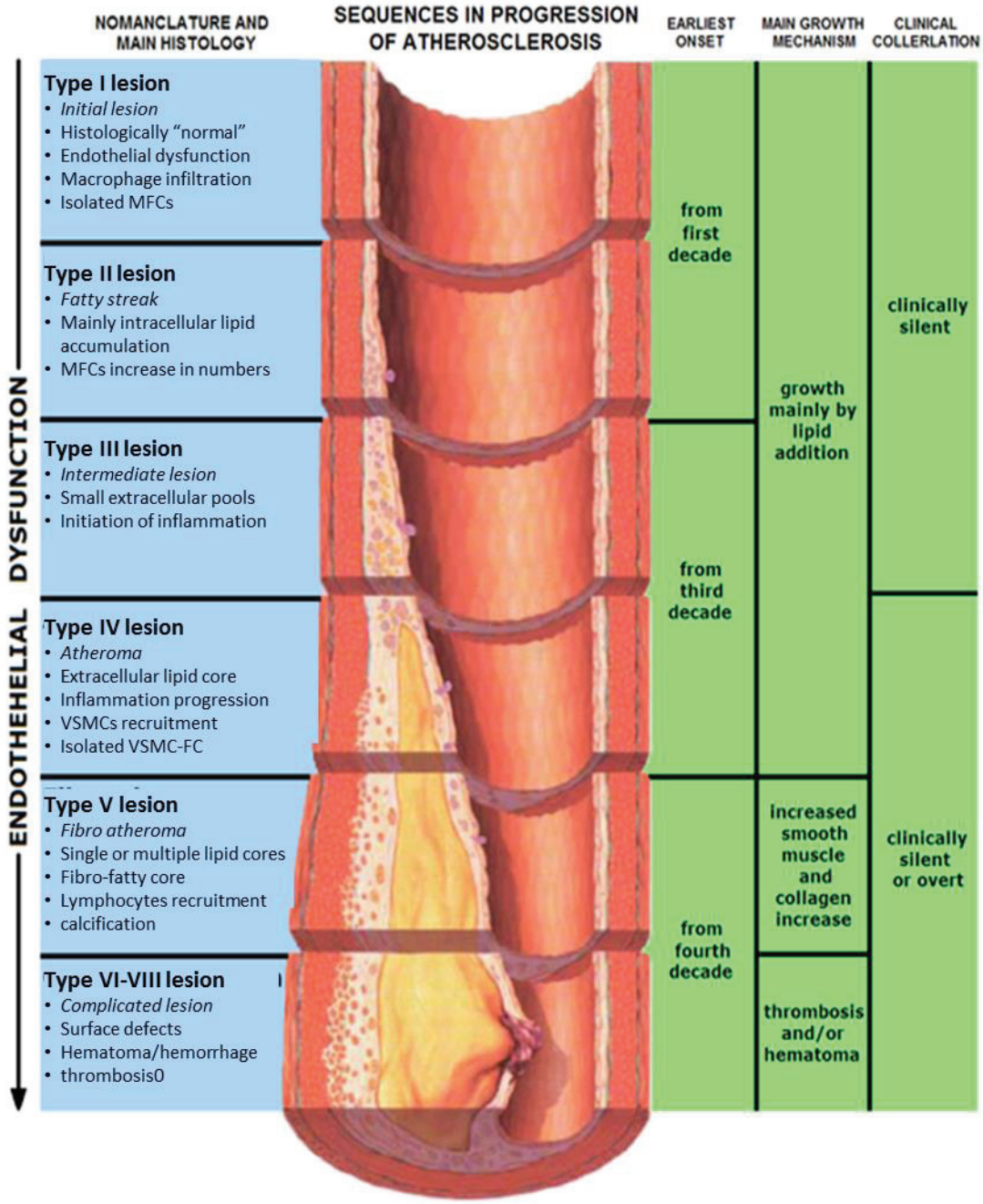

Figure I.4: The different stages of atheroma development. MFC, macrophage-derived foam cells; VSMC, vascular smooth muscle cell; VSMC-FC, vascular smooth muscle cell-derived foam cell. Adapted from https://commons.wikimedia.org/wiki/File%3AEndo_dysfunction_Athero.PNG.

Fibrous cap of ruptured plaques have more macrophages, lymphocytes and mast cells than non-ruptured plaques[152]. Macrophages secrete inflammatory cytokines and proteases, mainly MMPs[152], thus leading to ECM degradation. Also it was shown that the efferocytotic activity of macrophages decrease with plaque progression, which will help in apoptotic cells accumulation and thus increased pressure on the cap of the plaque[122]. In fact, accumulating apoptotic macrophages release excess inflammatory cytokines and ECM proteases, thus aiding in cap weakness. In addition, macrophages can induce VSMCs apoptosis by secreting

pro-apoptotic TNFα and NO, also by activating Fas pathway[76]. In fact, unstable plaques are usually associated with VSMCs apoptosis, which leads to thinning of the fibrous cap as a result of reduced cellular and matrix components[153]. Apoptotic cells may release IL-1a and IL-1b, which lead to the induction of MCP1, TNFα and IL-6 in non-apoptotic VSMCs and thus augmenting the inflammatory response in the lesion[154]. In apoE -/- mice, chronic low apoptosis was associated with two fold plaque growth with enhanced calcification, thickened fibrous cap and enlarged necrotic core[155]. In fact, the balance between VSMCs proliferation and apoptosis is a key determinant of atheroma progression[156], with VSMCs apoptosis leading to unstable and calcic plaques[155,157].

In addition to the cellular components, Hemorrahge[158], microcalcification in fibrous cap[159], high shear stress[160] and other factors are commonly associated with vulnerable plaques. Indeed, all these factors may lead to the formation of a thin cap fibroatheroma, which constitute a thin cap with few fibrous matrix and VSMCs (<65µm) and a large necrotic core constituting more than 30% of the plaque area[39]. This plaque may then be subjected to rupture (55-65%), erosion (30-35%) and/or calcified nodules formation (2-7%), which disrupt the endothelial layer and expose lipid core, collagen, tissue factors and other elements[39]. These factors may lead to disturbance in coagulation/fibrinolysis balance[161] and subsequent thrombi formation that continue to enlarge and occlude the lumen within hours-days. A study done on 30-59 years old patients had shown that 38% of advanced lesions in the aorta had thrombi on their surface[39]. The formed thrombi constitute layers of platelets with variable amounts of fibrin, red blood cells and acute inflammatory cells[18]. Plaque rupture usually occurs at the shoulders where low VSMCs and high inflammatory cells are present[39,157]. In some cases, small surface ulcerations may lead to small thrombi that may form, recur and incorporate in the plaque over the years, thus leading to an increase in lesion size and subsequent narrowing of the lumen[18]. Ruptures may heal by VSMCs infiltration, accompanied with ECM accumulation, neovascularization, inflammation and surface re-endothelialization[18,39].

I.2.8 Conclusion

In conclusion, atherosclerosis is a complex disease with multiple players exerting multiple mechanisms, and the combination of these mechanisms over the time course results in the development of the highly complex atheroma plaque. Although many studies addressed the mechanisms involved in atheroma development, most of these studies were *in vitro* studies

targeting certain mechanisms of one player or the other. In this regard, the need to study atherosclerotic processes in a systems biology approach is needed. Indeed, this will need high throughput techniques that investigate multiple players at the “omics” level, such as transcriptomic microarrays to identify altered gene expression, ChiP-seq to identify epigenetic modifications involved in the phenotypic changes of cells, and proteomic techniques (i.e. protein chips, mass spectrometry) to identify the pool of proteins that are interacting and playing their roles in shaping the atherosclerotic process.

I.3 THE RENIN-ANGIOTENSIN-ALDOSTERONE SYSTEM (RAAS)

I.3.1 Classical RAAS

The renin angiotensin system was originally defined as a circulating hormonal cascade that functions in the homeostatic control of arterial, pressure, tissue perfusion, and extracellular volume[162]. The system was first discovered in a 1898 by Tigerstedt and Bergmann that demonstrated the existence of a heat-labile substance in crude extracts of rabbit renal cortex that caused a sustained increase in arterial pressure. They called this substance "renin". Later on, studies had shown that the pressor activity of renin was indirect and resulted from its proteolytic action on a plasma substrate, "angiotensinogen", to liberate a direct-acting pressor peptide "angiotensin"[163].

In its classical endocrine view, RAAS includes several components and enzymatic cascades resulting in the conversion of the "inactive" substrate of the system, angiotensinogen (AGT) into the active peptide angiotensin II (Ang-II), which binds to its specific membrane receptors and elicits cellular effects[51]. AGT, the "inactive" substrate of RAAS, is a glycoprotein constituting 452 amino acids long produced primarily and continuously in the liver. In addition AGT is expressed and differentially regulated in multiple other tissues, including heart, blood vessels, kidneys and adipose tissue[51]. In the plasma, AGT exists in concentrations lower than Michaelis-Menten constant of renin (<1μM), thus providing a repository for the rapid formation of Ang-I under certain physiological conditions[164]. AGT production can be induced by several stimuli, including inflammation, insulin, estrogen, glucocorticoids, thyroid hormone and Ang-II.

In the plasma AGT is converted into the decapeptide angiotensin-I (1-10) (Ang-I) by the tightly regulated enzyme renin produced by the juxtaglomerular cells (JG) that line the afferent arteriole of the renal glomerulus[162]. In fact, this step is considered the rate limiting step of the system in the circulation[162]. Renin is synthesized from a 9 exons gene as a pre-pro-hormone cleaved by microsomes to form the preform, prorenin, which contains a 43-amino-acid prosegment peptide at its N-terminus[165]. Prorenin is then released as inactive precursor or can be converted by a variety of proteases into active intracellular renin that is stored in granules of the JG cells and is released by a stimulus-dependent exocytic process into the circulation[162]. Active renin secretion can be stimulated by 3 main inter-dependent factors: (1) a fall in perfusion pressure sensed by the renal baroreceptors of the afferent arteriole, (2) a fall in the delivery of NaCl to the *macula densa* cells of the distal tubule, and (3) sympathetic

nerve stimulation via beta-1 adrenergic receptors[162]. In addition, renin secretion can also be regulated by a negative feedback exerted by Ang-II on the JG cells[166].

Ang-I produced by renin is further processed by the angiotensin converting enzyme (ACE) which removes the C-terminal dipeptide to releases the octapeptide angiotensin II (1–8) (Ang-II). ACE was first described in horse plasma in 1956 as an enzyme that convert hypertensin I into hypertensin II; the latter two being the original names of Ang-I and Ang-II, respectively[167]. ACE is a membrane-bound exopeptidase localized on the plasma membranes of various cell types, mainly endothelial cells, and specifically those of the lungs and liver[162]. Indeed, ACE production is often used as an endothelial cell marker *in vitro*[168]. It is this membrane-bound ACE that is thought to be physiologically important. In addition, ACE can degrade a number of other vasodilating peptides, including Ang-(1-7), bradykinin and kallirein, thus playing a central role as a pressor enzyme[51,162]. Moreover, ACE can activate cellular signaling when bound to ACEi and bradykinin, leading to increased ACE and COX2 production via c-Jun N-terminal kinase (JNK) signaling[169].

Ang-II is the biologically active peptide of the system, which elicits its cellular effects by binding to its membrane receptors. Ang-II mediates effects via complex intracellular signaling pathways that are stimulated following binding of the peptide to its cell-surface receptors, angiotensin type I (AT1R) and type II (AT2R) receptors[170], which were identified as seven transmembrane receptors that share 34% of their nucleic acid sequence[171]. In the classical view, Ang-II is a circulating hormone that regulates blood pressure and electrolyte balance by acting on vascular tone, aldosterone secretion, renal sodium handling, thirst and water intake, sympathetic activity, and vasopressin release[51]. Indeed, all these effects are known to increase blood volume and pressure. However, molecular studies have shown that the activation of AT1R also exerts rapid (short term) and genetic (long term) effects at the cellular level[172]. By binding to the AT1R, Ang-II activates multiple intracellular signaling cascades, mainly mitogen-activated protein kinase cascades (MAPK) and tyrosine kinases, leading to cell growth, proliferation and migration[173]. In addition, AT1R activation leads to the activation of various transcription factors (TFs) that regulate genes coding for vasoactive hormones, growth factors, extracellular matrix components, cytokines, etc[173]. As a defense mechanism against extensive activation, AT1R undergoes rapid desensitization and internalization after agonist stimulation[51]. On the other hand, the AT2R acts mainly through Gi and tyrosine phosphatases to exert pre-dominantly inhibitory actions on cellular responses

mediated by the AT1 receptor, mainly by inhibition of cell growth and proliferation and promoting cell differentiation, in addition to vasodilation and reducing blood pressure[174].

One of the major effects of Ang-II is stimulating aldosterone synthesis and seretion by the adrenal cortex by stimulating the expression and activity of the aldosterone synthase, CYP11B2[175]. Aldosterone has emerged as the most important physiological regulator of extracellular fluid volume and blood pressure in mammals, and has been implicated in a variety of disease states in humans[176]. CYP11B2 production and activity can be regulated by several compounds, mainly the plasma potassium concentration, the activity of the renin-angiotensin system) and Adrenocorticotropic hormone (ACTH)[177]. Aldosterone acts in a variety of tissues through its mineralocorticoid receptor (MR) to influence extracellular fluid volume, blood pressure, salt exchange, but may also lead to pathological consequences, mainly tissue fibrosis[178].

I.3.2 Extended RAAS

Research in the last few decades supports the new concept of an extended RAAS (extRAAS) that includes multiple enzymatic pathways for the generation of different angiotensin peptides, with alternative enzymes and receptors that are expressed and exert their effects in a tissue- and condition-specific manner[179]. These effecrs may explain the dual role of the RAAS as both a circulating hormonal and tissue-specific regulatory system serving autocrine, paracrine and even intracrine functions. Based on literature and previous results obtained in our laboratory, extRAAS constitute 37 genes that could be obtained from the human renin-angiotensin pathway (hsa04614) and the steroid hormones biosynthesis pathway (hsa00140) from the KEGG database (http://www.genome. jp/kegg/pathway.html), in addition to other participants previously linked to the system that are not included in either KEGG pathways. The genes participating in the different pathways with the corresponding references are present in Table I.1.

Table I.1: extended renin angiotensin sstem (extRAAS) participants.

Pathway	Participant (gene symbol)	References
Aldosterone	CYP11B2	KEGG hsa00140 pathway
	GPER	Gros R 2013[180]
	NR3C1	KEGG hsa04960 pathway
	NR3C2	KEGG hsa04960 pathway
Ang-(1-7)	ACE	KEGG hsa04614 pathway
	ACE2	KEGG hsa04614 pathway
	CPA3	KEGG hsa04614 pathway
	CTSA	KEGG hsa04614 pathway
	MME	KEGG hsa04614 pathway
	NLN	KEGG hsa04614 pathway
	PREP	KEGG hsa04614 pathway
	THOP1	KEGG hsa04614 pathway
	MAS1	KEGG hsa04614 pathway
Ang-I	REN	KEGG hsa04614 pathway
	CTSD	Naseem RH et al. 2005[181]
	IGF2R	Batenburg and Danser 2012[182]
	ATP6AP2	Batenburg and Danser 2012[182]
Ang-II	ACE	KEGG hsa04614 pathway
	CMA1	KEGG hsa04614 pathway
	CTSG	KEGG hsa04614 pathway
	KLK1	Ideishi M et al. 1990[183]
	AGTR1	KEGG hsa04614 pathway
	AGTR2	KEGG hsa04614 pathway
	EGFR	Okada H. 2012[184]
Ang-III	ENPEP	KEGG hsa04614 pathway
	AGTR1	KEGG hsa04614 pathway
	AGTR2	KEGG hsa04614 pathway
Ang-IV	ANPEP	KEGG hsa04614 pathway
	DPP3	Dhanda et al. 2008[185]
	RNPEP	Carrera MP et al. 2006[186]

	AGTR1	Li et al. 2006 pathway[187]
	LNPEP	KEGG hsa04614 pathway
Corticosteroids	CYP11A1	KEGG hsa00140 pathway
	CYP17A1	KEGG hsa00140 pathway
	CYP21A2	KEGG hsa00140 pathway
Cortisol	AKR1C4	KEGG hsa00140 pathway
	AKR1D1	KEGG hsa00140 pathway
	CYP11B1	KEGG hsa00140 pathway
	HSD11B1	KEGG hsa00140 pathway
	HSD11B2	KEGG hsa00140 pathway
	NR3C1	KEGG hsa04960 pathway
	NR3C2	KEGG hsa04960 pathway

I.3.2.1 *Interaction between angiotensin and corticosteroids*

Several studies indicate that there is a reciprocal interaction between angiotensin and corticosteroids, mainly between Ang-II, aldosterone and their receptors, rather than just being Ang-II-induced aldosterone production[188–191]. Ang-II is the principal agonist of adrenal aldosterone synthesis and it maintains both the structure of the glomerulosa and the secretion of aldosterone, and at the same time, aldosterone-dependent sodium accumulation inhibits RAAS[192]; thus their levels and effects are tightly linked. In addition to systemic Ang-II, local RAAS can be a possible regulator of adrenal aldosterone production[193]. Local interaction between angiotensin and corticosteroids was described in several tissues, including the brain, VSMCs and ECs, and the myocardium[194]. More than 20 years ago it was shown that aldosterone stimulates expression of AT1R[195]. Similarly, Shelat et al. demonstrated that both activated MR and GR stimulated receptor specific binding of Ang-II to its AT1R in specific regions of the rat brain[196]. In addition to the AT1R, aldosterone treatment was also shown to activate ACE expression in cultured neonatal rat cardiomyocytes[197]. Thus it seems that aldosterone can alter both Ang-II generation and activity. Our team has recently shown that cortisol and angiotensin receptors are strongly correlated in the arterial wall, and that an auto-amplification loop exists between angiotensin and cortisol, which favor atherogenic signaling[198]. Moreover, some of the signaling pathways activated by the AT1R are dependent on the MR and vice versa[190]. For example, Ang-II was shown to activate MR-mediated gene transcription in coronary artery VSMCs via AT1R signaling, independent of aldosterone

synthesis[175]. These and other findings indicate that there is a strong interaction between angiotensin and corticosteroids, which suggest that enzymes and receptors involved in the metabolism and response to angiotensin and corticosteroids should be studied simultaneously.

I.3.3 Tissue RAAS

The first demonstration for the presence of a local tissue RAAS was in 1971[199], where a renin-like activity, independent of kidney and plasma renin, was found in the brain of dogs. This finding was then supported by the identification of peptides that are immunologically and pharmacologically similar to Ang-I with variable molecular weights in dog brain[200]. Since then, extensive studies were done to elucidate local angiotensin forming pathways and their physiological importance in different tissues. Indeed, local RAAS have been described in several organs and tissues[51,194,201–203], including the heart, blood vessels, kidney, brain, adipose tissue, adrenal gland, pancreas, liver, reproductive system, lymphatic tissue, placenta and the eye. In these tissues, RAAS acts independent from systemic RAAS in a paracrine and autocrine manner, but it may also interact with the systemic RAAS to exert endocrine effects[51]. Alterations in local RAAS were found to be associated with several pathological conditions, and the pharmacological inhibition of RAAS actions are widely used in the treatment of various diseases, such as hypertension, congestive heart failure, left ventricular dysfunction, pulmonary and systemic edema, diabetic nephropathy, diabetes and insulin resistance, liver cirrhosis, scleroderma, and migraines[204]. Detailed reviews on local RAAS can be found for each tissue and pathological condition.

The concept of tissue extRAAS is that **a specific combination of extRAAS components is expressed locally in each tissue, even in each cell type, leading to the production of a specific quantitative and qualitative combination of peptides, which result in a balanced local paracrine/autocrine effect that play a role in tissue physiology.** A change in the local expression of extRAAS components will lead to alteration in the balance obtained and thus may lead to pathophysiological consequences (figure I.6). In this regard, studies on extRAAS need to be shifted from the one peptide-one pathway approach toward a more general approach that take into account the different players and their respective interactions. Indeed, the knowledge obtained from the former approach may lead to an inconclusive view that may rely on the used protocol and model, with lack of information on other pathways that may balance the effect of the pathway in question. Therefore the use of high throughput

techniques such as Genomics, transcriptomics and metabolomics to measure the different components of extRAAS in a specific tissue/cell under a specific physiologic condition is of importance, specifically in the new era of systems biology.

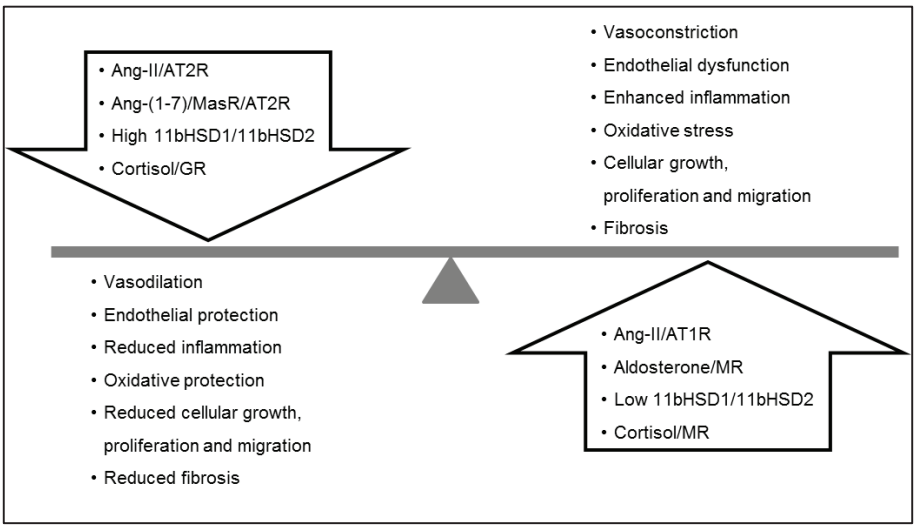

Figure I.5: tissue extRAAS play key roles in tissue homeostasis. ExtRAAS pathways exert antagonizing effects at the tissue level that balance each other to maintain tissue homeostasis. A change extRAAS components expression may shift the balance toward one direction, possibly leading to tissue physiopathology.

I.4 REVIEW MANUSCRIPT I

THE MULTIPLE PATHWAYS OF EXTENDED RENIN-ANGIOTESNIN-ALDOSTERONE SYSTEM IN ATHEROSCLEROSIS: EXPRESSION AND INTERACTIONS

Ali Nehme[1,2], Catherine Cerutti[1], Kazem Zibara[2]*, Giampiero Bricca[1]*.

[1] EA4173, Functional genomics of arterial hypertension, Hôpital Nord-Ouest, Villefranche-sur-Saône; Université Lyon1, Lyon, France.

[2] ER045, Laboratory of stem cells, Department of Biology, Faculty of sciences, Lebanese University, Beirut, Lebanon.

* Co-last and corresponding authors

Address correspondence to:

* Dr Giampiero BRICCA, EA4173, Functional genomics of arterial hypertension, Université Lyon1, Domaine Rockefeller, 8 avenue Rockefeller, France; email: giampiero. bricca@inserm. fr

*Dr Kazem ZIBARA, ER045, Laboratory of stem cells, Department of Biology, Faculty of Sciences, Lebanese University, Beirut – Lebanon; email: kzibara@ul. edu. lb

Short title: **Extended extRAAS tissue organization**

Word count: xxx

Grey scale illustrations: 6 (Figures 1-4 and tables 1&2)

Colored Illustrations: 3 (Figures 5-7)

I.4.1 Introduction

Atherosclerosis remains the main cause of death and morbidity in the world, mainly in developed countries[20,21]. According to the world health organization, ischemic heart disease and stroke, both mainly caused by atherosclerosis, were the major causes of death during the last decade, accounting for more than 50% of total death in the world[22]. Although many studies were done to elucidate the mechanisms by which atherosclerosis develop, many aspects of the disease remain unclear. This is mainly due to the high complexity of the disease, which is affected by a combination of direct local mechanisms that occur in the arterial wall, in addition to the effects and interactions of numerous risk factors such as life style, blood pressure, dyslipidemias, diabetes and metabolic syndrome[205]. However, the recent advances in molecular biology techniques has increased our knowledge in the disease and revealed many molecular bases of the different mechanisms involved in atherosclerosis development and progression[206]. One of the important systems that were found to be involved in and linking most of the atherosclerotic processes and risk factors is the renin-angiotensin-aldosterone system (RAAS).

RAAS is a complex bioactive peptidic system, involving different angiotensinogen metabolizing pathways leading to the generation and degradation of several bioactive peptides that may exert different cellular effects through molecular interactions with selective receptors. The specific combination of peptides and receptors defines the final response of a tissue toward the system. Initially thought as being just an endocrine system involved in blood pressure regulation and body electrolyte balance, RAAS is now considered a "ubiquitous" system present locally in various tissues[207] and exerting multiple paracrine/autocrine effects at the tissue level. Indeed, RAAS was shown to be involved in numerous molecular mechanisms that play key roles in tissue homeostasis and remodeling, including cellular growth, proliferation, differentiation, migration and apoptosis, in addition to extra cellular matrix (ECM) remodeling and inflammation[208]. Importantly, each of these processes may play a major role in atherosclerosis formation and progression.

We have recently proposed an extended RAAS (extRAAS)[209] that includes all the angiotensin peptides generation pathways with their alternative metabolizing enzymes and receptors. In addition this system includes enzymes and receptors involved in the metabolism and response to the two corticosteroids aldosterone and cortisol, which are tightly linked and interact with the angiotensin system at the tissue level. The substrates, metabolizing enzymes and receptors

should be locally present in a tissue for extRAAS to be functionally active independent of the circulating system. Several lines of evidence support the expression of extRAAS components in the arterial wall and their alteration in atherosclerotic lesions, thus participating in the atherosclerotic process. Since the local effects of angiotensin peptides are extensively reviewed, this review will briefly mention these effects and discuss the local differential production of extRAAS during atheroma development and its participation in processes leading to atherosclerotic lesion development.

I.4.2 The substrate angiotensinogen (AGT)

Several AGT polymorphisms were shown to be associated with atherosclerotic events and atherosclerotic risk factors[210–216].

Both AGT mRNA and protein were detected in several normal arterial beds[217–222] and their levels were found to be upregulated by balloon surgery-induced vascular injury[219], increased sodium diet[218] and bilateral nephrectomy[217]. The expression of extRAAS genes involved in the different pathways and their cellular distribution in atheroma is presented in Table I.2. In normal arterial mouse tissue, AGT is mainly expressed by medial VSMCs of the media and fibroblast cells of the adventitia[218,219,221]. Similar results were obtained by our team in carotid atherosclerotic lesions obtained by endarterectomy operation[223]. Since carotid samples contain no media and adventitia, AGT transcript was observed principally in the tunica media and in scattered cells of the subendothelial layer, whereas AGT immunoreactivity was mainly observed in the intimal layer, as well as in occasional vascular smooth muscle cells (VSMCs), suggesting that it is expressed by VSMCs and may be diffusing into the intimal layer from the blood stream. In order to investigate the functional aspects and due to the difficulty in obtaining normal human arterial tissue, we compared the results obtained from atheroma lesions to nearby macroscopically intact arterial tissue (MIT)[224]. Despite the fact that AGT expression in VSMCs could be influenced by risk factors of atherosclerosis such as type 2 diabetes (T2D), insulin resistance, and high cortisol[224–226], we couldn't observe significant difference in AGT expression between atheroma lesions and MIT[223].

Table I.2: extRAAS components expression in atheroma. "X" indicate of presence of gene's transcript/protein. "*" indicate that expression was validated in the same cell but in other organ.

Pathway	level in atheroma	Participating genes (gene symbol)	Expression				
			level in atheroma	EC	VSMC	Macrophage	Other cells
Aldosterone	Increase	CYP11B2		X	X		Mast cell*
		GPER		X	X	*	
		NR3C2	increase	X	X	X	
Ang-(1-7)	Decrease	ACE2	Increase	X	X	X	
		CPA3					Mast cell
		CTSA	Increase				Mast cell
		MAS1		X			
		MME					
		NLN					
		PREP					
		THOP1					
Ang-I	Increase	ATP6AP2			X		
		CTSD					
		IGF2R			x		
		REN		X			
Ang-II	Increase	ACE	Increase	X		X	X
		CMA1					Mast cell
		CTSG				X	Mast cell
		EGFR					
		KLK1					
Ang-III	Unknown	ENPEP					
Ang-IV	Unknown	ANPEP					
		DPP3					
		LNPEP		X			
		RNPEP					
Corticosteroids	Increase	CYP11A1					
		CYP17A1					
		CYP21A2					
Cortisol	Increase	AKR1C4					
		AKR1D1					
		CYP11B1					
		HSD11B1	increase	X			
		HSD11B2		X	X		
		NR3C1	decrease	X		X	
Shared	NA	AGT	Increase		X		
		AGTR1	Increase		X	X	X
		AGTR2	Increase/ Decrease		X		

I.4.3 Angiotensin (Ang)-I generating enzymes

As we discussed in the previous section, AGT is expressed in the vascular wall, mainly in VSMCs, and its expression is increased in atherosclerosis and under the influence of atherosclerotic risk factors. Although AGT is biologically inactive, it can exert atherosclerotic effects by fueling the production of bioactive angiotensin peptides that are known to play a major role in atheroma development and progression. Indeed, the blockage of AGT metabolism using renin inhibitor was shown to decrease atheroma development in Ldlr-deficient mice[227]. Renin is considered the major Ang-I producing enzyme due to its high ligand affinity and specificity. Although a huge debate occurred on the local expression of renin in the vascular wall, several studies have detected renin mRNA, protein and activity in VSMCs[228,229] and endothelial cells (ECs)[230] of the arterial wall in several species. In addition, vascular renin/prorenin receptor (R/PR) protein was found to be associated to renin activity in VSMCs of rat aorta and mesenteric artery, but also in the sub-endothelial VSMCs of coronary and kidney arteries[201,231,232], suggesting for another source of renin by recruitment from the circulation. Moreover, binding of prorenin to the R/PR was shown to directly enhance VSMCs proliferation via ROS generation and ERK1/2 activation[233]. Thus, this receptor may exert direct effects on atherosclerotic cells independent of Ang-II generation. However, the investigation of the direct effects of R/PR in atherosclerosis is still fresh and further studies to elucidate these effects and their mechanisms of action should be done. In addition to renin, alternative Ang-I-generating enzymes were also described in the vascular wall. Indeed, cathepsin D (CTSD), tonins and aspartyl proteases have been identifies in the vessel wall[234]. Although we were unable to detect renin mRNA in the vessel wall[223], Kaschina et al. interestingly showed that renin, R/PR and CTSD proteins were upregulated in human atherosclerotic compared to normal aortic tissue[235]. This suggest that in human atherosclerosis, renin may be recruited from the circulation rather than being expressed in situ, and that Ang-I generation takes place by the recruited renin and locally expressed CTSD in the lesion. Moreover, CTSD protein was found to be increased in abdominal aortic aneurysm (AAA) compared to atherosclerotic tissue[235], suggesting for an alternative role of this enzyme in the generation of AAA.

Alternatively, the newly discovered Ang-(1-12) was also detected in the medial layer of coronary arteries and vascular endothelium[236]. ACE was identified as the primary enzyme accounting for Ang-(1-12) metabolism in the circulation of both normal and hypertensive rats[237–239] and in isolated rat arteries[240], including the aorta and right and left common carotid

arteries. ACE is found on endothelial cells of both normal and atherosclerotic arteries, but also prominently expressed by monocytes and T-lymphocytes in advanced atherosclerotic lesions[241]. Interestingly, Ang-(1-12) significantly constricted the descending thoracic aorta, right and left common carotid arteries, abdominal aorta and superior mesenteric artery, with little effect on the femoral and renal arteries[240]. These effects of Ang-(1-12) were attenuated when either ACE or chymase were inhibited, with chymostatin displaying lesser potency, indicating that these effects most likely result fromAng-II production. Further information about ACE and its role in Ang-II generation will be discussed in the next section.

I.4.4 Ang-II pathway

Ang-II was initially thought to only exert indirect effects on atherosclerosis through hemodynamic actions; however, compelling evidence support that Ang-II can also act locally in atherosclerotic lesions where it exerts various effects leading to atheroma initiation and progression[242–244]. Several studies indicate that Ang-II blockage via ACE inhibitor (ACEi) or angiotensin type 1 receptor (AT1R) blockers (ARBs) inhibit the formation and progression and acute complications of atherosclerotic lesions independent of hypertension and other risk factors of atherosclerosis[244–246]. Ang-II was shown to play key roles in atherosclerotic lesion initiation by inducing endothelial dysfunction[247–249] and macrophages recruitment[250–255] to the vascular wall. In addition, Ang-II enhances VSMCs dysfunction[77,81,124] by inducing constriction[256], switching toward proinflammatory phenotype[257], growth[258], migration[259], proliferation[259–261] and survival[262,263]. Ang-II can also enhance foam cells formation by inducing low density lipoprotein (LDL) oxidation[264–266] and LDL-receptors expression on ECs, VSMCs and macrophages[267–271]. Moreover, Ang-II was shown to be a key inducer of local inflammation in atherosclerosis[243,272] by inducing local oxidative stress[273–276] and the production of various inflammatory cytokines[234,257,277,278]and chemokines[279], mainly through AT1R-mediated Nuclear factor kappa b (NFKB) activation[243,253,255,257,272,277,280], in addition to downregulating anti-inflammatory pathways[281]. In addition, Ang-II induces vascular ECM remodeling[282–288], apoptosis[249,289], calcification[290] and thrombosis[278,291–293], which are key markers of advanced lesion rupture.

Total Ang-II formation was shown to be significantly higher in atherosclerotic and aneurysmal lesions compared to normal aortas[294,295]. ACE is thought to be the major Ang-II producer in the intima of both normal and atherosclerotic vessels[278,296]. In healthy vessels, ACE was found to be restricted to both luminal and *vasa vasorum* ECs[297]. Whereas in

atherosclerotic lesions, ACE is predominantly expressed by macrophages, in addition to macrophage-derived foam cells (MFCs) and lymphocytes[241,296,297]. This was further supported by the expression of ACE by monocytes *in vitro*, which was upregulated during differentiation into macrophages and after LDL treatment[241,298]. Therefore, it seems that macrophages are the major source of ACE in atherosclerotic lesions, in addition to ECs, which may explain the increase in ACE levels during atheroma development[223]. However, vascular Ang-II production was shown not to be completely suppressed by ACEi, which suggested for the presence alternative Ang-II producing enzymes[295]. Indeed, ACE-independent pathways were found to be functional and important in the physiology of normal human arteries[299], with indication for the participation of non-ACE pathways for more than 40% of Ang-II generation in the vessel wall[300]. Although Chymase is restricted to mast cells in the tunica adventitia, Ihara et al. demonstrated that most of Ang-II forming activity *in vitro* was chymase-dependent in both normal and atherosclerotic human aortas[294]. Similar results were obtained in patients undergoing coronary artery bypass operation and in Syrian hamsters fed a high cholesterol diet where a significant positive correlation between serum cholesterol levels and arterial chymase-dependent Ang-II-forming activity was found[301]. However, they didn't observe any change in chymase levels between the two tissues[294], suggesting that the increase in Ang-II generation observed in atheroma could be due to increased ACE expression as a result of macrophage infiltration and high serum cholesterol, which may trigger upregulation of vascular chymase activity and facilitate the development of atherosclerosis. Moreover, our team had shown that the mRNA levels of cathepsin G (CTSG), another enzyme involved in Ang-II generation, increased in atherosclerotic lesion[223], possibly originating from infiltrating monocytes[302], thus participating in the increased in Ang-II formation in atheroma lesions.

To exert its effects, Ang-II acts through its two main receptors, angiotensin type 1 and type 2 receptors (AT1Rand AT2R, respectively), which are known to exert opposite effects in the vessel wall, mainly on VSMCs physiology. While the AT1R is associated with pro-atherogenic effects, the AT2R generally exerts athero-protective actions[303–305], such as endothelial protection[306–308], anti-inflamatory mechansims[309], apoptosis and vasodilatation. In support of these effects of both receptors, our team[223] previously showed that the AT1R expression decreases 2.5-folds in atherosclerotic compared to healthy vascular tissue. However, the AT2R remains very low[310,311], even decreases[312], during atherosclerotic lesion progression, although still exerting important effects in counterbalancing AT1R effects in

atheroma[304]. Thus, it seems that Ang-II exerts most of its effects through AT1R in the adult vasculature and in atherosclerosis[313], which is mainly expressed on VSMCs, where it can be upregulated in diabetic patients[224,225,314] and by LDL stimulation[315,316]. Therefore, the increased AT1R expression in atherosclerotic lesions can be explained by the LDL-induced production by proliferating VSMCs, in addition to infiltrating macrophages[317] and platelets[318] that were also shown to express the AT1R.

I.4.5 The Ang-(1-7) pathway

Although Ang-(1-7) pathway is considered the second main "arm" of RAAS, few studies were done to elucidate the expression of its components in the vessel wall. Indeed, the studies on the Ang-(1-7) in atherosclerosis started during the last decade, mainly focusing on the effects of this peptide in atherosclerosis rather than on its synthesis and presence in atherosclerotic lesions. Ang-(1-7) is a potential player in maintaining atherosclerotic lesion stability mainly by antagonizing the Ang-II/AT1R-mediated proatherogenic effects[319]. Ang-(1-7) plays a major role in preventing atherosclerotic lesions initiation by ameliorating endothelial function mediated through oxidative protection[51,319–322]. In addition, Ang-(1-7) is associated with atherosclerotic lesion stability[323–326], which can be mediated by inducing atheroprotective effects and inhibiting various pro-atherogenic effects, either directly or through Ang-II-dependent mechanisms[326–329]. Indeed, Ang-(1-7) treatment were associated with reduced vascular macrophages adhesion and recruitment[330,331], VSMCs dysfunction[332–335], Foam cells formation[336,337], inflammation[338] and ECM remodeling[332,339]. All these effects were inhibited after ACE2[324,326] or MasR[329,340] defeciency/inhibition. Therefore, it seems that Ang-(1-7) is mainly produced by ACE2 in the vessel wall and mediates most of its effects through MasR or by interfering with Ang-II/AT1R-mediated effects.

It seems that ACE2 is the major Ang-(1-7) producing enzyme in atherosclerosis[314,341] as shown by various studies that investigated the effects of ACE2 and Ang-(1-7) deficiency on atherosclerotic lesion development in various animal models. Both ACE2-deficiency and Ang-(1-7) inhibition in atherosclerosis produced similar effects in multiple studies, where they both enhanced atherosclerotic plaques progression by enhancing contents of lipids, macrophages, VSMCs and collagens in late lesions, in addition to upregulation of cytokines and MMPs expression and activity[324–326]. ACE2 protein was found to be present in human veins, non-diseased mammary arteries and atherosclerotic carotid arteries and expressed in endothelial cells, smooth muscle cells and macrophages[314,342,343]. ACE2 showed a differential

regulation of its expression during atherosclerotic lesion development with higher activity in the stable advanced atherosclerotic lesions compared to early and ruptured atherosclerotic lesions. Ang-(1-7) can also be produced by various non-ACE2 enzymes[319,344] including neurolysin, neprilysin, thimet oligopeptidase, prolyl-carboxypeptidase,prolyl-endoxypeptidase and carboxy peptidase A3[344–348]. However, the levels and activity of these enzymes in atheroma are not clear. In addition, rat mesenteric arteries were shown to possess CPA-like enzymes that are able to convert Ang-I and Ang-II into Ang-(1-9) and Ang-(1-7) independent of ACE2 and CTSA, respectively[349]. However, the identity of these CPA-like enzymes and their respective levels in normal and atherosclerotic arteries need further investigations. This CPA activity was supported by other studies that showed CPA expression in mast cells of atherosclerotic lesions[350]. Cathepsin A (CTSA) that is known for its Ang-(1-9) generating activity, thus providing a substrate for Ang-(1-7) generation, was shown to be expressed in mast cells and upregulated in atherosclerotic lesions. Ang-(1-9) was shown to exert some effects independent of Ang-(1-7) generation by potentiating bradykinin action on its receptor, thus contributing vascular protection.

Ang(1-7) generally performs its athero-protective roles in atheroma by binding mainly to its Mas receptor (MasR), and to a lower extent to the AT2R[304,341]. In the vessel wall, Ang-(1-7) was shown to bind both the Mas receptor (MasR) and AT2R on ECs under normal conditions[331,351,352]. Both receptors activation stimulates nitric oxide production and vasodilation[351,352], therefore maintaining endothelial function. Despite the fact that AT2R was shown to be lowly expressed in atherosclerotic lesions[310,311], to our knowledge, no data is available about the expression of MasR in this tissue. However, studies investigating the effects of MasR stimulation[329,340,353] indicate that MasR may be present and active in atherosclerosis, but its levels and response to local Ang-(1-7) need to be validated. A recent study on upstream and downstream regions of internal carotid plaques, showed MasR upregulation in the downstream portions of human stable carotid plaques as compared to unstable lesions[354]. Thus it seems that MasR possess a differential expression in atherosclerotic lesions and that its expression and activity may play a role in stabilizing the plaque from rupture. Although it was shown that AT2R expression was increased in aortic segments from the cardiovascular patients[355], its levels remain very low in both normal and healthy vessels[310]. AT2Rs have been detected in vessels such as mesenteric[356,357] and uterine[358,359] arteries.

Therefore, although both ACE2 and Ang-(1-7) levels may increase in atheroma, its atheroprotective effects remain overridden by the high Ang-II/AT1R proatherogenic activity[314]. Thus, the levels of Ang-(1-7) pathway components and its interaction with the Ang-II pathway should be further studies.

I.4.6 Ang-III/IV pathway

Although there is no clear evidence on the Ang-III and Ang-IV generation in normal and atherosclerotic vessels, studies have shown that both peptides treatment may exert local effects in the vessel wall. Ang-III mediates similar effects to Ang-II, such as vasopressor effects[319], activation of the transcription factors NF-KB and AP-1 with an increase in the expression of related pro-inflammatory genes, such as MCP-1, IL-6, TNF, ICAM-1, and PAI-1[360,361]. However, these effects were mainly mediated through Ang-III-mediated activation of AT2R[242], which indicate that AT2R can perform opposite effects in a ligand-dependent manner. Ang-IV peptide was also shown to induce MAPK, ERK1/2, NFKB and AP-1 activity via AT4R or AT1R activation in VSMCs or ECs[187,243,362,363]. On the contrary, Ang-IV may also confer vasoprotective effects in both normal and atherosclerotic vessels by improving endothelial function through both the AT2R and the AT4R[364–366]. The latter was shown to be present on ECs, but not on VSMCs, in pulmonary arteries, where it can induce dose-dependent vasodilation upon Ang-IV stimulation[364]. On the other hand, studies on rabbit carotid arteries showed that normal arteries express AT4R in VSMCs and in the vasa vasorum of the adventitia that was upregulated following balloon injury, with very low receptor levels in ECs[367]. Thus, it seems that that Ang-IV may exert both protective and atherosclerotic effects in the vessel wall depending on the stimulated receptor and the activated intracellular pathways. In addition, this may suggest that some of the effects induced by Ang-II may be mediated through downstream angiotensin peptides.

I.4.7 Corticosteroids

Like Ang-II, the vascular effects of Aldosterone were originally accredited to renal MR-mediated blood pressure elevation with secondary vascular consequences[368]. However, studies over the past years showed that aldosterone may also exert local effects on atherosclerotic cells independent of blood pressure. For example, several studies have shown that plasma aldosterone level is associated with atherosclerosis progression and subsequent cardiovascular events independent of blood pressure[369–373]. In addition, in the RALES[374] and EPHESUS[375] trials the doses of the MR antagonists used were below threshold for causing

significant renal effects. These findings support the direct local effects of aldosterone on the vasculature independent of hypertension. Aldosterone infusion, in the absence of vascular injury, had no significant effect on vascular remodeling, suggesting that aldosterone acts synergistically with mechanical endothelial damage to promote vascular remodeling[376]. Ex vivo treatment of mouse aortas with aldosterone identified 72 proatherogenic genes with enhanced Aldo-stimulated expression by MR and oxidative stress-dependent mechanism[368]. These genes are involved in regulating oxidative stress, vascular cell proliferation and angiogenesis, and extracellular matrix formation and degradation. Indeed, aldosterone in atherosclerosis contributes locally[377,378] to endothelial dysfunction[379,380], VSMCs dysfunction[175,379,381,381–385], vascular inflammation[380,386–388], oxidative stress[379,389,390], calcification[175,391,392] and ECM remodeling[393,394]; whereas MR antagonists inhibit these effects[378,395,396].

Compelling evidence support the local production of aldosterone in the vascular wall[175,376]. Both aldosterone synthase (CYP11B2) and aldosterone receptor (MR) mRNA and proteins were detected in ECs and VSMCs obtained from human pulmonary artery; however the levels of MR were less in ECs than VSMCs[383,397,398]. In addition, MR is expressed in macrophages, dendritic cells, and T and B lymphocytes[399]. However, the 11β-HSD2 should also be present and active for aldosterone to exert its effects freely on the MR that can also be bound by cortisol. Indeed, intact rat aortic rings were shown to express both functional 11β-HSD1 and 11β-HSD2. The latter, was present in both ECs and VSMCs, whereas the former was expressed in ECs only[175,398,400–402]. This was in line with the results showing that VSMCs respond directly to exogenous aldosterone and may produce aldosterone locally in an Ang-II-dependent and independent mechanisms[175,203,382,403]. This indicates that aldosterone is locally produced in in atherosclerotic lesions, and that the synthesis and response to aldosterone in atheroma may increase as a result of increased VSMCs proliferation and Ang-II production. In addition, aldosterone has been demonstrated to mediate part of its rapid non-genomic vascular effects via MR-independent pathways, which are yet to be determined[404]. Recent studies have shown that some of these MR-independent effects can be mediated via G-protein-coupled estrogen receptor (GPER)[180]. Aldosterone-mediated GPER activation was shown to induce contraction and apoptosis in VSMCs via phosphatidylinositol 3-kinase (PI3K)-mediated extracellular signal-regulated kinase (ERK) activation[180]. Aldosterone was also able to activate ERK signaling in vascular EC model with persistent expression of GPER but no detectable MR expression, indicating that this effect of aldosterone in ECs could be

completely dependent on MR-independent mechanisms, most possibly through GPER activation[180]. However, aldosterone-mediated ERK activation was inhibited by both the MR-selective antagonist, eplerenone, and the GPER-selective antagonist, G15, indicating that eplerenone could also inhibit aldosterone-mediated GPER activation through unknown mechanism. On the contrary, GPER agonist- or estradiol-mediated GPER effects induced differentiation and inhibit VSMCs proliferation by inhibiting ERK1/2 and Akt phosphorylation[405], suggesting that this receptor may act in a ligand-depndent manner and that the conclusive atheroprotective effects[406] of GPER should be carefully interpreted.

Although the presences of 11β-HSD1 in the vessel wall support the local production of cortisol, there is no study that shows it ratio to 11β-HSD2, and thus cortisol production/degradation ratio. Nevertheless, the general view that 11β-HSD1-deficiency/inhibition (lower cortisol level) is atheroprotective, whereas 11β-HSD2-deficiency/inhibition (higher cortisol level) accelerates atherosclerosis independent of systemic risk factors, reflects modulation of cortisol actions and inflammation within the vasculature[407]. Indeed, treatment of ApoE/11β-HSD2 double knockout mice (these mice should have high cortisol content) with eplerenone, an MR antagonist, reduced plaque development and macrophage infiltration while increasing collagen and VSMCs content with increased VCAM-1 expression on VSMCs compared to Apoe(-/-) mice, without any effect on systolic blood pressure. Similarly, aldosterone increased VCAM-1 expression in mouse aortic ECs, an effect mimicked by corticosterone only in the presence of an 11β-HSD2 inhibitor, indicating that cortisol mediate atherogenic effects at high levels through MR activation. Similarly, it was shown that 11β-HSD1 gene expression increases in the ascending aorta tissue of metabolic syndrome patients with coronary artery disease[408]. In addition, we recently showed using carotid atheroma samples that 11β-HSD1 is up to 10 folds higher in advanced atherosclerotic plaques compared to nearby macroscopically intact tissue, which the latter is considered a very early stage of atheroma[198]. Similar results were also obtained in vitro in lipid storing VSMCs, which is a prominent feature of VSMCs in advanced lesions, compared to contractile VSMCs[226]. Thus it seems that 11β-HSD1 increases during atherosclerotic lesion development and may play a role during atherosclerotic lesion progression. 11β-HSD1 was shown to be expressed and upregulated upon inflammatory stimuli *in vitro* both in macrophages[409] and VSMCs[410], in addition to promoting macrophages phagocytic capacity[411]. 11β-HSD1 deficiency/inhibition in ApoE-/- mice attenuated atherosclerosis with reduced lesion size, lipids accumulation, foam cells formation and local

inflammation, independent of plasma lipids or glucose[407,412,413].. However, cortisol may also exert atheroprotective effects through cortisol glucocorticoid receptor (GR) activation, which was shown to be expressed in atheroma[398]. In fact, glucocorticoids are assumed to act as antagonists of MR in kidney and heart, whereas in the vessel wall they act as agonists at high levels[414]. Recent studies demonstrated that GR exerts opposing effects to MR and that the balance between the two receptors may affect vascular remodeling. Indeed, In C57Bl/6J mice, neointimal proliferation was reduced by systemic or local glucocorticoid administration and by MR antagonist, whereas increased by the GR antagonist[415]. These effects were shown to be independent of 11β-HSD1 deficiency or antagonism[402,415,416], suggesting for a role of other glucocorticoids (GCs) than cortisol in GR-mediated atheroprotective effects[417]. Loss of GR from atherosclerotic cells induced a GC-mediated decrease in cellular proliferation and increase in apoptosis and collagen synthesis, which may be explained by the effects of GC elicited through MR[418]. On the contrary, mice lacking the endothelial GR developed more severe atherosclerotic lesions in the aorta, brachiocephalic artery, and aortic sinus, as well as enhanced local inflammation as evidenced by increased macrophage recruitment in the lesions[419]. Similarly, mice having a macrophage-specific GR knockout showed less calcification within the vasculature. In vitro studies using conditioned media from macrophages which had been stimulated with dexamethasone demonstrated a dose-dependent increase in calcium deposition by VSMCs[420], suggesting that GR may inhibit VSMCs calcification indirectly through macrophages. Moreover, GCs including cortisol have been shown to inhibit MCP-1 synthesis in a variety of cell types including arterial VSMC[421]. In the latter, GCs can also inhibit cell growth, migration, proliferation and lipid uptake in culture and in animal models of arterial injury[422–425]. In addition, GR activation inhibits oxLDL-induced macrophage growth by suppressing the expression of granulocyte/macrophage colony-stimulating factor[424]. These findings indicate that cortisol level is tightly regulated in the vessel wall to exert atheroprotective effects, and that when cortisol reaches high levels it may bind MR and exert similar pro-atherogenic effects like aldosterone-MR activation[426]. Therefore, aldosterone should be always studied in relation to cortisol, MR and GR levels to give non-false positive results about its possible effects in atheroma.

I.4.8 Pathways interactions

Recent studies have shown that ACE2-Ang-(1-7) axis may be regulated by Ang-II-AT1R pathway. Indeed, several studies have shown that Ang-II induces a dose-dependent decrease in ACE2 mRNA and protein expression[427–429], along with increased atherogenic reactions,

which can be restored by ARBs and Ang-(1-7) treatment[430,431]. AT1R blockade and Ang-(1-7) treatment attenuated the decrease in ACE2 mRNA and increased AT2R mRNA but did not affect AT1R mRNA. This was accompanied with attenuated neointimal area, VSMC proliferation, increases in the mRNA levels of MCP-1, TNF-α, and IL-1β, and ROS production in the injured artery. These effects of Ang-II/AT1R-axis on ACE2/Ang-(1-7)-axis were shown to be mediated by several mechanisms including the activation of signaling through ERK1/2, JNK and MAPK[432,433]. In addition, a very recent study had shown that ACE2 can also be inhibited by ROS derived from AT1-mediated proinflammatory signaling, which can be restored upon AT1R inhibition[434]. Therefore, Ang-II may exert a double effect in atherosclerosis by maintaining an atherogenic microenvironment in atherosclerotic lesions and at the same time it inhibits the Ang-(1-7)/MasR athero-protective effects. Thus, as the levels of Ang-II and its atherogenic effects in atherosclerotic lesions increase, the protecting arm of extRAAS that is known to counterbalance Ang-II atherogenic effects decreases, or may even be missing due to the loss of response through the Mas or AT1 receptors[434]. In contrast, the MasR was also shown to diminish Ang-II-induced inositol phosphates and mobilization of intracellular Ca^2 by the forming a hetero-oligomeric complex with the AT1R. In vivo in mice, this inhibition was shown to regulate the Ang-II-mediated vasoconstriction in mesenteric microvessels[435]. Moreover, in human ECs, Ang-(1-7) negatively modulates Ang-II/AT1R–activated c-Src and its downstream targets ERK1/2 and NAD(P)H oxidase[320].

There is a tight cross talk and mutual activation between MR and AT1R in VSMCs, leading to the regulation of atherogenic processes including increased vascular tone, inflammation, fibrosis and thrombosis[436]. Aldosterone and Ang-II synergistically stimulate migration in VSMCs via MR and AT1R signaling, respectively, through MEK and EGFR signalling[188,190]. In addition, aldosterone may act indirectly on the vessel wall by inducing Ang-II generation[389,437]. In vitro treatment of macrophages with aldosterone enhanced ACE expression and activity and increased their ROS production and LDL oxidation ability [389]. Only co-treatment of eplerenone with ramipril or losartan completelyblocked the oxidative effects of aldosterone, which indicate that the MR-induced pro-oxidative effects may be mediated via Ang-II production. Similarly, Ang-II mediates some of its effects through aldosterone synthesis and MR activation[438]. In rat aortic VSMCs, Ang-II induced aldosterone synthesis and VSMCs proliferation via the AT1R. Ang-II-induced proliferation was inhibited by spironolactone, suggesting that locally generated aldosterone may mediate the effects of Ang-II/AT1R in stimulating rat aortic VSMC proliferation[382,383]. It was recently shown that

Ang-II and aldosterone synergistic effects depend partly on their newly assigned receptors EGFR and GPER[439]. However, the significance of the aldosterone-mediated effects of Ang-II *in vivo* is still controversial and need further validation. Indeed, Cassis et al. showed that aldosterone infusion or MR blockade in apoE-/- mice did not influence the Ang-II-induced vascular pathologies of atherosclerosis or abdominal aortic aneurysms formation, which indicate that aldosterone does not contribute significantly to Ang-II-induced atherosclerosis or abdominal aortic aneurysms (AAA) formation in hyperlipidemic mice[440]. This could be attributed to the high aldosterone concentration used in the study, since aldosterone-mediated Ang-II potentiation was shown to occur at nanomolar aldosterone concentration, but disappear at micromolar concentration[439]. At the same time, Ang-II was shown to mediate some of its effects by activating the MR independent of aldosterone-mediated MR activation. Michel et al. showed that AT1R blockade completely abrogated aldosterone pro-angiogenic effects in mice treated with aldosterone[441]. This was then validated in human VSMCs where Ang-II was shown to activate MR gene transcription through AT1R activation, independent of aldosterone-MR binding[175].

The different extRAAS pathways, their local effects and their interaction in atherosclerosis is summarized in Figure I.7. As can be seen in the figure, the same peptide/metabolite may exert both proatherogenic and atheroprotective effects depending on the receptor to which it binds and activate. On the contrary, the same receptor may also bind different peptides/metabolite, however, exerting similar effects. Therefore, the study of extRAAS effects in atherosclerosis should be shifted from the peptide/metabolite-specific effects to receptor-specific effects. In general, it seems that the atheroprotective effects mediated through AT2R, AT4R, MasR and GR are overridden by the proatherogenic effects mediated via the highly expressed and activated AT1R and MR. The latter are maintained by a positive loop that exerted between Ang-II/AT1R and aldosterone/MR mutual induction and activation.

I.4.9 Summary and perspective

In summary, all bioactive angiotensin peptides could be produced in the arterial wall, and their production is altered in atherosclerosis as a result of cell-specific differential expression. Angiotensin peptides may also exert different, even opposite, cell-specific responses in normal and atherosclerotic vascular wall. Therefore, the pattern of expression of extRAAS components and their cellular distribution in both normal and atherosclerotic walls should be

investigated. This will provide a global view on the possible mechanisms by which the system is altered and exert local effects in atherosclerosis, which will provide a more stringent basis for finding the most specific and efficient extRAAS-targeting therapeutics in the treatment of atherosclerosis.

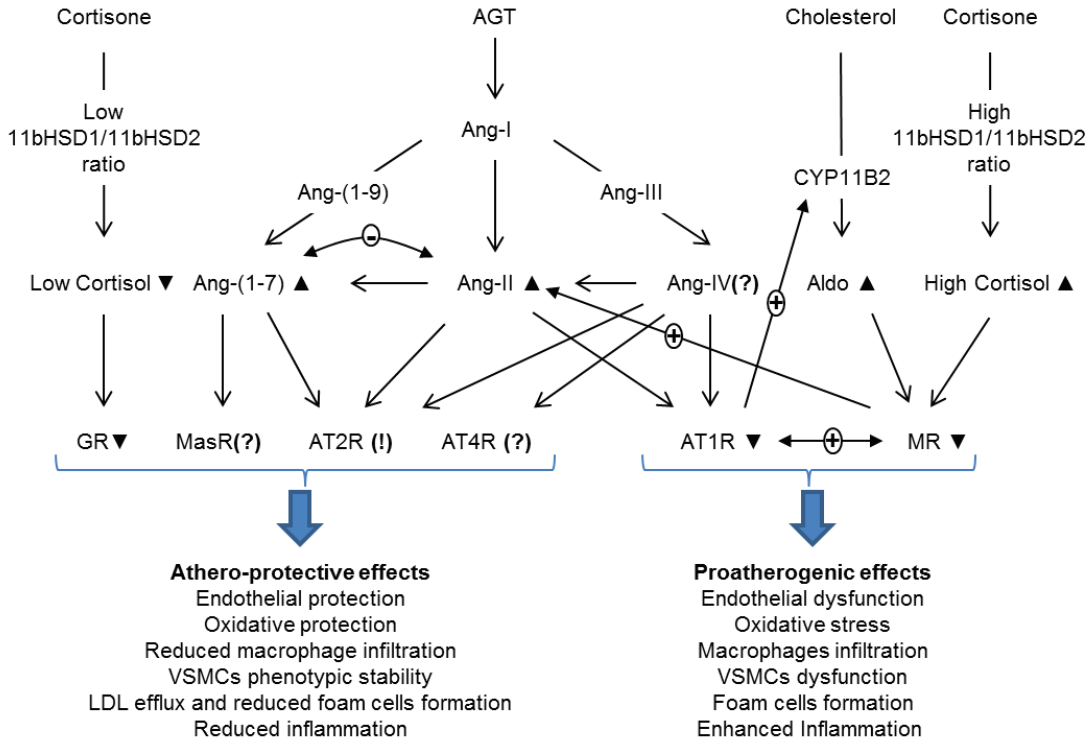

Figure I.6: interaction between angiotensin peptides in atherosclerosis. The final extRAAS outcome effects of extRAAS would be the result of the balance between its athero-protective and proatherogenic effects. The levels in atherosclerotic compared to normal vessel wall are indicated as follow: ▼, decrease;▲, increase, (!), contreversial; (?), unknown. Arrows aith positive (+) or negative (-) signs indicate positive and negative correlations, respectively. 11bHSD1, 11b-Hydroxysteroid dehydrogenase type 1; 11bHSD2, 11b-Hydroxysteroid dehydrogenase type 2; Aldo, aldosterone; Ang, angiotensin; AGT, angiotensinogen; AT1R, Angiotensin-II type 1 receptor; AT2R, Angiotensin-II type 2 receptor; CYP11B2, aldosterone synthase; GR, glucocorticoid receptor; MR, mineralocorticoid receptor; ; VSMC, vascular smooth muscle cell.

II. HYPOTHESIS AND OBJECTIVES

II.1 PRELIMINARY RESULTS

Our team has been investigating extRAAS expression and effects in atherosclerotic lesions from carotid atheroma. The earlier work of the team showed the existence of such a system in the arterial wall and described its alteration in atherosclerosis in relation to T2D in human and mice[223–226]. Indeed, we have identified Ang-I converting enzymes, including cathepsin D, cathepsin G and kallikriens that localize the production of active angiotensin peptides in the atherosclerotic lesion. Due to the difficulty in obtaining normal human vascular tissue, and in order to identify their association with atherosclerotic lesion progression, we have been comparing gene expression between atherosclerotic lesion and nearby "macroscopically intact" tissue (MIT) that can be obtained from the same carotid sample (figure II.1).

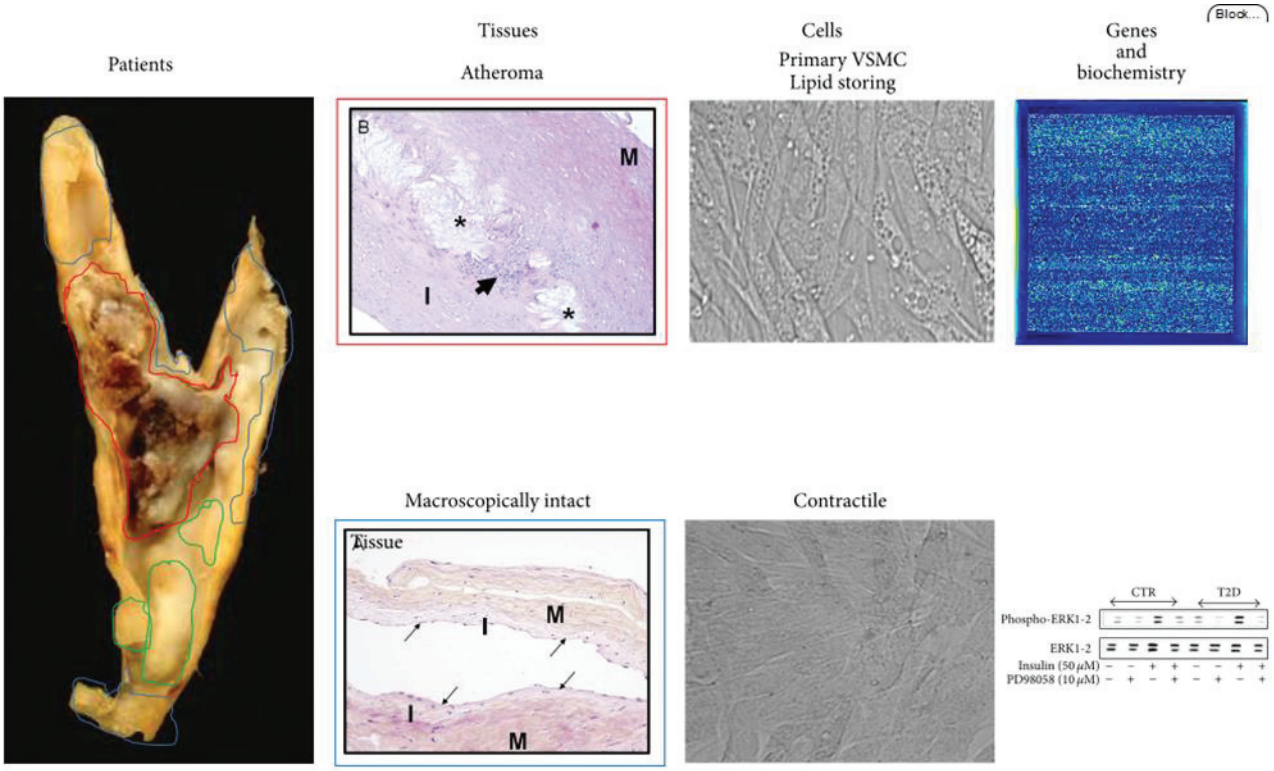

Figure II.1: human carotid atheroma as a study model of atheroma development. On the macroscopic view are drawn the dissections performed in a much remodeled carotid artery. Most often the three types of tissues, red: atheroma plaque, green: fatty streaks, and blue: macroscopically intact tissue, are more easy to delineate. Standard histological control confirms the grade of atherosclerotic remodeling higher than grade IV according to the classification of Stary for atheroma and lower than II for macroscopically intact tissue and tissues may be used for mRNA in situ hybridization and immunohistochemistry. From microscopically intact tissue, primary culture of vascular smooth muscle cells may be established and the responses are studied according to different phenotype in which cells can be conducted, "contractile" and "lipid storing." Interindividual variability and reproducibility of biochemical parameters may be assessed both in situ from the different segments dissected and from primary cells (source: Bricca et al. 2015).

Our team has recently obtained the transcriptome data (Affymetrix gene chip gene 1.0 ST array, 28869 transcripts) of the atherosclerotic lesion (stage IV and superior) and

corresponding MIT (stages I and II) obtained from 32 patient carotid samples. Using these data they examined extRAAS gene correlations through hierarchical clustering of gene transcripts. Interestingly, the correlations were highly similar in atherosclerotic lesion and MIT with minor differences. Indeed, a group of 10 strongly clustered transcripts was found in both tissues. With the exception of IGF2R, this group constitutes genes coding for angiotensin metabolizing peptidases whose expression increases in the atheromatous plaque compared to MIT (Figure II.2).

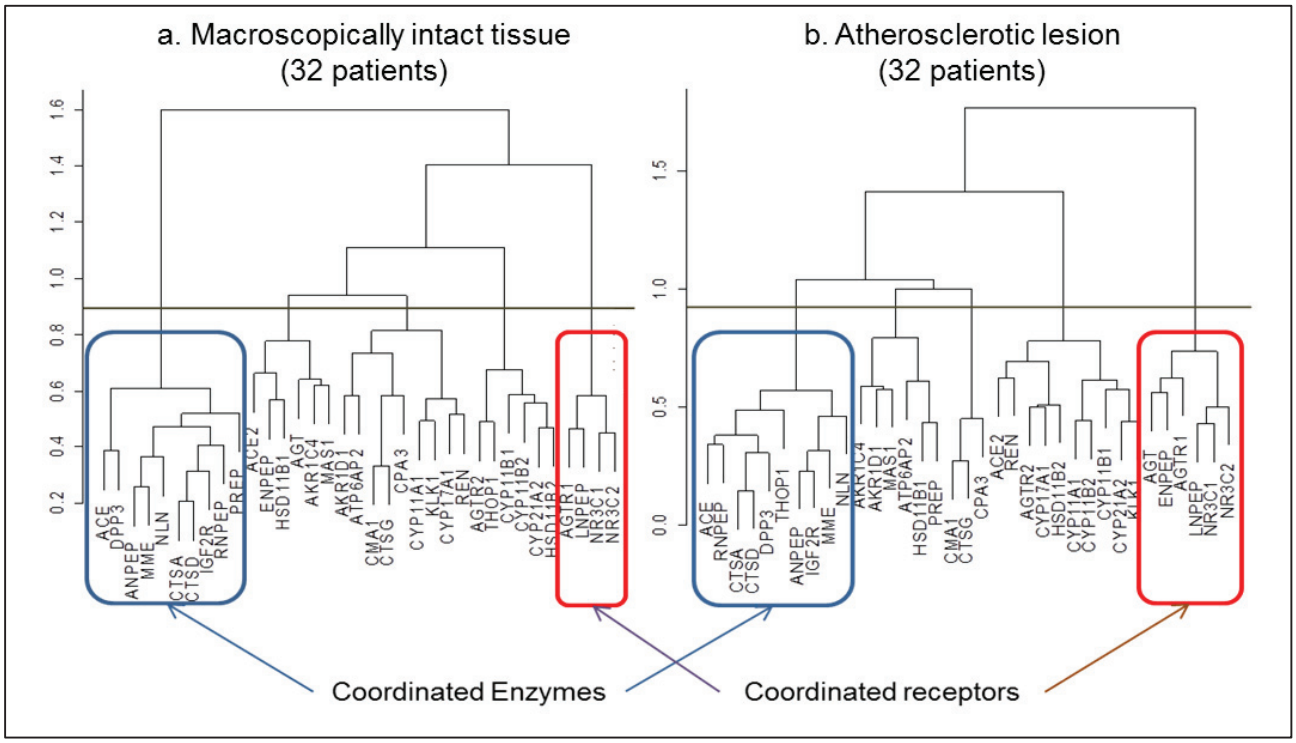

Figure II.2: dendrograms of 35 extRAAS transcripts in MIT (A) and ATH (B) of 32 patients. Hierarchical clustering used the "Cluster" package of R. The agglomerative coefficients were 0.71 in MIT and 0.75 in ATH. The dendrograms were cut in order to separate 5 clusters.

A second group associates genes coding for MR, GR, AT1R and AT4R also shows similar strong correlation between their genes, and interestingly strong negative correlation with the genes of peptidases (figure II.2). The comparison of these results to previously published microarray dataset available on the gene expression Omnibus (GEO) database (accession number: GSE10000) obtained from normal aortas of Apolipoprotein E-deficient mice (Apo-E -/-) and control mice permitted the confirmation of the results in relation with the development of atherosclerosis. Interestingly, the correlations between extRAAS transcripts obtained from our carotid atheroma samples and from ApoE-/- aortas were different from those obtained from control mouse aorta. This indicates that the organization of extRAAS in atherosclerosis in the vessel wall is mainly regulated at the transcriptional level. Interestingly

our team had also shown that the expression of extRAAS genes was altered through the atherosclerotic process where there is a general increase in the expression of the coordinated angiotensin metabolizing enzymes; however, a decrease in the coordinated receptors that are known to favor atheroma formation (LNPEP, AGT1R and MR) (figure II.3). In addition, AGTR2 and MAS1, which are both known to encode receptors that antagonize AT1R were found to be lowly expressed, they were even not detected. All these data were validated using qPCR. This indicates that the organization of extRAAS in the arterial wall is altered during early stages of atherosclerotic lesion development (in MIT) and retained during lesion progression, thus participating in both lesion initiation and progression.

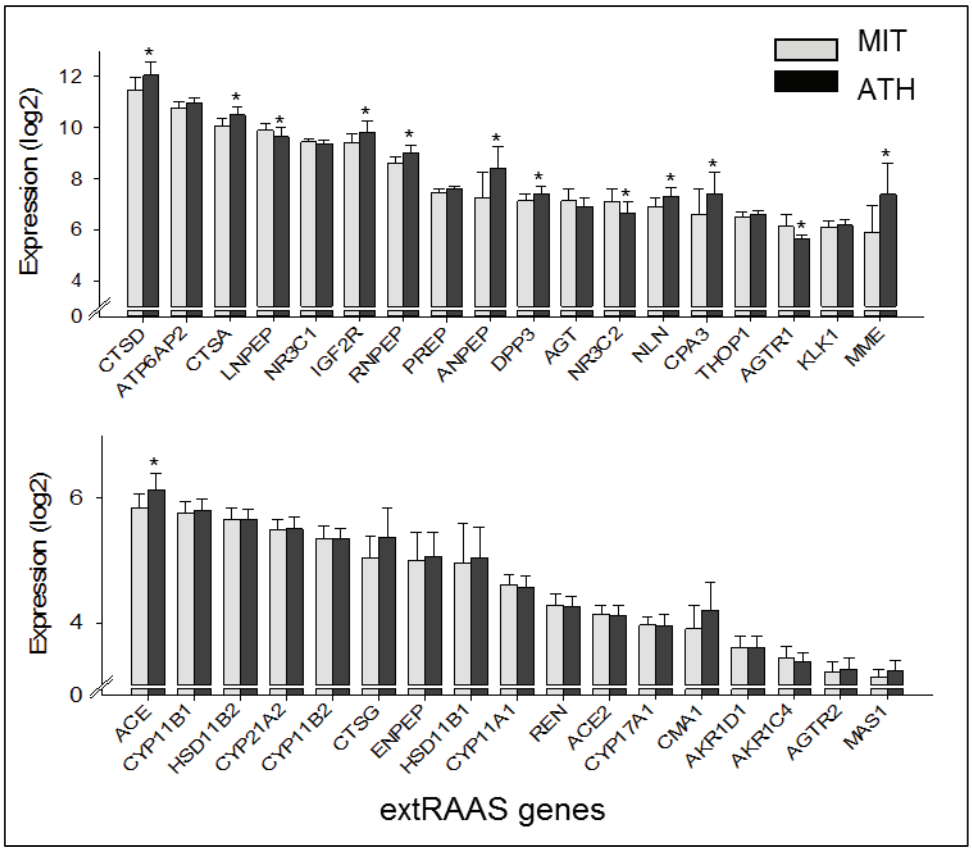

Figure II.3: expression of 35 extRAAS genes in macroscopically intact tissue (MIT) and atheroma plaque (ATH) of 32 patients (mean ± SD). Genes having mean expression level higher than the median value over the microarray in the upper graph, whereas genes having mean expression level lower than the median value over the microarray are present in the lower graph.

Therefore, we hypothesized that extRAAS has a specific organization in atheroma that plays a key role in atherosclerotic lesion development, and targeting this organization to get it back into its normal state through novel non-classical RAAS inhibitors may play a critical role in atherosclerosis treatment. However, the pharmaceutical targeting of this organization may affect the organization of extRAAS in other tissues, thus leading to side effects in these

tissues. Therefore, our objective in this study is to identify the tissue-specific characteristics of the organization of extRAAS in atherosclerotic lesion, which will allow a more specific and efficient treatment.

II.2 OBJECTIVES AND EXPERIMENTAL STRATEGIES

Objective1: Validate the tissue-specificity of extRAAS organization in atheroma

Since extRAAS is known to be expressed in various other tissues than the arterial wall, we checked whether the organization we have obtained from carotid atherosclerotic lesion is reproducible in other types of atheroma (coronary, renal, peripheral) and if it is specific for atheroma.

Objective 2: Identify the cellular source of extRAAS organization atheroma

Because the coordinated transcripts are found in initial atherosclerotic lesion stages with almost absent inflammatory cells (MIT) and in ApoE-/- aortas in the absence of hypercholesterolemic diet, which allows excluding the role of absent inflammatory cells in these samples. In addition, since carotid endarterectomy tissue contains no adventitial tissue, this also excludes the role of adventitial cells. Thus it is thus more likely that this organization originate from VSMCs, which are present in much higher numbers than EC in MIT, human atherosclerotic lesions and ApoE-/- aortas. However, VSMC in atherosclerotic lesions may present with large phenotypic variability from typical medial contractile cells to synthetic, lipid storing and calcified cells as was discussed in the introduction. Therefore, extRAAS organization was investigated using primary human VSMCs conducted to adopt different phenotypes related to vascular remodeling in atheroma: contractile, lipid storing or osteoblastic.

Objective 3: Identify the role of extRAAS organization in orienting the metabolism of active peptides in atheroma

Whether and how the correlations observed at the mRNA level translates into protein and signaling peptide production is of upmost importance. Using mass spectrometry (MS) we are analyzing the flow of Ang-I metabolism in atheroma by measuring downstream peptides. In addition we are measuring the protein levels of extRAAS components in carotid atherosclerotic lesions that will be also subject for correlation and system network analsysi.

Objective 4: Reveal the transcriptional regulatory mechanisms behind extRAAS organization in atheroma

Coordination between gene transcripts may rely on the activity of common TFs that may bind to the promoter of coordinated genes and simultaneously activate their transcription. Thus, we identified candidate TFs involved in extRAAS gene coordination using bioinformatics tools, that will need to be validated experimentally using molecular biology techniques in VSMCs.

III. EXPERIMENTAL APPROACHES

III.1 OBJECTIVE 1: VALIDATE THE TISSUE-SPECIFICITY OF EXTRAAS ORGANIZATION IN ATHEROMA

To check for the reproducibility of the organization of extRAAS in atheroma and its tissue-specificity we used previously published transcriptomic data available on the gene expression omnibus (GEO) database. Since analysis was done on different datasets obtained using different experimental protocols, microarray platforms and were normalized differently, analysis was done based on the workflow presented in Figure III.1. Experimental procedures in each step of the workflow are detailed in the next sections.

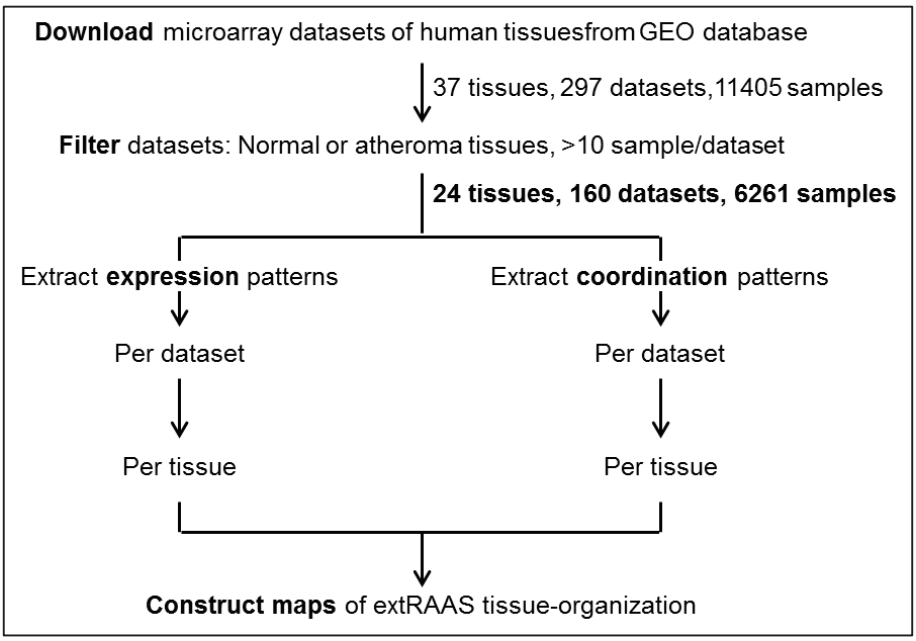

Figure III.1: workflow of the experimental approach to achieve objective 1. Microarrays were downloaded from the GEO database based on certain inclusion and exclusion criteria. Expression and coordination patterns were then extracted from each database. Results obtained from datasets of the same tissue were then joined and reproducible patterns of expression and coordination were identified. for each tissue, the identified reproducible patterns were then used to construct a map of extRAAS organization.

III.1.1 Downloading microarray datasets

Published microarray datasets were downloaded from the Gene Expression Omnibus database (http://www.ncbi.nlm.nih.gov/geo/). The search was done by tissue name and a filter was applied for organism (human or mouse), study type (expression profiling by array), attribute name (tissue) and sample count (>10). The results obtained were then checked for the study design used to check for the samples type (tissue, cells or explants), sample treatments (addition of exogenous substances, physical treatment) and their processing protocol. Only datasets with more than 10 normal tissue samples without any treatment that

are directly frozen or lysed for RNA extraction were retained. Atherosclerotic tissues were also retained. Since only normal samples were to be analyzed in other tissues than the vascular tissue, expression data of normal samples (usually control samples used in the study) were separated from the expression data of diseased samples in each dataset and saved into separate files. Except for atherosclerotic vascular tissue, all physio-pathological samples from each dataset were excluded and further analysis was only done on physiologically normal tissues. Age, gender, and ethnicity were not taken into account in selecting the datasets.

III.1.2 Extracting expression levels and quality control

After filtering, datasets were checked for the expression distribution of their individual samples. Datasets which showed large variability among samples were eliminated. Datasets were normalized by their authors using different methods including robust multichip average (RMA), GC-RMA or a global score method[442]; datasets lacking any transformation were log 2-transformed. Since datasets were obtained using different microarray platforms and since they were normalized differently, and in order to compare expression data between different datasets, the centile rank of a gene was calculated using the R-software by normalizing its mean expression level relative to the mean expression data distribution over the microarray (figure III.2). As an example, a gene with a centile rank equals to 68 in a specific dataset means that its expression is higher than 68% of the genes in the same dataset.

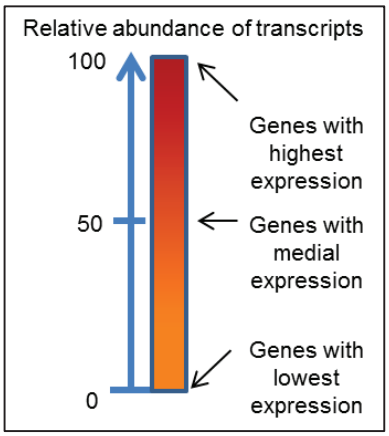

Figure III.2: the centile expression rank reflects the mRNA expression level of a gene relative to other genes of the genome.

III.1.3 Clustering of extRAAS genes per dataset

The R software was used for statistical description and clustering of the 37 extRAAS gene transcripts in each dataset, using the "Cluster" R library. ExtRAAS gene transcripts were hierarchically clustered in each dataset using Pearson correlation distance and Ward's agglomeration method[443]. Each of the obtained dendrograms was then cut at a given level to identify the gene clusters (figure III.3). The cut-off level was chosen on the basis of a balance between the level of clustering strength, assessed with the agglomerative coefficient and a minimum of 3 gene transcripts per cluster.

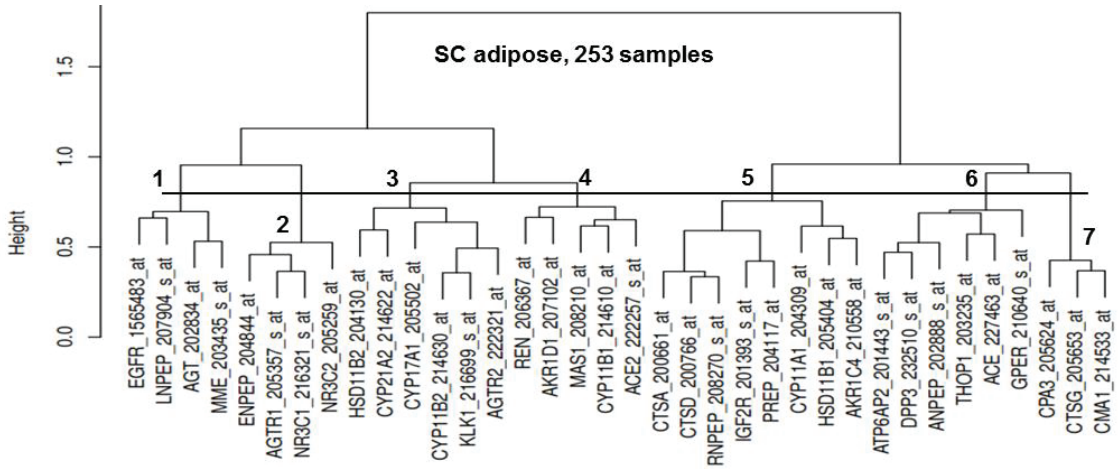

Figure III.3: cutting the dendrogram. This is a typical dendrogram of a dataset containing 253 subcutaneous (SC) adipose tissue samples. The cut-off level was chosen on the basis of a balance between the level of clustering strength, assessed with the agglomerative coefficient and a minimum of 3 gene transcripts per cluster. By cutting this dendrogram at the level indicated by straight horizontal line, we obtain 7 clusters with a minimum of three genes (cluster 7). Cutting at a higher level will produce to larger clusters, however, with lower clustering strength. On the other hand, cutting at a lower level will produce clusters with strong gene correlations, however, the genes will be scattered into many clusters.

III.1.4 Identifying local extRAAS co-expression modules in each tissue

A co-expression module was defined as a set of 2 or more genes that were coordinated across datasets of a given tissue (Table III.1). In the beginning, a co-expression module was defined as the genes that are totally clustered in more than 50% of the datasets of a given tissue. However, this may underestimate other genes that are clustered with the genes of a given co-expression module in some datasets. Therefore, co-expression modules were then extracted based on the average coordination rate (ACR) of genes within a module, which is the average percentage of coordinated genes within a module that were clustered across the different datasets in a specific tissue. For example, PREP in the first module in figure 3.x would have been eliminated from the module if co-expression modules were extracted based on the first method because it is clustered with all the genes of the module only in 3 of the 8 datasets

(<50% of datasets). However, based on the ACR method, it would be included because it is also clustered with other genes of the module in certain datasets.

Table III.1: extraction of co-expression modules. Cluster patterns from the different datasets of a give tissue are arranged in a table like the one in the figure above. The table shows the level of coordination of genes across 8 datasets of subcutaneous adipose tissue. Colors indicate clustered genes and the bugs indicate non-clustered genes in a dataset. A module is a set of coordinated genes with an average coordination rate (ACR) greater than 55%. ACR was calculated as the average % of genes that are coordinated across datasets. For example, 81% of the first module genes are coordinated across datasets in adipose tissues. The non-clustered genes are those which have a low correlation with any other genes across datasets, thus they don't belong to any module.

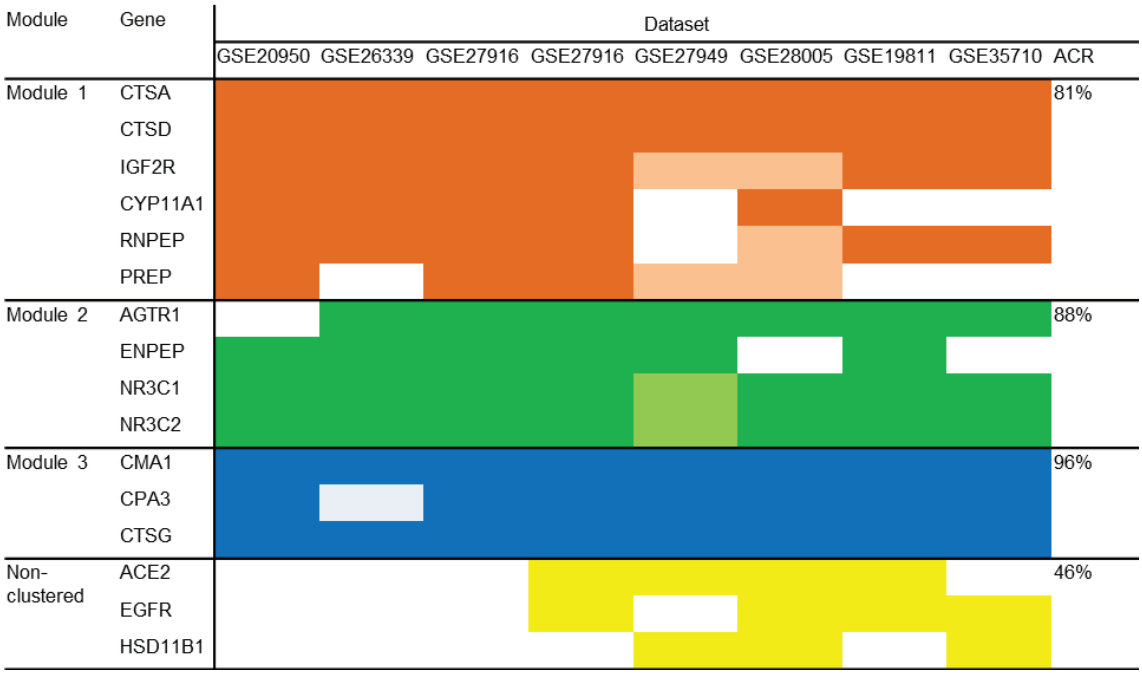

ACR was calculated based on the following equation:

$$\mathbf{ACR}=\frac{\sum_{i=0}^{n}(xi-ei+1)/z}{n}*100$$

Were *n* is the total number of datasets,

x is the total number of coordinated genes in a dataset,

e is the number sub-clusters in a dataset,

and *z* is the total number of genes in a module.

Therefore, ACR of module 1 in table III.1 would be calculated as follows:

$$\frac{\frac{6}{6}+\frac{5}{6}+\frac{6}{6}+\frac{6}{6}+\frac{(4-2+1)}{6}+\frac{6-2+1}{6}+\frac{4}{6}+\frac{4}{6}}{8}*100=\frac{6.5}{8}*100=81.3\sim 81\%$$

In this case, the larger the modules across datasets, the fewer the sub-clusters, and thus, the higher the ACR would be. Therefore, ACR reflects the strength of correlations between genes across all datasets. A threshold of >55% was the criterion used to define gene modules that were representative for a specific tissue.

III.1.5 Datasets quality control

In our first trial on extracting co-expression modules, we found that in tissues with multiple datasets, such as subcutaneous adipose tissue, certain datasets showed a different clustering when compared to the bulk of datasets in the same tissue. So, we hypothesized that these datasets may have a different expression profile due to a large difference in experimental protocol used. So, we checked for the expression profiles of extRAAS genes in these datasets and found that indeed they showed a large difference in their expression profiles compared to other datasets of the same tissue (figure III.4).

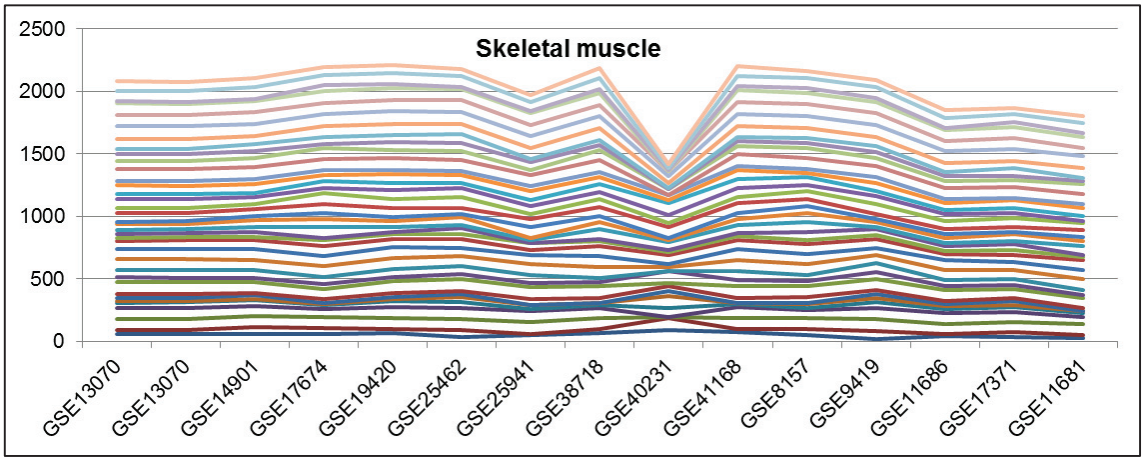

Figure III.4: expression profiles of extRAAS genes in all datasets of skeletal muscle before quality control. Each horizontal line corresponds to a the expression profile of one gene across the datasets. Each part of the horizontal axis corresponds to the expression of all genes within one dataset. A good profile in a dataset should have a consistent global change in its gene expression profile that leave the expression profile of individual genes parallel with the upstream and downstream dataset. In the graph above, the profile of GSE40231 is clearly different from all other datasets making deep changes in gene expression, with some increasing and the others decreasing.

However, to minimize manual manipulation in our analysis, datasets of a given tissue were then hierarchically clustered based on the obtained centile rank of extRAAS gene expression based on the average linkage method using cluster 3.0 [444] and Java TreeView 3.0[445] softwares. Non-clustered datasets were then eliminated from the study (figure III.5).

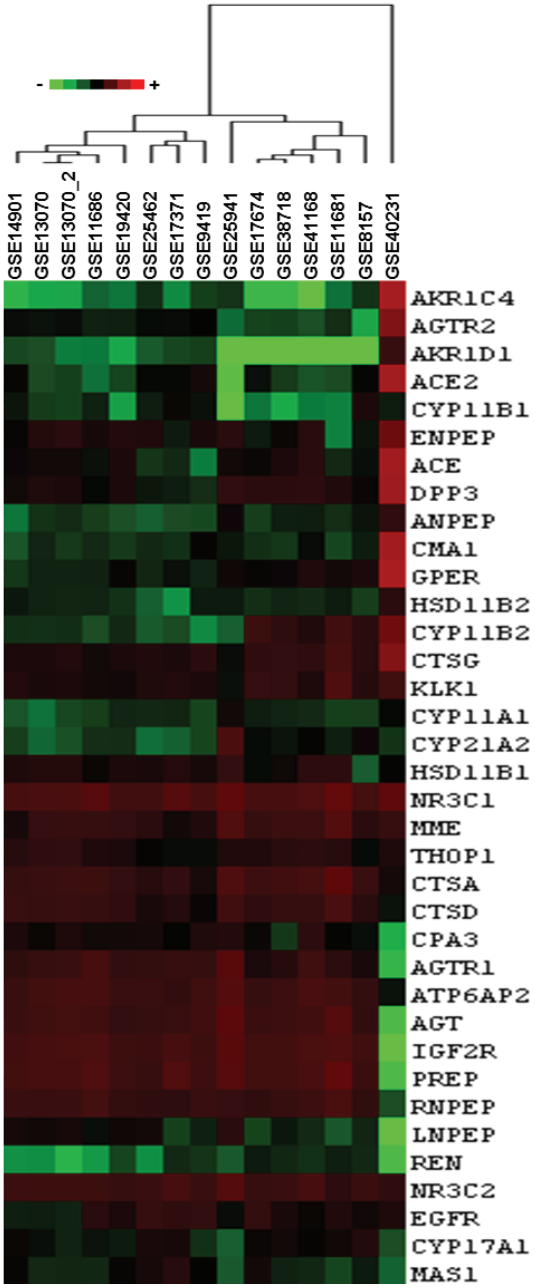

Figure III.5: quality control heatmap for skeletal muscle. The dendrogram was drawn based on the average linkage method (cluster 3.0 software) using the logged and normalized mean centile expression rank of extRAAS genes. Colors correspond to the relative logged centile rank in each dataset. It is very clear that GSE40231 (last column on the right) is not clustered with the bulk of datasets.

III.1.6 Statistical analysis

For centile rank expression levels, one MCR value was computed per tissue and one mean MCR for all tissues. These MCR values were presented as (1) mean ± SD to show intra- and

inter-tissue variation in extRAAS gene expression and (2) mean ± SEM to describe specific gene expression.

III.2 OBJECTIVE 2: IDENTIFY THE CELLULAR SOURCE OF EXTRAAS ORGANIZATION ATHEROMA

A summary of the experimental approach used to achieve objective 2 is present in figure III.6.

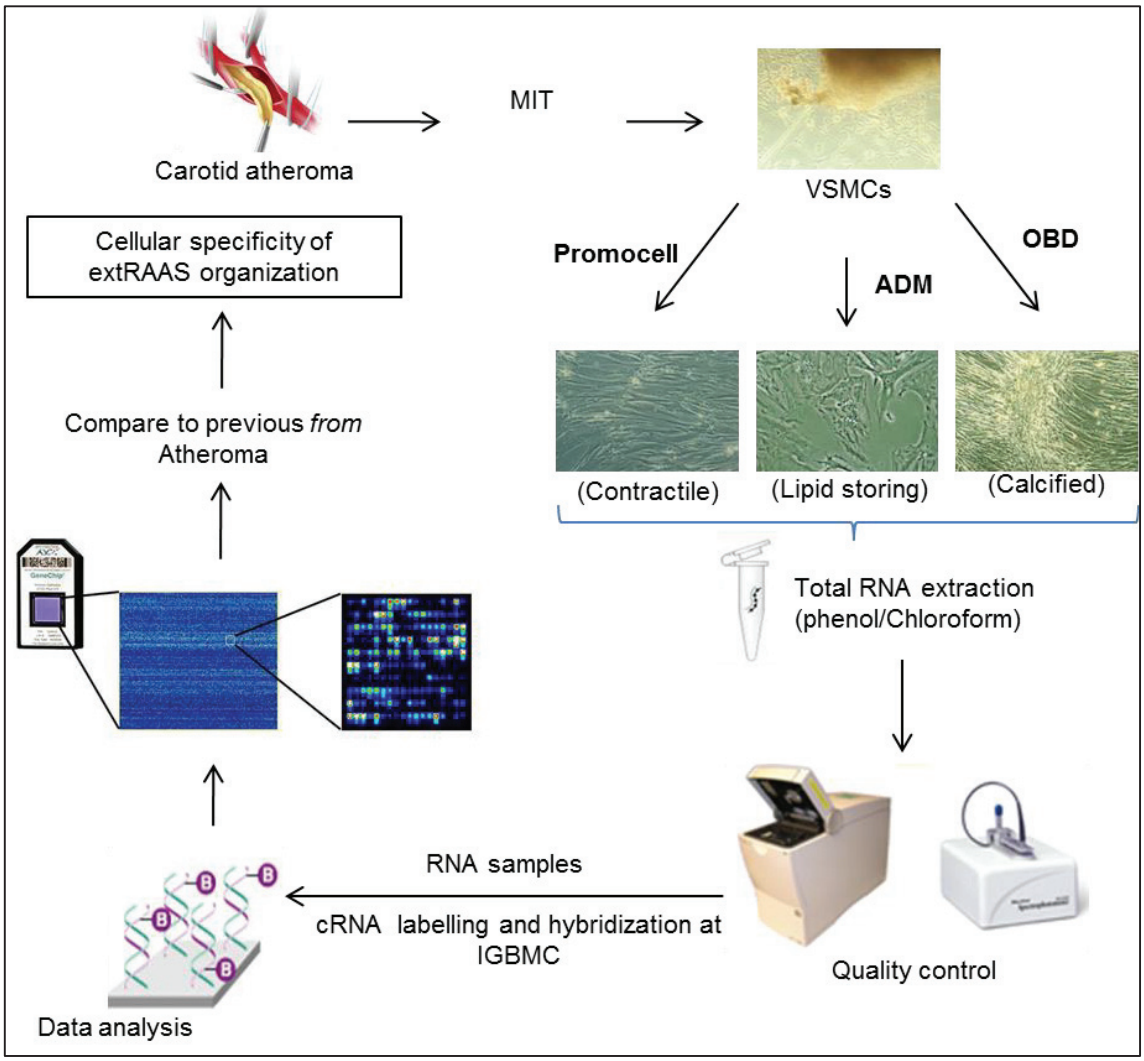

Figure III.6: workflow of the experimental approach to achieve objective 2. VSMCs obtained from MIT of carotid samples were stimulated to differentiated into lipid storing (adipocytic) and calcified (osteoblastic) phenotypes, in addition to a third set that are maintained with their contractile phenotype. RNA was then extracted from the each cell type and RNA with good quality and quantity was stored for microaaray hybridization. The obtained transcriptomic data will then be analyzed for extRAAS transcripts organization and compared to our previous data from atheroma so that we can identify the cellular source of extRAAS organization in atherosclerotic lesions.

III.2.1 Carotid samples preparation and storage.

The investigations were carried out according to the principles outlined by the Declaration of Helsinki, all procedures were approved by the local ethical committee, and the patients gave written informed consent[446]. Fresh carotid samples were brought from the operation block of Hôpital Edouard Herriot within 2 hours after carotid endarterectomy. The atherosclerotic lesion (calcification, hemorrhage, fatty streak) part was carefully separated from the nearby macroscopically intact tissue (MIT) part in each sample. A 0.5 cm² fragment of each part was then put in 4% paraformaldehyde (PFA) solution to be sent for biochemical analysis. Another fragment of 1-2 cm² was taken from the MIT for VSMCs extraction. The rest of both the atherosclerotic lesion and MIT were snap frozen in liquid nitrogen then stored at -80°C for further analysis.

III.2.2 VSMCs extraction from MIT

The 1-2 mm part of MIT was cut into 1-2 mm² pieces that were spread in a 25 cm² Falcon™ tissue culture treated flasks using a Pasteur pipette. After separating the small pieces, the flask is incubated 10 minutes at 37°C in 5% CO_2. The flask is then filled with 4-5 ml of complete Promocell medium for smooth muscle cell growth. (Promocell catalog number: C-22162) containing 1% penicillin; 0.2% funjizon and 0.2% nystatin This medium was used as the control medium for further treatment. The medium is changed every 2-3 days. After 4-8 weeks, when VSMCs grow and become more than 40% confluent, the cells are trypsinized and passed into another 25 cm² flask. These are considered passage 1 cells.

III.2.3 VSMCs differentiation protocol

VSMCs were obtained by an explant method originally described by Ross[447]. VSMCs in passage 3-5 were used in the protocol. After trypsinization, 1 x 10^5 cells were seeded per well in a 6 wells plate. The medium was changed every 2-3 days and treatment starts after the cells reach 70-80% of confluence. The lipid storing phenotype was stimulated using control medium with 1nM T3, 0.25mM IBMX, 1.2 µM insulin and 100 nM dexamethasone[448]. On the other hand VSMCs calcification was done using control medium with containing 1% penicillin; 0.5% funjizon, 0.5% nystatin, 10 mM sodium pyruvate, 10 mM β-glycerophosphate, 1 µM insulin, 50 µg/ml ascorbic acid and 100 nM dexamethasone[449] (in another protocol we used control medium containing a final phosphate concentration of 3.9 mM). Control cells were left treated with control medium. For the 3 phenotypic treatments, the medium was changed every 2-3 days for 2 weeks.

III.2.4 Total RNA extraction using TRIZOL-phenol/chloroform

Cells from each well were trypsinized and put into separate tubes. After lyzing the cells in 500 µl of TRIzol reagent, cell lysate was homogenized in 100µl of Choroform/Isoamyl alcohol with respective 24:1 ratio and incubated on ice for 5 minutes. The mixture was then centrifuged at 12000g for 10 min at 4°C, which result in 3 layers: an upper clear layer containing the RNA, an interphase containing proteins and the lower organic phase containing lipids and DNA. The upper clear phase containing RNA was transferred into a new tube, incubated overnight with an equal volume of 100% isopropanol, and then centrifuged at 14000g for 20 min at 4°C in order to precipitate the extracted RNA. The resulted RNA pellet was washed by 70% ethanol, left to dry out, and then reconstituted in 50µl Diethylpyrocarbonate (DPEC) water. After that, RNA was treated with DNase-I to remove DNA traces and the DNase was deactivated by heating at 70°C for 10 min. RNA was precipitated again overnight with 0.1V of 2M acetate (18 µl), 2.5V of cold 100% Ethanol and 1.5µl glycogen then centrifuged at 14000g for 20 min at 4°C and the resulted RNA pellet was washed by 70% ethanol, left to dry out, and then reconstituted in 10-15µl Diethylpyrocarbonate (DPEC) water. RNA quantity and quality were measured using nanodrop and agilent bioanalyzer, respectively. The RNA quality is evaluated by the O.D260/O.D280 $\geq$ 1.8 and O.D260/O.D230 relations. The absence of degradation was checked by the relation 18S/28S $\geq$ 1.6 and RIN > 6 (RNA integrity number) using the Agilent bio-analyzer. RNAs with quantity greater than 500 µg and quality that verify all criteria were stored at -80°C to be sent to the molecular and cellular biology institute (IGMCB) in Strasbourg where microarray experimental protocol will be performed.

III.2.5 Validation of lipid storing phenotype using RT-qPCR

Contractile and lipid storing phenotype of VSMCs was validated using microscopic examination and quantitative measurement of the mRNA expression of key genes involved in each phenotype. Contractile phenotype was validated by the expression of smooth muscle cell actin (α-SMA). Lipid storing phenotype was tested by the expression of adipocyte fatty acid binding protein (FABP4/aP2) and FAT atypical cadherin 4 (FAT4). Table III.2 shows the sequence and features of primers used for these measurements.

Table III.2: primer sequences for the validation of adipocytic differentiation by RT-qPCR.

Gene name	Gene symbol	Primers	Amplicon size	Melting Temp °C
FAT atypical cadherin 4	FAT4	TAACACAGAGTCTGGATCGGG GTTCCAGTTCCAGTCAAGGC	93	58
Fatty acid binding protein 4	FABP4	TGATGATCATGTTAGGTTTGGC TGGAAACTTGTCTCCAGTGAA	106	60
Smooth muscle alpha actin	a-SMA	TGCCTGATGGGCAAGTGA CTGGGCAGCGGAAACG	51	60

For quantitative measurements, 1 µg of total mRNA were reverse transcribed using 200U Superscript II (Invitrogen_18064-014), 200ng random hexamers (Invitrogen_N8080127), 10 nmole dNTPs, 250 nmole DTT and first strand buffer in a total volume of 25µl based on the suppliers protocol. iQ 96-well PCR plates (Cat#223-9441) and plate sealers(Cat#MSB-1001) were purchased from BioRad. Real-time polymerase chain reaction was performed in a MyIQ thermal cycler (Biorad) using iQ™ SYBR® Green Supermix (Cat #: 170-8882) and the appropriate set of primers based on the protocol of the iQ SYBR Green Supermix supplier. Briefly, 8µl of SYBR supermix were mixed with 4µl water, 100 pmol of forward primer, 100 pmol of reverse primer and 1µl of sample. All samples were run in duplicate along with dilutions of known amounts of target sequence to obtain standard curve, in addition to negative controls without template DNA. Cycling parameters were done using the following program:

Step	# Cycles	Temperature	Time
Enzyme activation	1x	95°C	3 min
Amplification	40x	95°C	10 sec
		Primers Tm	45 sec
		Fluorescence measurement	
Final elongation	1x	95°C	1 min
		55°C	1 min
Melting curve	80x	increasing steps of 0.5°C starting at 60°C	10 sec

qPCR results analysis was done using Bio-Rad, iCycler iQ Optical System Software. Cycle thresholds (Cts) were determined by the software automatically. By default, the baseline

cycles and the threshold are automatically calculated. The automatic threshold calculation is done to use standards defined on the experimental plate, the threshold is adjusted to attain the highest possible correlation coefficient value for the standard curve.

Results were expressed as the target over 18S RNA concentration ratio. mRNA levels were compared with two way analysis of variance for cell experiments (phenotype and treatment). Pearson correlation was used to test the relationship between mRNA levels of genes of interest. $P<0.05$ was considered significant.

III.2.6 Validation of VSMCs calcification by alkaline phosphatase assay or alizarin staining

VSMCs calcification was validated using alkaline phosphatase (AP) assay or alizarin red staining. AP is highly expressed and play major role in VSMC calcification (Narisawa S et al. 2007). Therefore, we tested for AP activity in ODM-treated VSMCs using BCIP/NBT (SigmaFast^{TM} BCIP-NBT; Sigma Aldrich Cat #: B5655) as a substrate, which stains cells blue-violet when AP is present. After removing the medium, cells were washed once using PBS without calcium or magnesium (PBS^-), then incubated in neutral buffered formalin (10%) for 1 minute (1 ml per one well of a 6-wells plate). The formalin was then removed and the cells were washed once with washing buffer (0.05% Tween 20 in PBS^-). BCIP/NBT substrate solution was then added to cover the cellular monolayer (1ml per well) and incubated at room temperature in the dark for 5-10 minutes. The dark blue color should now be clear in calcified cells expressing AP. Finally, the substrate solution was carefully aspirated and cells were washed with washing buffer then incubated in PBS^-.

Mineral deposition in cultured VSMCs was assessed by alizarin red staining. Alizarine red solution was prepared by 2 g Alizarin Red S (Sigma Aldrich Cat #: A5533) in 100 ml distilled water, PH adjusted to 4.2, then filtered stored in the dark. The following protocol is set for cells in 24-wells plate. Cells were first washed once with PBS^- then twice with 50% ethanol. After that, cells were incubated 5 minutes in 500 µl of 50% ethanol, then 5 minutes in 500 µl of 70% ethanol, and finally in 250 µl of alizarin red solution. The solution was then removed and cells were washed once by 50% ethanol. Undifferentiated cells should be slightly reddish, whereas mineralized should be bright orange-red.

III.3 OBJECTIVE 3: IDENTIFY THE ROLE OF EXTRAAS ORGANIZATION IN ORIENTING THE METABOLISM OF ACTIVE PEPTIDES IN ATHEROMA

Expression of extRAAS genes identified from the microarray data in atheroma and VSMCs (Objective 1 & 2) may provide an indirect view of the possible pathways favored in atheroma since they are analyzed at the mRNA level. However, to identify the expression of extRAAS in atheroma and their activity in orienting angiotensin metabolism we need to analyze the extRAAS components at the protein level. In this context, we will check the peptide flow of angiotensin metabolism by measuring the concentrations of downstream peptides obtained from a common labeled Ang-I (ang-I*) spiked into atheroma tissue explant. The label is incorporated on the fifth amino acid (DRVY-I*-HPFHL) which is present in all downstream peptides. This will insure that the measured peptides are all driven from the same initial Ang-I peptide added with known concentration.

A summary of the experimental approach used to achieve objective 3 is present in figure III.7.

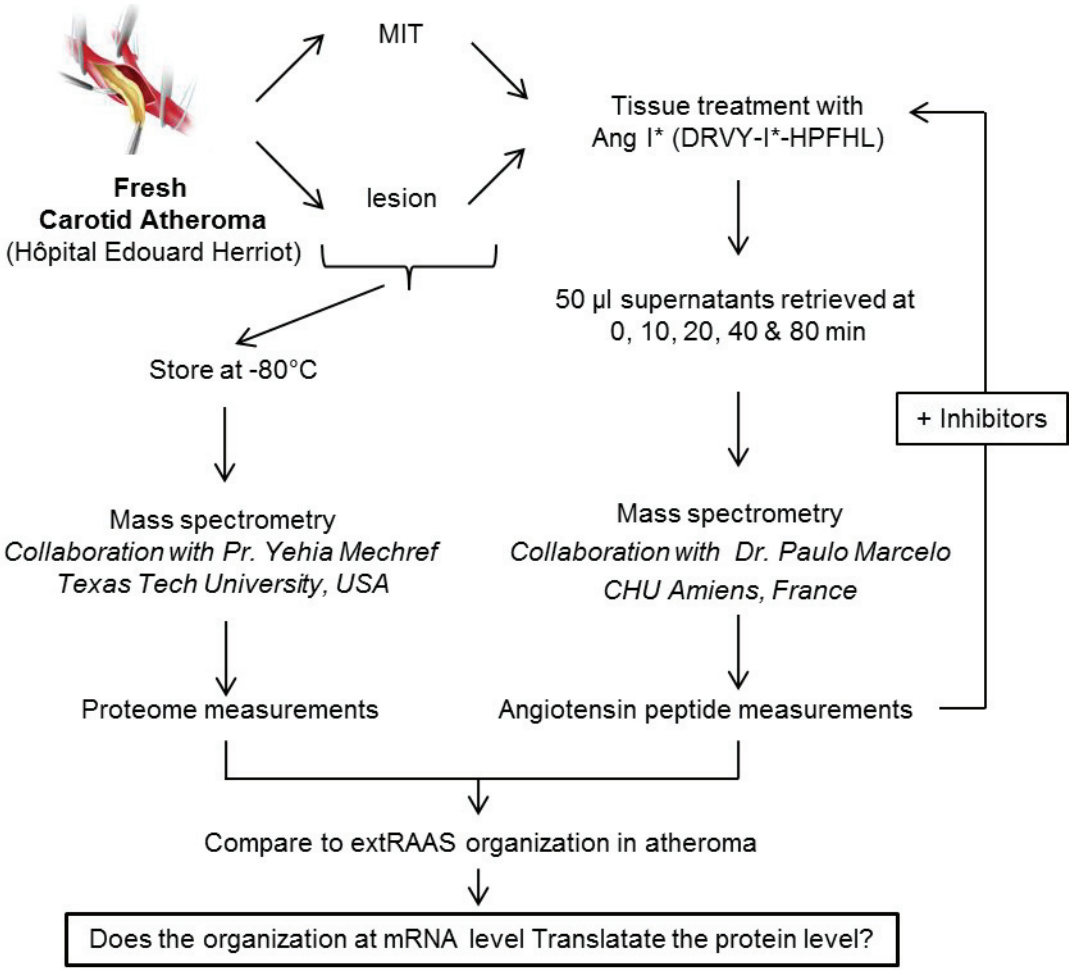

Figure III.7: workflow of the experimental approach to achieve objective 3. Fresh carotid sample is separated in to its constituent MIT and lesion, respectively. Each part is then devided into

two pieces: one piece will be used for total proteome measurement and the other piece will be used for the measurement of the kinetics of angiotensin metabolism.

III.3.1 Samples preparation and treatment

Fresh carotid samples are dissected to obtain respective MIT and advanced atherosclerotic lesions respectively. 10 mg of each tissue type is measured and washed 3 times in phosphate buffer saline (PBS). Each is then incubated in 1ml Krebs Hensleit solution (KHS: $MgSO_4$ 1.2 mM, KH_2PO_4 1.2 mM, KCl 4.7 mM, NaCl 118 mM, $CaCl_2$ 2.5 mM, $NaHCO_3$ 25 mM) for 5 minutes at room temperature and a 50 µl of the solution is taken to measure background concentrations. Labeled Ang-I* (DRVY-I*-HPFHL, Tebu-bio, catalog# 1168) is then added to reach a final concentration of 1µM and another 50 µl of the supernatants is taken directly to measure peptides concentrations at t_0= min. The mixture is then incubated at 37°C in 5% CO^2 and 50 µl of supernatants is taken respectively after 10, 20, 40 and 80 minutes. Supernatants are stored directly at -80°C. After removing the remaining solution the tissue was allowed to dry then weighed and cut into small pieces. The pieces are then grinded into powder in liquid nitrogen and transferred into an Eppendorf tube. 500 µl of lysis buffer (1% triton-X, PH= 7.4) was then added and the tissue was sonicated using a medial frequency 3 times, each for 10 seconds on ice. Total protein was then measured using the Bradford method. Dry tissue weight and/or total protein are used for normalization.

The rest of each of MIT and atherosclerotic lesions were used for proteomic measurements using mass spectrometry.

III.3.2 Mass spectrometry measurements

Frozen aliquots of supernatants obtained from treated tissues will then be thawed, filtered to eliminate strong background measurements. The samples will then be loaded directly on a reverse phase HPLC connected to electrospray ionization-mass spectrometry (LC-ESI-MS) for the measurement of produced angiotensin metabolites. This part of the work will be done in collaboration with Pr. Paulo Marcelo from CURS, CHU Amiens, France. We are still setting up the conditions for measurements.

As for proteome measurements in MIT and atherosclerotic lesions, this part will be done using a time-of-flight mass spectrometer (TOFMS) in collaboration with Pr. Yehia Mechref from Texas Tech University, USA.

III.4 OBJECTIVE 4: REVEAL THE TRANSCRIPTIONAL REGULATORY MECHANISMS BEHIND EXTRAAS ORGANIZATION IN ATHEROMA

Because at least part of the determinism of correlations must lie within the sequence of the mRNA or of its gene DNA, we will be first looking for the possible causes of extRAAS genes co-expression through TF binding to the majority of extRAAS genes promoters and/or identifying how genes coordinate with extRAAS in the studied tissue. This was conducted using Genomatix Software Suite[450] which offers numerous tools that will allow the identification of promoter sequences of extRAAS genes and corresponding TFs that regulate their expression. After that we scanned for candidate TFs that have common TF binding sites (TFBS) in the promoter of coordinated genes in atheroma. From these candidate TFs we are going to choose the 3-4 most relevant TFs to be validated by molecular biology techniques, such as siRNA transfection to knockdown a target TF and check for its effects on the expression of extRAAS genes.

A summary of the experimental approach used to achieve objective 4 is present in figure III.8.

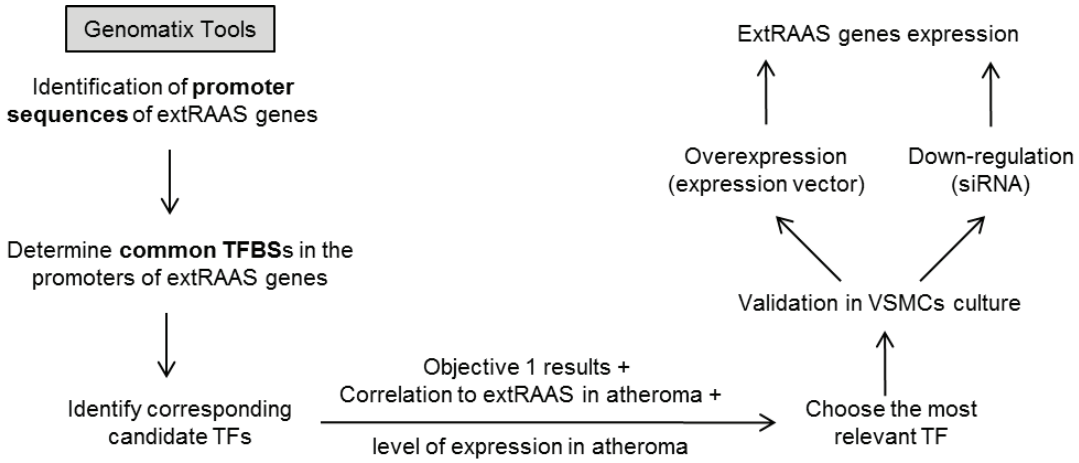

Figure III.8: workflow of the experimental approach to achieve objective 4. We are going to use the Genomatix software suite in order to identify candidate TFs that may simultaneously bind promoters of coordinated extRAAS genes in atheroma and regulate their expression. The Genomatix tools will allow the identification of TFBSs present in the promoter of coordinated genes with their corresponding TFs. From these TFs we are going to choose the most relevant ones to be validated experimentally in VSMCS using molecular biology techniques such as down-regulation using siRNA or overexpression using mammalian expression vectors. The choice of the relevant TFs will rely on the results obtained from objective 2 in addition to the transcriptional levels and coordination of these TFs to extRAAS genes.

III.4.1 Identification of candidate TFs using bioinformatics

The bioinformatics approach used for the identification of candidate TFs is written in the materials and methods of enclosed Scientific manuscript I. The different methods used will be explained in more details in the following sections.

III.4.1.1 *Promoter analysis of coordinated extRAAS genes*

Transcription start clusters (TSC) were identified using SwissRegulon genome map[451]. Alternatively, dbTSS database[452] was used to extract individual TSS in the region of active transcription for certain genes for which no TSC could be extracted. A TSC or TSS is considered active when the expression of downstream exons is >1.5 folds greater than the upstream exon. An example on AGT transcript is presented in figure III.9.

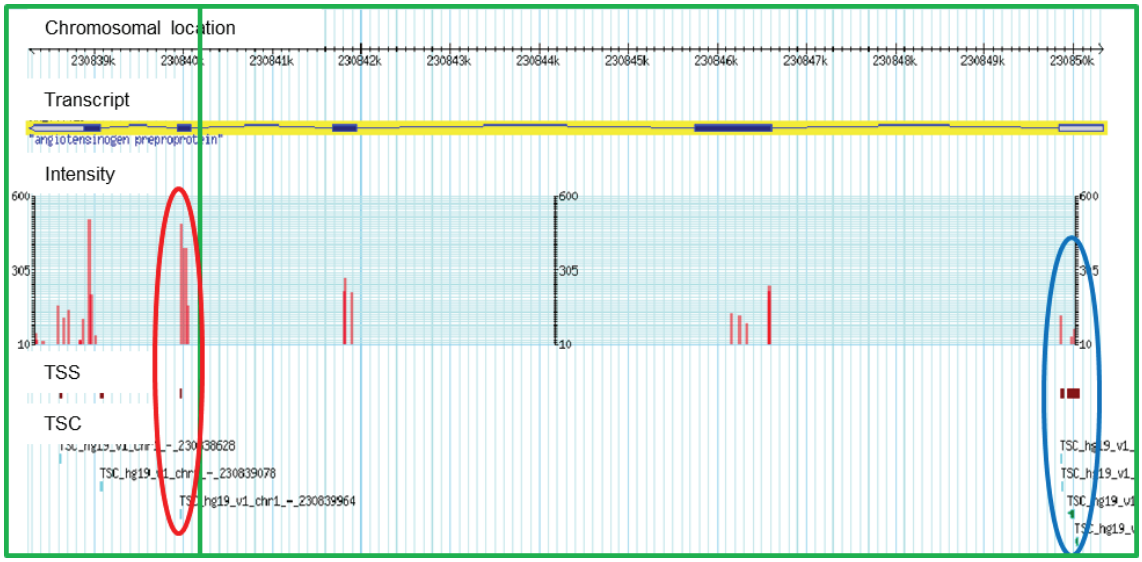

Figure III.9: AGT exon expression profile and transcription start sites. As can be seen in the figure that there are several transcription start clusters (TSCs) and transcription start site (TSSs). The first three clusters (on the right side, in blue oval shape) are close and seems to be active. Therefore, one common promoter was extracted for them. In addition, there is a sharp increase at a specific start site in the second last exon of the transcript, thus another promoter was extracted around this TSS.

Exon expression levels were obtained from raw expression data of the GSE43292 dataset obtained in our lab. After defining active TSCs, promoter sequences were extracted using the Genomatix database[450] and SwissRegulon human genome database. A promoter was defined by the sum of consecutive promoter sequences obtained by Genomatix around a specific TSC obtained from SwissRegulon. If no Genomatix promoter sequence could be obtained for a specific active TSC, then the promoter is considered as the 100-500 bp downstream and 400-700 bp upstream of the TSC in SwissRegulon genome viewer. For TSS obtained from the dbTSS, a promoter region of 600 bp is extracted, with 500 bp upstream and 100 bp

downstream the TSS using the NCBI genome viewer. An example of the latter case is presented in figure III.10. Promoter sequences of coordinated extRAAS genes were then analyzed simultaneously using the commonTF tool from Genomatix using default options in order to identify enriched transcription factor binding sites (TFBSs) in the promoters of coordinated genes. All of the position-weight matrices (each one associated with one TFBS) having at least one match in the studied promoters were obtained with their enrichment p-value in the group of studied promoters. One TFBS was taken as significantly enriched if its adjusted p-value (p-value/total number of position-weight matrices having at least one match in the studied promoters) was less than 0.05.

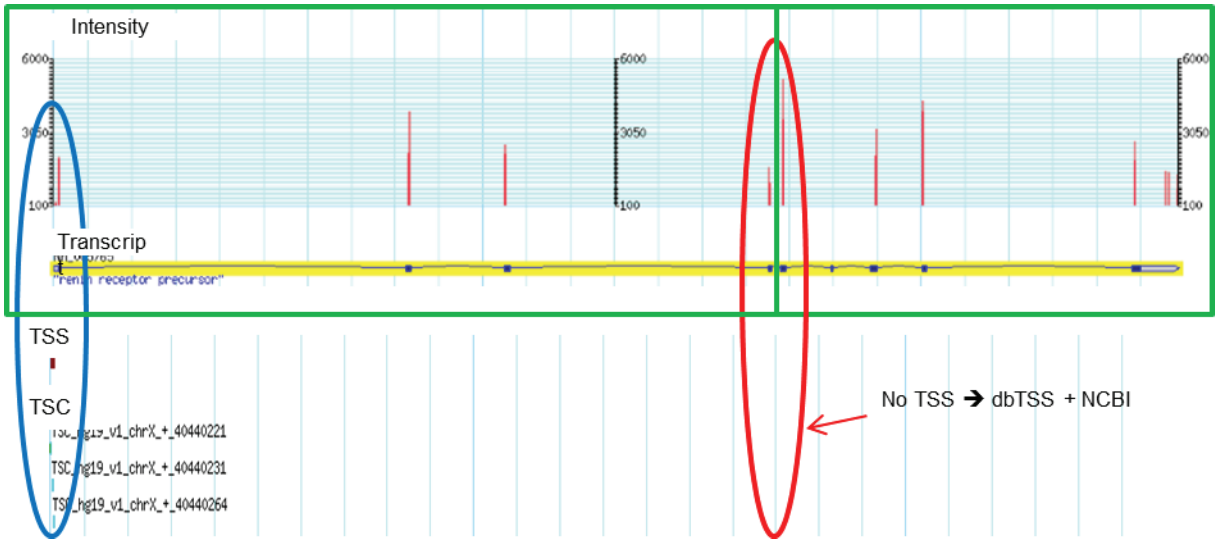

Figure III.10: ATP6AP2 exon expression profile and transcription start sites. There are several transcription start clusters (TSCs) and transcription start site (TSSs). The first three clusters (on the left side, in blue oval shape) are close and seems to be active. Therefore, one common promoter was extracted for them. In addition, there is a sharp increase in the fourth exon of the transcript. However, no TSC or TSS is present around this exon on SwissRegulon or on Genomatix. Therefore, the TSS for this point was extracted from the dbTSS and the corresponding promoter was extracted using the NCBI genome viewer.

III.4.2 Identification of relevant TFs

The identification of relevant TFs was done based on their transcriptional correlations with the coordinated extRAAS genes in atheroma (see Scientific manuscript I). The methods used to achieve this goal were the same as those used to achieve objective 1 but with the candidate TFs coding genes (obtained by applying methods in section 3.4.1) included.

III.4.3 Experimental validation of relevant TFs

Relevant TFs are to be validated using molecular biology techniques, specifically by TF knockdown using siRNA and TF overexpression using mammalian expression vectors. At this level, we are still setting up the experiments of siRNA transfection.

III.4.4 Setting-up siRNA transfection

In order to check for the relation between candidate TFs and coordinated extRAAS genes, we tried to knockdown a specific TF in VSMCs in vitro using small interfering RNA (siRNA) and check for its effect on extRAAS genes expression. Since IRF5 had been recently correlated to atherosclerotic lesion development[453], our first TF knockdown trial was done on IRF5 gene. IRF5 knockdown was done using Silencer® Select pre-designed siRNA against IRF5 supplied by Thermo Fisher Scientific (Cat. # 4392420). siRNA transfection was done using INTERFERin® transfection reagent (supplied by Polyplus Transfection™) according to the manufacturer's instructions (Figure III.11).

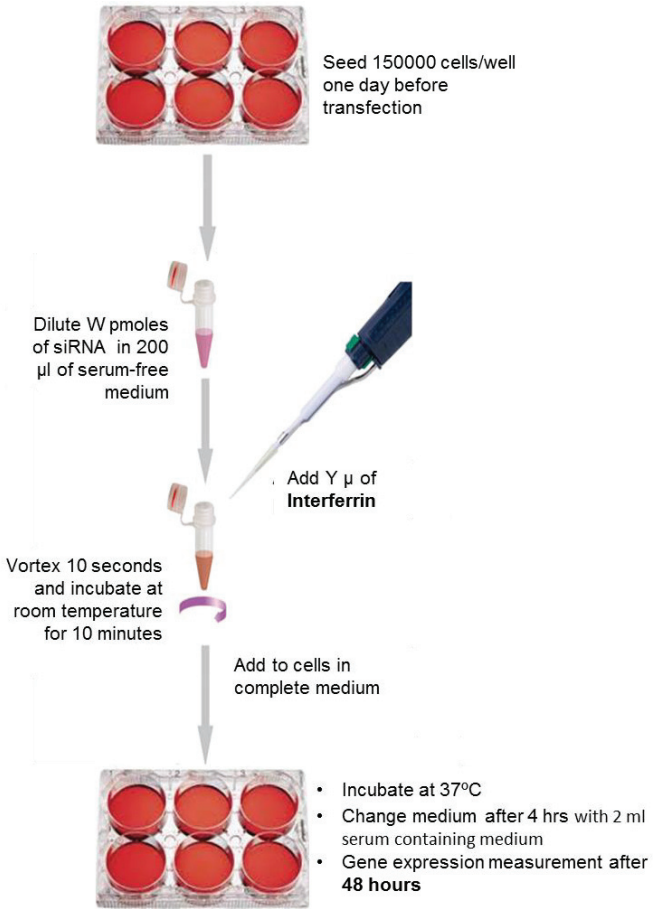

Figure III.11: siRNA transfection protocol using Transferrin transfection reagent. 150000 cells/well were seeded in 2 ml of control medium in a six well plate one day before the transfection. The next day, the desired amount (W) of siRNA to obtain the final desired concentration in 2 ml was diluted in 200µl of serum-free medium. The siRNA mix was then mixed with a specific volume of Transferrin, vortexed and stored 10 minutes at room temperature. The transfection mixture was then added into the cells in culture. The medium was changed 4 hours after transfection to reduce toxicity. Gene expression measurement was done 48 hours after transfection.

To set up the transfection protocol, transfection was done on 150000 cells in 6 wells plate using the following combinations of siRNA concentration and transfection reagent volume (IRF5-siRNA, INTERFERin): (5nM; 8µl) and (10nM; 12µl). Control cells were transfected with scrambled random siRNA (Cat. # sc-37007) using the same conditions. The transfection protocol is presented in figure 3.4. The different volumes of the reagents used are presented in Table III.3.

Table III.3: the different amounts of reagents used for siRNA transfection.

Conditions (siRNA concentration, Transferrin volume)	**# cells seeded**	**Volume of siRNA from a 5µM stock**	**Volume of serum-free medium**	INTERFERin **Volume**	**Final culture volume**
(5nM; 8µl)	150000	2.2	200	8	2.2
(10nM; 12µl)	150000	4.4	200	12	2.2

Gene expression measurement using RT-qPCR was done 48 hours after transfection for the following genes: 18S, IRF5, GR, MR, AGTR1, CTSA, ACE and MME. Results were expressed as the target over 18S RNA concentration ratio. The primer sequences used for gene measurement are presented in Table III.4.

Table III.4: primer features for measurement of extRAAS genes after IRF5 knockdown.

Gene symbol	Primers	Amplicon size	Melting Temp °C
MAX	GAACGAAAACGTAGGGACCA	152	60
	AAGGTGTGGCATTTCTGCAT		
ETS1	TTGGAAAAGCAAAACGCTCT	174	60
	CCCCGAGAATCCACTGATAA		
NR3C1	TAAGGACGGTCTGAAGAGCCA	122	60
	GATAAAACCGCTGCCAGTTCT		
CTSA	GTGCCCAGCCATTTTAGGTA	160	60
	AAGCAGCTGTTGTGTTGGTG		
MME	ACAGTCCAGGCAATTTCAGG	208	60
	CCTAGGGCCCATTTTCTTTC		
EP300	CAGATTGATCCCAGCTCCAT	215	60

	GAAAGAAGACTCGGCGTTTG		
LNPEP	TGAGTGACAAAGACCGAGCC	135	60
	CTTCGGTGATGGGTGCAGTA		
NR3C2	TTGCCTTGAGCTGGAGATCG	125	60
	GTGCATCCCCTGGCATAGTT		
SMAD1	AGCCGATGGACACAAACATG	74	60
	TAAGCAACCGCCTGAACATC		
AGTR1	TTTTCGTGCCGGTTTTCAGC	100	60
	TGCAACTTGACGACTACTGC		
IRF5	AGTGGATTTGGGCCAAGAAG	120	60
	TGCTCATGGCTGAATTTCCC		
ACE	GTGTGGAACGAGTATGCCGA	106	60
	GGGTGTGGTTGGCTATTTGC		

IV. RESULTS

IV.1 SCIENTIFIC ARTICLE I

Tissue distribution of renin-angiotensin-aldosterone system (RAAS) has attracted much attention because of its physiological and pharmacological implications; however, a clear definition of what is a tissue RAAS is still missing. The response of a tissue to the system is defined by the local organization of RAAS favoring specific pathways. Based on the hypothesis that a tissue-specific RAAS organization will refer to the co-expression of genes coding for specific subset of the potential participants, we investigated using public microarray data such organization of an extended RAAS (extRAAS) across 24 different normal human tissues. We defined extRAAS as the set of 36 genes encoding classical and newly discovered RAAS participants including substrate, enzymes and receptors. Microarray datasets were downloaded from the GEO database then filtered for normal samples (not diseased, no infection, not post-mortem). Only those containing more than 10 normal samples were retained. The R software was used to extract the mean expression levels and to cluster the 36 extRAAS genes (hierarchical clustering using correlation and Ward's agglomeration method) in each dataset. Reproducibility of gene clusters between the different datasets within each tissue was used to extract the extRAAS co-expression modules. Maps of the tissue-specific organization of extRAAS were constructed for each of the 24 tissues based on expression levels and coordination data. Our analysis included 152 datasets representing 24 different tissues (2 to 32 datasets per tissue) containing overall 5252 samples fulfilling the inclusion criteria. Expression data provided an overview of the local participants and thus the possible physiological response in a specific tissue. Gene coordination indicates the existence, at the mRNA level, of tissue specific modules organized or not around core groups of transcripts. Two core groups are composed of peptidases: 1) Cathepsin A and Cathepsin D, with or without other enzymes, and 2) Cathepsin G, Carboxypeptidase A3 and Chymase. The existence of these clusters of peptidases suggests that the coordinated expression may exert a strong effect in orientating the metabolism of angiotensin I. One core group involves receptors (GR, MR with AGTR1) that may orientate cell sensitivity. The latter core group may show certain negative coordination with the groups of enzymes in certain tissue (i.e. adipose). Using publicly available data with simple and robust statistical analysis applied to several independent large samples of human material, we propose a preliminary atlas of the organization of RAAS across 24 different normal human tissues. These maps showing expression levels and coordination of genes may help understand tissue specific effects of

RAAS and its targeting drugs. Tissue-specific modules indicate transcriptional coordination that may provide a frame for the identification of tissue specific modulators of RAAS.

SCIENTIFIC REPORTS

OPEN

Atlas of tissue renin-angiotensin-aldosterone system in human: A transcriptomic meta-analysis

Received: 12 November 2014
Accepted: 09 March 2015
Published: 20 May 2015

Ali Nehme[1,2], Catherine Cerutti[1], Nedra Dhaouadi[1], Marie Paule Gustin[1], Pierre-Yves Courand[1], Kazem Zibara[2] & Giampiero Bricca[1]

Tissue renin-angiotensin-aldosterone system (RAAS) has attracted much attention because of its physiological and pharmacological implications; however, a clear definition of tissue RAAS is still missing. We aimed to establish a preliminary atlas for the organization of RAAS across 23 different normal human tissues. A set of 37 genes encoding classical and novel RAAS participants including gluco- and mineralo-corticoids were defined as extended RAAS (extRAAS) system. Microarray data sets containing more than 10 normal tissues were downloaded from the GEO database. R software was used to extract expression levels and construct dendrograms of extRAAS genes within each data set. Tissue co-expression modules were then extracted from reproducible gene clusters across data sets. An atlas of the maps of tissue-specific organization of extRAAS was constructed from gene expression and coordination data. Our analysis included 143 data sets containing 4933 samples representing 23 different tissues. Expression data provided an insight on the favored pathways in a given tissue. Gene coordination indicated the existence of tissue-specific modules organized or not around conserved core groups of transcripts. The atlas of tissue-specific organization of extRAAS will help better understand tissue-specific effects of RAAS. This will provide a frame for developing more effective and selective pharmaceuticals targeting extRAAS.

Since the identification of renin by Tigerstedt and Bergmann in 1898, the renin-angiotensin-aldosterone system (RAAS) has been extensively studied. It is a major therapeutic target in cardiovascular diseases (CVD) due to its important role in maintaining cellular and tissue physiology[1,2].

In its classical endocrine view, angiotensinogen (AGT), produced by the liver, is cleaved in the plasma by the tightly regulated renin, produced by the kidney. This results in the release of the amino terminus decapeptide angiotensin I (1–10) (Ang I). Ang I is further processed by the angiotensin converting enzyme (ACE) which releases the active (1–8) octapeptide angiotensin II (Ang II). The latter binds to its specific membrane receptors and elicit cellular effects. The system is currently characterized by an increased complexity, with the discovery of new functional components such as the receptors for renin, for the heptapeptide angiotensin (1–7) and for the hexapeptide angiotensin IV (3–8), in addition to the enzymes leading to the production of active angiotensin peptides from Ang I. Until recently, renin was thought to be the rate limiting factor for the production of these active peptides due to its high specificity and affinity for angiotensinogen. However, the recent discovery of the angiotensin (1–12) peptide as a potential alternative of Ang I for cleavage by ACE, chymase or neprilysin raised the possibility of alternative renin-independent pathway(s) for the generation of active peptides from AGT[3,4]. Moreover,

[1]EA4173, Functional genomics of arterial hypertension, Hôpital Nord-Ouest, Villefranche-sur-Saône; Université Lyon1, Lyon, France. [2]ER045, Laboratory of stem cells, Department of Biology, Faculty of sciences, Lebanese University, Beirut, Lebanon. Correspondence and requests for materials should be addressed to K.Z. (email: kzibara@ul.edu.lb) or G.B. (email: giampiero.bricca@inserm.fr)

the known activity of cathepsin D, cathepsin G and tissue kallikrein to directly accept angiotensinogen, as a substrate to release Ang I or Ang II, further strengthens this hypothesis[5]. Altogether, this leads to the concept of tissue RAAS that was shown to act at the paracrine and autocrine levels, independently from the circulating RAAS.

Tissue RAAS has attracted much attention because of its physiological, pharmacological and therapeutic implications[6]. In fact, tissue RAAS is often investigated in the context of expression of specific enzymes or receptors, pharmacological responses to specific peptides, or pharmacological inhibition of specific enzymes. However, very few studies simultaneously compared several components of RAAS in several tissues[7,8]. We have compared the expression of several components of RAAS in the atheroma plaque relative to nearby low grade remodeling tissue. Indeed, we found that a specific pattern of expression modifications of both receptors and enzymes was found to be associated with the remodeling process[9,10]. Moreover, we showed that the trans-differentiation of vascular smooth muscle cells (VSMCs) could establish a positive loop between angiotensin II and corticosteroids signaling, thus functionally linking both systems[11]. In addition, this suggested that along with the expression levels, correlations between transcripts could hold a tissue- or process-specific property.

Based on literature and results obtained in our laboratory, we defined an extended renin-angiotensin-aldosterone system (extRAAS) which includes 37 gene products[3,11–15]. The extRAAS system contains the classical systemic RAAS participants (AGT-REN-ACE-AGTR1) in addition to novel enzymes and receptors[13,16] described at the tissue level (Fig. 1, see also Supplementary Table S1).

Our hypothesis is that a tissue-specific extRAAS organization should refer to the co-expression of genes coding for specific subsets of potential participants. In this study, we aimed to address the organization of extRAAS components in several human tissues. Owing to the availability of large public transcriptomic databases, we established the first atlas of tissue extRAAS in a large set of human tissues. Using this atlas, we showed that tissue specificity could be achieved through a specific pattern of expression and coordination of transcripts.

Material and Methods

Microarray data sets. Published microarray data sets of different human tissues were downloaded from the Gene Expression Omnibus database (http://www.ncbi.nlm.nih.gov/geo/). Data sets were then filtered for normal tissues, by excluding cell culture samples, post mortem tissues, diseased tissues (cancer or other), and tissues from pharmacologically treated individuals. Age, gender, and ethnicity were not taken into account in selecting the data sets. Only data sets with more than 10 normal samples were retained. Affymetrix microarray data sets were exclusively selected and only those containing all the probe sets were included for further analysis. The detailed procedure is shown in Fig. 2.

Expression level and quality control. After filtering, data sets were checked for the expression distribution of their individual samples. Data sets which showed large variability among samples were then eliminated. Data sets were normalized by their authors using different methods including robust multichip average (RMA), GC-RMA or a global score method[17]. Since data sets were obtained from different experiments, the data sets lacking any transformation were log2-transformed. In order to compare expression data between different data sets, the centile rank of a gene was calculated using R-software by normalizing its mean expression level relative to the mean expression data distribution over the microarray. As a quality control step to remove outliers, data sets of a given tissue were then hierarchically clustered based on the obtained centile rank of extRAAS gene expression (Cluster 3.0 software using the average linkage method, http://bonsai.hgc.jp/~mdehoon/software/cluster/, and Java TreeView 3.0, http://jtreeview.sourceforge.net free software tools)[18]. Non-clustered data sets were then eliminated from the study.

ExtRAAS expression profiles across tissues and tissue dendrogram. In order to reflect the relative abundance of extRAAS transcripts in a given tissue, the mean expression centile rank (MCR) of genes was calculated across data sets. After log transformation of MCR, a tissue dendrogram was built by hierarchical clustering of tissues based on the correlation between MCR profiles of extRAAS (Cluster 3.0 and TreeView 3.0). Principle component analysis (PCA) was also applied on tissues based on standardized MCR values, using the R software (ade4 package). Projection of tissues on the 3 principal axes (rgl package) was used to disclose specific groups of tissues[19].

Clustering of extRAAS genes per data set. The R software was used for statistical description and clustering of the 37 extRAAS gene transcripts in each data set, using the "Cluster" R library. ExtRAAS gene transcripts were hierarchically clustered in each data set using Pearson correlation distance and Ward's agglomeration method[20]. Each of the obtained dendrograms was then cut at a given level to identify the gene clusters. The cut-off level was chosen on the basis of a balance between the level of clustering strength, assessed with the agglomerative coefficient and a minimum of 3 gene transcripts per cluster.

Identifying local extRAAS co-expression modules. For a given tissue, a co-expression module was defined as a set of 2 or more genes that were coordinated across data sets. The average coordination

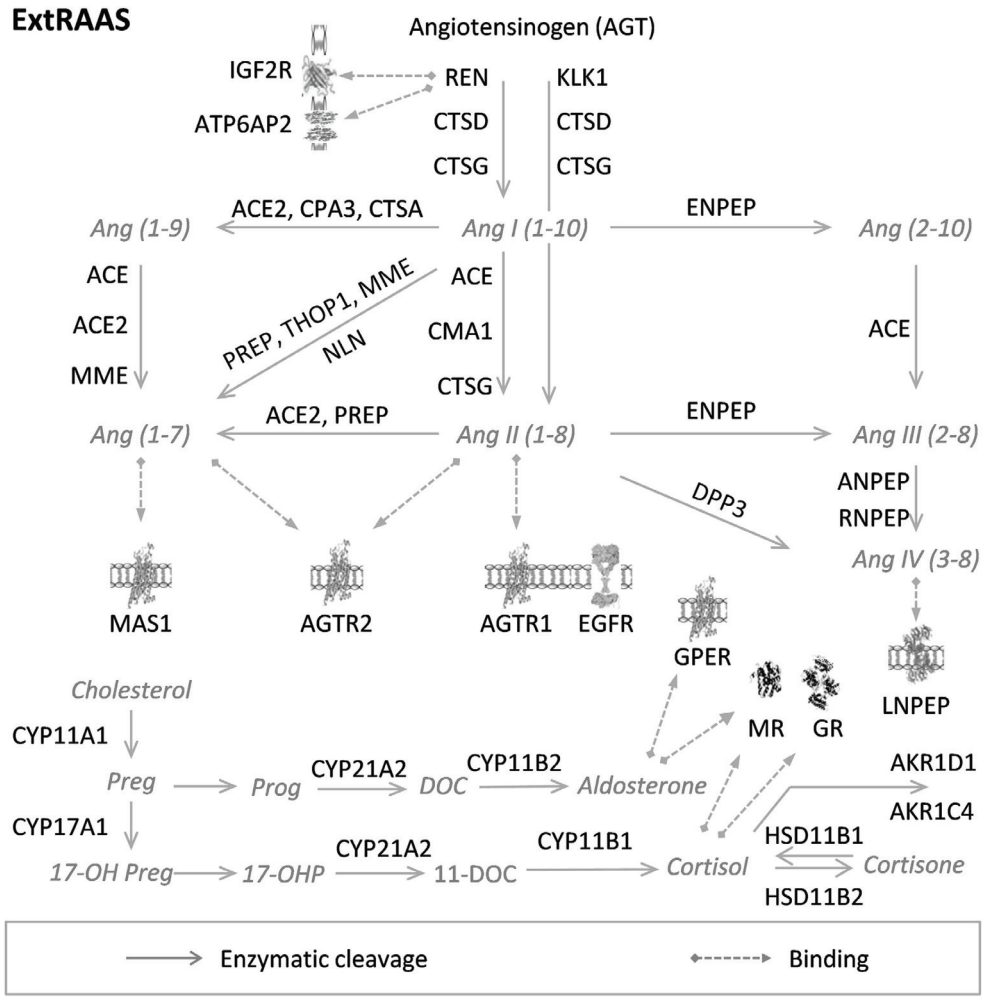

Figure 1. Extended Renin Angiotensin Aldosterone System (ExtRAAS). The metabolic cascades of angiotensin peptides, and cortico-and gluco-corticoid pathways have been represented using symbols of genes coding for the substrate, the enzymes and the receptors involved in the pathway. Angiotensin peptides and steroid hormones are represented in grey using their usual abbreviation. Ang, Angiotensin; Preg, Pregnanolone; Prog, Progesterone; DOC, deoxycortisol; 17-OHP, 17-OH Progesterone; ACE, angiotensin I converting enzyme; ACE2, angiotensin I converting enzyme type 2; AGTR1, angiotensin II type 1 receptor; AGTR2, angiotensin II type 2 receptor; AKRIC4, aldo-keto reductase family 1, member C4; AKRID1, aldo-keto reductase family 1, member D1; ANPEP, alanyl-aminopeptidase; ATP6AP2, prorenin/renin receptor; CMA1, chymase 1; CPA3, carboxypeptidase A3; CTSA, cathepsin A; CTSD, cathepsin D; CTSG, cathepsin G; CYP11A1, cytochrome P450, family 11, subfamily A, polypeptide 1; CYP11B1, cortisol synthase; CYP11B2, aldosterone synthase; CYP17A1, cytochrome P450, family 17, subfamily A, polypeptide 1; CYP21A2, cytochrome P450 enzyme, family 21, subfamily A, polypeptide 2; DPP3, dipeptidyl-peptidase 3; ENPEP, glutamyl aminopeptidase (aminopeptidase A); GR, glucocorticoid receptor; HSD11B1, hydroxysteroid (11-beta) dehydrogenase 1; HSD11B2, hydroxysteroid (11-beta) dehydrogenase 2; IGF2R , insulin-like growth factor 2 receptor; KLK1, tissue kallikrein; LNPEP, leucyl/cystinylaminopeptidase; MAS1, MAS1 proto-oncogene; MME, membrane metallo-endopeptidase; MR, mineralocorticoid receptor; NLN, neurolysin (metallopeptidase M3 family); PREP, prolylendopeptidase; REN, renin; RNPEP, arginyl aminopeptidase (aminopeptidase B); THOP1, thimetoligopeptidase 1. Images of IGF2R[36], ATP6AP2[37], MR[38], GR[39], G-protein coupled receptors (AGTR1, AGTR2, GPER and MAS1)[40] and LNPEP[41] were obtained from the Protein Data Bank in Europe (PDBe) with respective PDBe IDs: 2YDO, 3LBS, 1P93, 4P8Q, 2AA2. Image of EGFR[42] was obtained from Protein Data Bank DOI:10.2210/rcsb_pdb/mom_2010_6.

rate of genes within a module was calculated as the average percentage of coordinated genes within a module that were always clustered together across the different data sets in a specific tissue. A threshold of > 55% was the criterion used to define gene modules that were representative for a specific tissue.

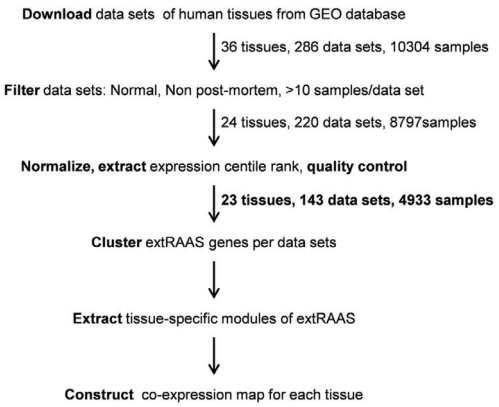

Figure 2. Experimental workflow. Microarray data sets obtained from tissue samples were downloaded from the Gene Expression Omnibus (GEO) database; then filtered for normal samples based on exclusion criteria. The data sets passing quality control were selected and their expression data were normalized by centile rank transformation. Each of the data sets was then submitted for extRAAS hierarchical clustering and expression profiling. The resulting dendrograms were then used to assess the level of reproducibility of the different clusters across different data sets obtained from the same tissue. Genes that were most often clustered together in different data sets of the same tissue were annotated as tissue-specific modules. For each tissue, a co-expression map was elaborated using both expression level and tissue-specific module belonging of each extRAAS gene.

Statistical analysis. For centile rank expression levels, one MCR value was computed per tissue and one mean MCR for all tissues. These MCR values were presented as (1) mean ± SD to show intra- and inter-tissue variation in extRAAS gene expression and (2) mean ± SEM to describe specific gene expression.

Results

Microarray data sets. Following filtering and applying the exclusion criteria, normalization of the data sets for normal tissues was done as described in Fig. 2. After quality control, 77 outlier data sets were removed from a total of 220. The retained 143 data sets contained a total of 4933 samples corresponding to 23 different tissues (Table 1, see detailed list in Supplementary Table S2). These tissues belong to different systems and have different physiological functions and embryological origins. The total number of data sets was variable between tissues and ranged between 2 (thyroid) and 17 (whole blood), whereas the total number of samples per tissue ranged between 54 (embryo) and 774 (whole blood). The average number of data sets per tissue was 6 ± 4, whereas that of samples per tissue was 214 ± 178. Some tissues, such as adrenal gland, vascular wall or brain, were absent from this study because it was impossible to obtain non post-mortem normal samples from these tissues.

ExtRAAS gene expression. Among the 37 extRAAS genes, neurolysin peptidase (NLN) was excluded from the analysis since it was not represented by any probe set in most of the microarray platforms. The MCR expression level of the remaining 36 extRAAS genes in each tissue was then calculated as the mean centile rank (MCR) of a gene transcript across data sets; thus supplying a complete and comparative assessment of mRNA abundance across tissues (Supplementary Table S3 and Supplementary Fig. S1). Using the MCR data, distribution of gene expression across tissues displayed the previously known classical RAAS features. The highest expression levels of key markers were found in their respective tissues[1], such as AGT in the liver, renin in the kidney, and ACE in the lung (Fig. 3a, 3b and 3c, respectively). Moreover, aldosterone sensitive tissues such as the kidney and the colon, along with skin and thyroid gland, contained the highest levels of HSD11B2 transcript (Fig. 3f). The MCR data revealed novel features for other extRAAS gene expression. For instance, the glucocorticoid receptor (GR) and the two potential prorenin and renin receptors, ATP6AP2 and IGF2R, were among the most abundant mRNAs in all tissues (Figs. 3g, 4a and 4b, respectively). Tissue-specific features could also be identified for the first time at the signal response level through AGTR2, MAS1, LNPEP-IRAP (Fig. 4d–f), GPER and EGFR (see Supplementary Fig. S1). In fact, MAS1 (Fig. 4e) and ACE2 (Fig. 4c) were highly expressed in the kidney and skeletal muscle while the LNPEP-IRAP (Fig. 4f) receptor was abundantly present in the omental adipose tissue, heart and pancreas, but not in the kidney. Similarly, this systematic comparison demonstrated new features such as the higher level of AGTR2 mRNA (Fig. 4d) in the large airways epithelium (bronchi) compared to small airways epithelium (bronchioles). On the other hand, HSD11B2 was expressed at relatively low levels in both types of airway tissues (Fig. 3f). Notably, lymphocytes were

Organ system	Tissue	Data sets	Samples
Urinary system	Kidney	4	84
Cardiovascular system	Heart	4	140
Adipose tissue	Sub-cutaneous adipose	9	474
	Omental adipose	4	86
Respiratory system	Large airways epithelium	5	101
	Small airways epithelium	8	357
	Lung	5	210
Reproductive system	Ovary	5	55
Fetal	Embryo	3	54
Digestive system	Colorectum	8	171
	Esophagus	3	83
	Liver	5	93
	Pancreas	3	100
	Oral mucosa	4	193
Blood	Lymphocytes	4	142
	Leukocytes	4	222
	PBMC	11	303
	Whole Blood	17	774
Other organ systems	Skin	7	222
	Thyroid	2	66
	Skeletal muscle	14	556
	Breast	6	239
	Bone marrow stem cells	8	208
Total	23	143	4933

Table 1. List of the studied human tissues. The final list of data sets obtained after filtering for normal samples and quality control. All selected data sets were obtained on the Affymetrix microarrays platform.

the only circulating blood cells found to contain high amounts of all angiotensin, renin and mineralocorticoid receptors mRNAs.

Classification of tissues according to extRAAS expression. Tissue dendrogram was drawn using MCR of extRAAS genes per tissue (Fig. 5). Interestingly, tissues belonging to the same system were clustered together. For example, peripheral blood mononuclear cells, whole blood cells, leukocytes and lymphocytes were found to be grouped with bone marrow. In addition, the epithelia from large and small respiratory airways were very close, as were omental and subcutaneous adipose tissues. On the other hand, the thyroid gland showed an extremely different expression profile and was not clustered with any of the other tissues. Finally, aldosterone-sensitive tissues (e.g. skin, colorectal and kidney), found to have high levels of HSD11B2 mRNAs, were not closely clustered. Similar results were obtained using PCA (data not shown).

ExtRAAS gene clustering in each data set. Hierarchical clustering of extRAAS genes in each data set indicated that all 36 genes could be strongly clustered with a mean agglomerative coefficient above 0.7, by default between 0 and 1, for all of the data sets in all tissues except lymphocytes, skeletal muscles and small airways. This showed that a clustering structure clearly exists within extRAAS transcripts.

ExtRAAS genes co-expression modules. Local extRAAS modules of co-expressed genes were then identified by calculating the average coordination rates of gene sets across data sets within tissues. Table 2 shows extRAAS co-expression modules and the corresponding gene expression levels for the kidney, heart, skin, and omental adipose tissues. A minimum of 5 modules per tissue was found in the kidney, omental adipose and total blood tissues, and a maximum of 8 modules was found in 10 tissues including the thyroid gland, liver, lung and subcutaneous adipose tissues (Supplementary Table S4). The largest module, comprising 11 transcripts, was found in the kidney. This module contained AGT, REN, ACE and ACE2 along with transcripts of other enzymes involved in the metabolism of angiotensin.

By comparing the modules in the different tissues, we found 3 types of transcript groups: (1) the first type comprised modules that were based on the presence of a "core group" of transcripts correlated in

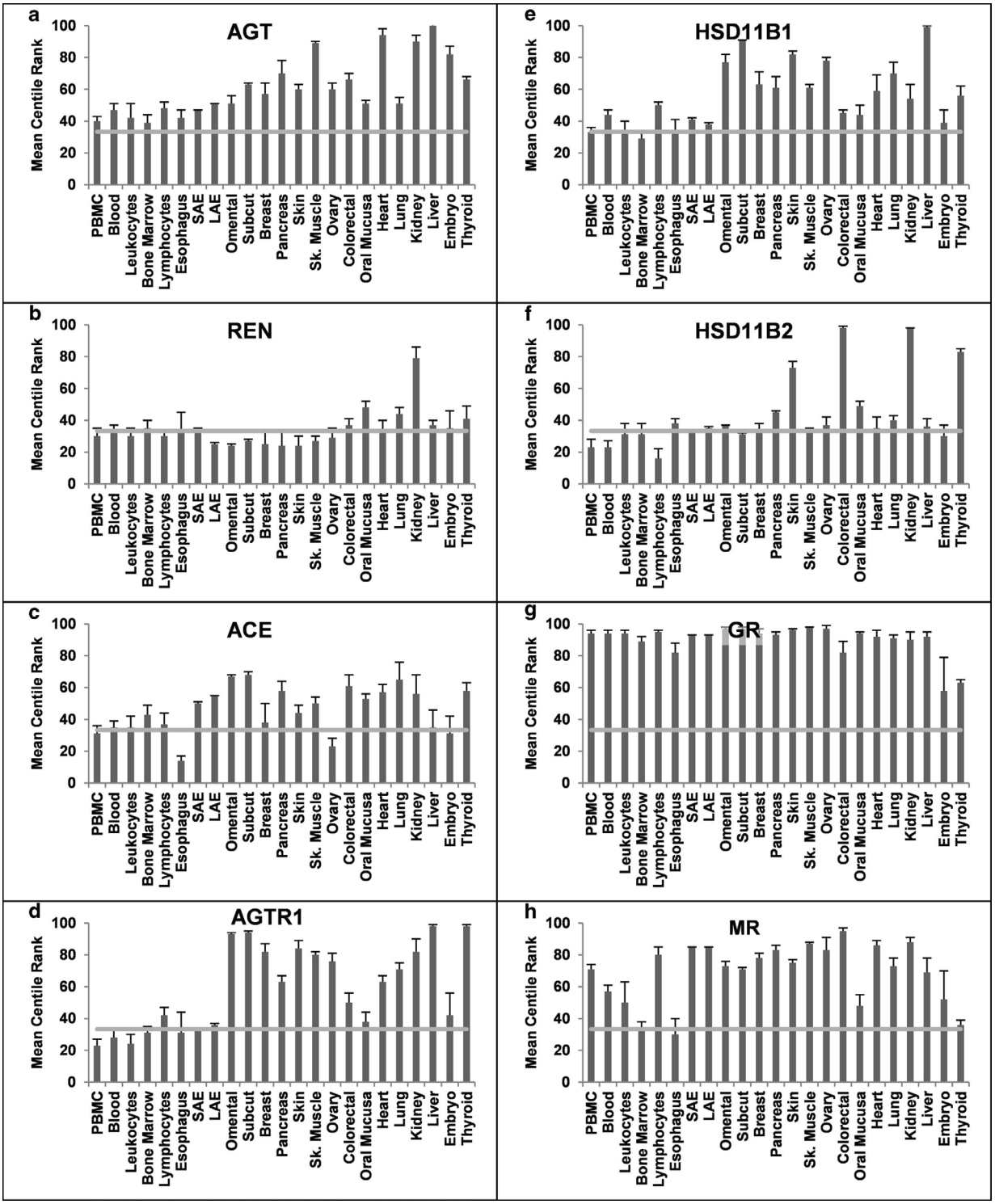

Figure 3. mRNA expression profile of classical RAAS and Corticosteroid system (COS) across tissues. The relative abundance of gene transcripts in each tissue is expressed as the mean expression centile rank (MCR) across data sets (Mean ± SEM). Classical RAAS genes (**a**-**d**): AGT, angiotensinogen; REN, renin; ACE, angiotensin converting enzyme; AGTR1, angiotensin II type 1 receptor. COS genes (**e**-**h**): HSD11B1, 11beta hydroxysteroid dehydrogenase type 1; HSD11B2, 11beta hydroxysteroid dehydrogenase type 2; GR, glucorticoid receptor; MR, mineralocorticoid receptor; PBMC, peripheral blood mononuclear cells; SAE, small airways epithelium; LAE, large airways epithelium; Omental, Omental adipose tissue; Subcut, subcutaneous adipose tissue; Sk. Muscle, Skeletal muscle.

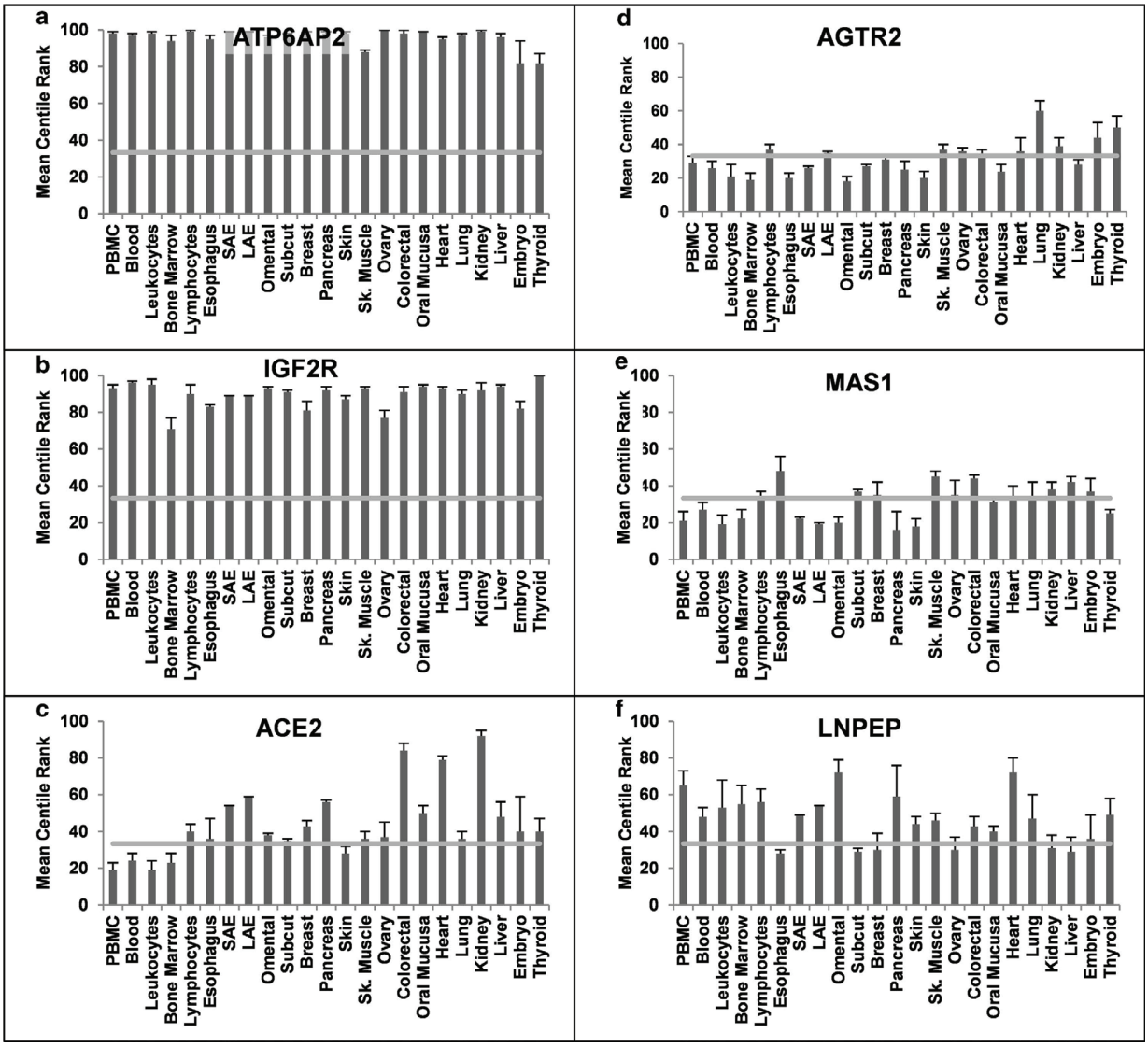

Figure 4. mRNA expression profile of key components of extRAAS across tissues. The relative abundance of gene transcripts in each tissue is expressed as the mean expression centile rank (MCR) across data sets (Mean ± SEM). (**a**-**b**). Renin receptors: ATP6AP2, ATPase, H + transporting, lysosomal accessory protein 2; IGF2R, insulin-like growth factor 2 receptor. **c**. ACE2, angiotensin converting enzyme type 2. (**d**-**e**). Angiotensin peptides receptors: AGTR2, angiotensin II type 2 receptor; MAS1, Ang (1–7) receptor; LNPEP, angiotensin IV receptor. PBMC, peripheral blood mononuclear cells; SAE, small airways epithelium; LAE, large airways epithelium; Omental, Omental adipose tissue; Subcut, sub-cutaneous adipose tissue; Sk. Muscle, Skeletal muscle. Expression profiles for the other investigated tissues are provided in supplemental data.

more than 50% of tissues. A total of 3 such modules were isolated, 2 of which were proteolytic enzymes modules. The first proteolytic module is based on CTSA and CTSD core group. These 2 transcripts were found to be coordinated with other proteolytic enzymes in numerous tissues, including the kidney. In fact, these 2 transcripts were coordinated with 9 other transcripts in the kidney and omental adipose tissue, making them the two largest modules detected. This module never contained receptors with the exception of the pancreas where both prorenin-renin receptors, ATP6AP2 and IGF2R, together with GR were associated (Supplementary Table S4). The second module of proteolytic enzymes was based on the core group of CPA3, CTSG, and CMA1 transcripts, which were often clustered together without any other genes (Table 2). This module was typically found in the subcutaneous adipose tissue, pancreas and skin. Interestingly, this module lacks CMA1 in the heart, which is replaced by ACE and included AGTR1. The third core group-based module contained receptor-coding transcripts: AGTR1, MR and GR (Table 2 and Supplementary Table S4). This cluster of receptors often contained only GR and MR.

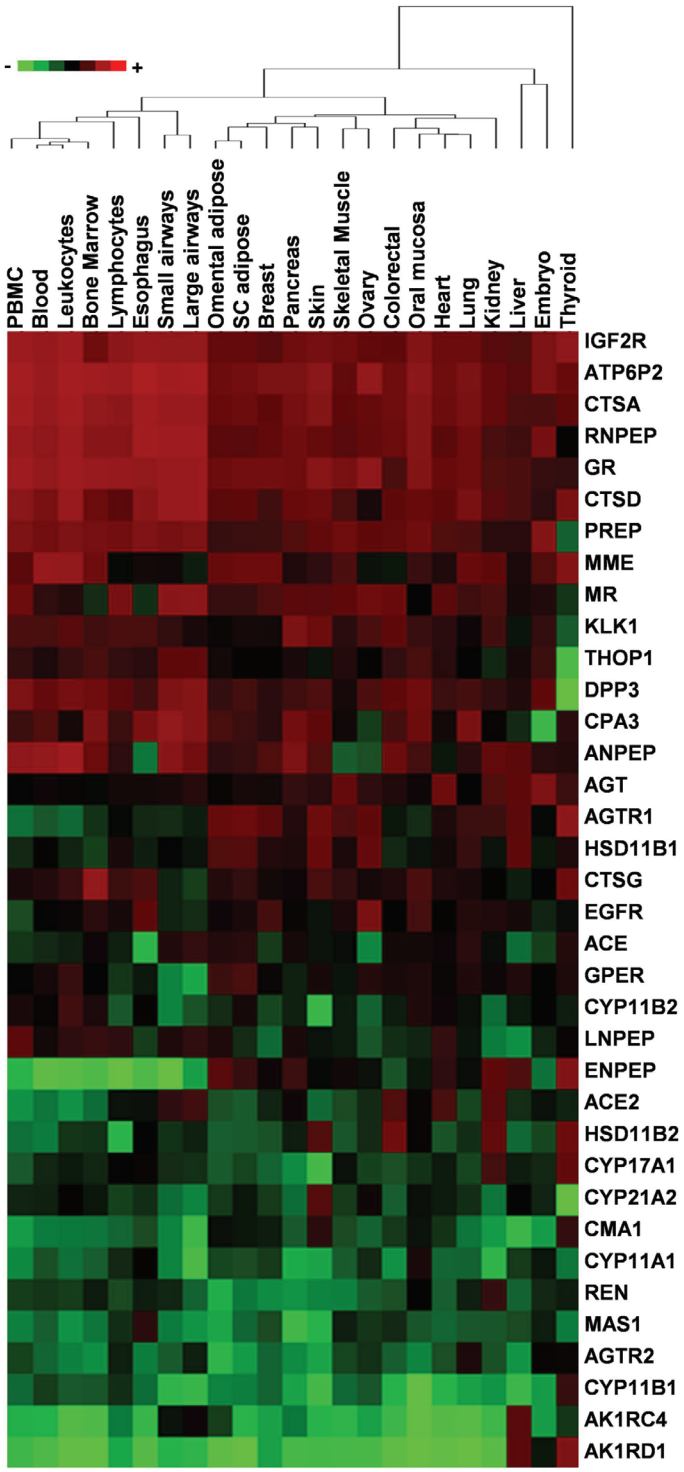

Figure 5. ExtRAAS-based tissue clustering. The tissue dendrogram was drawn based on the average linkage method (cluster 3.0 software) using the logged and normalized mean centile expression rank of extRAAS genes. Colors of the heatmap correspond to the relative log (MCR) in each tissue. PBMC, peripheral blood mononuclear cells.

(2) The second type of transcripts group constituted co-expression modules detected only in a single tissue. For example, only the heart tissue contained the IGF2R-MME-HSD11B1-AKR1D1 module (Table 2). At least one such module was detected in each tissue (Supplementary Table S4).

Tissues (data sets, samples)	Module 1		Module 2		Module 3		Module 4		Module 5		Module 6	
Kidney (4, 84)	84%		88%		85%		94%		80%			
	CTSA	**99**	ATP6AP2	99	**CTSG**	**59**	THOP1	48	PREP	74		
	ANPEP	98	**GR**	**90**	AGTR2	39	CYP11B2	34	**CPA3**	**60**		
	ENPEP	97	**MR**	**88**	MAS1	38	CYP21A2	32	HSD11B1	54		
	MME	97	**AGTR1**	**82**	AKR1C4	19	**CMA1**	**26**	LNPEP	31		
	ACE2	92			AKR1D1	11			CYP11A1	21		
	CTSD	**92**										
	AGT	90										
	CYP17A1	85										
	KLK1	84										
	REN	75										
	ACE	56										
Heart (4, 140)	77%		75%		80%		100%		81%		81%	
	CTSA	**94**	**GR**	**92**	**CTSG**	**64**	EGFR	54	KLK1	68	IGF2R	93
	AGT	94	ENPEP	69	**AGTR1**	**63**	REN	33	**CMA1**	**41**	MME	64
	CTSD	**88**			**CPA3**	**59**	MAS1	32	HSD11B2	35	HSD11B1	59
	DPP3	74			ACE	57			CYP11B1	20	AKR1D1	8
	THOP1	67			AKR1C4	11						
Skin (7, 222)	81%		57%		90%		71%		57%		71%	
	GPER	54	AGTR1	84	**CPA3**	**78**	THOP1	44	**GR**	**96**	ATP6AP2	98
	ACE	44	**MR**	**75**	**CTSG**	**70**	REN	24	HSD11B2	73	ACE2	28
	CYP11B2	16			**CMA1**	**60**						
Omental adipose (4, 86)	91%		83%		83%		85%		75%			
	ATP6AP2	96	**GR**	**97**	ACE	67	AGT	51	PREP	74		
	CTSA	**95**	MME	96	KLK1	57	ACE2	38	LNPEP	72		
	CTSD	**89**	**AGTR1**	**93**	CYP11B2	46	REN	24				
	RNPEP	86	IGF2R	93	CYP21A2	44	MAS1	20				
	HSD11B1	77	ENPEP	88	CYP11A1	37	AKR1D1	9				
	CPA3	**75**	GPER	75	HSD11B2	37						
	DPP3	72	**MR**	**73**	CYP17A1	36						
	CTSG	**65**	ANPEP	67	CYP11B1	33						
	THOP1	62	EGFR	67	AGTR2	18						
	CMA1	**51**										
	AKR1C4	49										

Table 2. ExtRAAS tissue modules. This table represents extRAAS co-expression modules (module 1–6) in the kidney, heart, skin and omental adipose tissues (data sets, samples). At the top of each module the average coordination rate is expressed as a percentage shown at the top of each module (average percentage of genes within a module that are always coordinated across the different data sets of a specific tissue). The mRNA abundance of each gene is present next to the gene symbol and is expressed in the mean MCR (mean centile rank, the percent level of the transcript within the transcriptome). Core-groups transcripts are in bold.

(3) The last type of transcripts group comprised the non-clustered transcripts. Their number could vary according to tissues, ranging between 4 in the kidney and up to 22 in the skin. Each of the extRAAS transcripts was found in this group in at least one tissue, except omental adipose which had all extRAAS genes included in co-expression modules.

ExtRAAS tissue atlas. extRAAS maps were built for each tissue using expression levels and co-expression modules (Supplementary Atlas S1). Degradation pathways leading to angiotensin peptides with no known activity, such as angiotensin (5–10) and angiotensin (1–5) pathways, in addition to the angiotensin (1–12) pathway, were not included in the maps. These maps clearly displayed different transcriptional organization between tissues, with only few strong similarities. As shown in Fig. 6, although

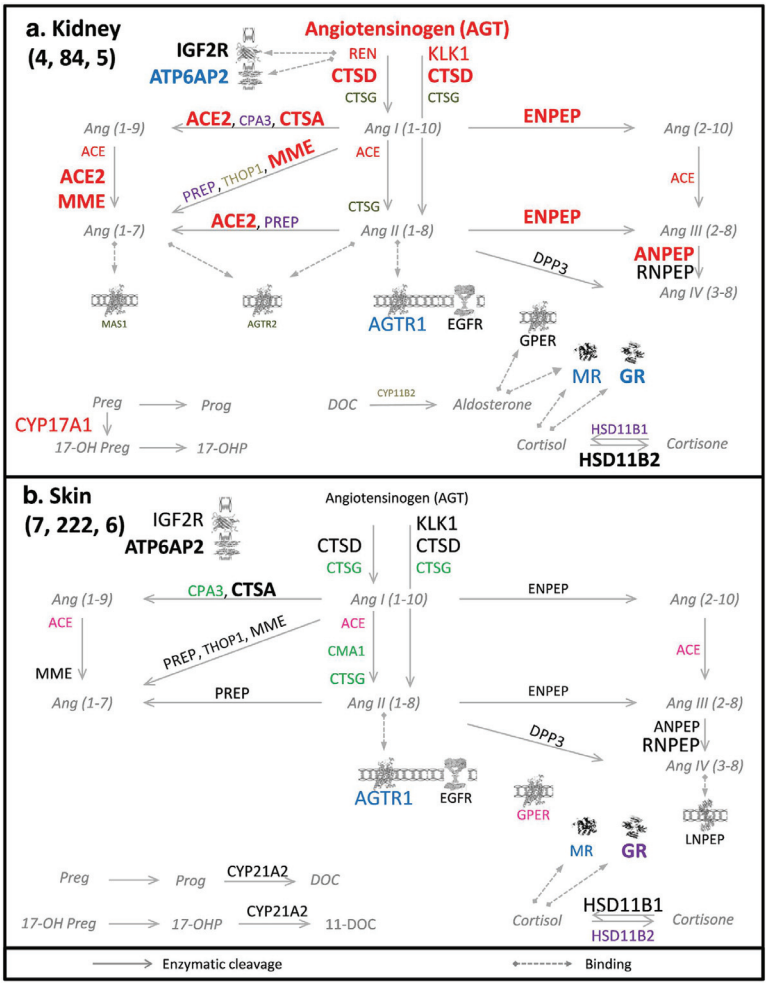

Figure 6. ExtRAAS maps in the kidney (a) and the skin (b). The number of data sets, samples and modules are represented between brackets (data sets, samples, modules) below tissue name in the upper left corner of the figure. Gene transcripts are represented by the corresponding official symbols. Genes are represented based on their coordination (same color = same module) and mean centile expression rank (MCR, different font size). Non-clustered genes are represented in black color. Gene transcripts below the first tertile (MCR < 33.3) in each tissue were excluded for simplicity. Angiotensin peptides and corticosteroid metabolites are represented in gray italics. Images of IGF2R[36], ATP6AP2[37], MR[38], GR[39], G-protein coupled receptors (AGTR1, AGTR2, GPER and MAS1)[40] and LNPEP[41] were obtained from the Protein Data Bank in Europe (PDBe) with respective PDBe IDs: 2YDO, 3LBS, 1P93, 4P8Q, 2AA2. Image of EGFR[42] was obtained from Protein Data Bank DOI:10.2210/ rcsb_pdb/mom_2010_6. Maps for the other investigated tissues are provided in supplemental data.

the kidney and the skin are both aldosterone sensitive tissues linked to water and salt homeostasis, their extRAAS maps showed different patterns of expression and coordination. Not only different expression patterns were observed, with the absence of MAS1, AGTR2, ACE2, REN and CYP17A1 transcripts in the skin compared to the kidney, but also the transcripts present in both tissues had different patterns of co-expression. The kidney showed a large CTSA-CTSD-based module associating highly expressed proteolytic enzymes and including the highly expressed AGT transcript (Fig. 6a, genes in red). In contrast, none of the genes of the red module in the kidney was found to be coordinated in the skin. On the other hand, the smaller proteolytic CTSG-CPA3-CMA1 module was present in the skin, but not in the kidney (Fig. 6b, genes in green). Similarly, the AGTR1-MR-GR-based receptor module was present in the kidney (Fig. 6a, genes in blue), but not in the skin.

In the same way, both the heart and the adipose tissues, which are known for their active local RAAS, showed abundant levels of angiotensin metabolizing enzymes and receptors mRNAs. However, there were large differences in clustering patterns between both tissues. In the heart, the CTSG and CPA3 core transcripts were coordinated with ACE, rather than CMA1 (Fig. 7a). In addition, the CTSA-CTSD proteolytic module was present in the heart (Fig. 7a), including the AGT transcript

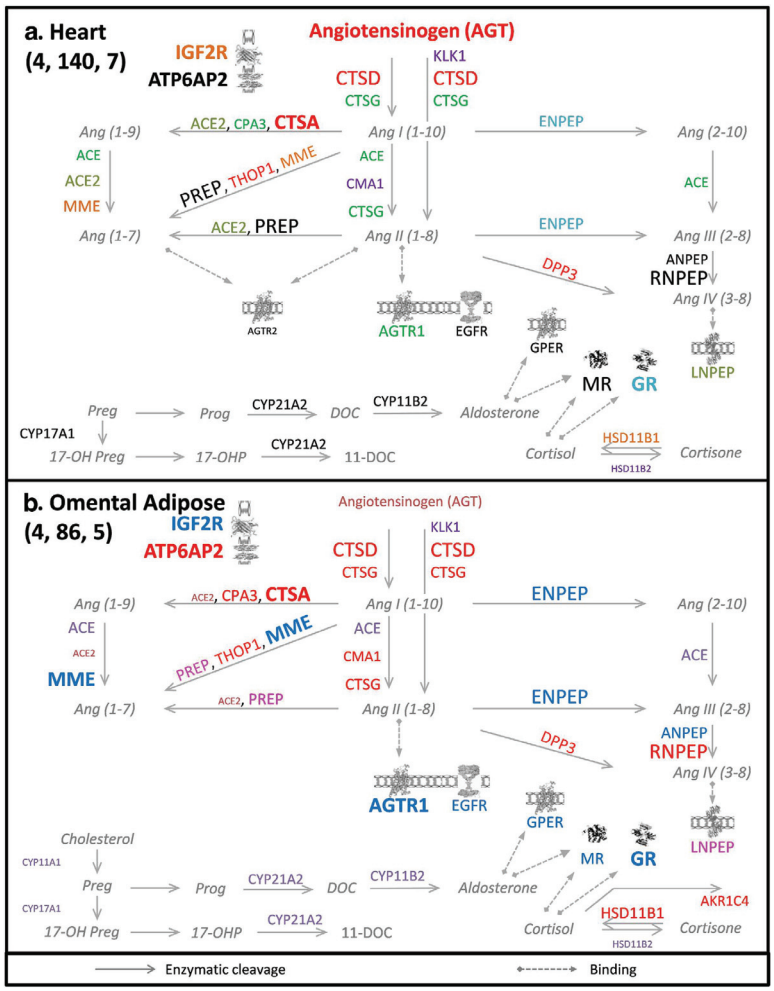

Figure 7. ExtRAAS maps in the heart (a) and the omental adipose tissue (b). The number of data sets, samples and modules are represented between brackets (data sets, samples, modules) below tissue name in the upper left corner of the figure. Gene transcripts are represented by the corresponding official symbols. The genes are represented based on their coordination (same color = same module) and mean centile expression rank (MCR, different font size). Non-clustered genes are represented in black color. Gene transcripts below the first tertile (MCR < 33.3) in each tissue were excluded for simplicity. Angiotensin peptides and corticosteroid metabolites are represented in gray italics. Images of IGF2R[36], ATP6AP2[37], MR[38], GR[39], G-protein coupled receptors (AGTR1, GTR2, GPER and MAS1)[40] and LNPEP[41] were obtained from the Protein Data Bank in Europe (PDBe) with respective PDBe IDs: 2YDO, 3LBS, 1P93, 4P8Q, 2AA2. Image of EGFR[42] was obtained from Protein Data Bank DOI:10.2210/rcsb_pdb/mom_2010_6. Maps for the other investigated tissues are provided in the supplemental data.

and two other enzymes transcripts DPP3 and THOP1). On the other hand, the CTSA-CTSD and the CTSG-CPA3-CMA1 proteolytic modules were combined in the omental adipose tissue (Fig. 7b), forming a larger module that included up to 11 gene transcripts. Moreover, the omental adipose tissue had the largest receptor-containing module which included the GR-MR-AGTR1 core group, GPER, IGF2R and EGFR gene transcripts, in addition to three enzyme-coding transcripts, MME, ENPEP and ANPEP. On the contrary, co-expression of receptor-coding gene transcripts was not detected in the heart.

Although similarities in patterns of expression can be detected between tissues, co-expression similarities were mainly limited to the core group-transcripts. For instance, the omental and adipose tissue were very similar in their expression patterns; however, they had very different patterns of coordination.

Discussion

In this study, we propose for the first time an extensive atlas of the mRNA organization of extRAAS across 23 different normal human tissues. These maps were generated using a large amount of publicly available

transcriptomic data in combination with a statistical meta-analysis, based on hierarchical clustering. Using expression levels and coordination of genes, tissue maps were generated for all 23 tissues. These maps displayed the tissue-specific features and may represent a reference for the analysis of pathological situations. Indeed, we showed that tissue specificity of extRAAS may be achieved through a specific pattern of expression and coordination of transcripts. When comparing the different maps, it appears that tissue-specific co-expression patterns are achieved through the combination of: (1) tissue-specific patterns of mRNA abundance; (2) modules of co-expressed transcripts; and (3) a specific combination of expression and coordination patterns.

Because this study was performed only at the mRNA level, it exclusively explored the gene expression properties of cells composing each tissue. It indicated the existence, at the mRNA level, of tissue-specific modules organized or not around core groups of transcripts. Two such core groups were enzymatic groups of peptidases suggesting that their coordinated expression could exert a strong effect in orienting the metabolism of angiotensin I. The other core group was a receptor group involving GR-MR with AGTR1 which may orient cell sensitivity. It is important to note that the substrate AGT mRNA is abundant in almost all tissues, as previously reported[21]. However, it is clustered only in the kidney and the heart, where it associates within the CTSA-CTSD module. The key quantitative role of AGT gene expression in determining blood pressure has been demonstrated both in humans and animals[22,23]. Our maps suggest that this effect may be associated with increased activity of specific components of the extRAAS in the heart and kidney tissues while the increased AGT expression in other tissues would fuel independent enzymatic pathways.

For each tissue, the meta-analysis included 2 to 17 data sets fulfilling the inclusion criteria. The number of data sets and the number of observations greater than 10 within each data set allowed robust estimation of gene expression levels and robust identification of co-expression modules. The mapping was found to fit perfectly with most known tissue distribution of transcript levels when a threshold was applied at the first tertile of the microarray expression distribution (MCR < 33 taken as non-expressed, Supplementary Atlas S1)[3,24]. In addition, we provide here a primary information in tissues where only scarce information was available, such as the ovary, thyroid gland, pancreas, skeletal muscle, circulating cells, and airways epithelia[25,26] (Supplementary Atlas S1). Interestingly, bone marrow cells showed almost the same map as total blood cells, leukocytes, or peripheral blood mononuclear cells indicating that the transcriptional coordination may be preserved during "cell lineage". Moreover, although the expression patterns were similar in subcutaneous and omental fat, there were important differences between the coordination patterns of both these tissues. This suggests that the differences observed between the two adipose tissues in obese patients[27] may likely be due to local differences in expression regulatory mechanisms.

All tissues appeared to have abundant mRNAs coding for GR and the two potential prorenin-renin receptors ATP6AP2 and IGFR2. Receptors mRNAs were all found to be abundant only in colorectal mucosa, skeletal muscle and lymphocytes. In all other tissues, at least one angiotensin peptide receptor was expressed confirming the very high tissue specificity of the responses through the combined activation of the different subsets of receptors. Interestingly, although there was often a strong coordination between angiotensin signaling receptors and steroid receptors, the metabolic pathways appeared to be structured only for the angiotensin proteases, with rare association with one or the other enzymes of the steroid pathway. The maps also suggest that the "active" metabolic pathways could lead to a dead-end with no receptors for peptides such as LNPEP-IRAP receptor in the kidney, or MAS1 receptor in the heart.

Altogether our results suggest that the extRAAS signaling pathways are regulated at the mRNA level in different tissues according to the 3 following targets that seem to be independent. First, the substrate AGT had scarce and limited coodination, except in the heart and kidney, suggesting that it is involved in other independent regulation(s). Second, the signal generation where the peptidic cascades showed 2 almost independent coordinated modules around CTSA-CTSD and CTSG-CMA1-CPA3, possibly orienting peptide flow. Third, the cell response where there was a strong core group of receptors GR-MR-AGTR1 which provide cell sensitivity. Although strong inter-relationships have been previously described for receptors[28–31], it is the first time that these relationships are detected for extRAAS enzymes. A major difference also appeared between peptide and steroid hormones. While the peptidic angiotensin cascade displayed high tissue organization, few and dispersed coordination was observed in the steroid biosynthetic pathway. Most of the local steroid synthesis regulation seemed to rely not only on CYP11B1 and CYP11B2 but mostly on both HSD11B1 and HSD11B2. On the other hand, the complete aldosterone synthetic pathway was present in adipose tissue, as expected from Biones *et al.*[32], as well as most of the features of local corticoid generation and metabolism[33]. Finally, the non-clustered transcripts, or those with dispersed coordination across tissues, were also of interest because they could represent bottle necks in the pathways and/or be linked to other cellular functions or pathways.

The identified modules of gene transcripts may hold a great functional importance. Their correlations may result from tissue and intercellular properties, but also from intracellular properties. It has been hypothesized from transcriptomic analysis that co-expressed genes may share common regulation either on the transcriptional side or the RNA degradation one. Indeed, we recently showed, in the field of TGFβ regulation in the human arterial wall, that the coordination between transcripts could be reproduced in cell culture as the result of common transcription factors activation[34]. Using a different approach, Zhou *et al.*[35] recently showed, in a human proximal tubular cell line, that different ligands of the Wnt/β-catenin

pathway could stimulate the expression of several classical RAAS genes simultaneously. Indeed, all these transcripts were included in the large specific module identified in the kidney. This raises several questions, first about the fate of other members of the coordinated groups in the cellular model, and second about the role of β-catenin pathway in the coordination observed *in situ*. Whatever the responses are, this strengthens the hypothesis that gene co-expression observed *in situ* has a cellular origin, and that it may result from the actions of transcription factors, which can be identified and tested.

In conclusion, our meta-analysis made possible the emergence of conserved results for each tissue and across data sets that are robust by definition. This study allowed extracting three levels of information. First, the expression levels revealed the features of the "endocrine RAAS" and permitted to get new insights of tissue distribution among the alternative players, such as MAS1, prorenin and renin receptors, and LNPEP-IRAP. A second level of information was the identification of core modules of transcripts that were robustly identified in several tissues, such as CTSA-CTSD, CTSG-CMA1-CPA3 and GR-MR-AGTR1. These clusters seemed to dissociate signal production from signal reception pathways, and could also orient the peptide cascade. A third level was about tissue-specific coordination of extRAAS transcripts, which built up by combining tissue-specific clusters, with modification and/or combination of the core modules.

The atlas we have established in this study provides the basis for further more elaborate studies that would take into account the variability in each tissue, due to age, gender or ethnicity. In addition, cellular and molecular mechanisms within this organization need to be elucidated, as well as how they translate into enzymatic activity, peptide production and signaling. Finally, the extensive atlas of the extRAAS organization across normal human tissues that we propose here will considerably help understand the tissue-specific effects of extRAAS and of its targeting drugs.

References

1. Robertson, J. I. S., Nichools, M. G. & August, P. *The renin-angiotensin system*. (Mosby, 1993).
2. Michel, J.-B. *Médecine cardiovasculaire du système rénine angiotensine*. (Ed. Pradel, 1992).
3. Paul, M., Mehr, A. P. & Kreutz, R. Physiology of Local Renin-Angiotensin Systems. *Physiol. Rev.* **86,** 747–803 (2006).
4. Ahmad, S. *et al.* Chymase-dependent generation of angiotensin II from angiotensin-(1–12) in human atrial tissue. *PloS One*, **6,** e28501 (2011).
5. Uehara, Y., Miura, S., Yahiro, E. & Saku, K. Non-ACE pathway-induced angiotensin II production. *Curr. Pharm. Des.* **19,** 3054–3059 (2013).
6. Kramkowski, K., Mogielnicki, A. & Buczko, W. The physiological significance of the alternative pathways of angiotensin II production. *J. Physiol. Pharmacol. Off. J. Pol. Physiol. Soc.* **57,** 529–539 (2006).
7. Akasu, M. *et al.* Differences in tissue angiotensin II-forming pathways by species and organs *in vitro*. *Hypertension* **32,** 514–520 (1998).
8. Engeli, S. *et al.* Co-expression of renin-angiotensin system genes in human adipose tissue. *J. Hypertens.* **17,** 555–560 (1999).
9. Legedz, L. *et al.* Cathepsin G is associated with atheroma formation in human carotid artery. *J. Hypertens. January 2004* **22,** 157–166 (2004).
10. Legedz, L. *et al.* Induction of tissue kallikrein in human carotid atheroma does not lead to kallikrein-kinins pathway activation. *J. Hypertens.* **23,** 359–366 (2005).
11. Ayari, H. *et al.* Mutual amplification of corticosteroids and angiotensin systems in human vascular smooth muscle cells and carotid atheroma. *J. Mol. Med. Berl. Ger.* (2014). doi:10.1007/s00109-014-1193-7
12. Ribeiro-Oliveira, A. *et al.* The renin-angiotensin system and diabetes: An update. *Vasc. Health Risk Manag.* **4,** 787–803 (2008).
13. Schwacke, J. H. *et al.* Network Modeling Reveals Steps in Angiotensin Peptide Processing. *Hypertension* **61,** 690–700 (2013).
14. Hodroj, W. *et al.* Increased Insulin-Stimulated Expression of Arterial Angiotensinogen and Angiotensin Type 1 Receptor in Patients With Type 2 Diabetes Mellitus and Atheroma. *Arterioscler. Thromb. Vasc. Biol.* **27,** 525–531 (2007).
15. Speth, R. C. & Giese, M. J. Update on the Renin-Angiotensin System (2013). *J. Pharmacol. Clin. Toxicol.* Available at: <http://www.jscimedcentral.com/Pharmacology/Articles/pharmacology-1-1004.php>. (Accessed: 10th February 2015).
16. Suski, M. *et al.* The influence of angiotensin-(1–7) Mas receptor agonist (AVE 0991) on mitochondrial proteome in kidneys of apoE knockout mice. *Biochim. Biophys. Acta.* **1834,** 2463–2469 (2013).
17. Irizarry, R. A. *et al.* Exploration, normalization, and summaries of high density oligonucleotide array probe level data. *Biostat. Oxf. Engl.* **4,** 249–264 (2003).
18. Eisen, M. B., Spellman, P. T., Brown, P. O. & Botstein, D. Cluster analysis and display of genome-wide expression patterns. *Proc. Natl. Acad. Sci.* **95,** 14863–14868 (1998).
19. Ringnér, M. What is principal component analysis? *Nat. Biotechnol.* **26,** 303–304 (2008).
20. Kaufman, L. & Rousseeuw, P. J. *Introduction, in Finding Groups in Data: An Introduction to Cluster Analysis*, Ch. 1, doi:10.1002/9780470316801.ch1 (John Wiley & Sons, Inc., Hoboken, NJ, USA, 1990).
21. Campbell, D. J. & Habener, J. F. Angiotensinogen gene is expressed and differentially regulated in multiple tissues of the rat. *J. Clin. Invest.* **78,** 31–39 (1986).
22. Jeunemaitre, X. *et al.* Molecular basis of human hypertension: role of angiotensinogen. *Cell* **71,** 169–180 (1992).
23. Smithies, O. & Kim, H. S. Targeted gene duplication and disruption for analyzing quantitative genetic traits in mice. *Proc. Natl. Acad. Sci. USA*. **91,** 3612–3615 (1994).
24. Lutterotti, N. von, Catanzaro, D. F., Sealey, J. E. & Laragh, J. H. Renin is not synthesized by cardiac and extrarenal vascular tissues. A review of experimental evidence. *Circulation* **89,** 458–470 (1994).
25. Itskovitz, J. & Sealey, J. E. Ovarian prorenin-renin-angiotensin system. *Obstet. Gynecol. Surv.* **42,** 545–551 (1987).
26. Shrikrishna, D., Astin, R., Kemp, P. R. & Hopkinson, N. S. Renin-angiotensin system blockade: a novel therapeutic approach in chronic obstructive pulmonary disease. *Clin. Sci. Lond. Engl. 1979* **123,** 487–498 (2012).
27. Giacchetti, G. *et al.* Gene expression of angiotensinogen in adipose tissue of obese patients. *Int. J. Obes. Relat. Metab. Disord. J. Int. Assoc. Study Obes.* **24 Suppl 2** S142–143 (2000).
28. Ayari, H. *et al.* Mutual amplification of corticosteroids and angiotensin systems in human vascular smooth muscle cells and carotid atheroma. *J. Mol. Med.* 1–8 (2014). doi:10.1007/s00109-014-1193-7
29. Rautureau, Y., Paradis, P. & Schiffrin, E. L. Cross-talk between aldosterone and angiotensin signaling in vascular smooth muscle cells. *Steroids* **76,** 834–839 (2011).

30. Jaffe, I. Z. & Mendelsohn, M. E. Angiotensin II and aldosterone regulate gene transcription via functional mineralocortocoid receptors in human coronary artery smooth muscle cells. *Circ. Res.* **96,** 643–650 (2005).
31. Ayari, H. *et al.* Auto-amplification of cortisol actions in human carotid atheroma is linked to arterial remodeling and stroke. *Fundam. Clin. Pharmacol.* **28,** 53–64 (2014).
32. Briones, A. M. *et al.* Adipocytes produce aldosterone through calcineurin-dependent signaling pathways: implications in diabetes mellitus-associated obesity and vascular dysfunction. *Hypertension* **59,** 1069–1078 (2012).
33. Chapman, K., Holmes, M. & Seckl, J. 11β-hydroxysteroid dehydrogenases: intracellular gate-keepers of tissue glucocorticoid action. *Physiol. Rev.* **93,** 1139–1206 (2013).
34. Dhaouadi, N. *et al.* Computational identification of potential transcriptional regulators of TGF-ß1 in human atherosclerotic arteries. *Genomics* **103,** 357–370 (2014).
35. Zhou, L. *et al.* Multiple Genes of the Renin-Angiotensin System Are Novel Targets of Wnt/β-Catenin Signaling. *J. Am. Soc. Nephrol. JASN* (2014). doi:10.1681/ASN.2014010085
36. Williams, C., Rezgui, D., Prince, S. N., Zaccheo, O. J., Foulstone, E. J., Forbes, B.E., Norton, R.S., Crosby, J., Hassan, A.B. & Crump, M.P. Structural Insights into the Interaction of Insulin-like Growth Factor 2 with IGF2R Domain 11. *Structure* **15,** 1065 (2007). PDBe ID: 2CNJ (doi:10.2210/pdb2cnj/pdb).
37. Zhang, Y., Gao, X. & Michael Garavito, R. Structural analysis of the intracellular domain of (pro)renin receptor fused to maltose-binding protein. *Biochem.Biophys.Res.Commun.* **407** 674–679 (2011). PDBe ID: 3LBS (doi:10.2210/pdb3lbs/pdb).
38. Bledsoe, R. K., Madauss, K. P., Holt, J. A., Apolito, C. J., Lambert, M. H., Pearce, K. H., Stanley, T. B., Stewart, E. L., Trump, R. P., Willson, T. M., Williams, S. P. A Ligand-mediated Hydrogen Bond Network Required for the Activation of the Mineralocorticoid Receptor. *J.Biol.Chem.* **280** 31283–31293 (2005). PDBe ID: 2AA2 (doi:10.2210/pdb2aa2/pdb).
39. Kauppi, B., Jakob, C., Farnegardh, M., Yang, J., Ahola, H., Alarcon, M., Calles, K., Engstrom, O., Harlan, J., Muchmore, S., Ramqvist, A.-K., Thorell, S., Ohman, L., Greer, J., Gustafsson, J.-A., Carlstedt-Duke, J. & Carlquist, M. The three-dimensional structures of antagonistic and agonistic forms of the glucocorticoid receptor ligand-binding domain: RU-486 induces a transconformation that leads to active antagonism. *J.Biol.Chem.* **278** 22748–22754 (2003). PDBe ID: 1P93 (doi:10.2210/pdb1p93/pdb).
40. Lebon, G., Warne, T., Edwards, P. C., Bennett, K., Langmead, C. J., Leslie, A. G. W. & Tate, C. G. Agonist-Bound Adenosine A(2A) Receptor Structures Reveal Common Features of Gpcr Activation. *Nature* **474** 521 (2011). PDBe ID: 2YDO (doi: 10.2210/pdb2ydo/pdb).
41. Hermans, S. J., Ascher, D. B., Hancock, N. C., Holien, J. K., Michell, B. J., Yeen Chai, S., Morton, C. J. & Parker, M. W. Crystal structure of human insulin-regulated aminopeptidase with specificity for cyclic peptides. *Protein Sci.* **24** 190–199 (2015). PDBe ID: 4P8Q (doi:10.2210/pdb4p8q/pdb).
42. Epidermal Growth Factor. June 2010 Molecule of the Month by David Goodsell. (doi: 10.2210/rcsb_pdb/mom_2010_6).

Acknowledgements

A.N. was awarded a scholarship from Association of Scientific Orientation and Specialization (ASOS). This work was supported by a Campus France grant from Coopération pour l'Évaluation et le Développement de la Recherche (CEDRE).

Author Contributions

A.N. performed experiments, analyzed data and wrote the manuscript. C.C. and M.P.G. provided the scripts on R-software and performed statistical analyses. N.D. and P.Y.C. prepared supplementary tables. G.B. and K.Z. designed the study, analyzed data and wrote the manuscript.

Additional Information

Supplementary information accompanies this paper at http://www.nature.com/srep

Competing financial interests: The authors declare no competing financial interests.

How to cite this article: Nehme, A. *et al.* Atlas of tissue renin-angiotensin-aldosterone system in human: A transcriptomic meta-analysis. *Sci. Rep.* **5**, 10035; doi: 10.1038/srep10035 (2015).

ATLAS OF TISSUE RENIN-ANGIOTENSIN-ALDOSTERONE SYSTEM IN HUMAN: A TRANSCRIPTOMIC META-ANALYSIS

Supplemental data

Ali Nehme, Catherine Cerutti, Nedra Dhaouadi, Marie Paule Gustin, Pierre-Yves Courand, Kazem Zibara*, Giampiero Bricca*.

* Co-last and corresponding authors

Address correspondence to:

* Dr Giampiero BRICCA, EA4173, Functional genomics of arterial hypertension, Université Lyon1, Domaine Rockefeller, 8 avenue Rockefeller, France; email: giampiero.bricca@inserm.fr

*Dr Kazem ZIBARA, ER045, Laboratory of stem cells, Department of Biology, Faculty of Sciences, Lebanese University, Beirut – Lebanon; email: kzibara@ul.edu.lb

Table of Contents

Supplementary Table S1: Extended Renin-Angiotensin-Aldosterone System (ExtRAAS) Genes

Supplementary Table S1: Extended renin-angiotensin-aldosterone system (ExtRAAS) gene. ExtRAAS constitute 36 genes; 25 encode for the renin-angiotensin system (RAS) components corresponding to angiotensinogen (AGT) 18 enzymes and 6 receptors; and 11 genes encode for corticosteroid system (COS) proteins corresponding to 9 enzymes and 2 receptors. RAS, renin-angiotensin system; COS, corticosteroid system; GeneID, gene refseq ID.

System	Gene Symbol	Gene Description	GeneID
RAS	ACE	angiotensin I converting enzyme (peptidyl-dipeptidase A) 1	1636
RAS	ACE2	angiotensin I converting enzyme (peptidyl-dipeptidase A) 2	59272
RAS	AGT	angiotensinogen (serpin peptidase inhibitor, clade A, member 8)	183
RAS	AGTR1	angiotensin II receptor, type 1	185
RAS	AGTR2	angiotensin II receptor, type 2	186
RAS	ANPEP	alanyl (membrane) aminopeptidase	290
RAS	ATP6AP2	ATPase, H+ transporting, lysosomal accessory protein 2	10159
RAS	CMA1	chymase 1, mast cell	1215
RAS	CPA3	carboxypeptidase A3 (mast cell)	1359
RAS	CTSA	cathepsin A	5476
RAS	CTSD	cathepsin D	1509
RAS	CTSG	cathepsin G	1511
RAS	DPP3	dipeptidyl-peptidase 3	10072
RAS	EGFR	epidermal growth factor receptor	1956
RAS	ENPEP	glutamyl aminopeptidase (aminopeptidase A)	2028
RAS	IGF2R	insulin-like growth factor 2 receptor	3482
RAS	KLK1	kallikrein 1	3816
RAS	LNPEP	leucyl/cystinyl aminopeptidase	4012
RAS	MAS1	MAS1 oncogene	4142
RAS	MME	membrane metallo-endopeptidase	4311
RAS	NLN	neurolysin (metallopeptidase M3 family)	57486
RAS	PREP	prolyl endopeptidase	5550
RAS	REN	renin	5972
RAS	RNPEP	arginyl aminopeptidase (aminopeptidase B)	6051
RAS	THOP1	thimet oligopeptidase 1	7064
COS	AKR1C4	aldo-keto reductase family 1, member C4	1109
COS	AKR1D1	aldo-keto reductase family 1, member D1	6718
COS	CYP11A1	cytochrome P450, family 11, subfamily A, polypeptide 1	1583
COS	CYP11B1	cytochrome P450, family 11, subfamily B, polypeptide 1	1584
COS	CYP11B2	cytochrome P450, family 11, subfamily B, polypeptide 2	1585
COS	CYP17A1	cytochrome P450, family 17, subfamily A, polypeptide 1	1586
COS	CYP21A2	cytochrome P450, family 21, subfamily A, polypeptide 2	1589
COS	GPER	G protein-coupled estrogen receptor 1	2852
COS	HSD11B1	hydroxysteroid (11-beta) dehydrogenase 1	3290
COS	HSD11B2	hydroxysteroid (11-beta) dehydrogenase 2	3291
COS	NR3C1	nuclear receptor subfamily 3, group C, member 1 (glucocorticoid receptor)	2908
COS	NR3C2	nuclear receptor subfamily 3, group C, member 2	4306

Supplementary Table S2: Detailed Inventory of Studied Datasets

Supplementary Table S2: Detailed inventory of studied datasets. Dataset ID, data set accession number in Gene expression omnibus (GEO) database; Platform ID, GEO accession number of platform; species, species from which tissues where obtained; Normal = number of normal samples in the dataset; Algorithm, normalization method used by authors; Cut height, the level at which the dendrogram was cut; MAC = mean agglomerative coefficient of dendrogram.

Dataset ID	Platform ID	Species	Tissue	Normal	algorithm	Cut height	MAC
GSE45460	GPL6244	Homo Sapiens	B cell progenitors	31	RMA	1	0.84
GSE18723	GPL96	Homo Sapiens	B cells	40	MAS 5	0.9	0.47
GSE16028	GPL570	Homo Sapiens	Blood	109	Quantile	0.82	0.48
GSE46480	GPL570	Homo Sapiens	Blood	98	Quantile	0.767	0.74
GSE10041	GPL570	Homo Sapiens	Blood	72	Global scaling	0.8	0.66
GSE19743	GPL570	Homo Sapiens	Blood	63	MBEI	0.8	0.63
GSE33580	GPL570	Homo Sapiens	Blood	43	MAS 5	0.89	0.57
GSE26049	GPL570	Homo Sapiens	Blood	42	RMA	0.9	0.67
GSE27263	GPL570	Homo Sapiens	Blood	26	RMA	0.82	0.79
GSE45536	GPL570	Homo Sapiens	Blood	24	RMA	0.987	0.71
GSE19314	GPL570	Homo sapiens	Blood	21	RMA	0.88	0.68
GSE22255	GPL570	Homo sapiens	Blood	20	RMA	0.93	0.71
GSE28750	GPL570	Homo Sapiens	Blood	20	RMA	0.9	0.8
GSE37171	GPL570	Homo Sapiens	Blood	20	RMA	0.8	0.8
GSE33341	GPL571	Homo sapiens	Blood	43	RMA	1	0.73
GSE21592	GPL571	Homo sapiens	Blood	20	RMA	1	0.83
GSE47199	GPL6244	Homo Sapiens	Blood	21	RMA	0.76	0.85
GSE12288	GPL96	Homo sapiens	Blood	112	MAS 5.0	0.785	0.56
GSE14795	GPL96	Homo Sapiens	Blood	20	MAS 5.0	0.94	0.62
GSE11504	GPL570	Homo Sapiens	BM cells	25	RMA	1	0.79
GSE16334	GPL96	Homo Sapiens	BM cells	11	RMA	1.02	0.84
GSE32719	GPL570	Homo Sapiens	BM cells	27	RMA	0.88	0.58
GSE24870	GPL571	Homo Sapiens	BM cells	20	MAS 5	1.033	0.75
GSE35010	GPL6244	Homo Sapiens	BM cells	16	RMA	0.875	0.86
GSE29431	GPL570	Homo Sapiens	Breast	12	RMA	1	0.86
GSE42568	GPL570	Homo Sapiens	Breast	17	gcRMA	1	0.78
GSE5364	GPL96	Homo sapiens	Breast	13	Global scaling	1	0.8
GSE20437	GPL96	Homo sapiens	Breast	24	MAS 5,0	0.8	0.74
GSE21947	GPL96	Homo Sapiens	Breast	30	Mean expression	1.03	0.75

Dataset ID	Platform ID	Species	Tissue	Normal	algorithm	Cut height	MAC
GSE10780	GPL570	Homo Sapiens	Breast	143	RMA	0.83	0.65
GSE19429	GPL570	Homo Sapiens	CD34+ cells	17	RMA	1	0.81
GSE31773	GPL570	Homo Sapiens	CD8 & CD4	17	RMA	1	0.85
GSE41328	GPL570	Homo sapiens	colon	10	PLIER	1	0.82
GSE13367	GPL570	Homo sapiens	colonic mucosa	38	RMA	1	0.77
GSE37364	GPL570	Homo sapiens	colonic mucosa	38	MAS 5,0	0.91	0.63
GSE24514	GPL96	Homo sapiens	colonic mucosa	15	Quantile	0.92	0.77
GSE22598	GPL570	Homo Sapiens	Colorectal	17	RMA	1	0.8
GSE23878	GPL570	Homo sapiens	Colorectal	24	PLIER	1	0.75
GSE32323	GPL570	Homo Sapiens	Colorectal	17	RMA	1	0.8
GSE9348	GPL570	Homo Sapiens	Colorectal	12	Global scaling	1.12	0.79
GSE15744	GPL570	Homo sapiens	Embryo	18	Global scaling	1	0.72
GSE18290	GPL570	Homo sapiens	Embryo	18	dChip signal intensity	0.81	0.79
GSE18887	GPL96	Homo sapiens	Embryo	18	RMA	1	0.79
GSE33168	GPL570	Homo sapiens	Embryonic fluid	12	Quantile	0.9	0.7
GSE20347	GPL571	Homo Sapiens	Esophagus	17	RMA	1	0.8
GSE23400	GPL96	Homo Sapiens	Esophagus	53	RMA	0.92	0.75
GSE5364	GPL96	Homo sapiens	Esophagus	13	Global scaling	1	0.83
GSE16134	GPL570	Homo Sapiens	Gingiva	70	RMA	0.93	0.71
GSE10334	GPL570	Homo Sapiens	Gingiva	64	RMA	1	0.71
GSE22253	GPL6244	Homo Sapiens	Heart	108	gcRMA	1	0.65
GSE22459	GPL570	Homo Sapiens	Kidney	25	MAS 5	1.08	0.75
GSE9489	GPL570	Homo Sapiens	Kidney	13	Global scaling	1.08	0.78
GSE15641	GPL96	Homo Sapiens	Kidney	23	dChip	1	0.8
GSE11906	GPL570	Homo Sapiens	Large airway epithelium	21	RMA	1	0.6
GSE10135	GPL570	Homo Sapiens	Large airway epithelium	21	Global scaling	1	0.6
GSE16696	GPL570	Homo sapiens	Large airway epithelium	20	Global scaling	1	0.64
GSE18637	GPL570	Homo sapiens	Large airway epithelium	20	Global scaling	1	0.67
GSE22047	GPL570	Homo sapiens	Large airway epithelium	19	Global scaling	1.01	0.64

Dataset ID	Platform ID	Species	Tissue	Normal	algorithm	Cut height	MAC
GSE11375	GPL570	Homo Sapiens	Leukocytes	26	Global scaling	0.85	0.75
GSE38941	GPL570	Homo sapiens	Liver	10	Median normalization	0.9	0.77
GSE45267	GPL570	Homo Sapiens	Liver	41	gcRMA	1	0.73
GSE29721	GPL570	Homo Sapiens	Liver	10	RMA	1	0.85
GSE14323	GPL571	Homo Sapiens	Liver	19	RMA	1.08	0.8
GSE41258	GPL96	Homo sapiens	Liver	13	LOWSESS	0.92	0.77
GSE19804	GPL570	Homo sapiens	Lung tissue	60	RMA	1	0.68
GSE18842	GPL570	Homo sapiens	Lung tissue	45	RMA	1	0.69
GSE31552	GPL6244	Homo sapiens	Lung tissue	36	RMA	1	0.83
GSE31547	GPL96	Homo sapiens	Lung tissue	20	Quantile	1	0.74
GSE10072	GPL96	Homo Sapiens	Lung tissue	49	RMA	0.785	0.75
GSE39540	GPL571	Homo Sapiens	mesenchymal stem cells	61	Quantile	1	0.74
GSE29819	GPL570	Homo sapiens	Myocardial	12	MAS 5.0	1	0.7
GSE12485	GPL570	Homo sapiens	Myocardial	10	RMA	1.09	0.78
GSE12486	GPL570	Homo sapiens	Myocardial	10	RMA	1	0.83
GSE13070	GPL570	Homo Sapiens	Omental	40	MAS 5.0	0.9	0.67
GSE15773	GPL570	Homo Sapiens	Omental	10	RMA and SAM	0.9	79
GSE20950	GPL570	Homo Sapiens	Omental	20	RMA	0.77	0.77
GSE41168	GPL570	Homo Sapiens	Omental	46	RMA	0.8	0.64
GSE20571	GPL6244	Homo Sapiens	Omental	13	Global Median	0.78	0.86
GSE25401	GPL6244	Homo Sapiens	Omental	56	Global Median	0.66	0.77
GSE17913	GPL570	Homo Sapiens	Oral mucosa	40	RMA	0.9	0.68
GSE37265	GPL570	Homo Sapiens	Oral mucosa	19	RMA	0.85	0.76
GSE14407	GPL570	Homo Sapiens	Ovary surface epithelium	12	MAS 5	1.06	0.74
GSE38666	GPL570	Homo Sapiens	Ovary surface epithelium	12	MAS 5	1.06	0.74
GSE29220	GPL570	Homo Sapiens	Ovary surface epithelium	11	gcRMA	1.154	0.81
GSE29450	GPL570	Homo Sapiens	Ovary surface epithelium	10	RMA	1.09	0.81
GSE26712	GPL96	Homo Sapiens	Ovary surface epithelium	10	RMA	1.16	0.76
GSE16515	GPL570	Homo Sapiens	Pancreatic tissue	16	gcRMA	0.8	0.86

Dataset ID	Platform ID	Species	Tissue	Normal	algorithm	Cut height	MAC
GSE15471	GPL570	Homo Sapiens	Pancreatic tissue	39	RMA	1	0.82
GSE28735	GPL6244	Homo sapiens	pancreatic tissue	45	RMA	1	0.79
GSE27562	GPL570	Homo sapiens	PBMC	46	RMA	0.93	0.71
GSE11761	GPL570	Homo Sapiens	PBMC	40	gcRMA	1.05	0.79
GSE14642	GPL570	Homo Sapiens	PBMC	40	gcRMA	0.93	0.78
GSE15932	GPL570	Homo sapiens	PBMC	32	VSN	0.84	0.6
GSE21942	GPL570	Homo Sapiens	PBMC	15	gcRMA	0.99	0.7
GSE17114	GPL570	Homo sapiens	PBMC	14	RMA	0.875	0.73
GSE43553	GPL571	Homo Sapiens	PBMC	34	Global scaling	0.9	0.79
GSE41890	GPL6244	Homo Sapiens	PBMC	24	gcRMA	0.91	0.77
GSE28686	GPL6244	Homo Sapiens	PBMC	20	gcRMA	0.78	0.82
GSE12585	GPL96	Homo Sapiens	PBMC	23	RMA	1	0.74
GSE14577	GPL96	Homo Sapiens	PBMC	15	RMA	1	0.75
GSE25507	GPL570	Homo sapiens	Periheral lymphocytes	64	RMA	0.85	0.66
GSE7638	GPL571	Homo sapiens	Peripheral monocytes	160	NUSE	0.86	0.72
GSE36895	GPL570	Homo Sapiens	Renal cortex	23	RMA	1	0.72
GSE15773	GPL570	Homo Sapiens	Subcutaneous adipose	9	RMA and SAM	1	0.84
GSE20950	GPL570	Homo Sapiens	Subcutaneous adipose	19	RMA	0.85	0.82
GSE26339	GPL570	Homo Sapiens	Subcutaneous adipose	35	Mas 5	1	0.75
GSE27657	GPL570	Homo Sapiens	Subcutaneous adipose	9	RMA	1	0.79
GSE27916	GPL570	Homo Sapiens	Subcutaneous adipose	253	PLIER	0.93	0.72
GSE27916	GPL570	Homo Sapiens	Subcutaneous adipose	120	PLIER	0.94	0.69
GSE27949	GPL570	Homo Sapiens	Subcutaneous adipose	11	MAS5	0.82	0.82
GSE28005	GPL570	Homo Sapiens	Subcutaneous adipose	38	RMA	0.867	0.73
GSE29718	GPL6244	Homo Sapiens	Subcutaneous adipose	15	RMA	0.91	0.81
GSE34302	GPL6244	Homo Sapiens	Subcutaneous adipose	10	Global scaling	0.917	0.78
GSE19811	GPL96	Homo Sapiens	Subcutaneous adipose	13	RMA	0.9	0.81
GSE35710	GPL96	Homo Sapiens	Subcutaneous adipose	48	PLIER	1	0.74
GSE18206	GPL570	Homo sapiens	Skin	21	VSN	1	0.74

Dataset ID	Platform ID	Species	Tissue	Normal	algorithm	Cut height	MAC
GSE30999	GPL570	Homo sapiens	Skin	85	gcRMA	1	0.77
GSE34248	GPL570	Homo sapiens	Skin	14	Rosetta resolver	0.92	0.76
GSE36842	GPL570	Homo sapiens	Skin	23	fRMA	0.88	0.75
GSE41662	GPL570	Homo sapiens	Skin	24	Rosetta resolver	0.8	0.69
GSE41663	GPL570	Homo sapiens	Skin	15	Rosetta resolver	0.86	0.76
GSE32407	GPL571	Homo sapiens	Skin	40	gcRMA	1.088	0.78
GSE11784	GPL570	Homo sapiens	small airway epithelium	63	MAS 5,0	0.93	0.72
GSE22047	GPL570	Homo sapiens	small airway epithelium	60	Global scaling	0.93	0.62
GSE30063	GPL570	Homo sapiens	small airway epithelium	60	Global scaling	0.93	0.62
GSE19667	GPL570	Homo sapiens	small airway epithelium	48	MAS 5,0	0.84	0.58
GSE19407	GPL570	Homo Sapiens	small airway epithelium	47	MAS 5	0.86	0.72
GSE11906	GPL570	Homo Sapiens	small airway epithelium	35	RMA	1	0.74
GSE13933	GPL570	Homo sapiens	small airway epithelium	23	MAS 5,0	1.05	0.66
GSE27681	GPL570	Homo sapiens	small airway epithelium	21	Global scaling	1	0.7
GSE14924	GPL570	Homo Sapiens	T cells	21	MAS 5	1	0.62
GSE29265	GPL570	Homo Sapiens	Thyroid	20	RMA	0.71	0.71
GSE33630	GPL570	Homo Sapiens	Thyroid	46	RMA	0.69	0.69
GSE13601	GPL8300	Homo Sapiens	Tongue	27	MAS 5	0.88	0.72
GSE13070	GPL570	Homo Sapiens	Vastus lateralis	87	MAS 5.0	0.82	0.65
GSE13070	GPL570	Homo Sapiens	Vastus lateralis	53	MAS 5.0	0.85	0.67
GSE14901	GPL570	Homo Sapiens	Vastus lateralis	72	MAS 5	1.04	0.61
GSE17674	GPL570	Homo Sapiens	Vastus lateralis	18	RMA	0.925	0.8
GSE19420	GPL570	Homo sapiens	Vastus lateralis	24	MAS 5,0	1	0.63
GSE25462	GPL570	Homo sapiens	Vastus lateralis	50	MAS 5,0	1	0.6
GSE25941	GPL570	Homo Sapiens	Vastus lateralis	36	Global scaling	0.9	0.54
GSE38718	GPL570	Homo Sapiens	Vastus lateralis	22	RMA	1	0.73
GSE41168	GPL570	Homo Sapiens	Vastus lateralis	47	RMA	0.79	0.54
GSE8157	GPL570	Homo sapiens	Vastus lateralis	43	RMA	1.16	0.78
GSE9419	GPL570	Homo Sapiens	Vastus lateralis	66	MAS 5	0.803	0.52

Dataset ID	Platform ID	Species	Tissue	Normal	algorithm	Cut height	MAC
GSE11681	GPL96	Homo sapiens	Vastus lateralis	10	RMA	1	0.78
GSE11686	GPL96	Homo Sapiens	Vastus lateralis	16	MAS5	1	0.68
GSE17371	GPL96	Homo sapiens	Vastus lateralis	12	MAS 5,0	0.9	0.72
GSE13985	GPL570	Homo sapiens	WBC	10	RMA	0.82	0.8
GSE28498	GPL6244	Homo Sapiens	WBC	26	RMA	0.6	0.82

Supplementary Table S3: Tissue Expression Profiles of ExtRAAS Genes

Supplementary Table S3: Tissue expression profiles extRAAS genes. Tissues are arranged based on the tissue dendrogram of figure 5 in the article (see figure on the right). PBMC, peripheral blood mononuclear cells; small airways, small airways epithelium; large airways, large airways epithelium; SC adipose, sub-cutaneous adipose tissue.

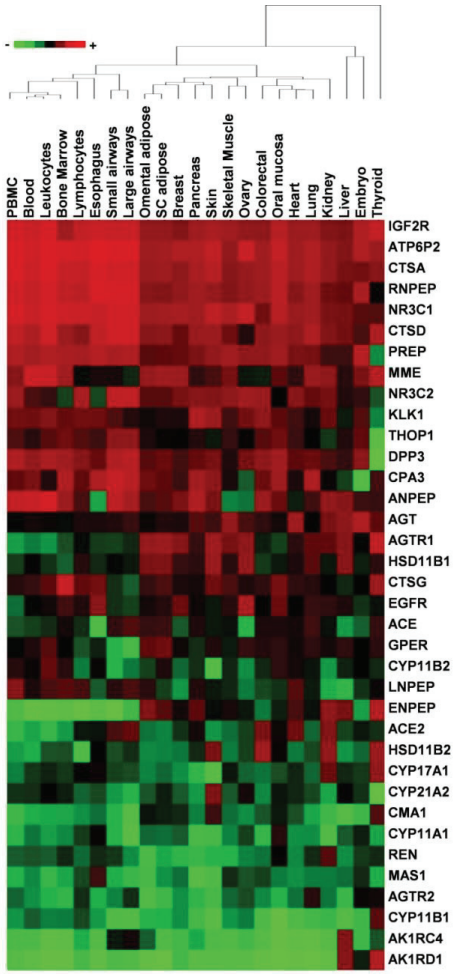

Gene symbol	PBMC	Blood	Leukocytes	Bone Marrow	Lymphocytes	Esophagus	Small airways	Large airways
ACE	31 ± 5	35 ± 4	36 ± 7	43 ± 6	37 ± 7	14 ± 3	50 ± 1	55 ± 0
ACE2	20 ± 4	24 ± 4	19 ± 5	23 ± 5	40 ± 4	36 ± 11	54 ± 0	59 ± 0
AGT	41 ± 3	47 ± 4	42 ± 9	39 ± 5	49 ± 4	43 ± 5	47 ± 0	51 ± 0
AGTR1	24 ± 4	28 ± 5	25 ± 6	31 ± 4	42 ± 5	32 ± 13	33 ± 1	36 ± 1
AGTR2	30 ± 4	26 ± 4	21 ± 7	20 ± 4	37 ± 3	21 ± 3	26 ± 1	35 ± 1
AKR1C4	16 ± 4	17 ± 3	10 ± 2	11 ± 2	23 ± 5	13 ± 5	38 ± 1	44 ± 0
AKR1D1	13 ± 4	11 ± 3	6 ± 3	6 ± 3	18 ± 5	8 ± 6	16 ± 1	15 ± 0
ANPEP	86 ± 4	94 ± 1	96 ± 2	71 ± 7	57 ± 10	21 ± 6	84 ± 0	75 ± 0
ATP6AP2	98 ± 1	97 ± 1	98 ± 1	94 ± 3	99 ± 1	95 ± 2	99 ± 0	99 ± 0
CMA1	18 ± 2	23 ± 2	22 ± 3	22 ± 3	26 ± 3	26 ± 7	21 ± 1	13 ± 1
CPA3	58 ± 5	67 ± 3	46 ± 12	76 ± 11	62 ± 5	72 ± 6	89 ± 0	82 ± 0
CTSA	98 ± 1	96 ± 1	98 ± 1	87 ± 4	90 ± 4	91 ± 3	93 ± 0	92 ± 0
CTSD	85 ± 3	82 ± 2	91 ± 4	71 ± 4	70 ± 6	78 ± 3	93 ± 0	93 ± 0
CTSG	48 ± 3	53 ± 3	56 ± 10	87 ± 7	62 ± 4	57 ± 5	35 ± 1	30 ± 0
CYP11A1	20 ± 3	29 ± 2	23 ± 4	25 ± 3	36 ± 6	39 ± 5	21 ± 2	11 ± 1
CYP11B1	25 ± 6	32 ± 6	26 ± 13	26 ± 7	34 ± 7	22 ± 10	15 ± 1	14 ± 1
CYP11B2	47 ± 6	45 ± 5	58 ± 10	47 ± 6	29 ± 13	39 ± 9	21 ± 2	27 ± 0
CYP17A1	27 ± 4	36 ± 4	36 ± 7	33 ± 6	43 ± 2	40 ± 8	33 ± 1	32 ± 1
CYP21A2	34 ± 5	37 ± 4	42 ± 5	37 ± 4	31 ± 9	30 ± 9	24 ± 1	21 ± 1
DPP3	78 ± 3	74 ± 4	75 ± 3	72 ± 5	71 ± 9	56 ± 8	79 ± 1	82 ± 0
EGFR	28 ± 7	43 ± 5	43 ± 7	51 ± 8	49 ± 9	62 ± 16	35 ± 1	33 ± 0
ENPEP	15 ± 5	7 ± 3	8 ± 3	11 ± 3	3 ± 1	11 ± 6	4 ± 1	18 ± 1
GPER	41 ± 6	49 ± 4	56 ± 1	40 ± 7	34 ± 8	34 ± 7	21 ± 1	17 ± 0
HSD11B1	34 ± 3	44 ± 3	34 ± 6	29 ± 5	50 ± 2	34 ± 8	41 ± 1	38 ± 1
HSD11B2	23 ± 5	23 ± 4	31 ± 7	31 ± 7	16 ± 6	38 ± 3	32 ± 1	35 ± 1
IGF2R	93 ± 2	96 ± 1	95 ± 3	72 ± 6	91 ± 5	84 ± 1	89 ± 0	89 ± 0
KLK1	62 ± 3	64 ± 3	64 ± 6	58 ± 6	65 ± 3	57 ± 2	55 ± 1	47 ± 0
LNPEP	66 ± 8	48 ± 5	53 ± 15	55 ± 10	56 ± 7	28 ± 2	49 ± 0	54 ± 0
MAS1	21 ± 5	27 ± 4	19 ± 5	23 ± 5	35 ± 3	48 ± 8	22 ± 1	19 ± 1
MME	66 ± 8	95 ± 3	88 ± 10	72 ± 9	43 ± 16	42 ± 14	45 ± 1	36 ± 1
NR3C1	94 ± 2	94 ± 2	95 ± 2	89 ± 3	95 ± 1	82 ± 6	93 ± 0	93 ± 0
NR3C2	71 ± 3	57 ± 4	50 ± 13	32 ± 6	80 ± 5	30 ± 10	85 ± 0	85 ± 0
PREP	79 ± 2	79 ± 2	78 ± 2	74 ± 4	79 ± 5	75 ± 5	77 ± 0	79 ± 0
REN	30 ± 5	33 ± 4	30 ± 5	36 ± 5	30 ± 4	33 ± 12	34 ± 1	25 ± 1
RNPEP	91 ± 1	91 ± 2	94 ± 2	82 ± 5	87 ± 2	92 ± 1	96 ± 0	96 ± 0
THOP1	55 ± 3	51 ± 4	55 ± 5	59 ± 7	58 ± 5	48 ± 7	68 ± 0	68 ± 0

Gene symbol	Omental adipose	SC adipose	Breast	Pancreas	Skin	Skeletal Muscle	Ovary	Colorectal
ACE	67 ± 1	68 ± 4	38 ± 12	58 ± 6	44 ± 5	50 ± 4	23 ± 5	61 ± 7
ACE2	38 ± 1	34 ± 3	44 ± 3	56 ± 1	28 ± 4	36 ± 4	37 ± 8	84 ± 4
AGT	58 ± 8	62 ± 3	58 ± 7	70 ± 8	60 ± 3	89 ± 1	60 ± 4	66 ± 4
AGTR1	94 ± 2	95 ± 1	82 ± 5	63 ± 4	84 ± 5	80 ± 2	76 ± 5	51 ± 6
AGTR2	21 ± 4	25 ± 3	31 ± 3	25 ± 5	20 ± 4	37 ± 3	36 ± 2	34 ± 3
AKR1C4	40 ± 17	20 ± 6	22 ± 5	28 ± 8	18 ± 3	19 ± 2	20 ± 6	18 ± 4
AKR1D1	9 ± 3	4 ± 1	23 ± 9	15 ± 6	14 ± 4	15 ± 3	13 ± 4	9 ± 4
ANPEP	72 ± 3	73 ± 4	79 ± 3	99 ± 1	73 ± 6	33 ± 2	31 ± 5	96 ± 1
ATP6AP2	98 ± 1	98 ± 1	98 ± 1	98 ± 1	98 ± 1	88 ± 1	100 ± 0	98 ± 2
CMA1	52 ± 2	50 ± 5	45 ± 6	33 ± 4	60 ± 7	36 ± 2	28 ± 5	41 ± 5
CPA3	81 ± 4	75 ± 4	65 ± 9	94 ± 2	78 ± 6	57 ± 2	34 ± 12	80 ± 5
CTSA	95 ± 1	96 ± 0	85 ± 4	95 ± 2	94 ± 1	85 ± 2	79 ± 3	99 ± 1
CTSD	89 ± 3	88 ± 2	74 ± 6	90 ± 5	83 ± 3	78 ± 2	53 ± 9	91 ± 2
CTSG	69 ± 2	71 ± 4	57 ± 9	56 ± 7	70 ± 5	69 ± 2	52 ± 1	67 ± 3
CYP11A1	39 ± 2	38 ± 3	38 ± 3	21 ± 10	20 ± 6	33 ± 2	37 ± 7	27 ± 4
CYP11B1	28 ± 9	28 ± 5	31 ± 9	22 ± 11	14 ± 1	31 ± 4	30 ± 6	22 ± 7
CYP11B2	45 ± 8	60 ± 3	37 ± 9	44 ± 15	16 ± 6	46 ± 6	28 ± 7	48 ± 7
CYP17A1	35 ± 2	38 ± 3	31 ± 7	25 ± 12	14 ± 5	49 ± 3	33 ± 8	38 ± 4
CYP21A2	41 ± 7	49 ± 3	38 ± 9	30 ± 11	74 ± 11	39 ± 4	50 ± 7	34 ± 7
DPP3	74 ± 3	79 ± 3	66 ± 9	74 ± 8	72 ± 3	59 ± 3	70 ± 3	92 ± 2
EGFR	60 ± 9	62 ± 6	75 ± 3	54 ± 21	44 ± 4	61 ± 4	86 ± 5	55 ± 9
ENPEP	87 ± 1	73 ± 6	56 ± 8	72 ± 3	46 ± 6	57 ± 4	43 ± 9	37 ± 9
GPER	77 ± 3	81 ± 2	54 ± 12	44 ± 5	54 ± 5	48 ± 3	57 ± 4	63 ± 5
HSD11B1	85 ± 6	85 ± 5	64 ± 8	61 ± 7	82 ± 2	61 ± 2	78 ± 2	46 ± 2
HSD11B2	34 ± 2	34 ± 2	34 ± 4	45 ± 1	73 ± 4	34 ± 1	37 ± 5	98 ± 1
IGF2R	94 ± 1	92 ± 1	81 ± 5	92 ± 2	87 ± 2	93 ± 1	77 ± 4	92 ± 3
KLK1	59 ± 3	61 ± 2	58 ± 4	98 ± 1	83 ± 3	67 ± 2	69 ± 2	91 ± 2
LNPEP	65 ± 10	43 ± 8	31 ± 9	59 ± 17	44 ± 4	46 ± 4	30 ± 7	43 ± 5
MAS1	23 ± 5	32 ± 4	35 ± 7	16 ± 10	18 ± 4	45 ± 3	35 ± 8	45 ± 2
MME	95 ± 2	96 ± 1	91 ± 3	62 ± 8	62 ± 4	79 ± 2	43 ± 11	50 ± 7
NR3C1	97 ± 1	97 ± 1	94 ± 3	93 ± 2	96 ± 1	98 ± 0	97 ± 2	82 ± 7
NR3C2	75 ± 4	73 ± 3	78 ± 3	83 ± 3	75 ± 2	87 ± 1	83 ± 8	95 ± 2
PREP	76 ± 4	75 ± 2	74 ± 5	80 ± 3	79 ± 2	94 ± 0	76 ± 1	92 ± 2
REN	23 ± 3	29 ± 2	25 ± 8	24 ± 10	24 ± 6	27 ± 3	29 ± 6	38 ± 4
RNPEP	88 ± 2	86 ± 1	87 ± 2	93 ± 2	81 ± 3	83 ± 1	78 ± 5	96 ± 1
THOP1	61 ± 2	56 ± 3	52 ± 5	59 ± 3	44 ± 8	64 ± 3	47 ± 4	75 ± 3

Gene symbol	Oral Mucosa	Heart	Lung	Kidney	Liver	Embryo	Thyroid
ACE	53 ± 3	57 ± 5	65 ± 11	56 ± 12	35 ± 11	31 ± 11	58 ± 5
ACE2	50 ± 4	79 ± 2	36 ± 4	92 ± 3	48 ± 8	40 ± 19	40 ± 7
AGT	51 ± 2	94 ± 4	51 ± 4	90 ± 4	100 ± 1	82 ± 5	66 ± 2
AGTR1	38 ± 6	63 ± 4	71 ± 4	82 ± 8	98 ± 1	42 ± 14	98 ± 1
AGTR2	24 ± 4	36 ± 8	60 ± 6	39 ± 5	28 ± 3	44 ± 9	50 ± 7
AKR1C4	7 ± 2	11 ± 3	10 ± 2	19 ± 6	96 ± 2	19 ± 7	36 ± 4
AKR1D1	3 ± 0	8 ± 3	5 ± 3	11 ± 6	97 ± 2	39 ± 12	91 ± 0
ANPEP	69 ± 3	48 ± 4	65 ± 11	98 ± 1	98 ± 1	54 ± 13	58 ± 4
ATP6AP2	99 ± 0	95 ± 1	97 ± 1	99 ± 1	96 ± 2	82 ± 12	82 ± 5
CMA1	44 ± 4	41 ± 5	28 ± 5	26 ± 2	20 ± 3	19 ± 7	63 ± 4
CPA3	84 ± 7	59 ± 8	96 ± 1	60 ± 1	49 ± 6	14 ± 8	60 ± 12
CTSA	95 ± 1	94 ± 0	96 ± 1	99 ± 0	93 ± 2	64 ± 14	77 ± 11
CTSD	83 ± 1	88 ± 4	96 ± 1	92 ± 1	91 ± 2	56 ± 5	89 ± 3
CTSG	72 ± 2	64 ± 9	59 ± 6	59 ± 2	53 ± 11	43 ± 5	83 ± 2
CYP11A1	55 ± 2	32 ± 3	31 ± 5	21 ± 4	45 ± 8	39 ± 8	26 ± 6
CYP11B1	7 ± 1	20 ± 9	22 ± 7	27 ± 9	20 ± 12	19 ± 5	65 ± 0
CYP11B2	57 ± 4	57 ± 10	48 ± 4	34 ± 13	54 ± 7	43 ± 8	41 ± 12
CYP17A1	37 ± 3	47 ± 9	36 ± 4	85 ± 4	53 ± 6	35 ± 6	79 ± 7
CYP21A2	45 ± 4	47 ± 4	40 ± 4	32 ± 8	61 ± 9	36 ± 7	6 ± 0
DPP3	86 ± 2	74 ± 3	75 ± 5	77 ± 5	74 ± 5	70 ± 7	4 ± 1
EGFR	69 ± 3	54 ± 9	63 ± 7	70 ± 11	68 ± 7	36 ± 16	45 ± 6
ENPEP	43 ± 9	69 ± 4	49 ± 9	97 ± 1	93 ± 2	24 ± 12	92 ± 4
GPER	57 ± 2	56 ± 2	61 ± 4	63 ± 9	73 ± 9	43 ± 10	56 ± 3
HSD11B1	44 ± 6	59 ± 10	70 ± 7	54 ± 9	99 ± 1	39 ± 8	56 ± 6
HSD11B2	49 ± 3	35 ± 7	40 ± 3	98 ± 0	36 ± 5	30 ± 7	83 ± 2
IGF2R	94 ± 1	93 ± 1	90 ± 2	92 ± 4	94 ± 1	82 ± 4	100 ± 0
KLK1	66 ± 3	68 ± 6	55 ± 5	84 ± 2	56 ± 7	57 ± 7	30 ± 3
LNPEP	40 ± 3	72 ± 8	47 ± 13	31 ± 7	29 ± 8	36 ± 13	49 ± 9
MAS1	31 ± 2	32 ± 8	33 ± 9	38 ± 4	42 ± 3	37 ± 7	25 ± 2
MME	66 ± 3	64 ± 7	89 ± 2	97 ± 1	71 ± 7	66 ± 4	93 ± 1
NR3C1	94 ± 1	92 ± 4	91 ± 2	90 ± 5	92 ± 3	58 ± 21	63 ± 2
NR3C2	48 ± 7	86 ± 3	73 ± 5	88 ± 3	69 ± 9	52 ± 18	36 ± 3
PREP	86 ± 1	82 ± 2	77 ± 3	74 ± 5	77 ± 7	84 ± 4	29 ± 8
REN	48 ± 4	33 ± 7	44 ± 4	79 ± 7	37 ± 3	35 ± 11	41 ± 8
RNPEP	95 ± 1	85 ± 1	91 ± 2	86 ± 5	87 ± 2	79 ± 9	48 ± 4
THOP1	71 ± 2	67 ± 3	51 ± 9	48 ± 11	69 ± 7	60 ± 8	12 ± 1

Supplementary Table S4: ExtRAAS Co-expression Modules in All 23 Studied Tissues

Supplementary Table S4: ExtRAAS co-expression modules in all 23 studied tissue. Below each tissue the number of datasets and corresponding samples are represented as (datasets, samples). At the top of each module the average coordination rate is expressed in percentage (average percentage of genes within a module that are always coordinated across the different datasets of a specific tissue). Next to each gene name the abundance of the mRNA is expressed in mean MCR (Mean expression centile rank). Tissues are arranged based on the tissue dendrogram of figure 5 in the article (see figure on the right).

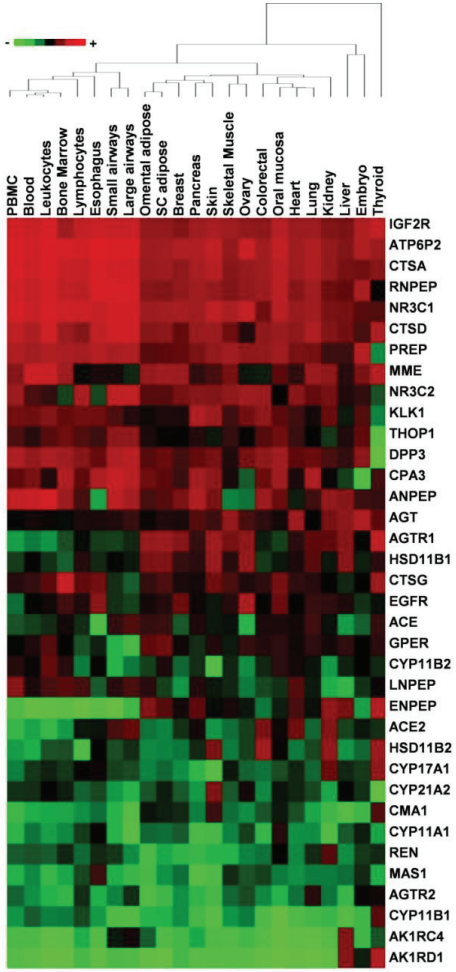

Tissues (datasets, samples)	Module 1		Module 2		Module 3		Module 4		Module 5		Module 6		Module 7		Module 8		Non-clustered genes	
Thyroid	100%		100%		100%		100%		100%		100%							
(2, 66)	CTSD	89	ATP6AP2	82	**MME**	**93**	CYP11B2	41	**AGTR1**	**98**	**AKR1D1**	**91**	PREP	**29**			**IGF2R**	**100**
	CYP17A1	79	GR	63	CTSG	83	KLK1	30	**ENPEP**	**92**	CYP11B1	65	THOP1	12			CTSA	77
	RNPEP	48	GPER	56	CMA1	63			HSD11B2	83	AKR1C4	36					AGT	66
			ACE2	40	CPA3	60			ACE	58							ANPEP	58
					HSD11B1	56											AGTR2	50
																	EGFR	45
																	NR3C2	36
																	CYP11A1	26
																	MAS1	25
																	CYP21A2	6
																	DPP3	4
Embryo	81%		83%		83%		83%		100%		75%		81%		83%			
(4, 66)	ATP6AP2	82	MR	52	CTSG	43	AGT	82	CYP11B2	43	GR	58	PREP	84	ANPEP	54	IGF2R	82
	RNPEP	79	CYP21A2	36	CMA1	19	AGTR1	42	ACE	31	CYP11A1	39	KLK1	57	REN	35	MME	66
	DPP3	70	LNPEP	36			AKR1D1	39					AGTR2	44	ENPEP	24	CTSA	64
	THOP1	60											HSD11B1	39			CTSD	56
																	GPER	43
																	ACE2	40
																	MAS1	37
																	EGFR	36
																	HSD11B2	30
																	AKR1C4	19
																	CPA3	14
Liver	83%		60%		87%		80%		80%		74%		74%		67%			
(5, 93)	**ATP6AP2**	**96**	**AGTR1**	**98**	**HSD11B1**	**99**	EGFR	68	**ANPEP**	**98**	MAS1	42	**ENPEP**	**93**	CYP11B2	54	**AGT**	**100**
	IGF2R	**94**	**GR**	**92**	**AKR1D1**	**97**	REN	37	KLK1	56	LNPEP	29	MME	71	CYP17A1	53	RNPEP	87
	CTSA	**93**			**AKR1C4**	**96**	CYP11B1	20	HSD11B2	36	AGTR2	28	MR	69	CYP11A1	45	PREP	77
	CTSD	**91**															GPER	73
	DPP3	74															THOP1	69
	CYP21A2	61															CTSG	53
	ACE	35															CPA3	49
																	ACE2	48
																	CMA1	20
Kidney	84%		88%		85%		94%		80%									
(4, 84)	**CTSA**	**99**	**ATP6AP2**	**99**	CTSG	59	THOP1	48	PREP	74							**HSD11B2**	**98**
	ANPEP	**98**	**GR**	**90**	AGTR2	39	CYP11B2	34	CPA3	60							**IGF2R**	**92**
	ENPEP	**97**	MR	88	MAS1	38	CYP21A2	32	HSD11B1	54							RNPEP	86
	MME	**97**	AGTR1	82	AKR1C4	19	CMA1	26	LNPEP	31							DPP3	77
	ACE2	**92**			AKR1D1	11			CYP11A1	21							EGFR	70
	CTSD	**92**															GPER	63
	AGT	**90**															CYP11B1	27
	CYP17A1	85																
	KLK1	84																
	REN	75																
	ACE	56																

Lung	90%		85%		100%		80%		86%		93%		80%		100%			
(5, 210)	**CTSD**	**96**	**CPA3**	**96**	CTSG	59	KLK1	55	EGFR	63	**ATP6AP2**	**97**	CYP11B2	48	AKR1C4	10	ACE	65
	CTSA	**96**	**GR**	**91**	CMA1	28	HSD11B2	40	REN	44	**IGF2R**	**90**	CYP21A2	40	AKR1D1	5	GPER	61
	RNPEP	**91**	MME	89			CYP11A1	31	MAS1	33	PREP	77					AGTR2	60
	DPP3	75	MR	73			CYP11B1	22									AGT	51
	ANPEP	65	AGTR1	71													THOP1	51
	LNPEP	47	HSD11B1	70													ACE2	36
			ENPEP	49													CYP17A1	36
Heart	77%		75%		80%		100%		81%		81%		75%					
(4, 140)	**CTSA**	**94**	**GR**	**92**	CTSG	64	EGFR	54	KLK1	68	**IGF2R**	**93**	ACE2	79			**ATP6AP2**	**95**
	AGT	**94**	ENPEP	69	AGTR1	63	REN	33	CMA1	41	MME	64	LNPEP	72			NR3C2	86
	CTSD	88			CPA3	59	MAS1	32	HSD11B2	35	HSD11B1	59					RNPEP	85
	DPP3	74			ACE	57			CYP11B1	20	AKR1D1	8					PREP	82
	THOP1	67			AKR1C4	11											CYP11B2	57
																	GPER	56
																	ANPEP	48
																	CYP21A2	47
																	CYP17A1	47
																	AGTR2	36
																	CYP11A1	32
Oral mucosa	81%		71%		96%		75%		87%		75%		75%		83%			
(4, 193)	**CTSA**	**95**	**GR**	**94**	CPA3	84	REN	48	**RNPEP**	**95**	KLK1	66	ACE2	50	AGT	69	**ATP6AP2**	**99**
	DPP3	86	MR	48	CTSG	72	MAS1	31	**IGF2R**	**94**	HSD11B2	49	LNPEP	40	AKR1C4	51	CYP11B2	57
	THOP1	71			ANPEP	69	AGTR2	24	PREP	86					EGFR	7	GPER	57
	CYP11A1	55			MME	66	CYP11B1	7	CTSD	83							ACE	53
					HSD11B1	44	AKR1D1	3									CYP21A2	45
					CMA1	44											AGTR1	38
					ENPEP	43											CYP17A1	37
Colorectal	82%		78%		96%		80%		83%		75%		75%		62%			
(8, 171)	**CTSA**	**98**	**ATP6AP2**	**98**	CPA3	80	**RNPEP**	**96**	**ANPEP**	**96**	AGT	66	EGFR	55	ACE	61	LNPEP	43
	HSD11B2	**98**	GR	82	CTSG	66	**PREP**	**92**	ACE2	84	CYP11B2	48	CYP17A1	37	MME	50	REN	37
	MR	**95**	GPER	63	CMA1	41	**DPP3**	**91**	MAS1	44	AGTR2	34					ENPEP	36
	IGF2R	**91**	AGTR1	50			**KLK1**	**91**	AKR1C4	18	CYP21A2	34					CYP11A1	26
	CTSD	**91**	HSD11B1	45			THOP1	74	AKR1D1	9	CYP11B1	21						
Ovary	85%		80%		80%		88%		90%		84%		85%		85%			
(5, 55)	CTSA	79	**GR**	**97**	EGFR	86	CTSG	52	THOP1	47	**ATP6AP2**	**100**	KLK1	69	AGT	60	RNPEP	78
	IGF2R	77	MR	83	CYP17A1	33	ACE2	37	MME	43	HSD11B1	78	CYP21A2	50	CTSD	53	PREP	76
	DPP3	70	CYP11B1	30	REN	29	MAS1	35	HSD11B2	37	AGTR1	76	CYP11B2	28	AGTR2	36	LNPEP	30
	GPER	57			CMA1	28	AKR1C4	20	CYP11A1	37	ENPEP	43	ACE	23	ANPEP	31		
							AKR1D1	13			CPA3	34						
Skeletal Muscle	64%		76%		57%		74%		67%		57%							
(14, 556)	CTSA	85	**GR**	**98**	CPA3	57	KLK1	67	CYP11B2	46	ATP6AP2	88					**PREP**	**94**
	RNPEP	83	**IGF2R**	**93**	CMA1	36	CYP17A1	49	CYP21A2	39	AGTR1	80					AGT	89
	CTSD	78	MR	87			REN	27	AKR1C4	19							MME	79
																	CTSG	69
																	THOP1	64
																	HSD11B1	61
																	EGFR	61
																	DPP3	59
																	ENPEP	57

																	ACE	50
																	GPER	48
																	LNPEP	46
																	MAS1	45
																	AGTR2	37
																	ACE2	36
																	HSD11B2	34
																	CYP11A1	33
																	ANPEP	33
																	CYP11B1	31
																	AKR1D1	15
																	AKR1C4	22
Skin	81%		57%		90%		71%		57%		71%							
(7, 222)	GPER	54	AGTR1	84	CPA3	78	THOP1	44	**GR**	**96**	**ATP6AP2**	**98**					**CTSA**	**94**
	ACE	44	MR	75	CTSG	70	REN	24	HSD11B2	73	ACE2	28					IGF2R	87
	CYP11B2	16			CMA1	60											CTSD	83
																	KLK1	83
																	HSD11B1	82
																	RNPEP	81
																	PREP	79
																	CYP21A2	74
																	ANPEP	73
																	DPP3	72
																	MME	62
																	AGT	60
																	ENPEP	46
																	EGFR	44
																	LNPEP	44
																	CYP11A1	20
																	AGTR2	20
																	MAS1	18
																	AKR1C4	18
																	AKR1D1	14
																	CYP11B1	14
																	CYP17A1	14
Pancreas	100%		100%		100%		100%		100%		100%							
(3, 100)	**ATP6AP2**	**98**	DPP3	74	**CPA3**	**94**	**RNPEP**	**93**	CYP11B2	44	**ANPEP**	**99**					MR	83
	CTSA	**95**	THOP1	59	CTSG	56	PREP	80	CYP21A2	30	**KLK1**	**98**					AGT	70
	GR	**93**			CMA1	33	ACE	58	AGTR2	25	MAS1	16					AGTR1	63
	IGF2R	**92**					ACE2	56	CYP17A1	25							MME	62
	CTSD	**90**					HSD11B2	45	REN	24							EGFR	54
	ENPEP	72							CYP11B1	22							GPER	44
	HSD11B1	61							AKR1D1	15							AKR1C4	28
	LNPEP	59															CYP11A1	21
Sub-cutaneous adipose	92%		77%		97%		67%		64%		64%							
(12, 580)	**CTSA**	**95**	**GR**	**97**	CPA3	75	KLK1	60	MAS1	32	**ATP6AP2**	**97**					**MME**	**95**
	CTSD	88	**AGTR1**	**94**	CTSG	71	CYP11B2	60	REN	29	HSD11B1	84					**IGF2R**	**91**
			ENPEP	73	CMA1	49			CYP11B1	28	ANPEP	73					RNPEP	85
			MR	73													GPER	80
																	DPP3	78

																	PREP	75
																	ACE	67
																	EGFR	62
																	AGT	61
																	THOP1	55
																	CYP21A2	49
																	LNPEP	43
																	CYP17A1	38
																	CYP11A1	37
																	HSD11B2	34
																	ACE2	34
																	AGTR2	24
																	AKR1C4	20
																	AKR1D1	4
Omental adipose	67%		83%		100%		83%		83%		67%							
(6, 185)	**CTSA**	**95**	**GR**	**97**	CPA3	81	KLK1	58	CYP17A1	35	**ATP6AP2**	**97**					**MME**	**94**
	CTSD	88	**AGTR1**	**94**	CTSG	68	CYP11B2	44	CYP11B1	28	HSD11B1	85					**IGF2R**	**93**
			ENPEP	87	CMA1	52			MAS1	23							RNPEP	88
			MR	75					REN	23							GPER	77
																	PREP	75
																	DPP3	74
																	ANPEP	72
																	ACE	67
																	LNPEP	65
																	THOP1	61
																	EGFR	59
																	AGT	57
																	CYP21A2	41
																	AKR1C4	40
																	CYP11A1	39
																	ACE2	37
																	HSD11B2	34
																	AGTR2	20
																	AKR1D1	9
Breast	86%		83%		73%		84%		83%		75%		83%					
(6, 239)	RNPEP	86	**ATP6AP2**	**98**	CPA3	65	EGFR	75	ACE2	43	AGT	57	ANPEP	79			**MME**	**90**
	CTSA	85	**GR**	**94**	CTSG	57	MAS1	35	REN	25	ACE	38	HSD11B2	34			HSD11B1	63
	CTSD	74	AGTR1	82	CMA1	45	AGTR2	31			CYP11A1	38					KLK1	57
	PREP	73	IGF2R	81							CYP11B1	31					GPER	54
	DPP3	66	MR	78													CYP21A2	38
	THOP1	52	ENPEP	55													CYP11B2	36
																	CYP17A1	31
																	LNPEP	30
																	AKR1D1	22

Large airways	96%		93%		100%		96%		95%		93%		73%		80%							
(5, 101)	**RNPEP**	**96**	**ATP6AP2**	**99**	CPA3	82	ANPEP	75	EGFR	33	HSD11B1	38	IGF2R	89	CYP17A1	32	AGT	51				
	CTSD	**93**	**GR**	**93**	AKR1C4	44	ACE	55	REN	25	HSD11B2	35	DPP3	82	CMA1	13	KLK1	47				
	CTSA	**92**	MR	85	CTSG	30	MME	36	MAS1	19	CYP21A2	21	AKR1D1	15			CYP11B1	14				
	PREP	79	ACE2	59	CYP11A1	11	AGTR1	36	ENPEP	18												
	THOP1	68	LNPEP	54			CYP11B2	27														
			AGTR2	35			GPER	17														
Small airways	96%		100%		90%		88%		78%		91%		88%									
(8, 357)	**RNPEP**	**96**	**GR**	**93**	CPA3	89	REN	34	MME	45	**ATP6AP2**	**99**	CYP21A2	24			KLK1	55				
	CTSD	**93**	MR	85	EGFR	35	AGTR1	33	AGTR2	26	AGT	47	CYP11B2	21			ACE	50				
	CTSA	**93**			CTSG	35	CYP17A1	33	AKR1D1	16	HSD11B1	41					LNPEP	49				
	IGF2R	89			HSD11B2	32	CYP11A1	21	ENPEP	4	AKR1C4	38					MAS1	22				
	ANPEP	84					CMA1	21									GPER	21				
	DPP3	79					CYP11B1	15														
	PREP	77																				
	THOP1	68																				
	ACE2	54																				
Esophagus	92%		92%		92%		100%		92%		92%											
(3, 83)	**RNPEP**	**91**	GR	82	CPA3	72	AGT	42	CYP21A2	30	**ATP6AP2**	**95**					EGFR	62				
	CTSA	**90**	AGTR1	31	CTSG	57	GPER	34	ACE	14	IGF2R	83					KLK1	56				
	CTSD	78	MR	30	CMA1	26	HSD11B1	33	AKR1C4	13	LNPEP	28					MAS1	48				
	PREP	74	ENPEP	10													MME	42				
	DPP3	55															CYP17A1	40				
	THOP1	48															CYP11B2	39				
	CYP11A1	39															HSD11B2	38				
	ACE2	36															REN	33				
																	CYP11B1	22				
																	ANPEP	21				
																	AGTR2	20				
																	AKR1D1	8				
Lymphocytes	77%		95%		83%		93%		83%		79%		75%									
(6, 184)	**IGF2R**	**90**	**ATP6AP2**	**99**	CTSG	61	EGFR	49	CYP17A1	43	KLK1	65	CTSD	70			HSD11B1	50				
	CTSA	**90**	**GR**	**95**	ANPEP	56	AGT	48	ACE	37	CPA3	61	THOP1	58			HSD11B2	16				
	RNPEP	87	**MR**	**90**	MME	42	REN	30	AGTR2	37	LNPEP	56	GPER	33								
	PREP	79			AGTR1	42	AKR1C4	23	CYP11A1	35	ACE2	40	CYP21A2	31								
	DPP3	70			MAS1	34	AKR1D1	18														
	CYP11B1	34			CMA1	26																
	CYP11B2	28																				
	ENPEP	3																				
Bone marrow	72%		75%		71%		73%		78%		75%		**72%**		67%							
(8, 208)	CTSA	86	GR	89	CTSG	87	CYP21A2	36	EGFR	51	CYP17A1	33	ACE	43	KLK1	57	**ATP6AP2**	**94**				
	RNPEP	82	ANPEP	70	CPA3	76	MR	32	GPER	40	AGTR1	31	AGT	39	CYP11B2	47	MME	72				
	PREP	74	LNPEP	55	DPP3	72	CYP11B1	26	HSD11B2	31	MAS1	22	REN	35	HSD11B1	29	THOP1	59				
	IGF2R	71					CYP11A1	25	ENPEP	10	AKR1D1	6	ACE2	23								
	CTSD	70					AGTR2	19					CMA1	22								
							AKR1C4	10														

Leukocytes	83%		75%		75%		88%		79%		75%		75%		75%					
(4, 222)	**ATP6AP2**	**98**	MR	50	CTSG	56	CYP17A1	36	KLK1	64	AGT	42	CYP11B1	26	AGTR2	21	**ANPEP**	**96**
	CTSA	**97**	CPA3	46	ENPEP	8	ACE	35	CYP11B2	58	AGTR1	24	AKR1D1	6	AKR1C4	9	**IGF2R**	**95**
	RNPEP	**93**					HSD11B2	31	GPER	55							**NR3C1**	**95**
	CTSD	**91**					REN	30	CYP21A2	41							MME	88
	PREP	78					CMA1	22	HSD11B1	34							THOP1	55
	DPP3	75					ACE2	19	CYP11A1	23							LNPEP	53
																	EGFR	43
																	MAS1	19
Whole Blood	76%		69%		65%		71%		69%									
(17, 774)	**IGF2R**	**96**	**ATP6AP2**	**97**	PREP	79	HSD11B1	44	REN	33							CPA3	67
	CTSA	**96**	**GR**	**94**	DPP3	74	CYP17A1	36	CYP11B1	32							KLK1	64
	MME	**95**	MR	57					AKR1D1	11							CTSG	53
	ANPEP	**94**	LNPEP	48													THOP1	51
	RNPEP	**91**															GPER	49
	CTSD	82															AGT	47
																	CYP11B2	45
																	EGFR	43
																	CYP21A2	37
																	ACE	35
																	CYP11A1	29
																	AGTR1	28
																	MAS1	27
																	AGTR2	26
																	ACE2	24
																	CMA1	23
																	HSD11B2	23
																	AKR1C4	17
																	ENPEP	7
PBMC	71%		77%		70%		68%		79%		79%							
(11, 303)	**CTSA**	**97**	**ATP6AP2**	**98**	AGTR2	29	AGT	40	KLK1	61	CYP17A1	26					ANPEP	86
	IGF2R	**93**	**GR**	**94**	AGTR1	23	ACE	31	CYP11B2	47	CYP11A1	20					PREP	79
	RNPEP	**91**	MR	71	AKR1D1	13	REN	30	GPER	40	ENPEP	15					DPP3	78
	CTSD	84	LNPEP	65			MAS1	21									MME	66
	THOP1	54															CPA3	58
																	CTSG	48
																	CYP21A2	34
																	HSD11B1	34
																	EGFR	28
																	CYP11B1	25
																	HSD11B2	23
																	ACE2	20
																	CMA1	18
																	AKR1C4	16

Supplementary Figure S1: ExtRAAS Genes Expression Profiles Across Studied Tissues

Supplementary Figure S1: ExtRAAS genes expression profiles across studied tissues. The expression profile of each of the extRAAS genes across all studied tissues represented in a bar-graph as mean expression centile rank (MCR) ± SEM. A horizontal cut-off line was drawn at the MCR level 33.3.

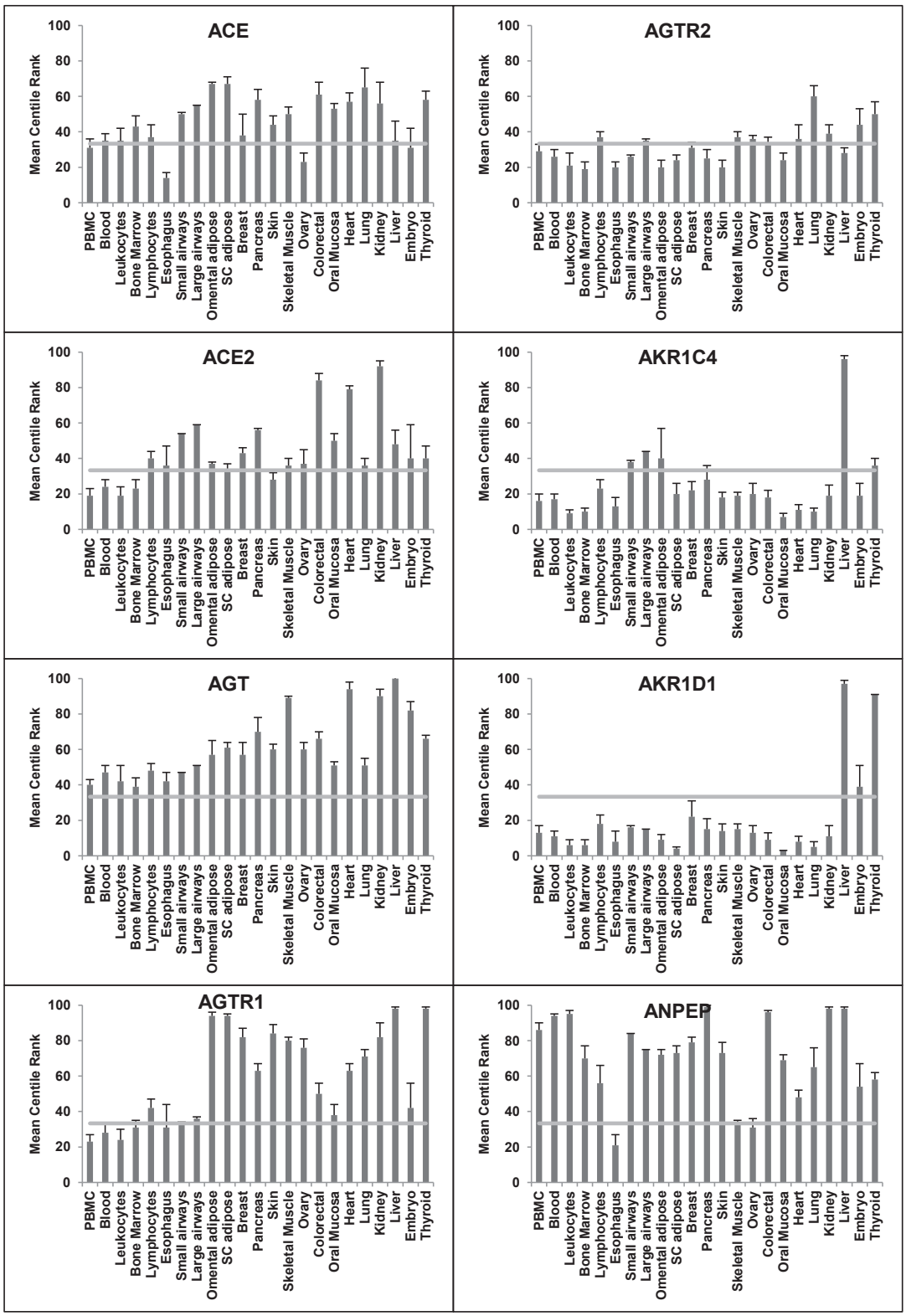
ACE
AGTR2
ACE2
AKR1C4
AGT
AKR1D1
AGTR1
ANPEP
Mean Centile Rank
0
20
40
60
80
100
PBMC
Blood
Leukocytes
Bone Marrow
Lymphocytes
Esophagus
Small airways
Large airways
Omental adipose
SC adipose
Breast
Pancreas
Skin
Skeletal Muscle
Ovary
Colorectal
Oral Mucosa
Heart
Lung
Kidney
Liver
Embryo
Thyroid

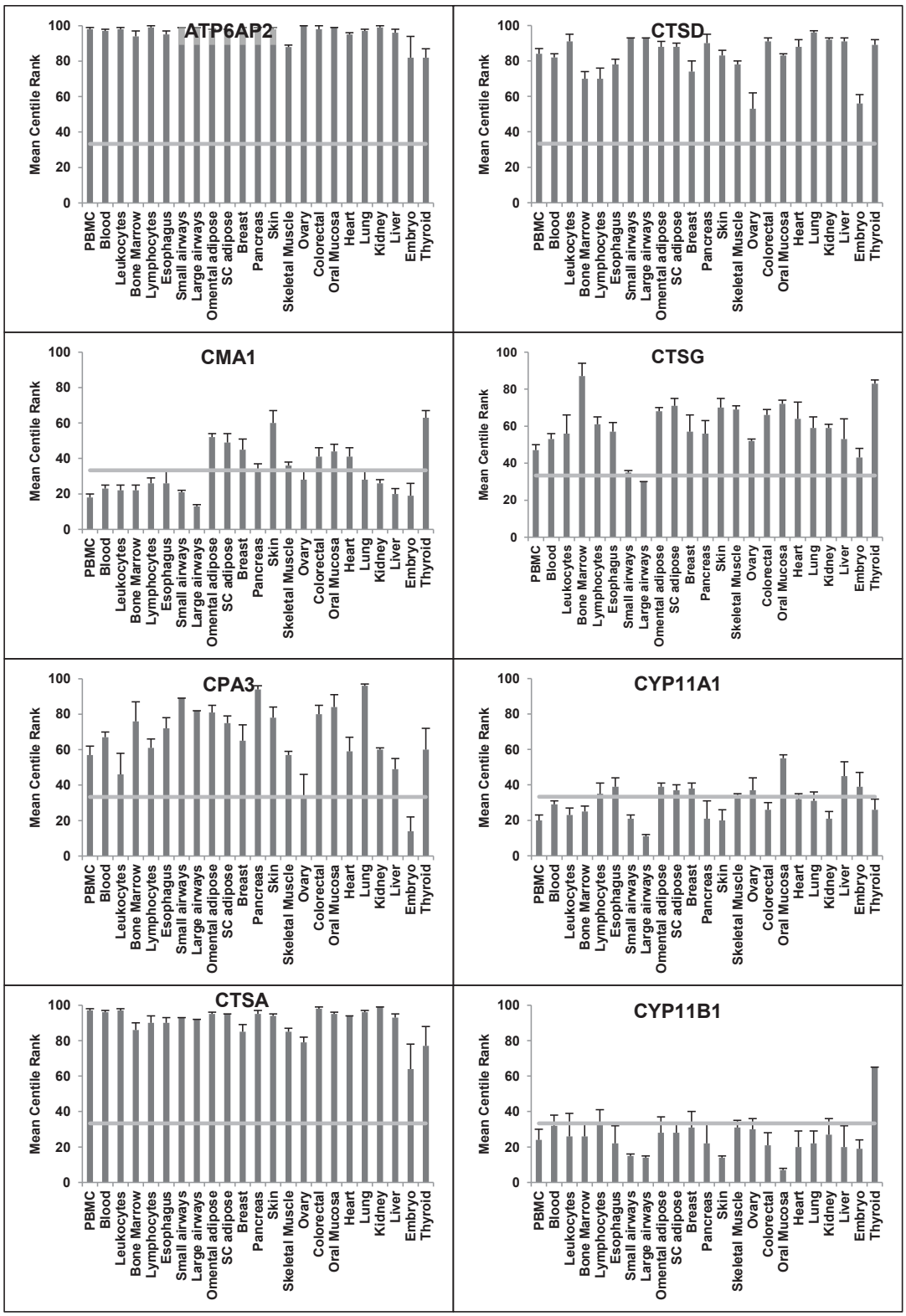
ATP6AP2
CTSD
CMA1
CTSG
CPA3
CYP11A1
CTSA
CYP11B1
Mean Centile Rank
0
20
40
60
80
100
PBMC
Blood
Leukocytes
Bone Marrow
Lymphocytes
Esophagus
Small airways
Large airways
Omental adipose
SC adipose
Breast
Pancreas
Skin
Skeletal Muscle
Ovary
Colorectal
Oral Mucosa
Heart
Lung
Kidney
Liver
Embryo
Thyroid

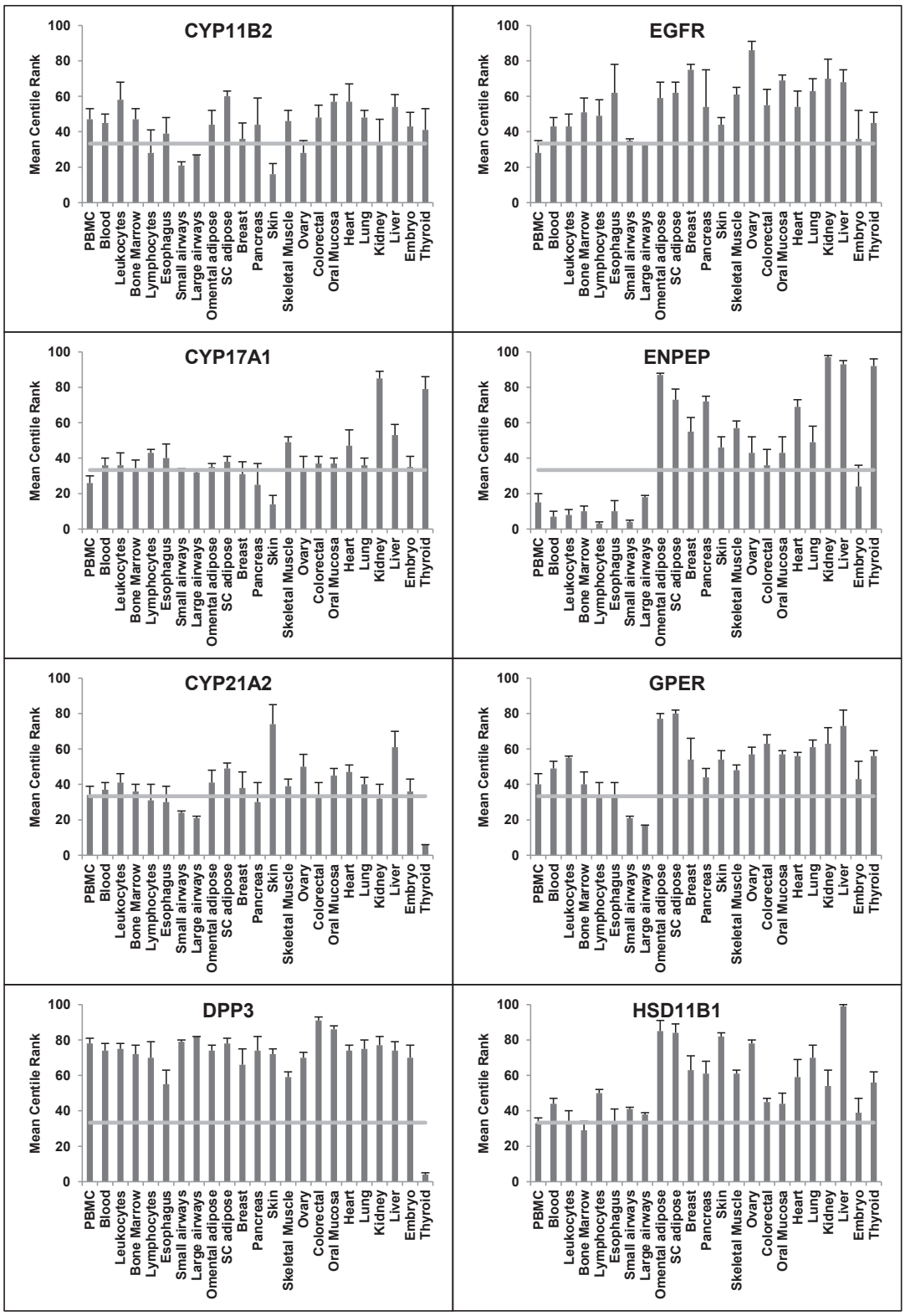
CYP11B2
EGFR
CYP17A1
ENPEP
CYP21A2
GPER
DPP3
HSD11B1
Mean Centile Rank
0
20
40
60
80
100
PBMC
Blood
Leukocytes
Bone Marrow
Lymphocytes
Esophagus
Small airways
Large airways
Omental adipose
SC adipose
Breast
Pancreas
Skin
Skeletal Muscle
Ovary
Colorectal
Oral Mucosa
Heart
Lung
Kidney
Liver
Embryo
Thyroid

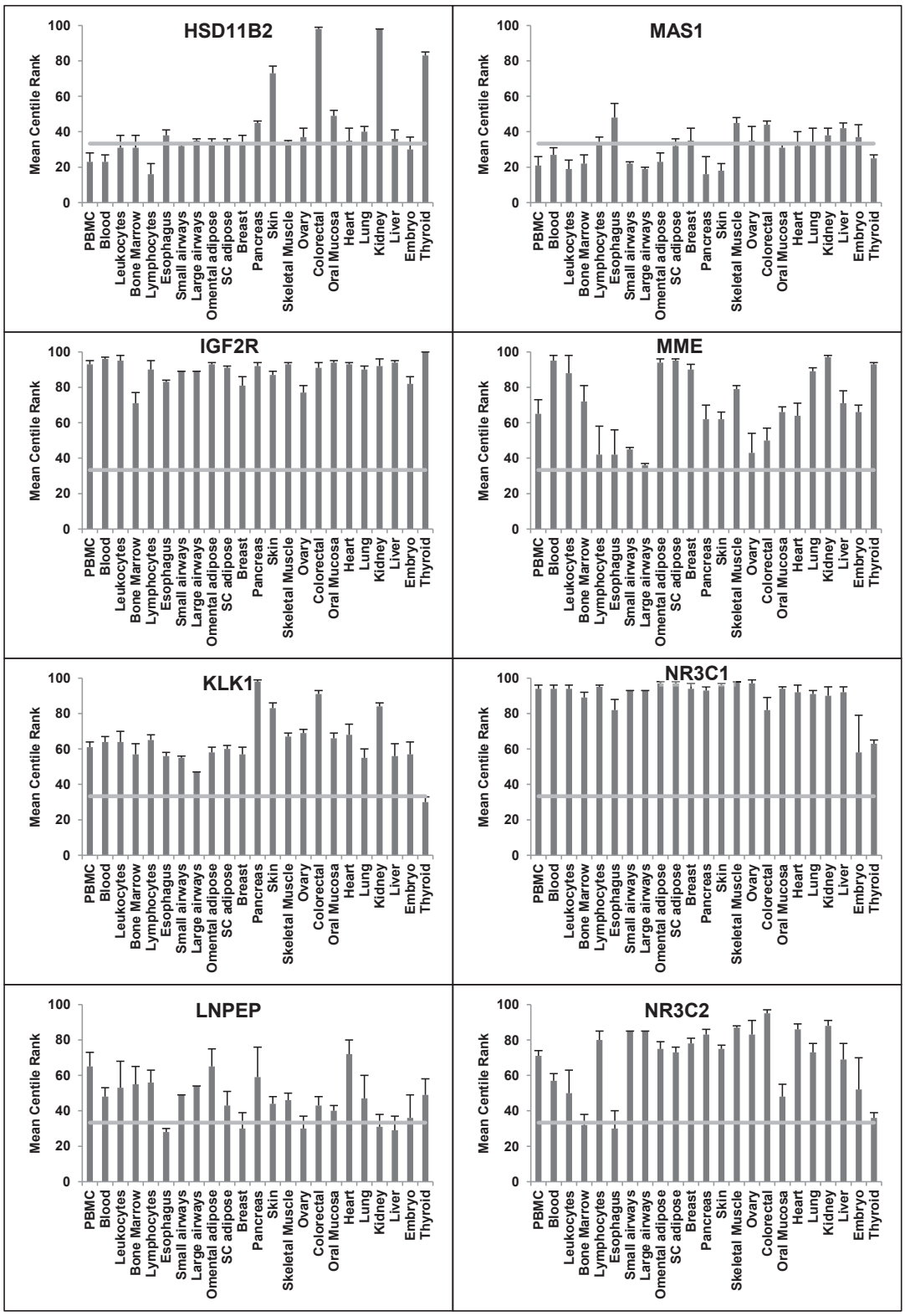
HSD11B2
MAS1
IGF2R
MME
KLK1
NR3C1
LNPEP
NR3C2
Mean Centile Rank
0
20
40
60
80
100
PBMC
Blood
Leukocytes
Bone Marrow
Lymphocytes
Esophagus
Small airways
Large airways
Omental adipose
SC adipose
Breast
Pancreas
Skin
Skeletal Muscle
Ovary
Colorectal
Oral Mucosa
Heart
Lung
Kidney
Liver
Embryo
Thyroid

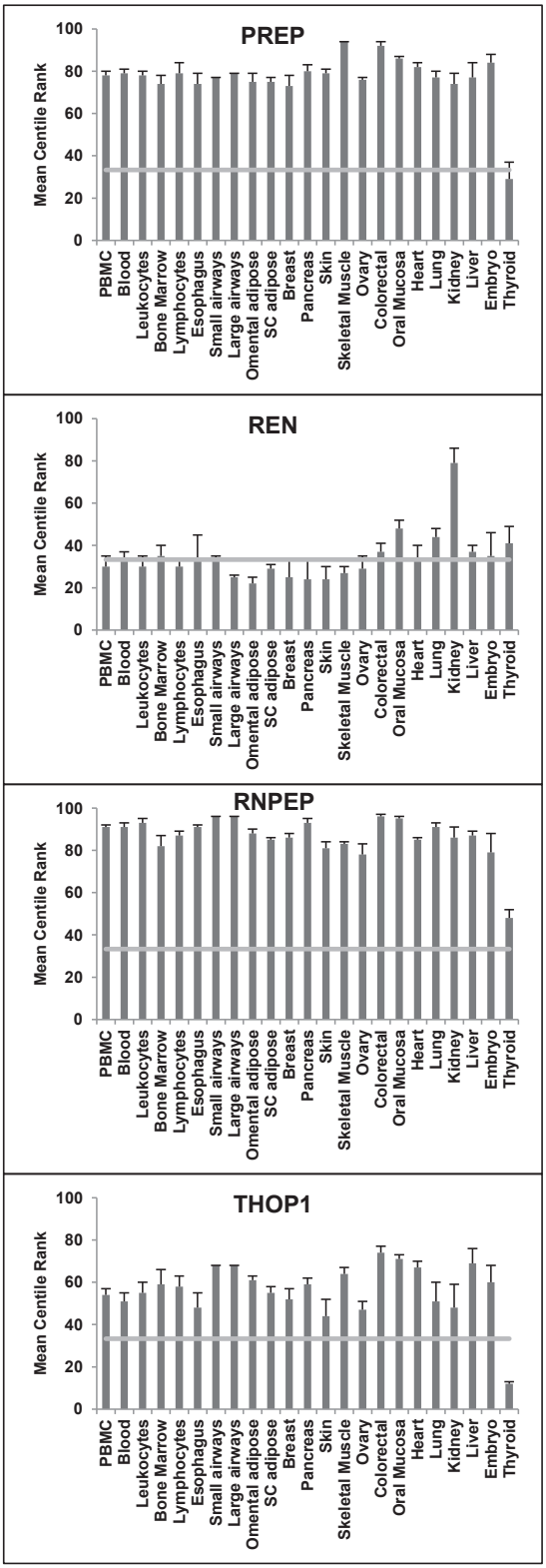
PREP
REN
RNPEP
THOP1
Mean Centile Rank
0
20
40
60
80
100
PBMC
Blood
Leukocytes
Bone Marrow
Lymphocytes
Esophagus
Small airways
Large airways
Omental adipose
SC adipose
Breast
Pancreas
Skin
Skeletal Muscle
Ovary
Colorectal
Oral Mucosa
Heart
Lung
Kidney
Liver
Embryo
Thyroid

Supplementary Atlas S1: ExtRAAS Maps in All Studied Tissues

Supplementary Atlas S1: ExtRAAS maps in in all studied tissues. Gene transcripts are represented by the corresponding official symbols. The genes are represented in the map based on their coordination (same color = same cluster) and mean centile expression rank (MCR, 4 level each with different font size). Genes below the first tertile (MCR ≤ 33) in each tissue were omitted for simplicity. Angiotensin peptides and corticosteroid metabolites are represented in gray italics. Below each map the expression profile of all genes within the corresponding tissue are represented using a bar graph. Tissues are arranged based on the tissue dendrogram of figure 5 in the article (see figure below).

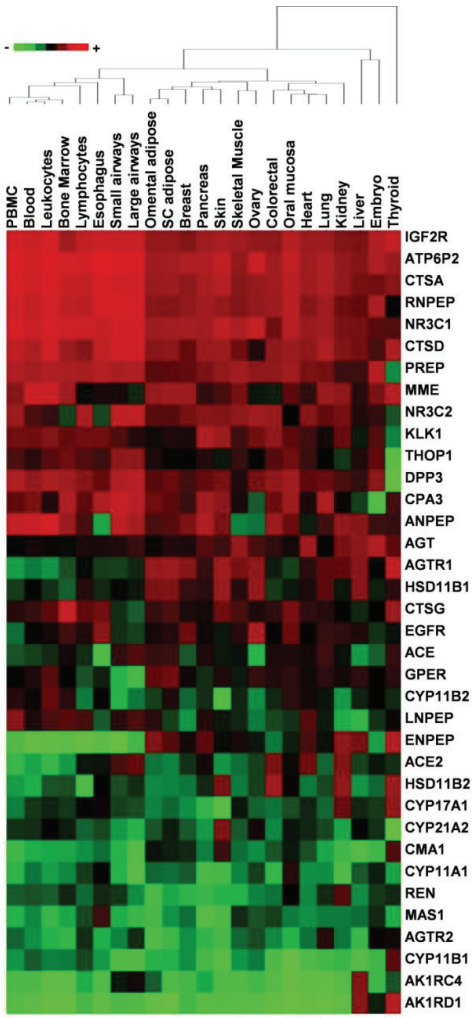

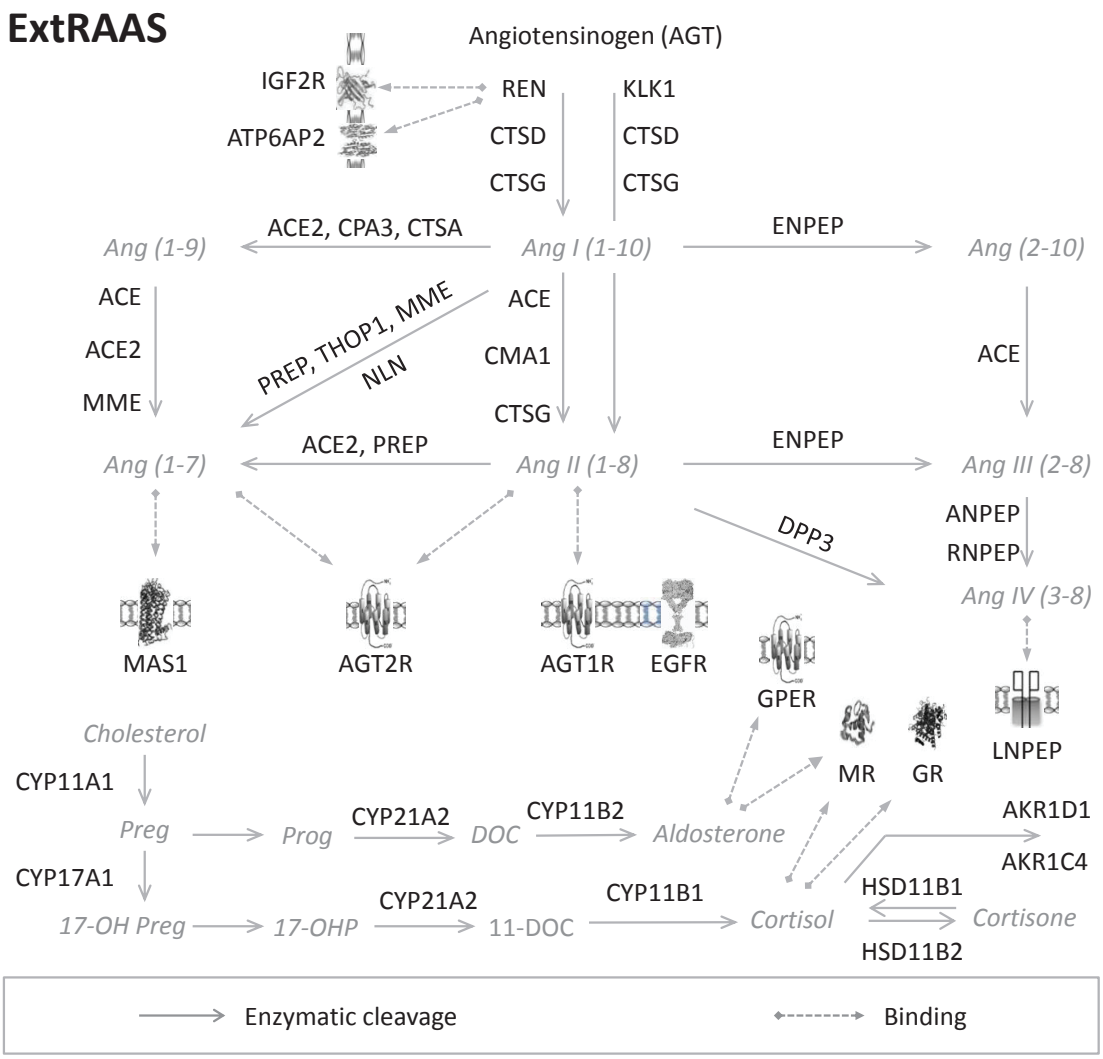

Figure font size

≤ 33 ➔ eleminated

34-40 ➔ 9

41-60 ➔ 11

61-80 ➔ 14

81-90 ➔ 18

91-100 ➔ 18

Thyroid (2, 66)

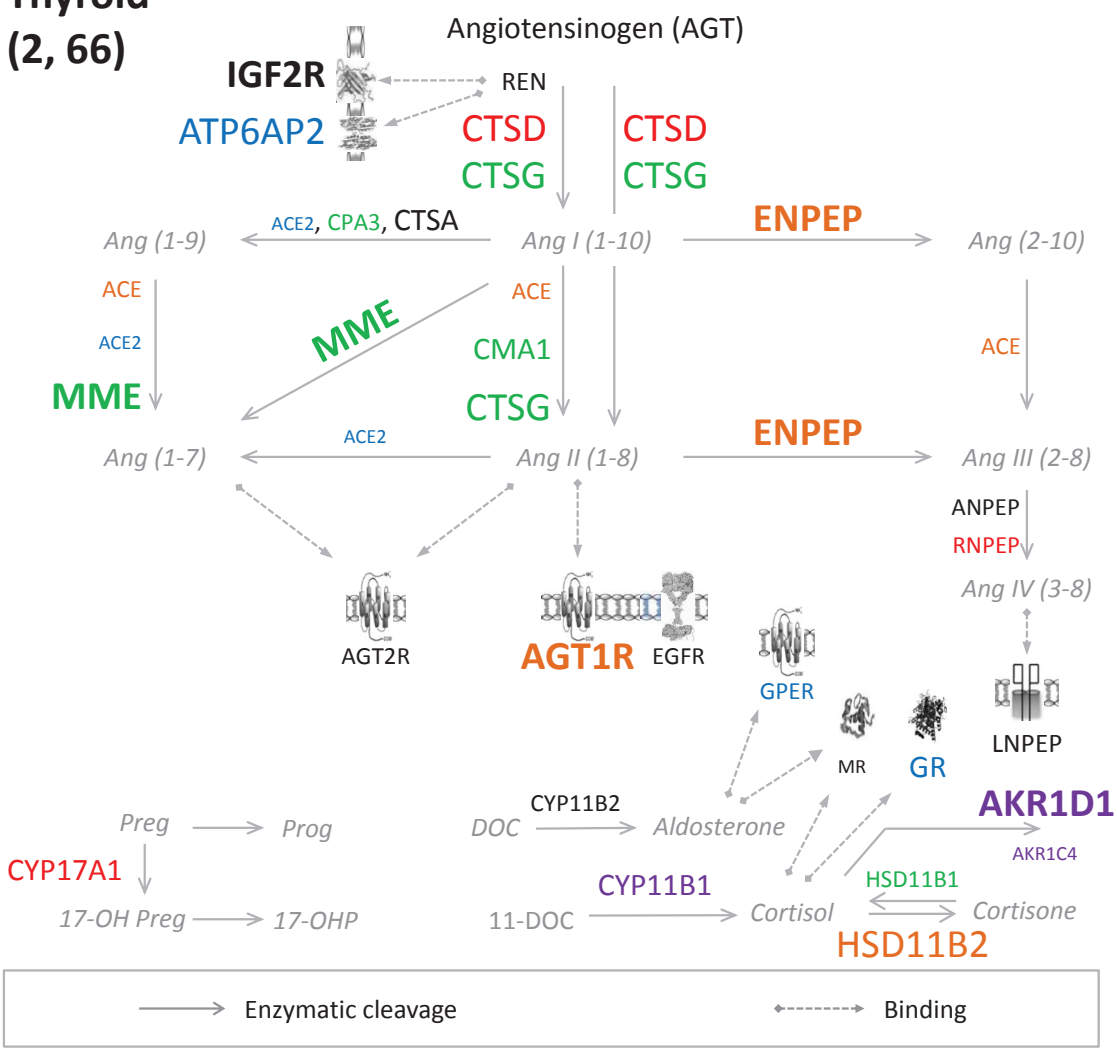
Angiotensinogen (AGT)
IGF2R
ATP6AP2
REN
CTSD
CTSG
CTSD
CTSG
ACE2, CPA3, CTSA
ENPEP
Ang (1-9)
Ang I (1-10)
Ang (2-10)
ACE
ACE2
MME
ACE
CMA1
CTSG
ACE
MME
ACE2
ENPEP
Ang (1-7)
Ang II (1-8)
Ang III (2-8)
ANPEP
RNPEP
Ang IV (3-8)
AGT2R
AGT1R
EGFR
GPER
LNPEP
MR
GR
AKR1D1
AKR1C4
Preg
Prog
DOC
CYP11B2
Aldosterone
CYP17A1
17-OH Preg
17-OHP
CYP11B1
HSD11B1
11-DOC
Cortisol
Cortisone
HSD11B2
Enzymatic cleavage
Binding

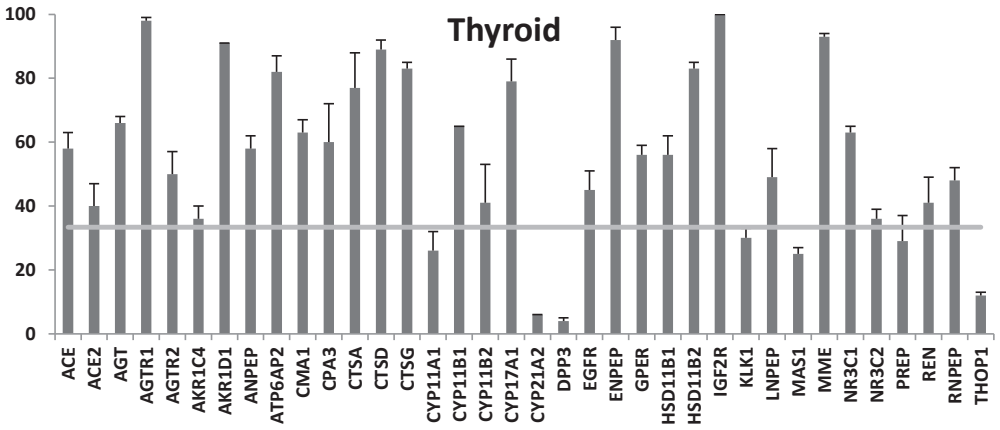
Thyroid
100
80
60
40
20
0
ACE
ACE2
AGT
AGTR1
AGTR2
AKR1C4
AKR1D1
ANPEP
ATP6AP2
CMA1
CPA3
CTSA
CTSD
CTSG
CYP11A1
CYP11B1
CYP11B2
CYP17A1
CYP21A2
DPP3
EGFR
ENPEP
GPER
HSD11B1
HSD11B2
IGF2R
KLK1
LNPEP
MAS1
MME
NR3C1
NR3C2
PREP
REN
RNPEP
THOP1

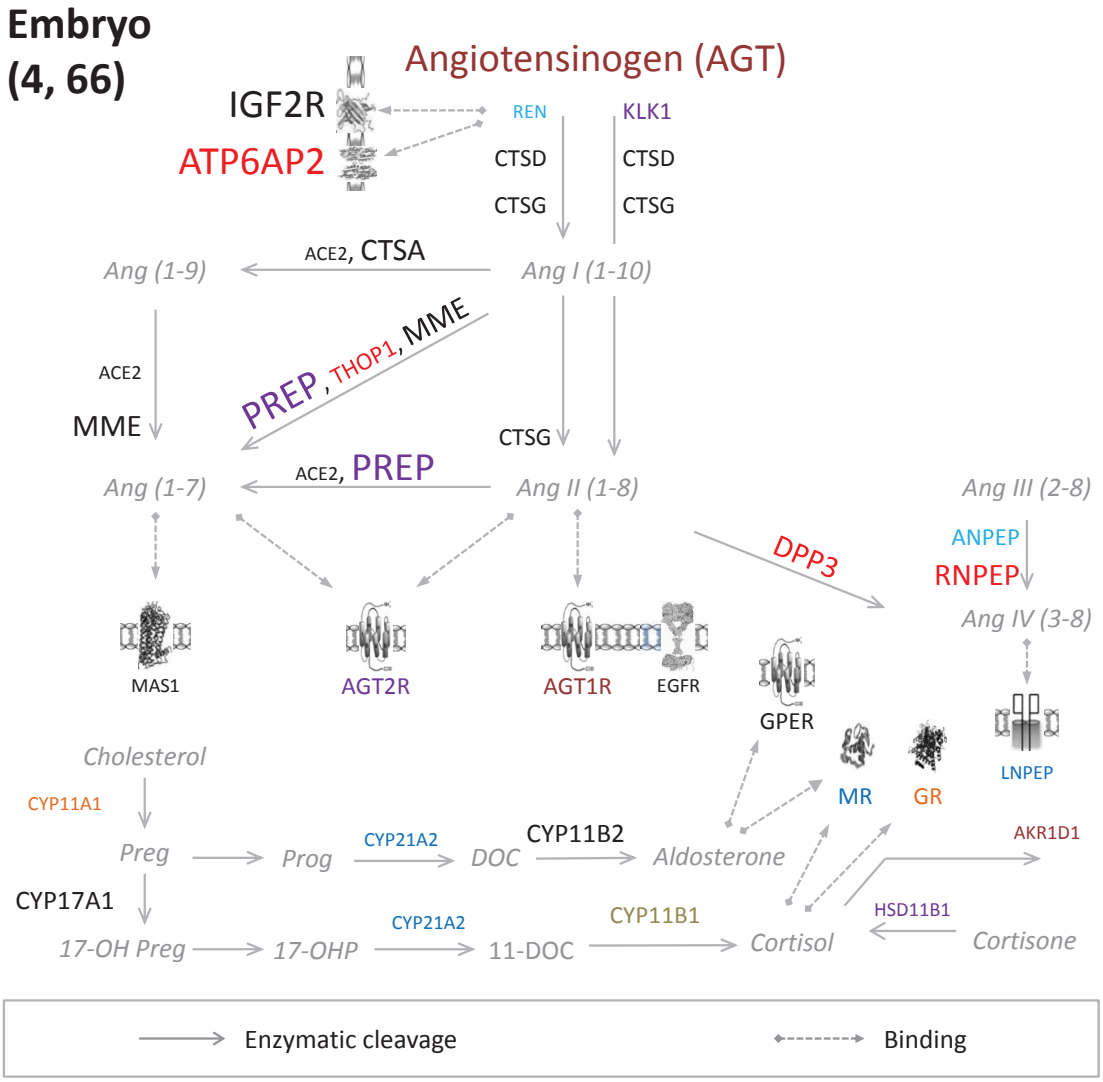
Embryo
(4, 66)
Angiotensinogen (AGT)
IGF2R
ATP6AP2
REN
KLK1
CTSD
CTSG
CTSD
CTSG
ACE2, CTSA
Ang (1-9)
Ang I (1-10)
ACE2
MME
PREP, THOP1, MME
CTSG
ACE2, PREP
Ang (1-7)
Ang II (1-8)
Ang III (2-8)
DPP3
ANPEP
RNPEP
Ang IV (3-8)
MAS1
AGT2R
AGT1R
EGFR
GPER
LNPEP
MR
GR
Cholesterol
CYP11A1
Preg
Prog
CYP21A2
DOC
CYP11B2
Aldosterone
AKR1D1
CYP17A1
17-OH Preg
17-OHP
CYP21A2
11-DOC
CYP11B1
Cortisol
HSD11B1
Cortisone
Enzymatic cleavage
Binding

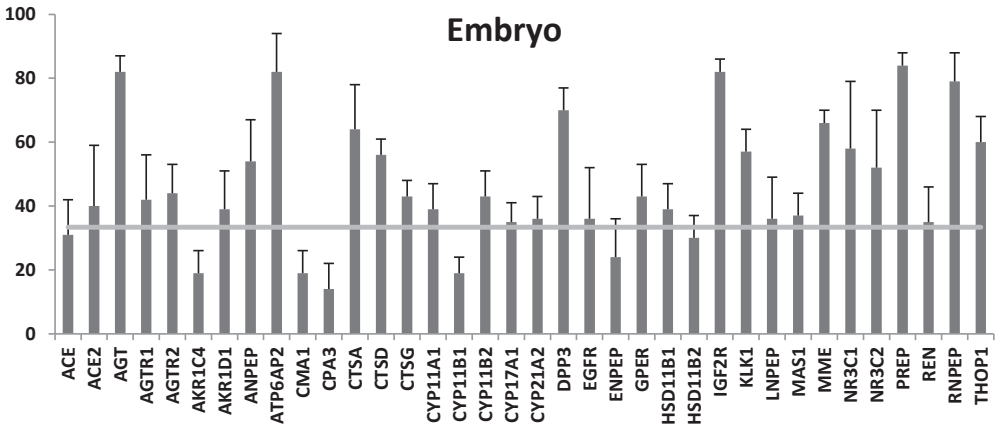
Embryo
100
80
60
40
20
0
ACE
ACE2
AGT
AGTR1
AGTR2
AKR1C4
AKR1D1
ANPEP
ATP6AP2
CMA1
CPA3
CTSA
CTSD
CTSG
CYP11A1
CYP11B1
CYP11B2
CYP17A1
CYP21A2
DPP3
EGFR
ENPEP
GPER
HSD11B1
HSD11B2
IGF2R
KLK1
LNPEP
MAS1
MME
NR3C1
NR3C2
PREP
REN
RNPEP
THOP1

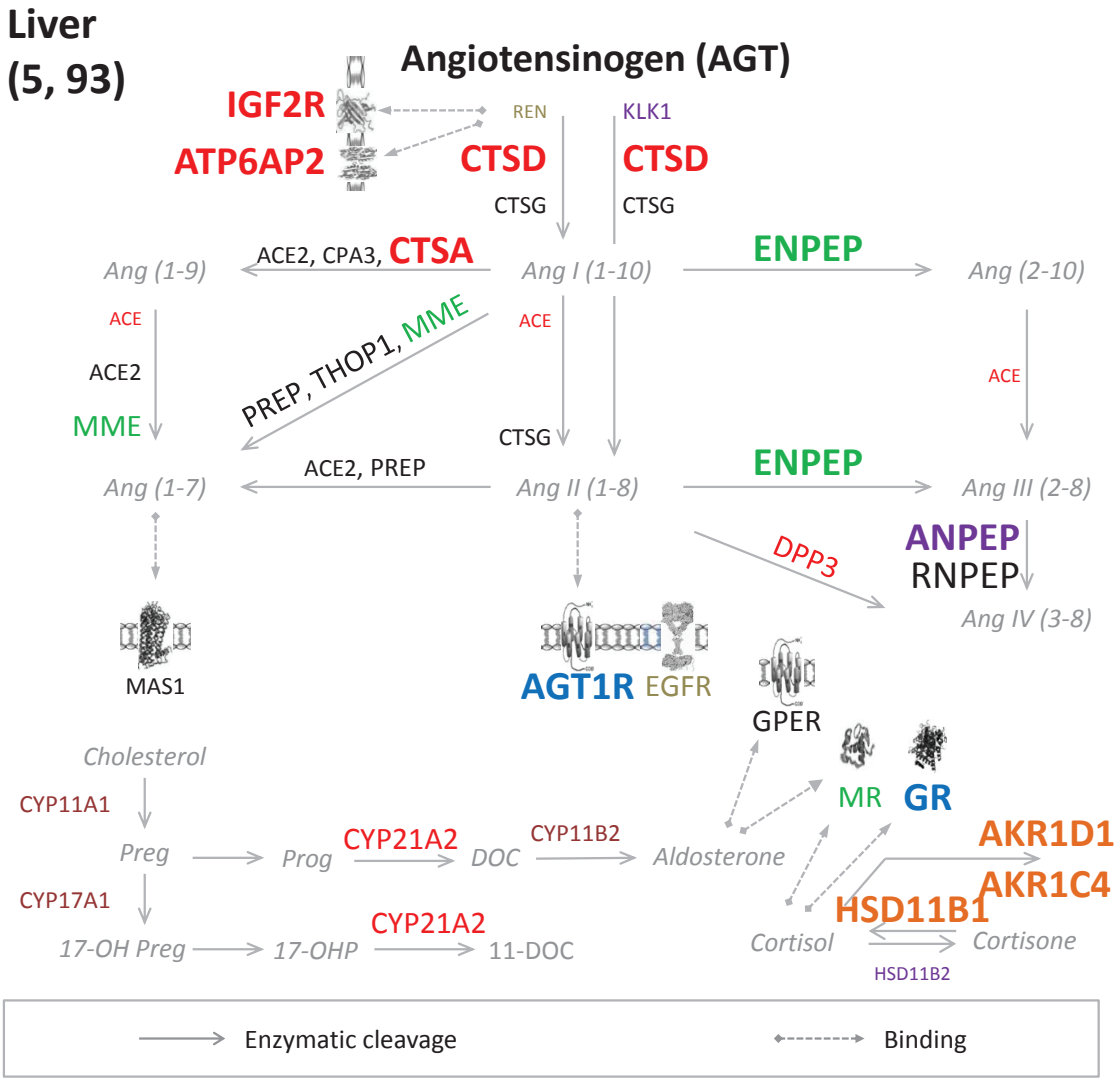
Liver
(5, 93)
Angiotensinogen (AGT)
IGF2R
ATP6AP2
REN
KLK1
CTSD
CTSD
CTSG
CTSG
ACE2, CPA3, CTSA
ENPEP
Ang (1-9)
Ang I (1-10)
Ang (2-10)
ACE
ACE2
MME
PREP, THOP1, MME
ACE
CTSG
ACE
ACE2, PREP
ENPEP
Ang (1-7)
Ang II (1-8)
Ang III (2-8)
DPP3
ANPEP
RNPEP
Ang IV (3-8)
MAS1
AGT1R
EGFR
GPER
MR
GR
Cholesterol
CYP11A1
Preg
Prog
CYP21A2
DOC
CYP11B2
Aldosterone
AKR1D1
AKR1C4
CYP17A1
HSD11B1
17-OH Preg
17-OHP
CYP21A2
11-DOC
Cortisol
Cortisone
HSD11B2
Enzymatic cleavage
Binding

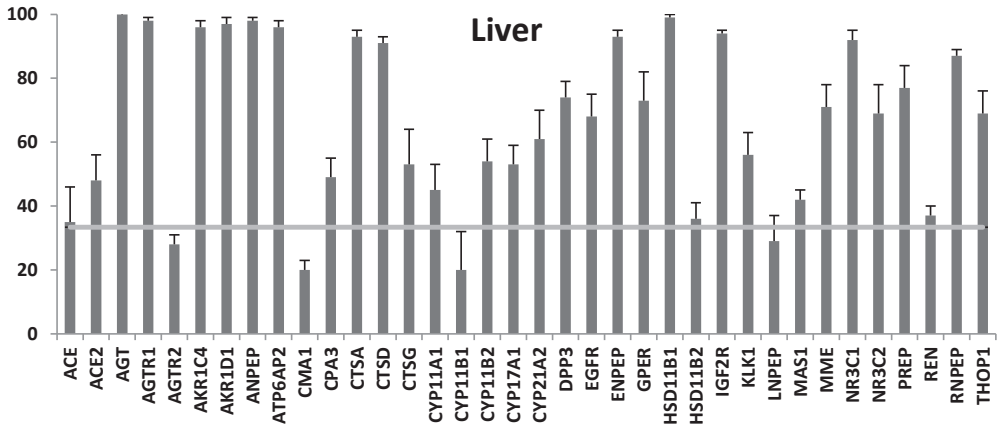
Liver
100
80
60
40
20
0
ACE
ACE2
AGT
AGTR1
AGTR2
AKR1C4
AKR1D1
ANPEP
ATP6AP2
CMA1
CPA3
CTSA
CTSD
CTSG
CYP11A1
CYP11B1
CYP11B2
CYP17A1
CYP21A2
DPP3
EGFR
ENPEP
GPER
HSD11B1
HSD11B2
IGF2R
KLK1
LNPEP
MAS1
MME
NR3C1
NR3C2
PREP
REN
RNPEP
THOP1

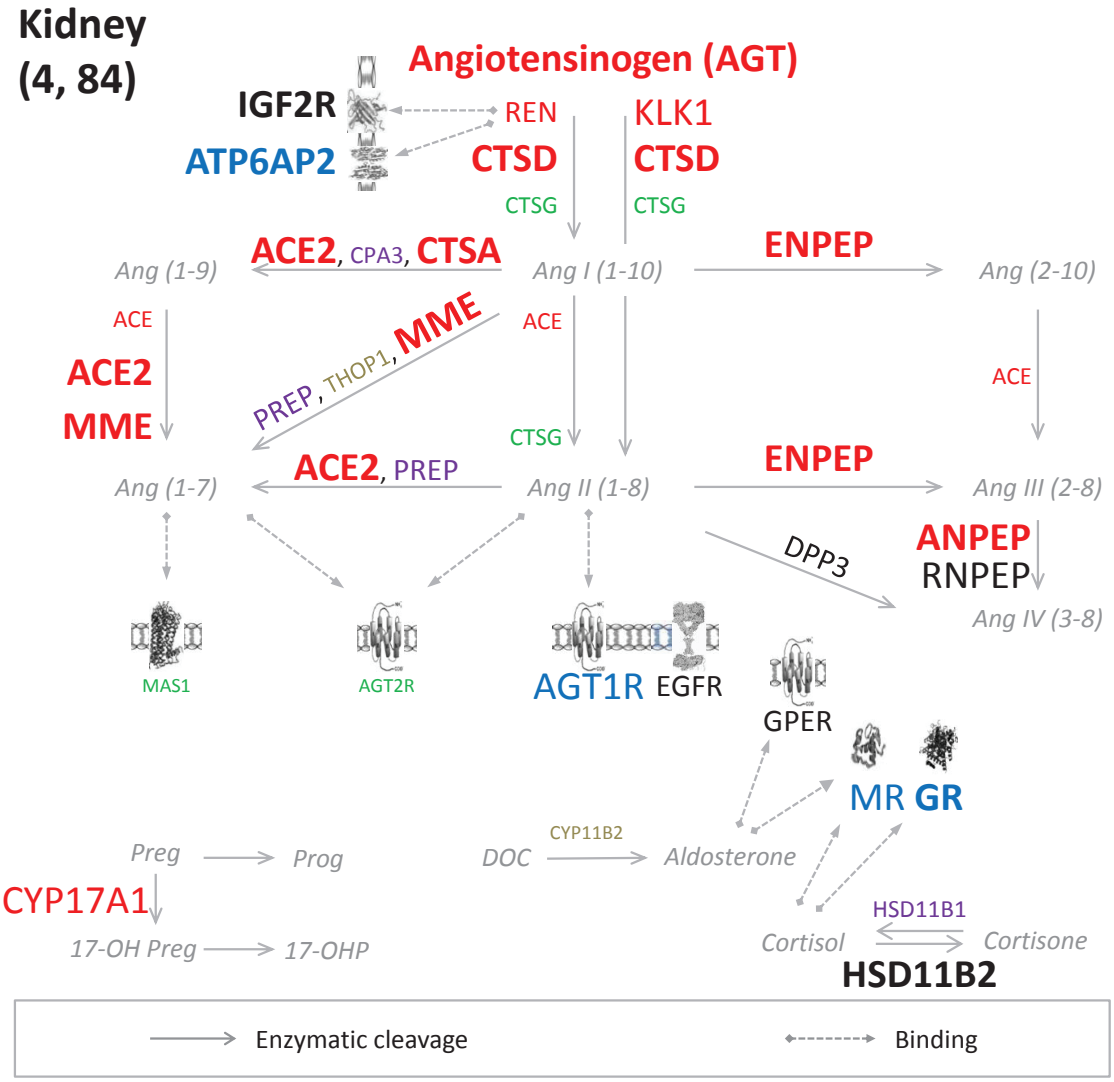
Kidney
(4, 84)
Angiotensinogen (AGT)
IGF2R
ATP6AP2
REN
CTSD
KLK1
CTSD
CTSG
CTSG
ACE2, CPA3, CTSA
ENPEP
Ang (1-9)
Ang I (1-10)
Ang (2-10)
ACE
ACE2
MME
PREP, THOP1, MME
ACE
ACE
CTSG
ACE2, PREP
ENPEP
Ang (1-7)
Ang II (1-8)
Ang III (2-8)
DPP3
ANPEP
RNPEP
Ang IV (3-8)
MAS1
AGT2R
AGT1R
EGFR
GPER
MR
GR
CYP11B2
Preg
Prog
DOC
Aldosterone
CYP17A1
HSD11B1
17-OH Preg
17-OHP
Cortisol
Cortisone
HSD11B2
Enzymatic cleavage
Binding

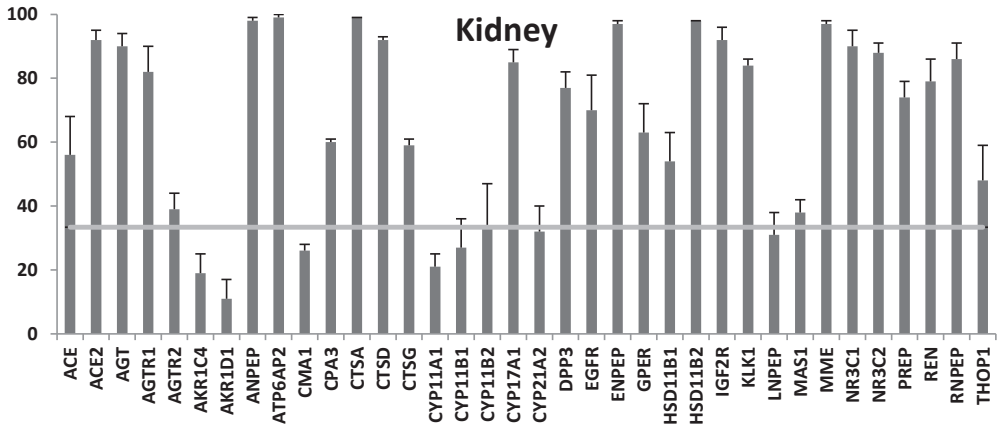
Kidney
100
80
60
40
20
0
ACE
ACE2
AGT
AGTR1
AGTR2
AKR1C4
AKR1D1
ANPEP
ATP6AP2
CMA1
CPA3
CTSA
CTSD
CTSG
CYP11A1
CYP11B1
CYP11B2
CYP17A1
CYP21A2
DPP3
EGFR
ENPEP
GPER
HSD11B1
HSD11B2
IGF2R
KLK1
LNPEP
MAS1
MME
NR3C1
NR3C2
PREP
REN
RNPEP
THOP1

Lung (5, 210)

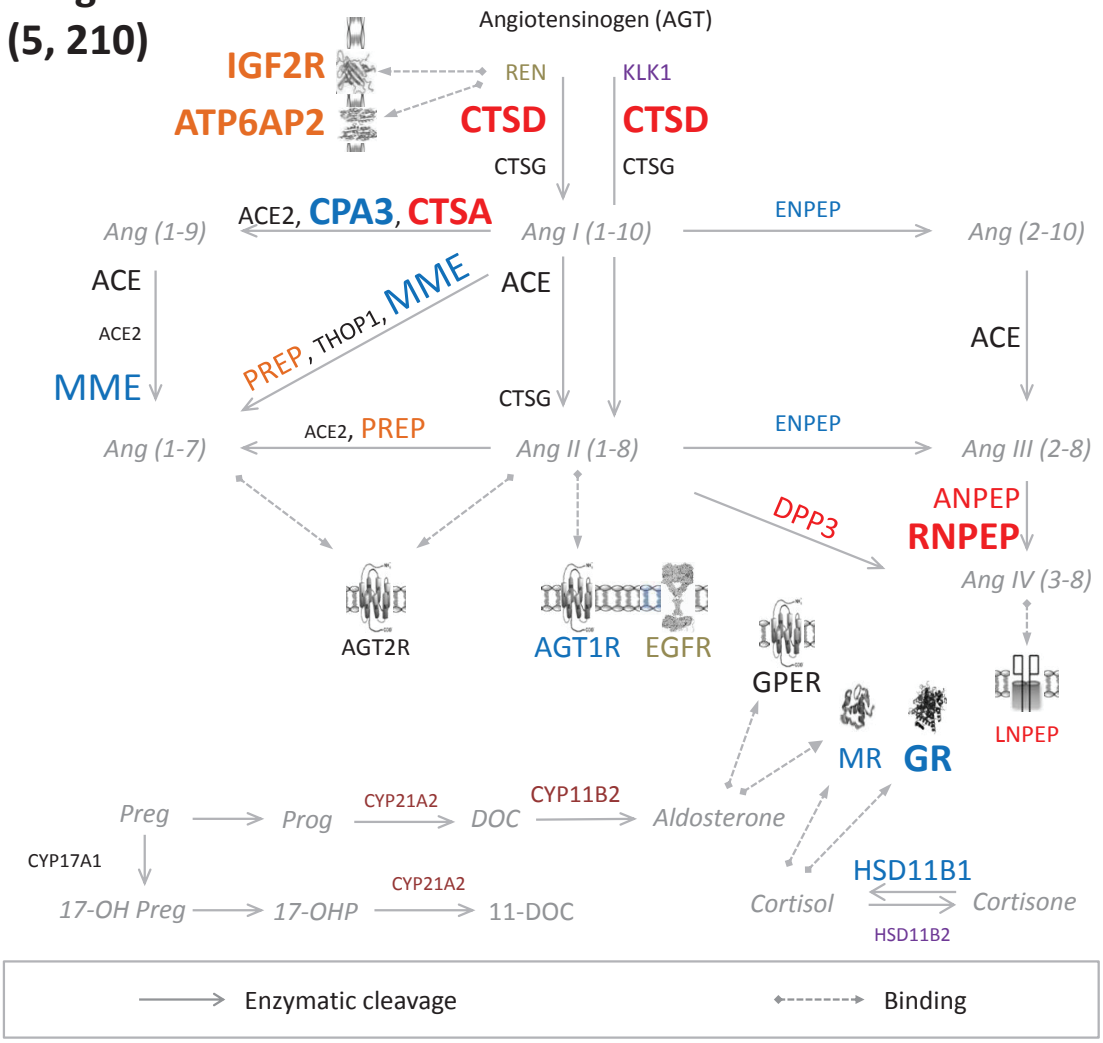
Angiotensinogen (AGT)
IGF2R
ATP6AP2
REN
KLK1
CTSD
CTSD
CTSG
CTSG
ACE2, CPA3, CTSA
Ang (1-9)
Ang I (1-10)
ENPEP
Ang (2-10)
ACE
ACE2
MME
PREP, THOP1, MME
ACE
CTSG
ACE
ACE2, PREP
Ang (1-7)
Ang II (1-8)
ENPEP
Ang III (2-8)
DPP3
ANPEP
RNPEP
Ang IV (3-8)
AGT2R
AGT1R
EGFR
GPER
LNPEP
MR
GR
Preg
Prog
CYP21A2
DOC
CYP11B2
Aldosterone
CYP17A1
17-OH Preg
17-OHP
CYP21A2
11-DOC
HSD11B1
Cortisol
Cortisone
HSD11B2
Enzymatic cleavage
Binding

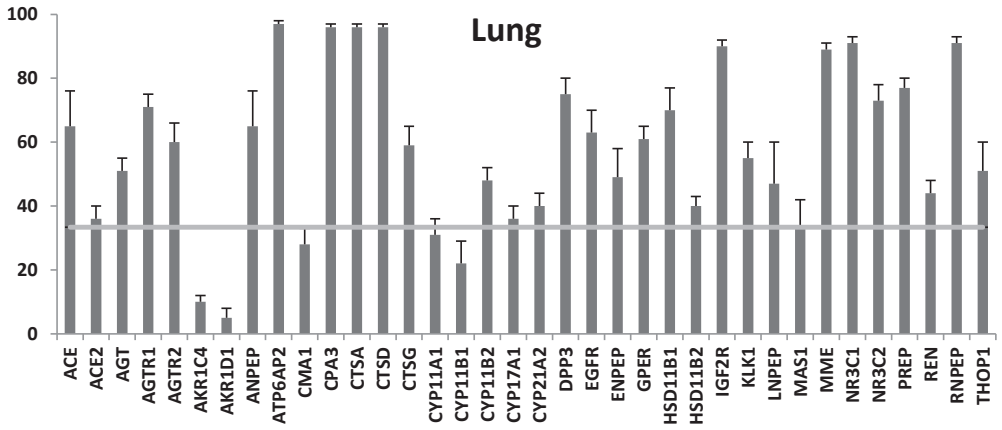
Lung
100
80
60
40
20
0
ACE
ACE2
AGT
AGTR1
AGTR2
AKR1C4
AKR1D1
ANPEP
ATP6AP2
CMA1
CPA3
CTSA
CTSD
CTSG
CYP11A1
CYP11B1
CYP11B2
CYP17A1
CYP21A2
DPP3
EGFR
ENPEP
GPER
HSD11B1
HSD11B2
IGF2R
KLK1
LNPEP
MAS1
MME
NR3C1
NR3C2
PREP
REN
RNPEP
THOP1

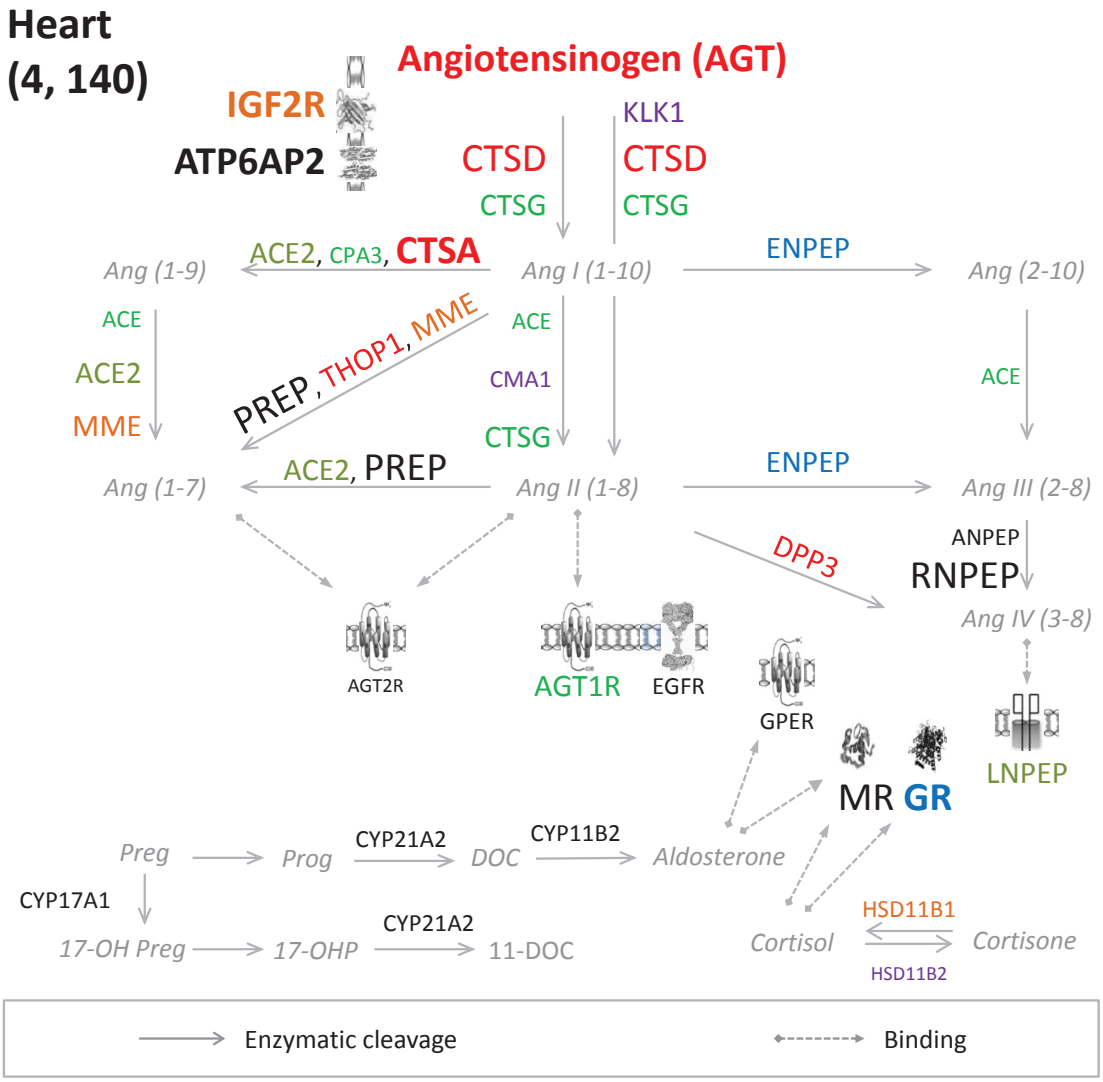
Heart
(4, 140)
Angiotensinogen (AGT)
IGF2R
ATP6AP2
KLK1
CTSD
CTSG
CTSD
CTSG
ACE2, CPA3, CTSA
ENPEP
Ang (1-9)
Ang I (1-10)
Ang (2-10)
ACE
ACE2
MME
PREP, THOP1, MME
ACE
CMA1
CTSG
ACE
ACE2, PREP
ENPEP
Ang (1-7)
Ang II (1-8)
Ang III (2-8)
DPP3
ANPEP
RNPEP
Ang IV (3-8)
AGT2R
AGT1R
EGFR
GPER
LNPEP
MR
GR
Preg
Prog
CYP21A2
DOC
CYP11B2
Aldosterone
CYP17A1
17-OH Preg
17-OHP
CYP21A2
11-DOC
Cortisol
HSD11B1
HSD11B2
Cortisone
Enzymatic cleavage
Binding

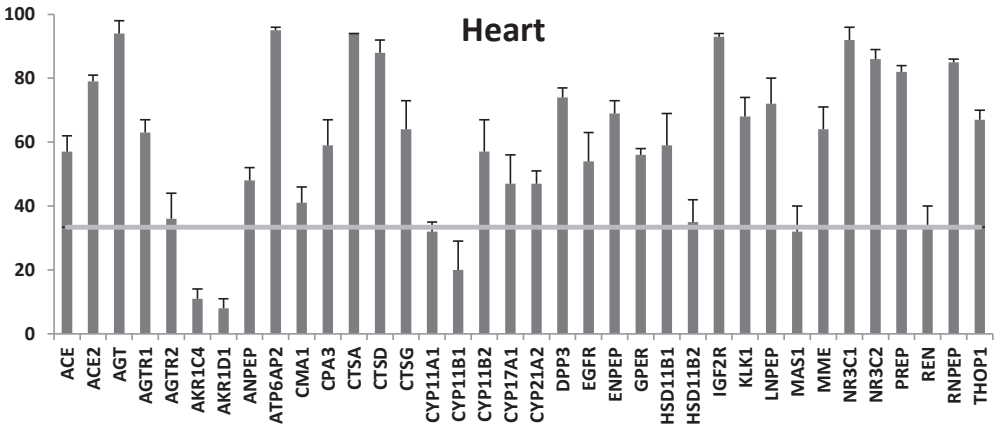
Heart
100
80
60
40
20
0
ACE
ACE2
AGT
AGTR1
AGTR2
AKR1C4
AKR1D1
ANPEP
ATP6AP2
CMA1
CPA3
CTSA
CTSD
CTSG
CYP11A1
CYP11B1
CYP11B2
CYP17A1
CYP21A2
DPP3
EGFR
ENPEP
GPER
HSD11B1
HSD11B2
IGF2R
KLK1
LNPEP
MAS1
MME
NR3C1
NR3C2
PREP
REN
RNPEP
THOP1

Oral Mucosa (4, 193)

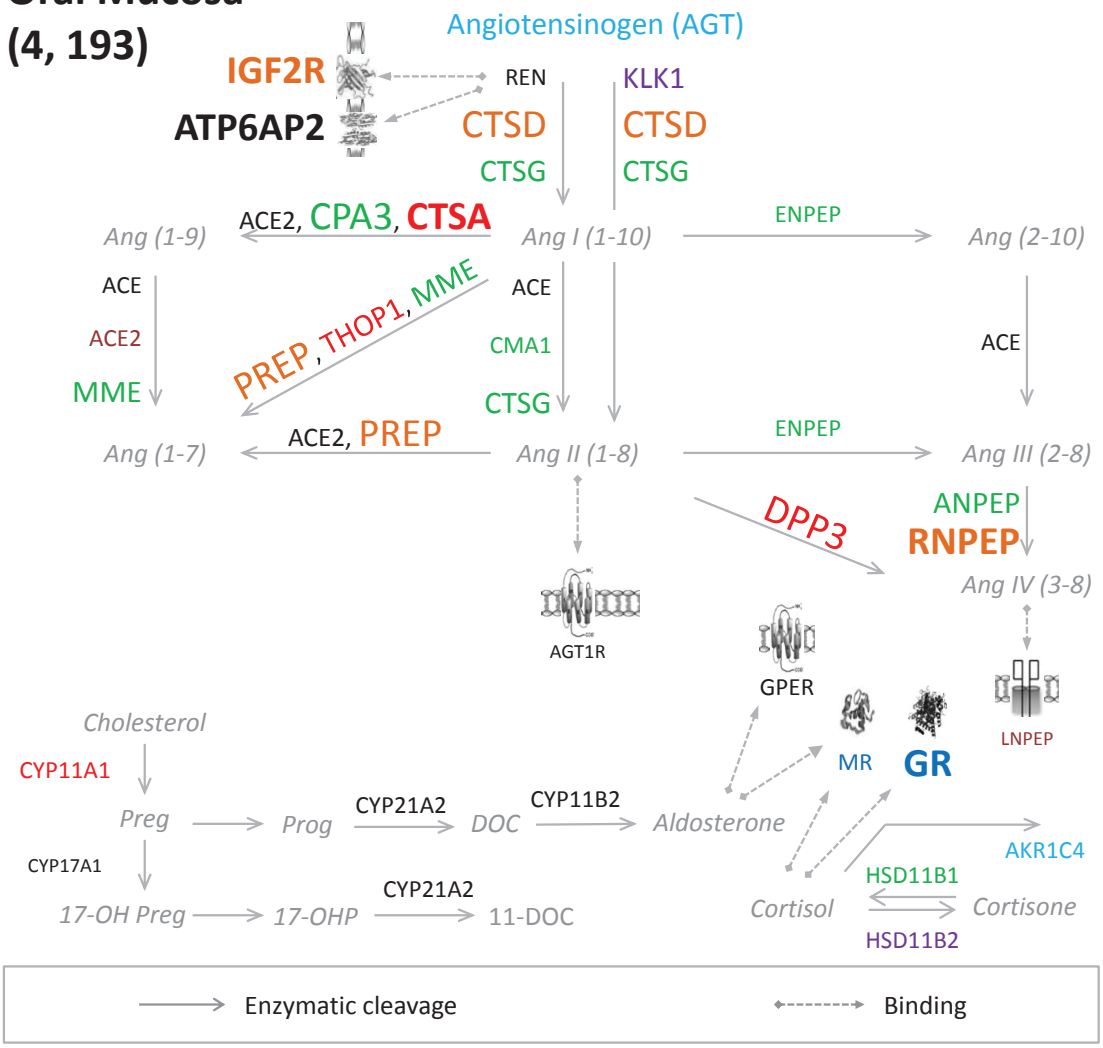

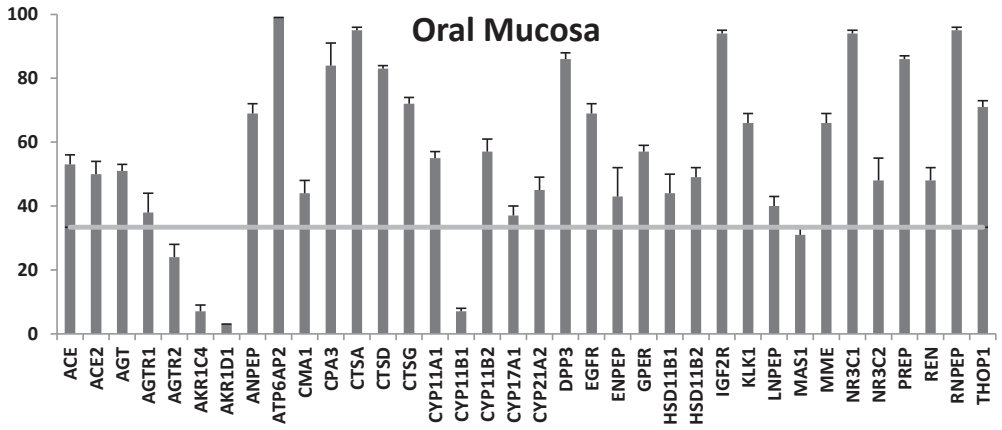

Colorectal (8, 171)

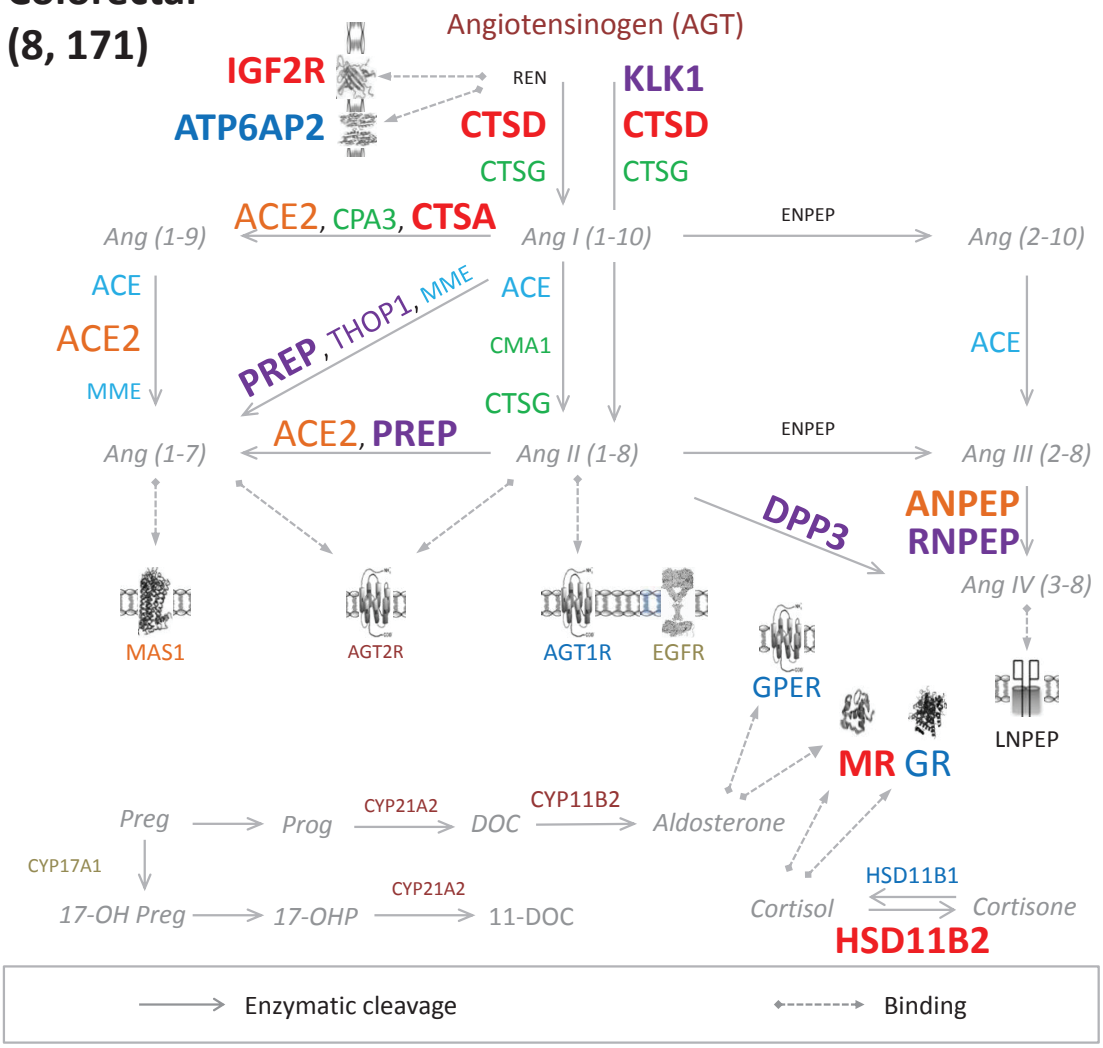

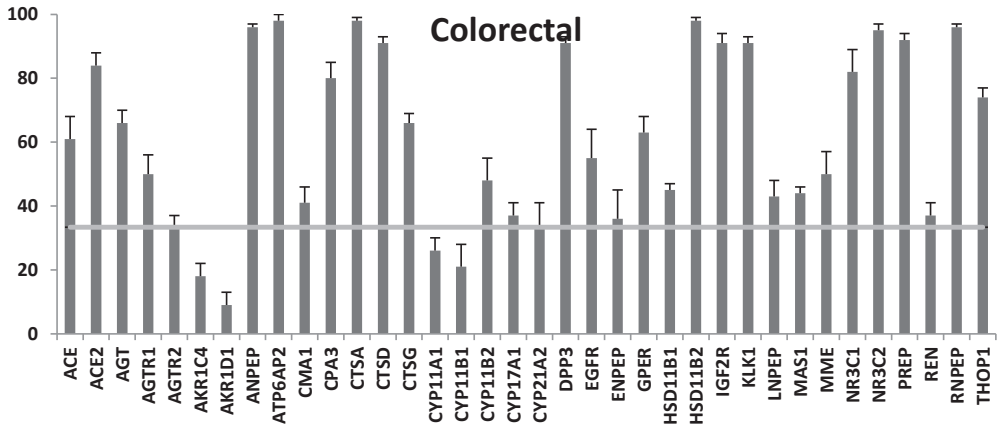

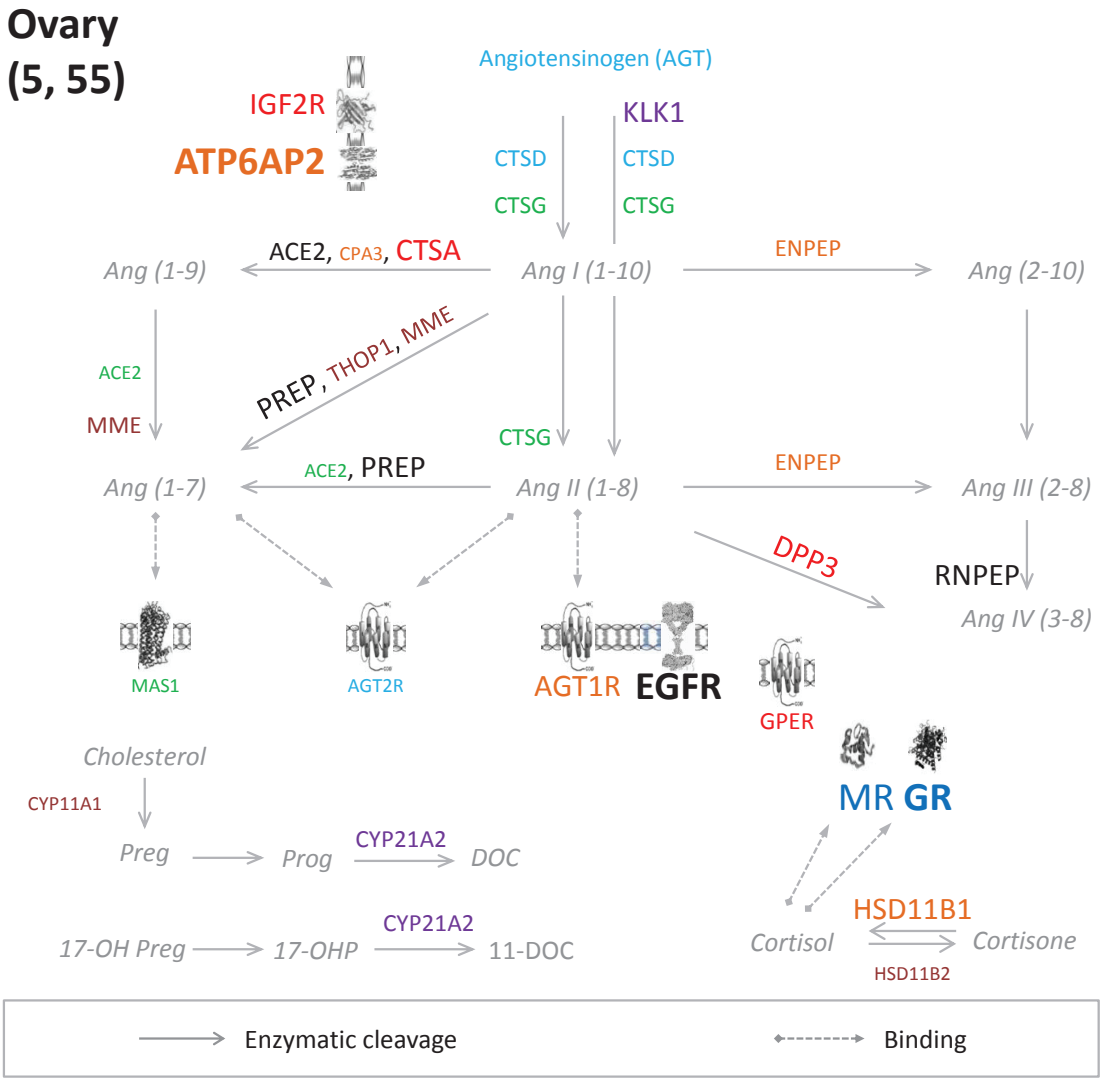
Ovary
(5, 55)
IGF2R
ATP6AP2
Angiotensinogen (AGT)
KLK1
CTSD
CTSG
CTSD
CTSG
ACE2, CPA3, CTSA
Ang (1-9)
Ang I (1-10)
ENPEP
Ang (2-10)
ACE2
MME
PREP, THOP1, MME
CTSG
ACE2, PREP
Ang (1-7)
Ang II (1-8)
ENPEP
Ang III (2-8)
DPP3
RNPEP
Ang IV (3-8)
MAS1
AGT2R
AGT1R
EGFR
GPER
MR
GR
Cholesterol
CYP11A1
Preg
Prog
CYP21A2
DOC
17-OH Preg
17-OHP
CYP21A2
11-DOC
HSD11B1
Cortisol
Cortisone
HSD11B2
Enzymatic cleavage
Binding

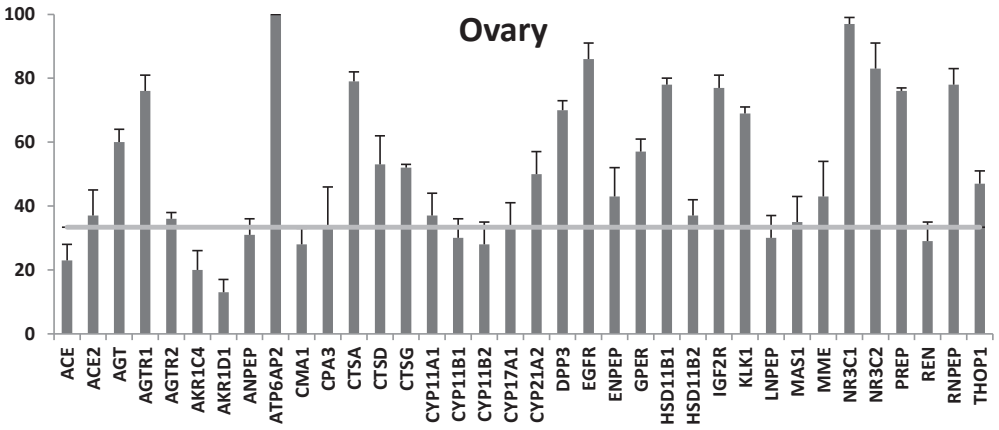
Ovary
100
80
60
40
20
0
ACE
ACE2
AGT
AGTR1
AGTR2
AKR1C4
AKR1D1
ANPEP
ATP6AP2
CMA1
CPA3
CTSA
CTSD
CTSG
CYP11A1
CYP11B1
CYP11B2
CYP17A1
CYP21A2
DPP3
EGFR
ENPEP
GPER
HSD11B1
HSD11B2
IGF2R
KLK1
LNPEP
MAS1
MME
NR3C1
NR3C2
PREP
REN
RNPEP
THOP1

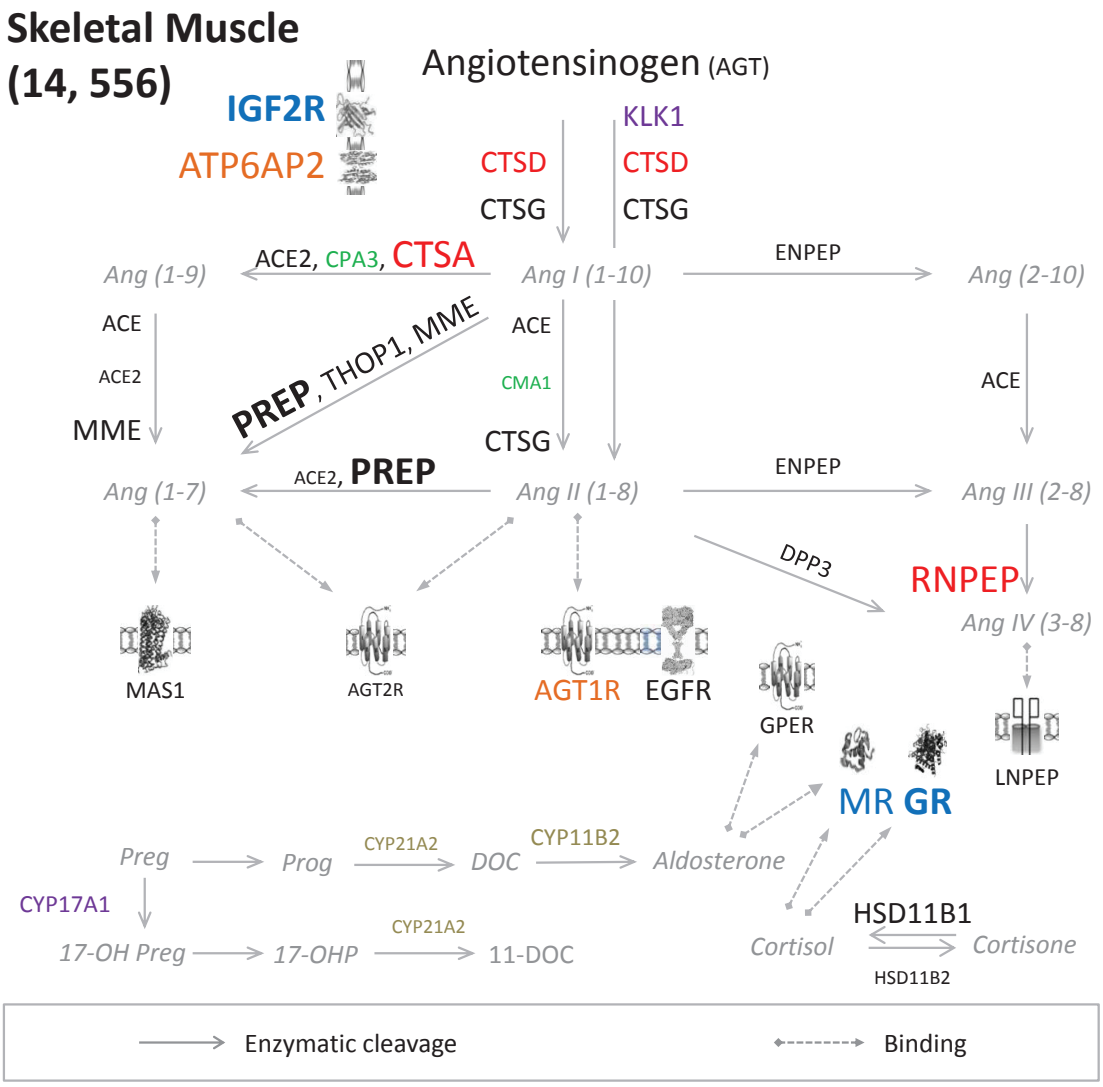
Skeletal Muscle
(14, 556)
Angiotensinogen (AGT)
IGF2R
ATP6AP2
KLK1
CTSD
CTSG
CTSD
CTSG
ACE2, CPA3, CTSA
ENPEP
Ang (1-9)
Ang I (1-10)
Ang (2-10)
ACE
ACE2
MME
PREP, THOP1, MME
ACE
CMA1
CTSG
ACE
ACE2, PREP
ENPEP
Ang (1-7)
Ang II (1-8)
Ang III (2-8)
DPP3
RNPEP
Ang IV (3-8)
MAS1
AGT2R
AGT1R
EGFR
GPER
LNPEP
MR
GR
Preg
Prog
CYP21A2
DOC
CYP11B2
Aldosterone
CYP17A1
17-OH Preg
17-OHP
CYP21A2
11-DOC
Cortisol
HSD11B1
Cortisone
HSD11B2
Enzymatic cleavage
Binding

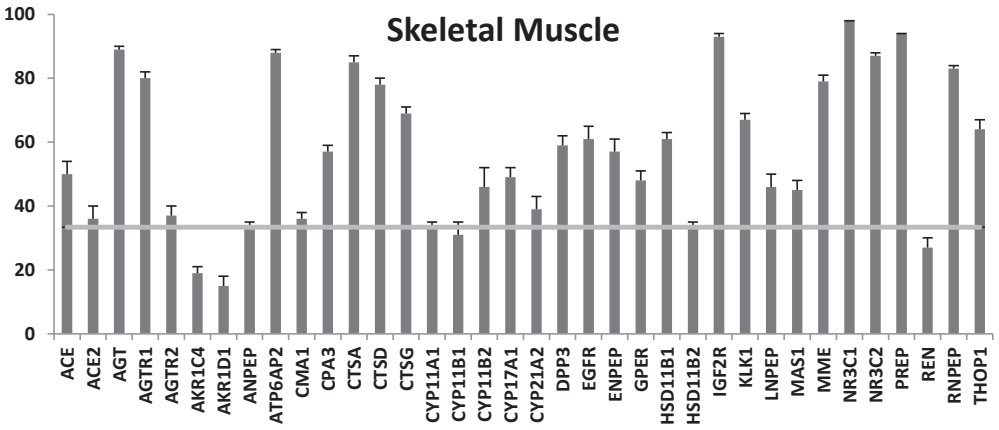
Skeletal Muscle
100
80
60
40
20
0
ACE
ACE2
AGT
AGTR1
AGTR2
AKR1C4
AKR1D1
ANPEP
ATP6AP2
CMA1
CPA3
CTSA
CTSD
CTSG
CYP11A1
CYP11B1
CYP11B2
CYP17A1
CYP21A2
DPP3
EGFR
ENPEP
GPER
HSD11B1
HSD11B2
IGF2R
KLK1
LNPEP
MAS1
MME
NR3C1
NR3C2
PREP
REN
RNPEP
THOP1

Skin (7, 222)

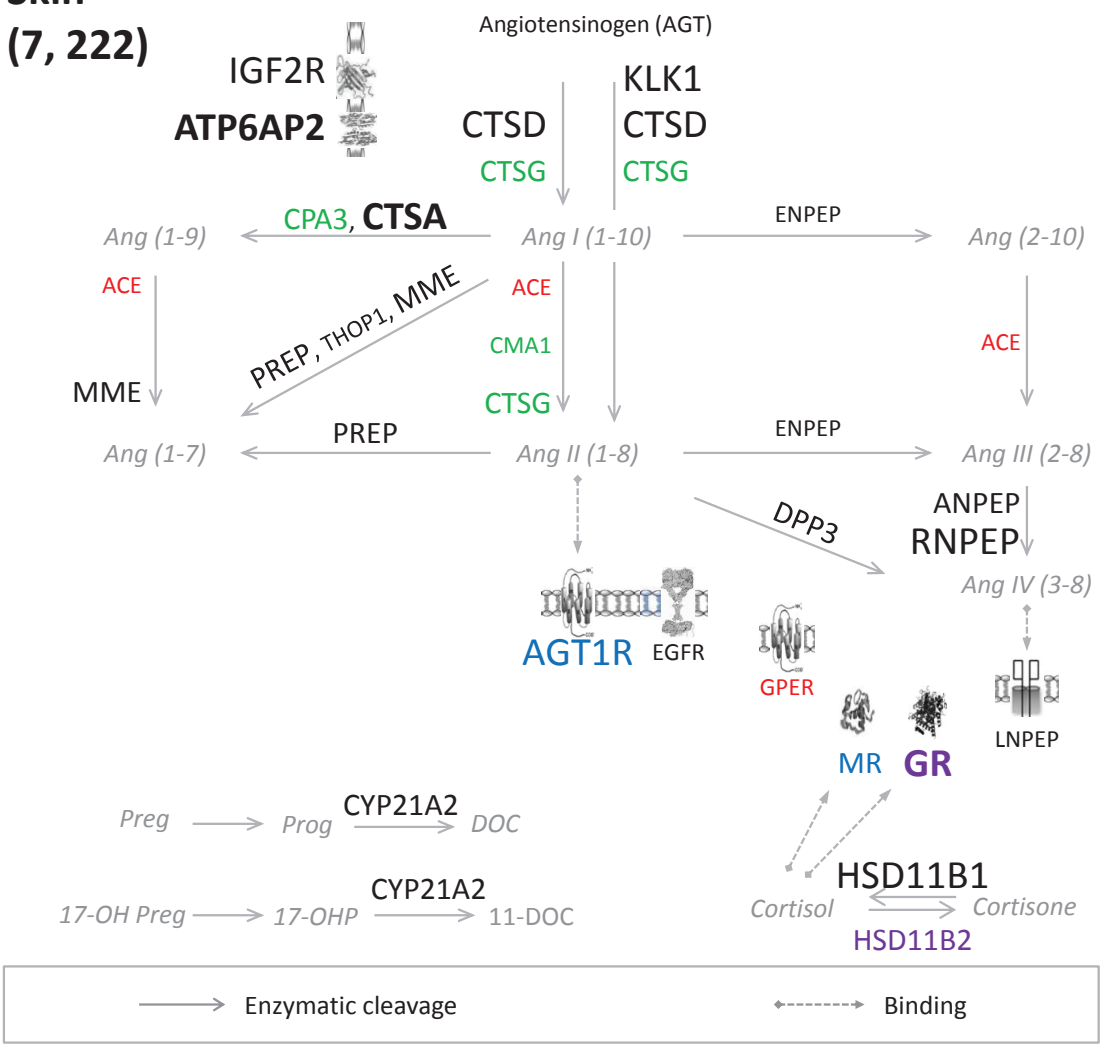
Angiotensinogen (AGT)
IGF2R
ATP6AP2
CTSD
CTSG
KLK1
CTSD
CTSG
CPA3, CTSA
Ang (1-9)
Ang I (1-10)
ENPEP
Ang (2-10)
ACE
ACE
ACE
PREP, THOP1, MME
CMA1
CTSG
MME
PREP
Ang (1-7)
Ang II (1-8)
ENPEP
Ang III (2-8)
DPP3
ANPEP
RNPEP
Ang IV (3-8)
AGT1R
EGFR
GPER
LNPEP
MR
GR
Preg
Prog
CYP21A2
DOC
17-OH Preg
17-OHP
CYP21A2
11-DOC
HSD11B1
Cortisol
Cortisone
HSD11B2
Enzymatic cleavage
Binding

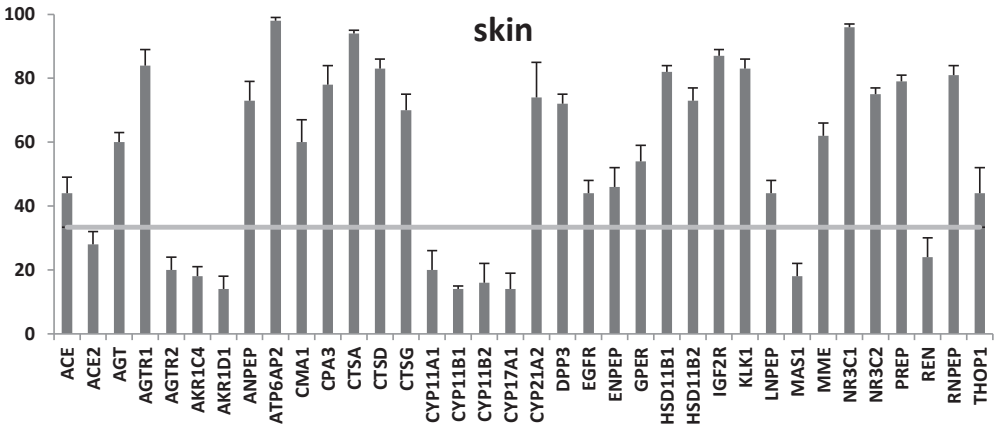
skin
100
80
60
40
20
0
ACE
ACE2
AGT
AGTR1
AGTR2
AKR1C4
AKR1D1
ANPEP
ATP6AP2
CMA1
CPA3
CTSA
CTSD
CTSG
CYP11A1
CYP11B1
CYP11B2
CYP17A1
CYP21A2
DPP3
EGFR
ENPEP
GPER
HSD11B1
HSD11B2
IGF2R
KLK1
LNPEP
MAS1
MME
NR3C1
NR3C2
PREP
REN
RNPEP
THOP1

Pancreas (3, 100)

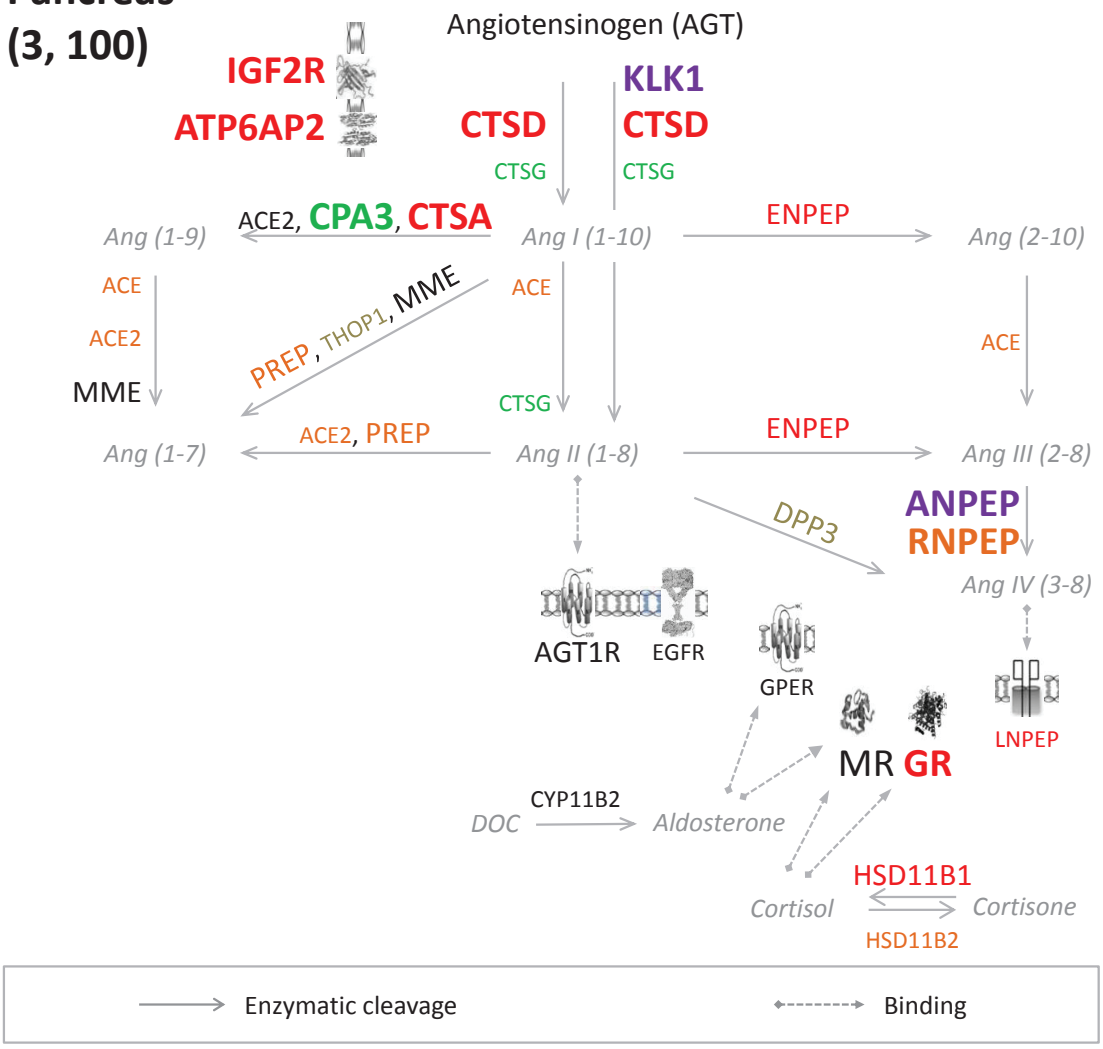

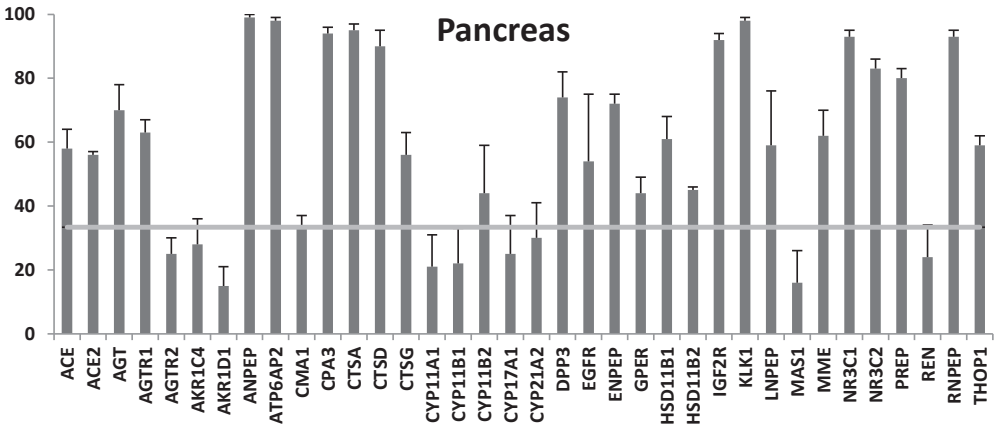

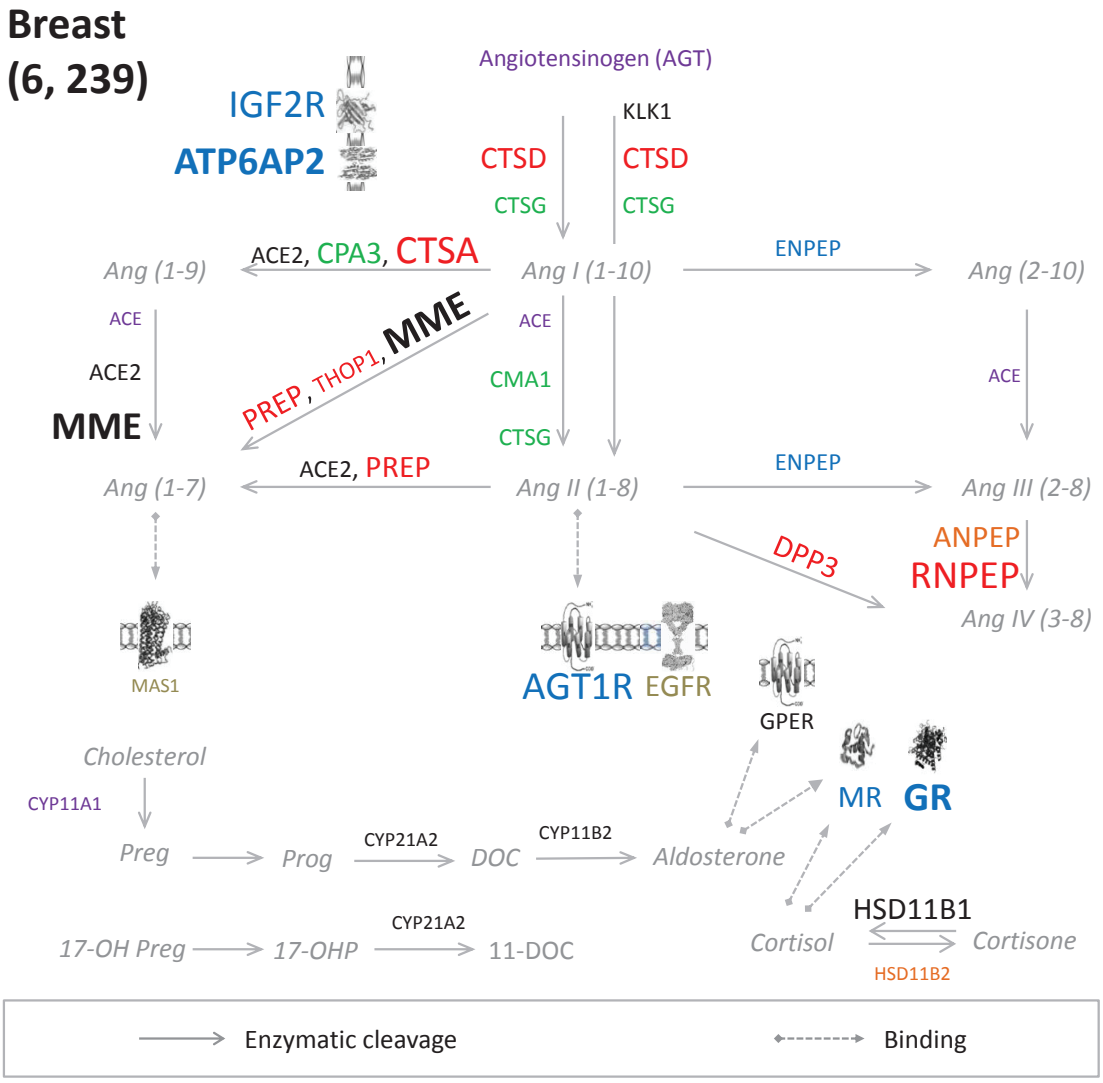
Breast
(6, 239)
Angiotensinogen (AGT)
IGF2R
ATP6AP2
KLK1
CTSD
CTSD
CTSG
CTSG
ACE2, CPA3, CTSA
ENPEP
Ang (1-9)
Ang I (1-10)
Ang (2-10)
ACE
ACE
ACE
ACE2
CMA1
MME
PREP, THOP1, MME
CTSG
ACE2, PREP
ENPEP
Ang (1-7)
Ang II (1-8)
Ang III (2-8)
DPP3
ANPEP
RNPEP
Ang IV (3-8)
MAS1
AGT1R
EGFR
GPER
Cholesterol
CYP11A1
MR
GR
Preg
Prog
CYP21A2
DOC
CYP11B2
Aldosterone
HSD11B1
17-OH Preg
17-OHP
CYP21A2
11-DOC
Cortisol
Cortisone
HSD11B2
Enzymatic cleavage
Binding

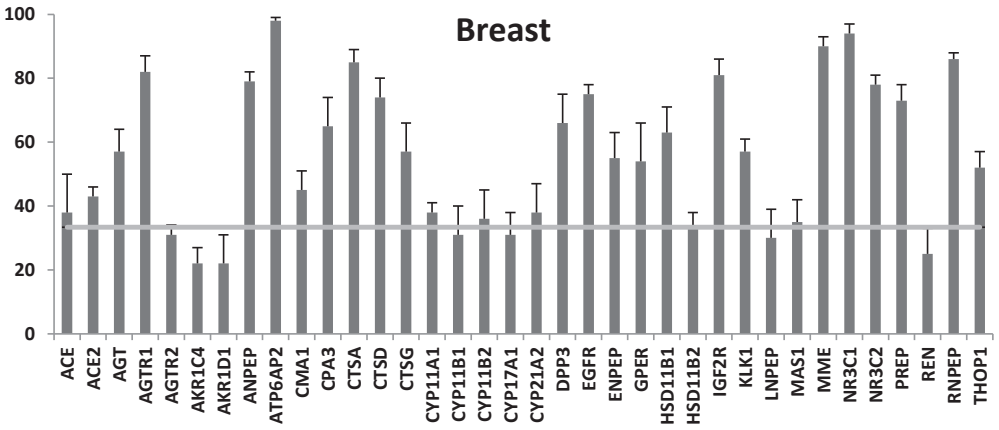
Breast
100
80
60
40
20
0
ACE
ACE2
AGT
AGTR1
AGTR2
AKR1C4
AKR1D1
ANPEP
ATP6AP2
CMA1
CPA3
CTSA
CTSD
CTSG
CYP11A1
CYP11B1
CYP11B2
CYP17A1
CYP21A2
DPP3
EGFR
ENPEP
GPER
HSD11B1
HSD11B2
IGF2R
KLK1
LNPEP
MAS1
MME
NR3C1
NR3C2
PREP
REN
RNPEP
THOP1

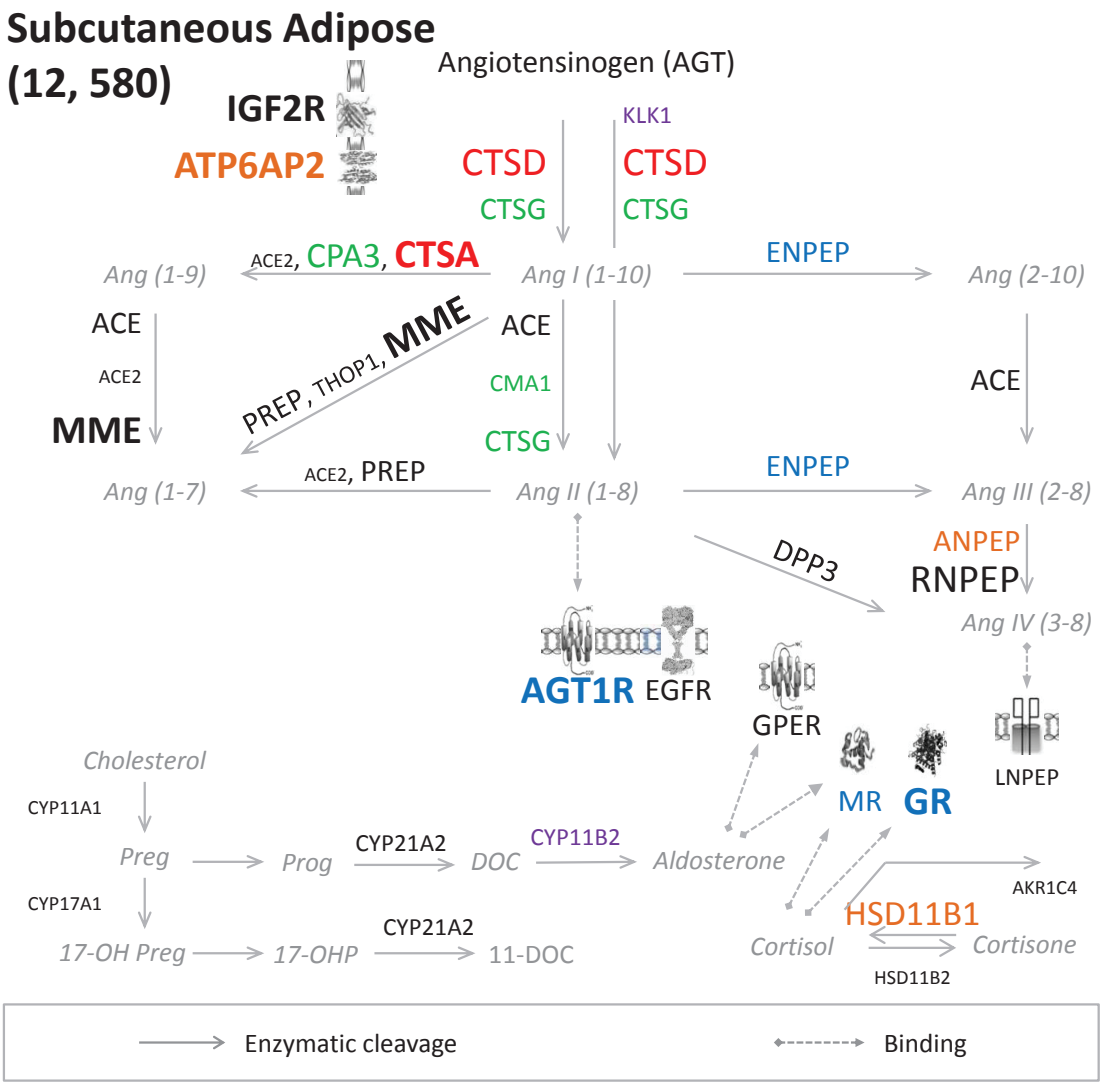
Subcutaneous Adipose
(12, 580)
Angiotensinogen (AGT)
IGF2R
ATP6AP2
KLK1
CTSD
CTSG
CTSD
CTSG
ACE2, CPA3, CTSA
Ang (1-9)
Ang I (1-10)
ENPEP
Ang (2-10)
ACE
ACE2
MME
PREP, THOP1, MME
ACE
CMA1
CTSG
ACE
ACE2, PREP
Ang (1-7)
Ang II (1-8)
ENPEP
Ang III (2-8)
DPP3
ANPEP
RNPEP
Ang IV (3-8)
AGT1R
EGFR
GPER
LNPEP
MR
GR
Cholesterol
CYP11A1
Preg
Prog
CYP21A2
DOC
CYP11B2
Aldosterone
AKR1C4
CYP17A1
17-OH Preg
17-OHP
CYP21A2
11-DOC
Cortisol
HSD11B1
Cortisone
HSD11B2
Enzymatic cleavage
Binding

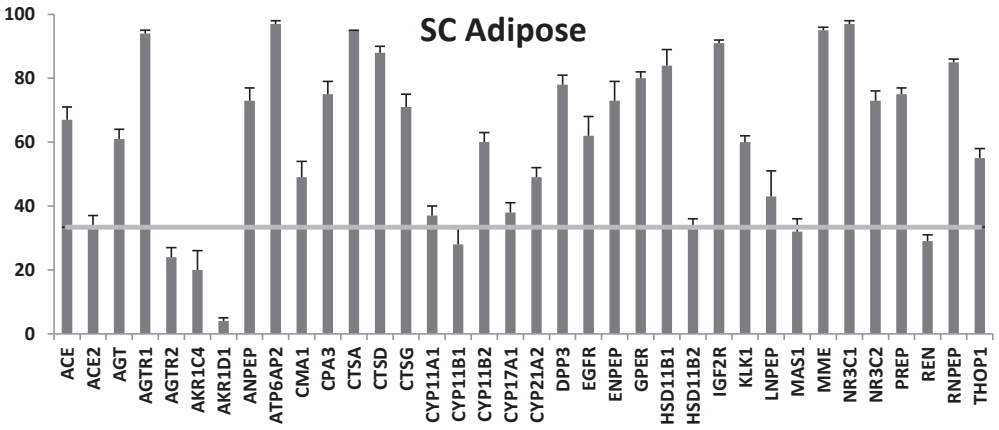
SC Adipose
100
80
60
40
20
0
ACE
ACE2
AGT
AGTR1
AGTR2
AKR1C4
AKR1D1
ANPEP
ATP6AP2
CMA1
CPA3
CTSA
CTSD
CTSG
CYP11A1
CYP11B1
CYP11B2
CYP17A1
CYP21A2
DPP3
EGFR
ENPEP
GPER
HSD11B1
HSD11B2
IGF2R
KLK1
LNPEP
MAS1
MME
NR3C1
NR3C2
PREP
REN
RNPEP
THOP1

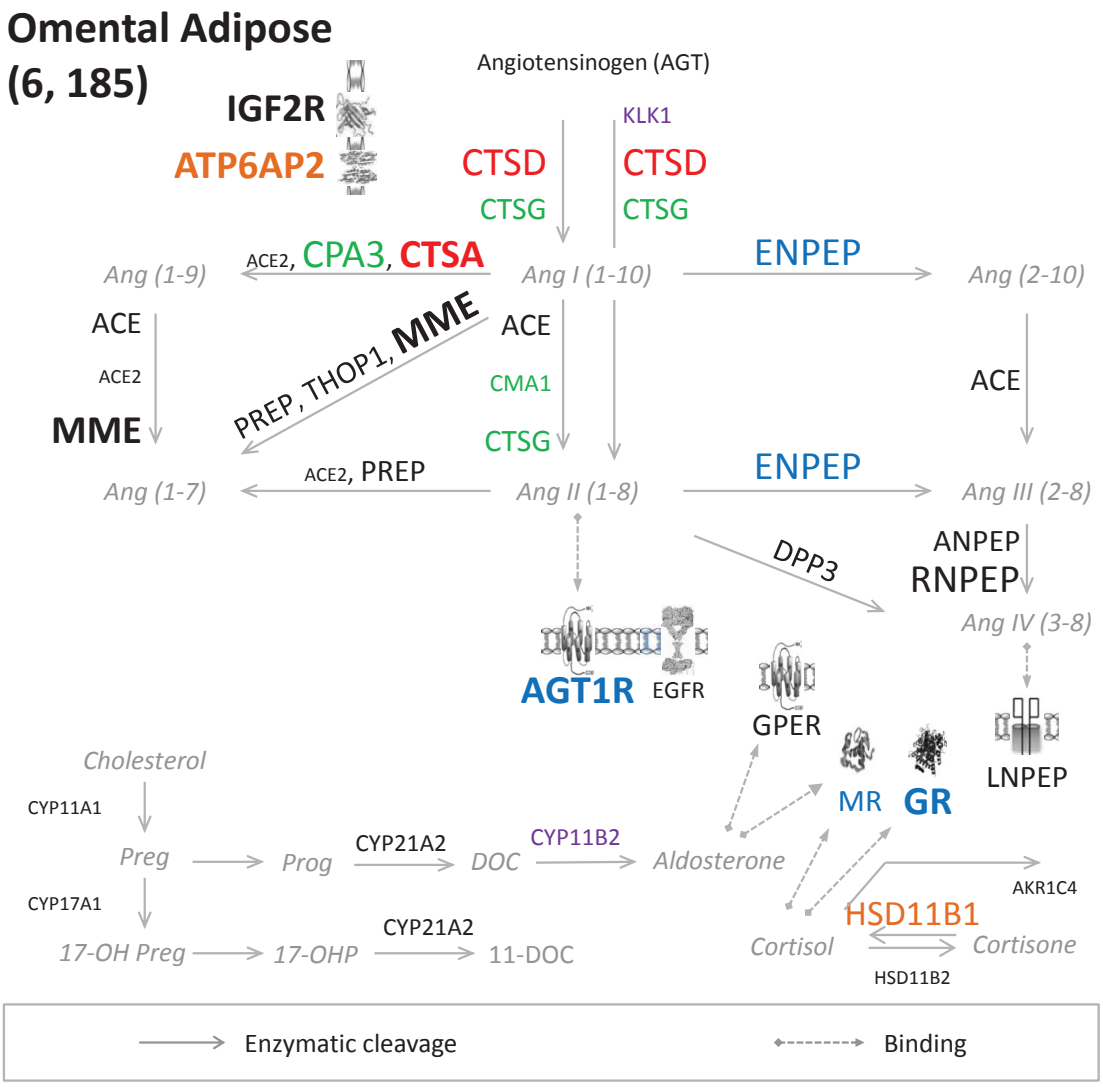
Omental Adipose
(6, 185)
IGF2R
ATP6AP2
Angiotensinogen (AGT)
KLK1
CTSD
CTSG
CTSD
CTSG
ACE2, CPA3, CTSA
ENPEP
Ang (1-9)
Ang I (1-10)
Ang (2-10)
ACE
ACE2
MME
PREP, THOP1, MME
ACE
CMA1
CTSG
ACE
ACE2, PREP
ENPEP
Ang (1-7)
Ang II (1-8)
Ang III (2-8)
DPP3
ANPEP
RNPEP
Ang IV (3-8)
AGT1R
EGFR
GPER
LNPEP
MR
GR
Cholesterol
CYP11A1
Preg
Prog
CYP21A2
DOC
CYP11B2
Aldosterone
AKR1C4
CYP17A1
17-OH Preg
17-OHP
CYP21A2
11-DOC
Cortisol
HSD11B1
Cortisone
HSD11B2
Enzymatic cleavage
Binding

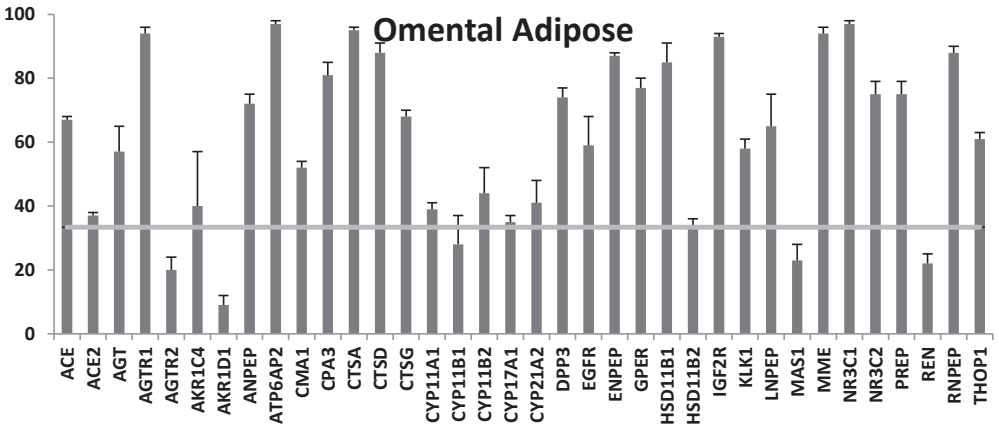
Omental Adipose
100
80
60
40
20
0
ACE
ACE2
AGT
AGTR1
AGTR2
AKR1C4
AKR1D1
ANPEP
ATP6AP2
CMA1
CPA3
CTSA
CTSD
CTSG
CYP11A1
CYP11B1
CYP11B2
CYP17A1
CYP21A2
DPP3
EGFR
ENPEP
GPER
HSD11B1
HSD11B2
IGF2R
KLK1
LNPEP
MAS1
MME
NR3C1
NR3C2
PREP
REN
RNPEP
THOP1

Large Airways Epithelium (5, 101)

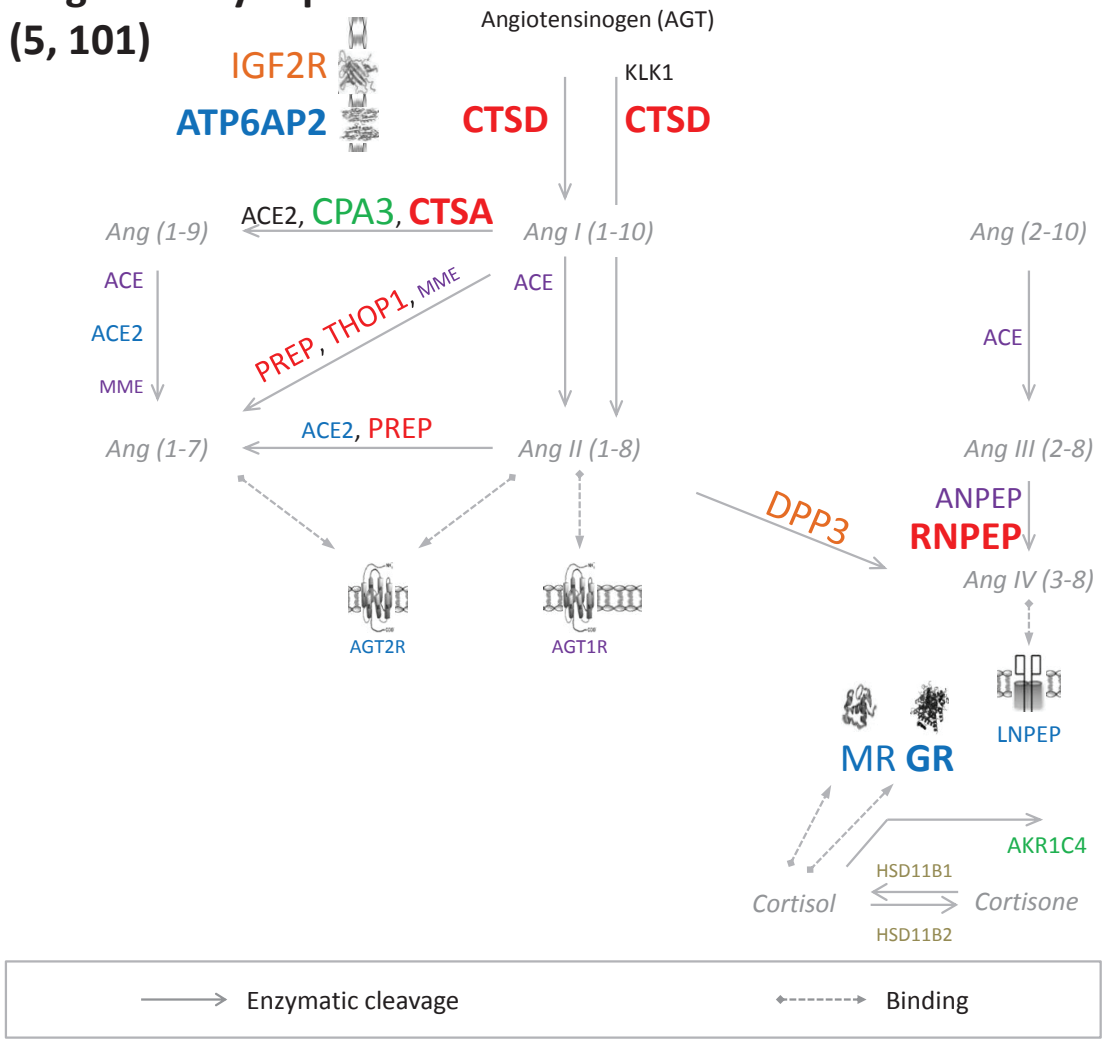

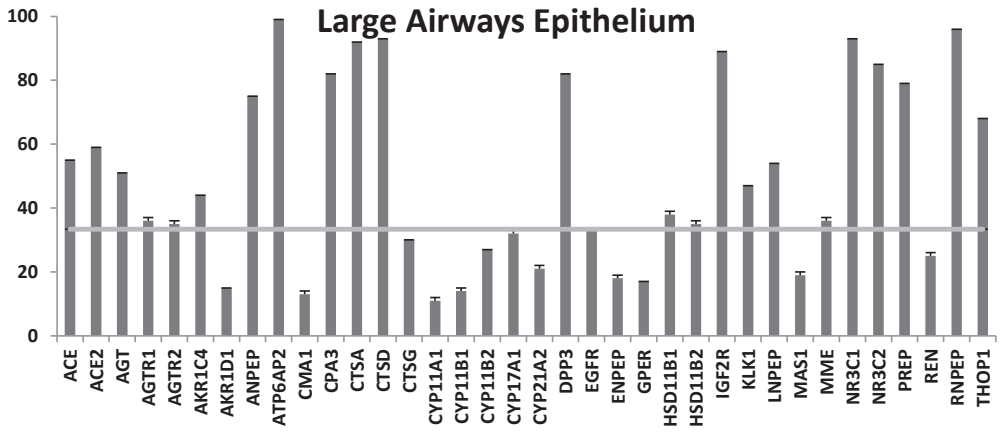

Small Airways Epithelium (8, 57)

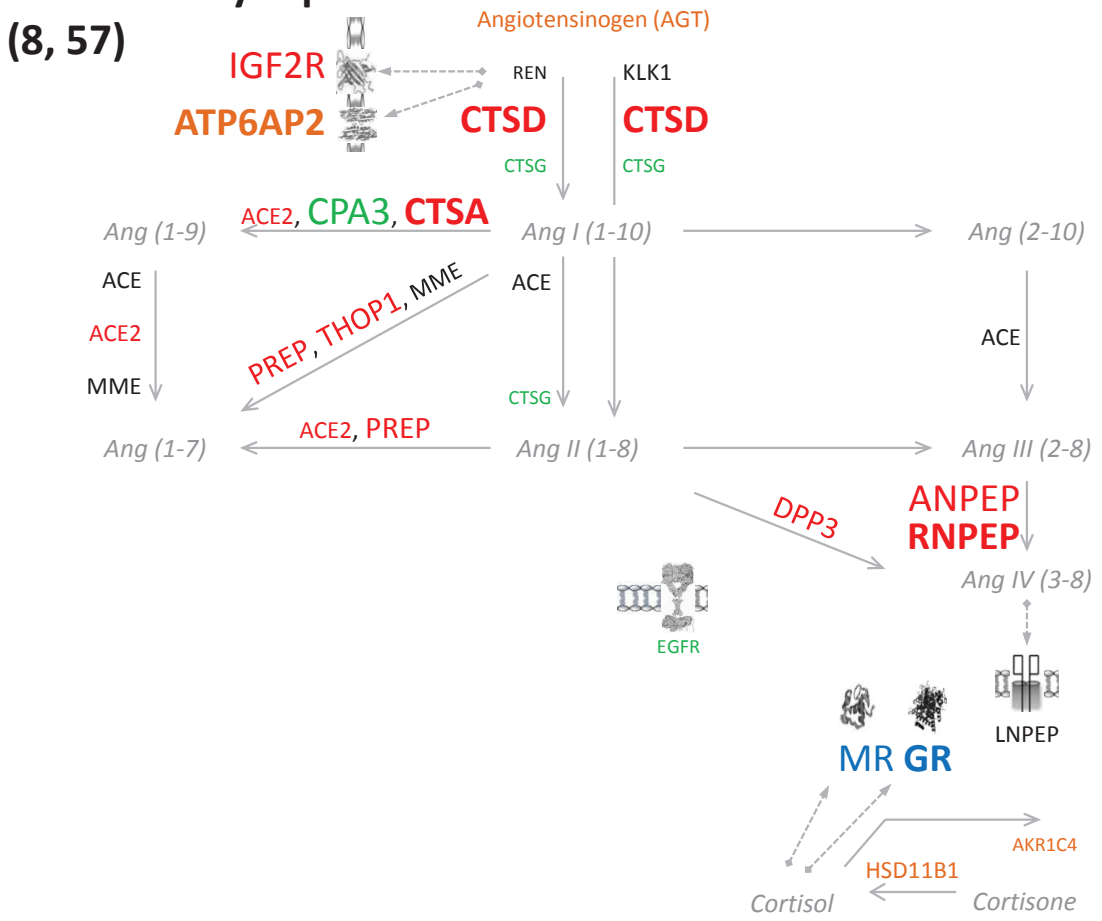

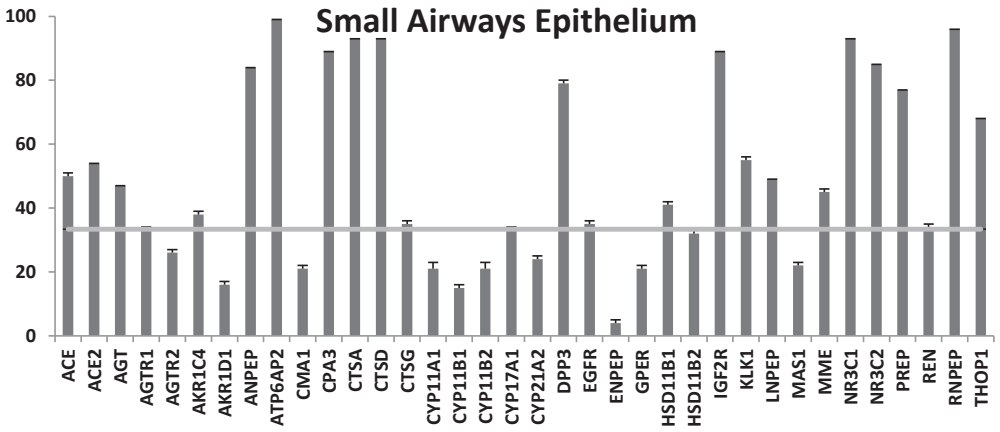

Esophagus (3, 83)

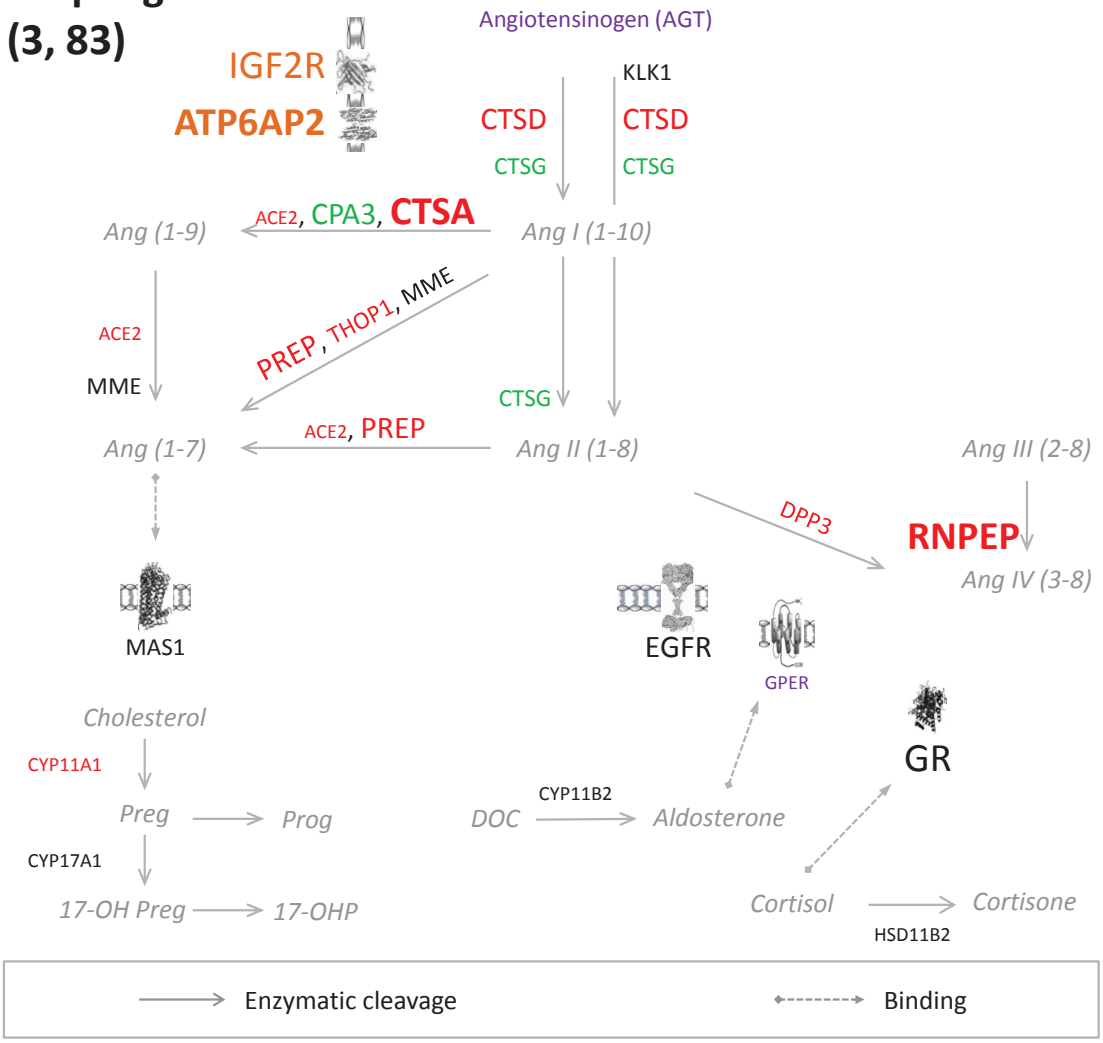

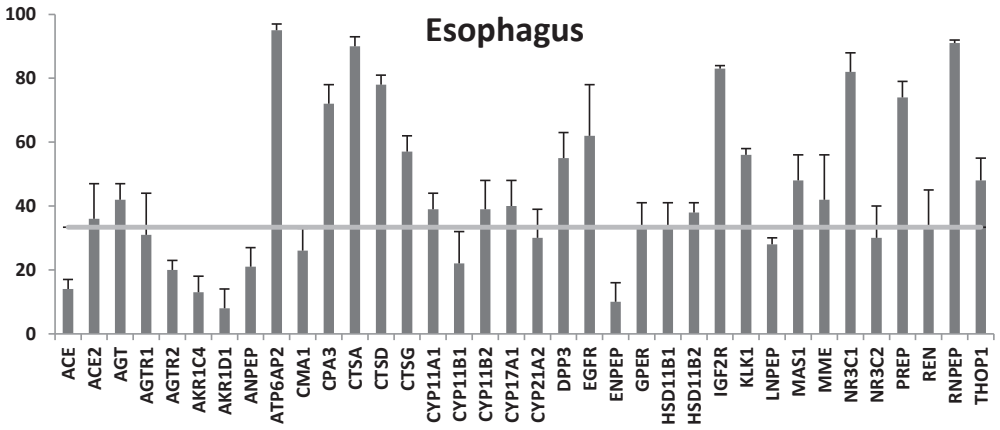

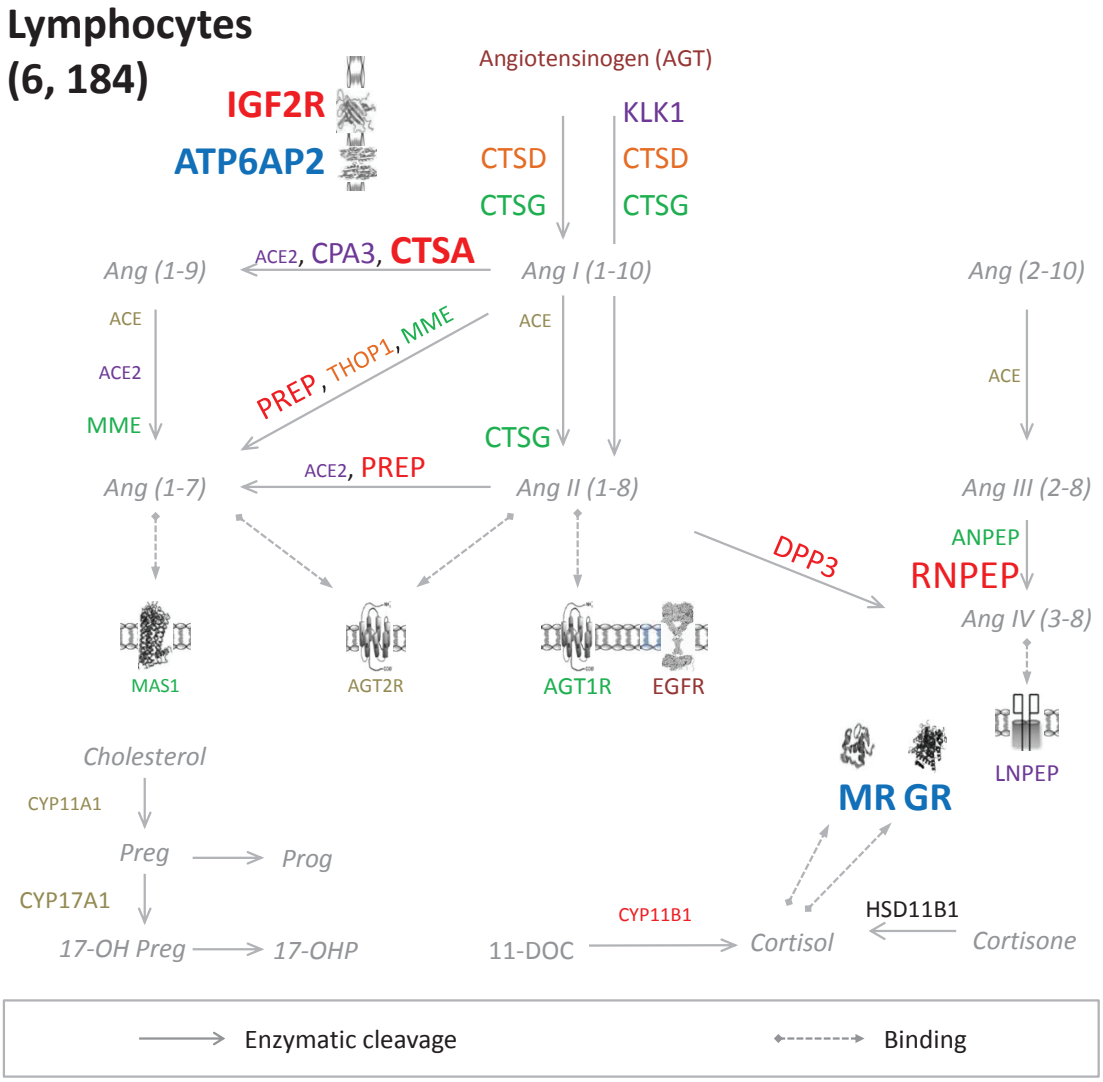
Lymphocytes
(6, 184)
IGF2R
ATP6AP2
Angiotensinogen (AGT)
KLK1
CTSD
CTSG
CTSD
CTSG
ACE2, CPA3, CTSA
Ang (1-9)
Ang I (1-10)
Ang (2-10)
ACE
ACE2
MME
ACE
PREP, THOP1, MME
CTSG
ACE
ACE2, PREP
Ang (1-7)
Ang II (1-8)
Ang III (2-8)
DPP3
ANPEP
RNPEP
Ang IV (3-8)
MAS1
AGT2R
AGT1R
EGFR
LNPEP
MR GR
Cholesterol
CYP11A1
Preg
Prog
CYP17A1
17-OH Preg
17-OHP
CYP11B1
11-DOC
Cortisol
HSD11B1
Cortisone
Enzymatic cleavage
Binding

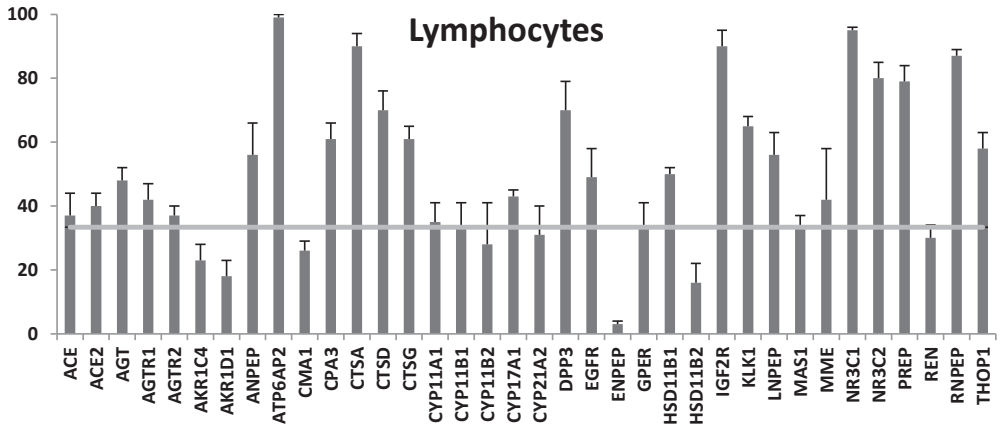
Lymphocytes
100
80
60
40
20
0
ACE
ACE2
AGT
AGTR1
AGTR2
AKR1C4
AKR1D1
ANPEP
ATP6AP2
CMA1
CPA3
CTSA
CTSD
CTSG
CYP11A1
CYP11B1
CYP11B2
CYP17A1
CYP21A2
DPP3
EGFR
ENPEP
GPER
HSD11B1
HSD11B2
IGF2R
KLK1
LNPEP
MAS1
MME
NR3C1
NR3C2
PREP
REN
RNPEP
THOP1

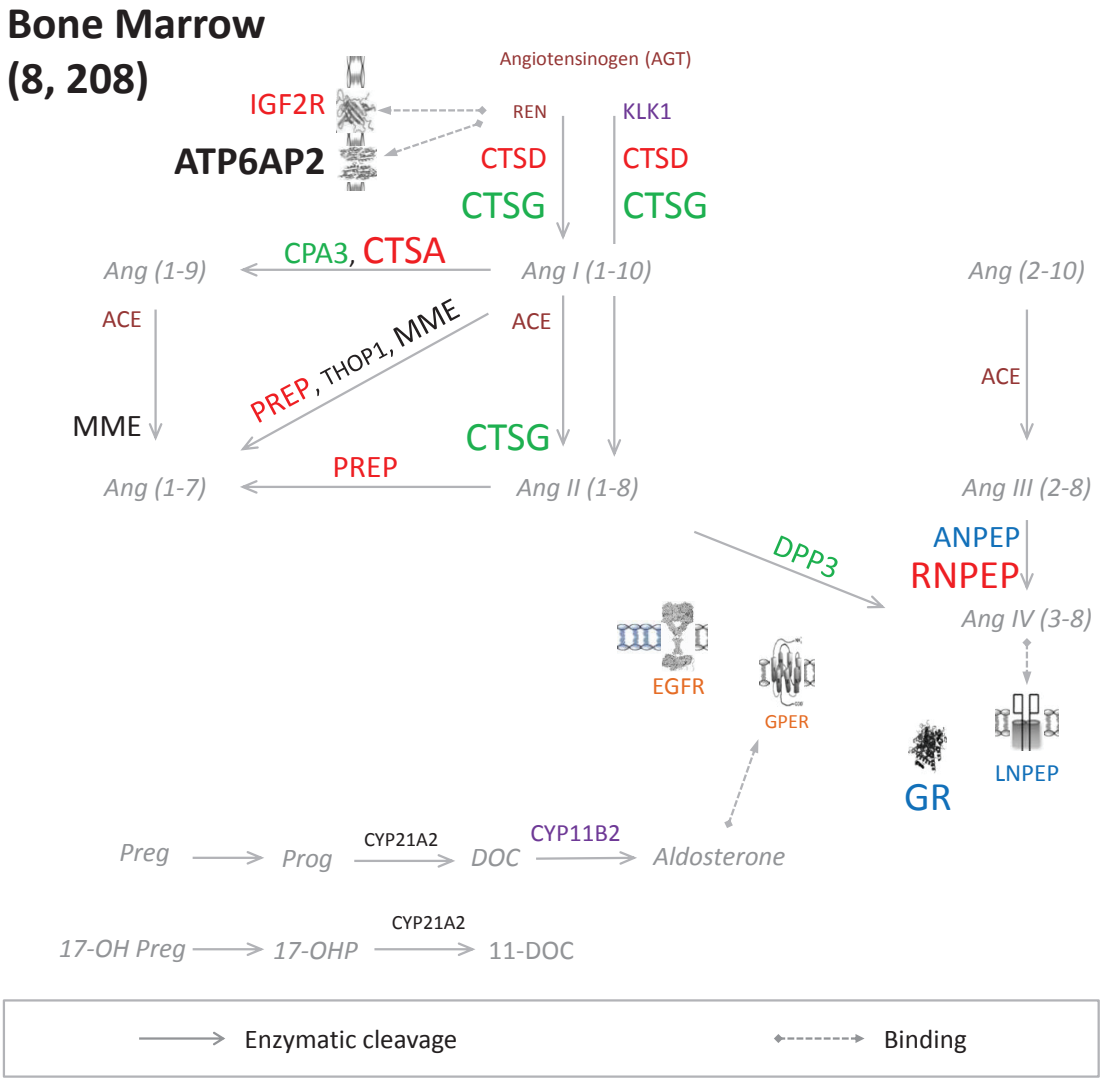
Bone Marrow
(8, 208)
IGF2R
ATP6AP2
Angiotensinogen (AGT)
REN
KLK1
CTSD
CTSG
CTSD
CTSG
CPA3, CTSA
Ang (1-9)
Ang I (1-10)
Ang (2-10)
ACE
ACE
ACE
MME
PREP, THOP1, MME
CTSG
PREP
Ang (1-7)
Ang II (1-8)
Ang III (2-8)
DPP3
ANPEP
RNPEP
Ang IV (3-8)
EGFR
GPER
LNPEP
GR
Preg
Prog
CYP21A2
DOC
CYP11B2
Aldosterone
17-OH Preg
17-OHP
CYP21A2
11-DOC
Enzymatic cleavage
Binding

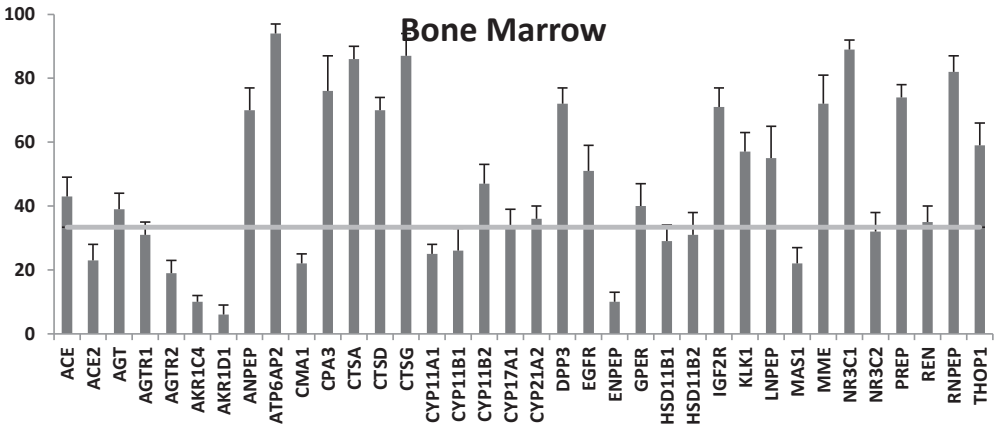
Bone Marrow
100
80
60
40
20
0
ACE
ACE2
AGT
AGTR1
AGTR2
AKR1C4
AKR1D1
ANPEP
ATP6AP2
CMA1
CPA3
CTSA
CTSD
CTSG
CYP11A1
CYP11B1
CYP11B2
CYP17A1
CYP21A2
DPP3
EGFR
ENPEP
GPER
HSD11B1
HSD11B2
IGF2R
KLK1
LNPEP
MAS1
MME
NR3C1
NR3C2
PREP
REN
RNPEP
THOP1

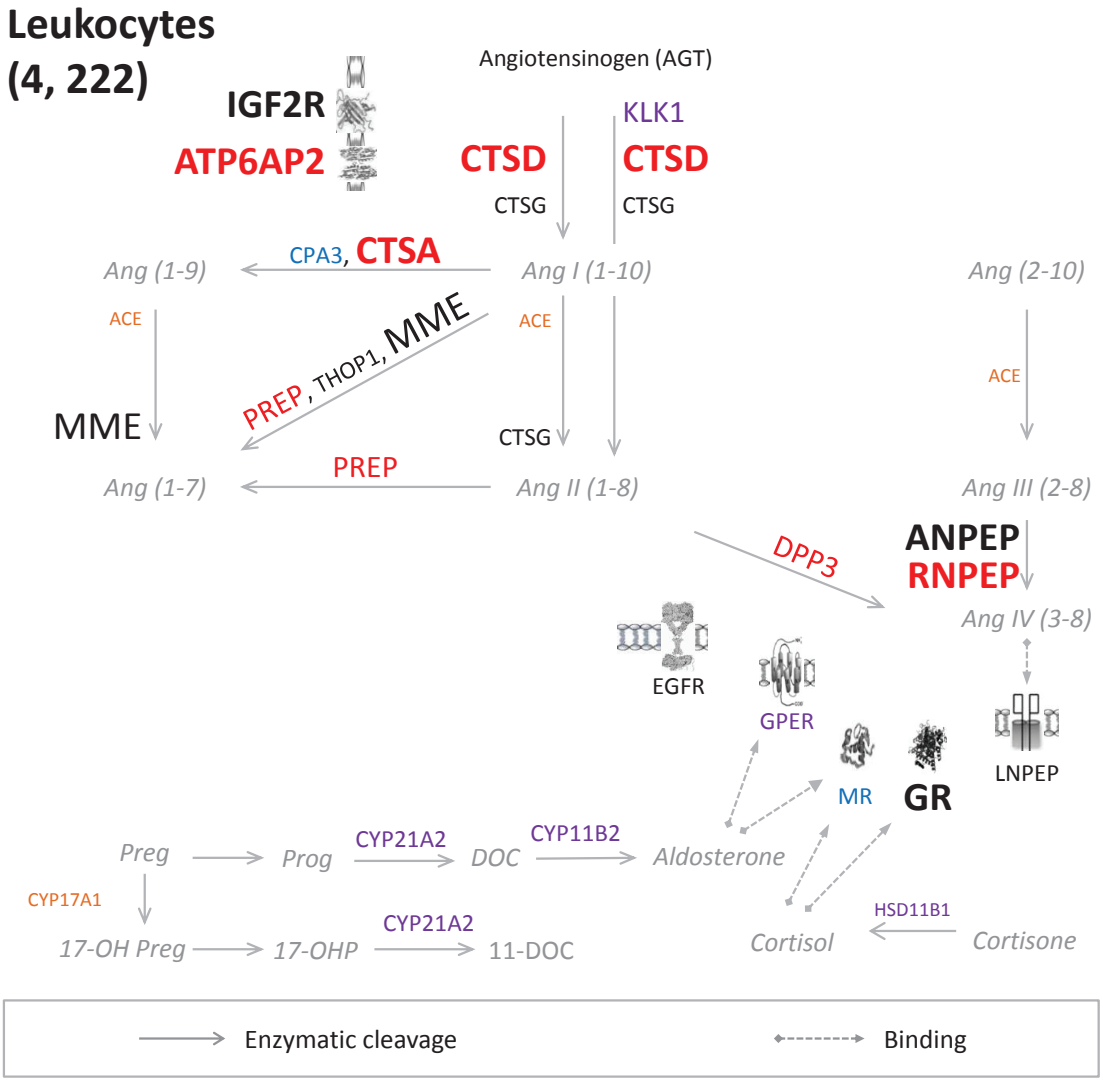
Leukocytes
(4, 222)
IGF2R
ATP6AP2
Angiotensinogen (AGT)
KLK1
CTSD
CTSD
CTSG
CTSG
CPA3, CTSA
Ang (1-9)
Ang I (1-10)
Ang (2-10)
ACE
ACE
ACE
MME
PREP, THOP1, MME
CTSG
PREP
Ang (1-7)
Ang II (1-8)
Ang III (2-8)
DPP3
ANPEP
RNPEP
Ang IV (3-8)
EGFR
GPER
LNPEP
MR
GR
Preg
Prog
CYP21A2
DOC
CYP11B2
Aldosterone
CYP17A1
17-OH Preg
17-OHP
CYP21A2
11-DOC
HSD11B1
Cortisol
Cortisone
Enzymatic cleavage
Binding

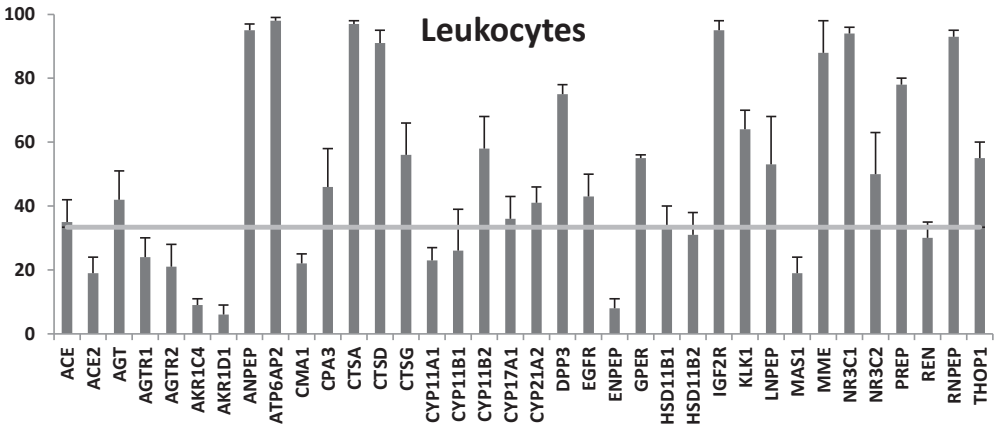
Leukocytes
100
80
60
40
20
0
ACE
ACE2
AGT
AGTR1
AGTR2
AKR1C4
AKR1D1
ANPEP
ATP6AP2
CMA1
CPA3
CTSA
CTSD
CTSG
CYP11A1
CYP11B1
CYP11B2
CYP17A1
CYP21A2
DPP3
EGFR
ENPEP
GPER
HSD11B1
HSD11B2
IGF2R
KLK1
LNPEP
MAS1
MME
NR3C1
NR3C2
PREP
REN
RNPEP
THOP1

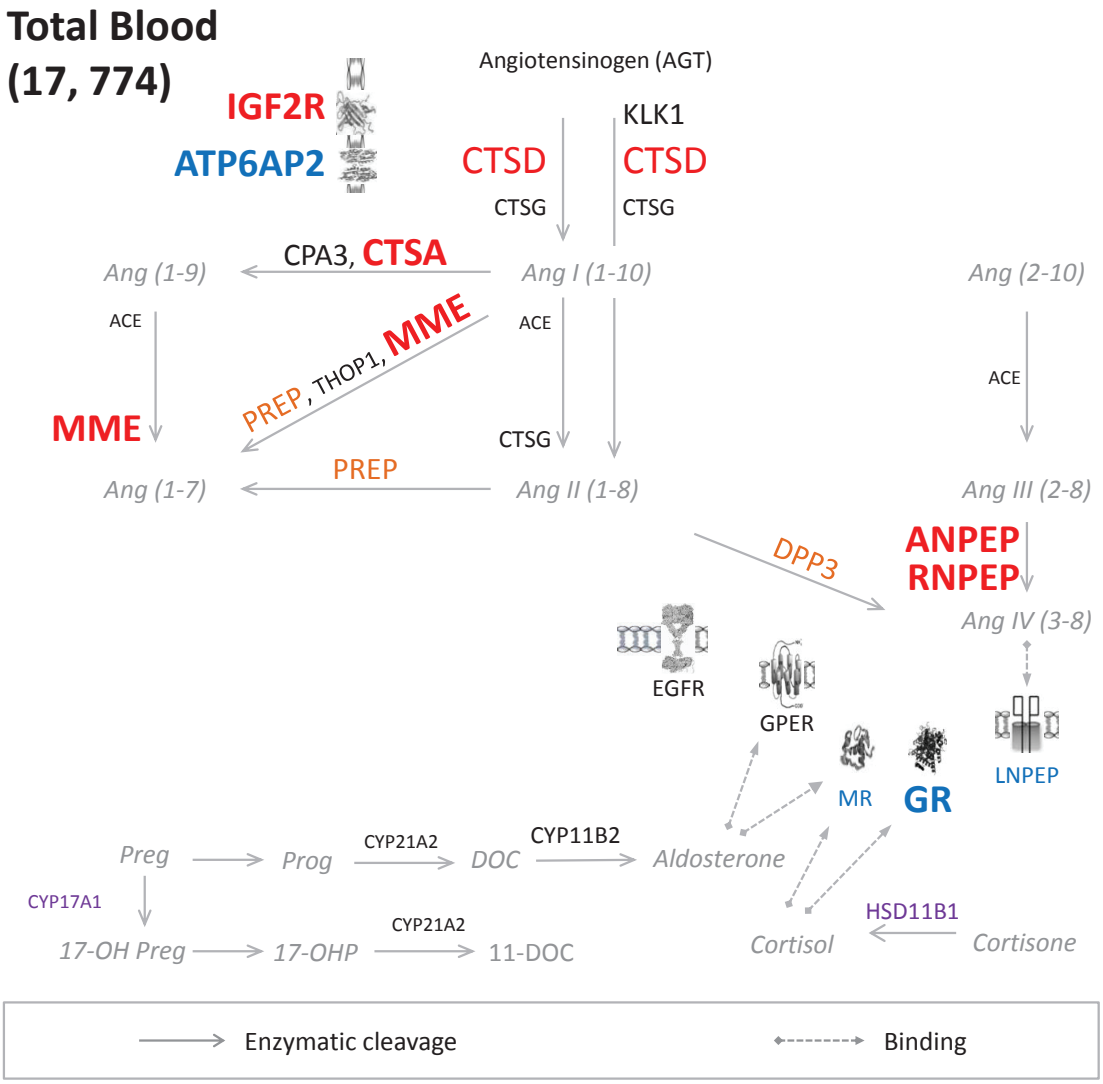
Total Blood
(17, 774)
IGF2R
ATP6AP2
Angiotensinogen (AGT)
KLK1
CTSD
CTSD
CTSG
CTSG
CPA3, CTSA
Ang (1-9)
Ang I (1-10)
Ang (2-10)
ACE
ACE
ACE
MME
PREP, THOP1, MME
CTSG
PREP
Ang (1-7)
Ang II (1-8)
Ang III (2-8)
DPP3
ANPEP
RNPEP
Ang IV (3-8)
EGFR
GPER
LNPEP
MR
GR
Preg
Prog
CYP21A2
DOC
CYP11B2
Aldosterone
CYP17A1
17-OH Preg
17-OHP
CYP21A2
11-DOC
HSD11B1
Cortisol
Cortisone
Enzymatic cleavage
Binding

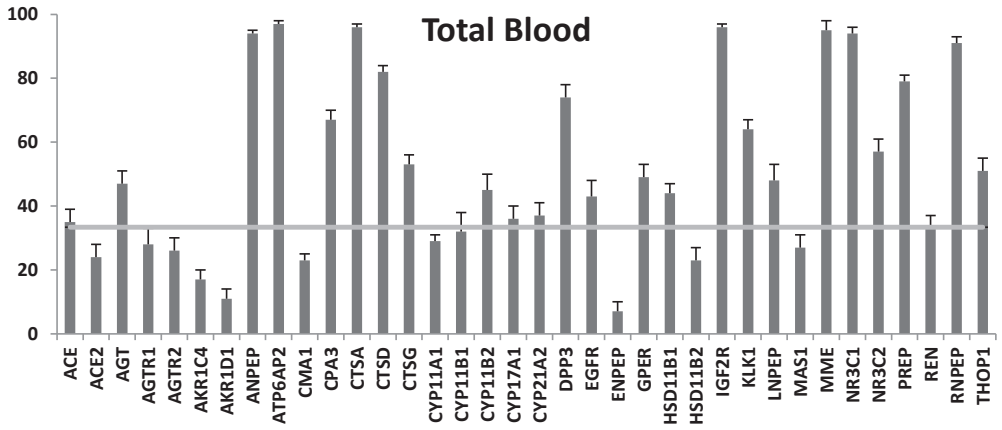
Total Blood
100
80
60
40
20
0
ACE
ACE2
AGT
AGTR1
AGTR2
AKR1C4
AKR1D1
ANPEP
ATP6AP2
CMA1
CPA3
CTSA
CTSD
CTSG
CYP11A1
CYP11B1
CYP11B2
CYP17A1
CYP21A2
DPP3
EGFR
ENPEP
GPER
HSD11B1
HSD11B2
IGF2R
KLK1
LNPEP
MAS1
MME
NR3C1
NR3C2
PREP
REN
RNPEP
THOP1

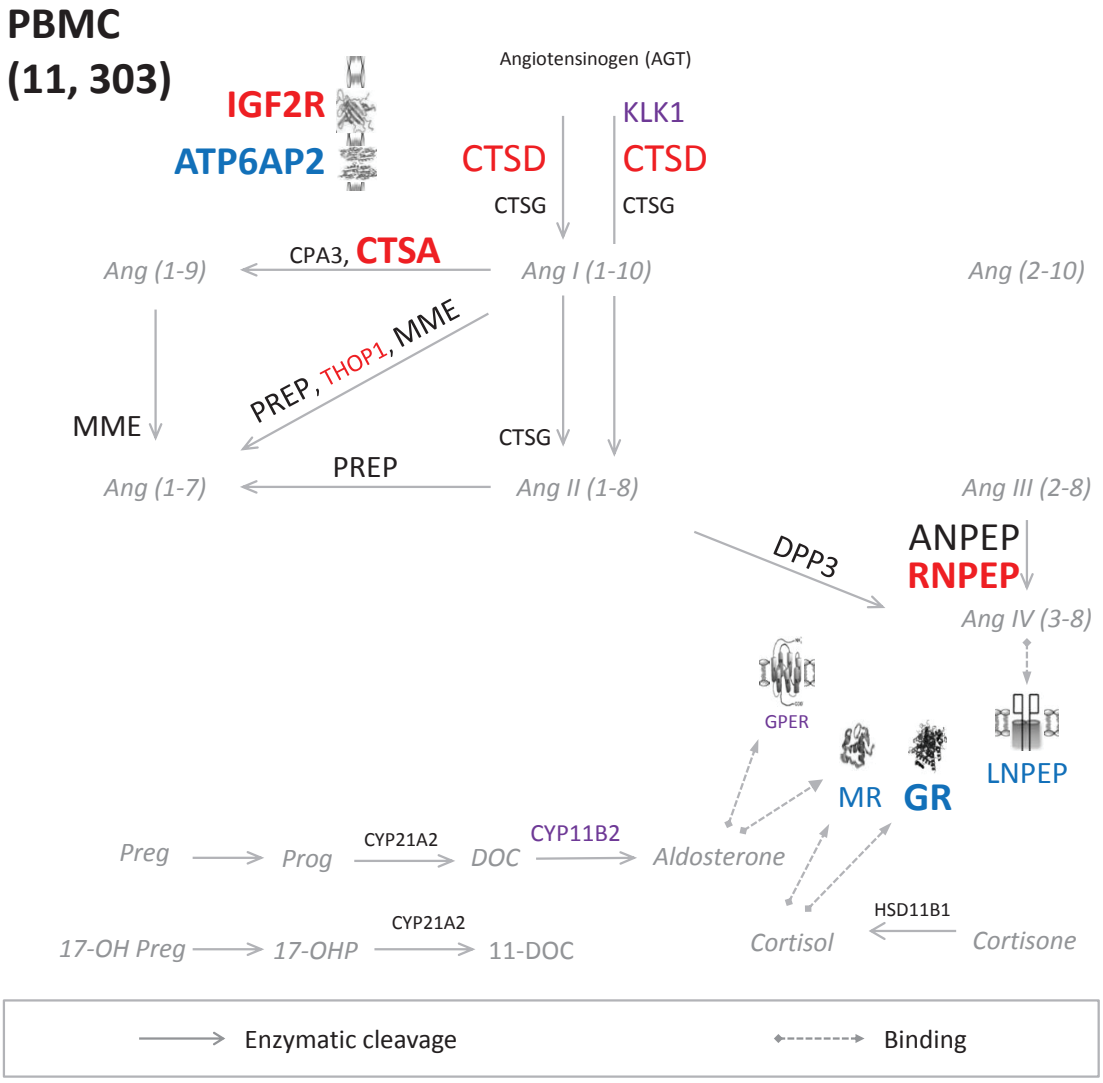
PBMC
(11, 303)
IGF2R
ATP6AP2
Angiotensinogen (AGT)
KLK1
CTSD
CTSD
CTSG
CTSG
CPA3, CTSA
Ang (1-9)
Ang I (1-10)
Ang (2-10)
PREP, THOP1, MME
MME
CTSG
PREP
Ang (1-7)
Ang II (1-8)
Ang III (2-8)
DPP3
ANPEP
RNPEP
Ang IV (3-8)
GPER
LNPEP
MR
GR
Preg
Prog
CYP21A2
DOC
CYP11B2
Aldosterone
17-OH Preg
17-OHP
CYP21A2
11-DOC
HSD11B1
Cortisol
Cortisone
Enzymatic cleavage
Binding

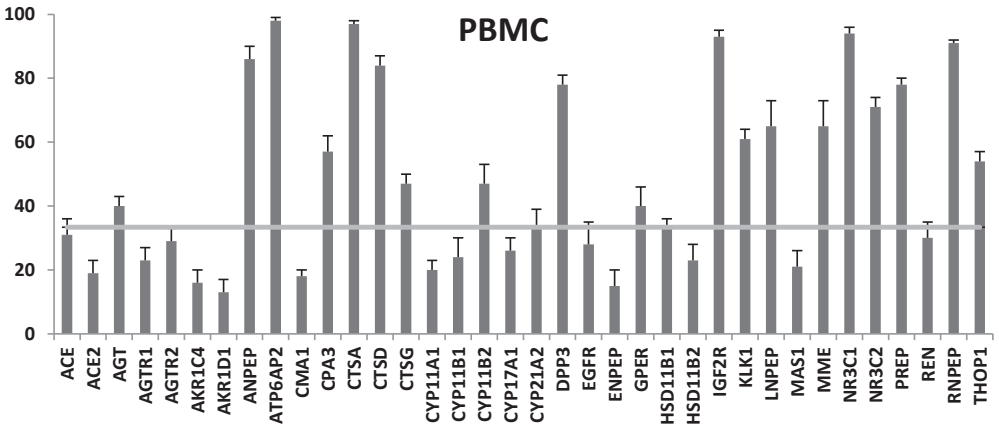
PBMC
100
80
60
40
20
0
ACE
ACE2
AGT
AGTR1
AGTR2
AKR1C4
AKR1D1
ANPEP
ATP6AP2
CMA1
CPA3
CTSA
CTSD
CTSG
CYP11A1
CYP11B1
CYP11B2
CYP17A1
CYP21A2
DPP3
EGFR
ENPEP
GPER
HSD11B1
HSD11B2
IGF2R
KLK1
LNPEP
MAS1
MME
NR3C1
NR3C2
PREP
REN
RNPEP
THOP1

IV.1.1 Summary of Scientitific article 1

In this work we used simple, but robust, statistical analysis of previously published data available on the GEO database. The atlas of tissue-RAAS can be a reference of extRAAS for scientists that are interested in the system in one or the other tissue. Indeed, we were the first to publish such a huge set of data on extRAAS, including both expression and coordination patterns for all participants in a wide range of tissues. The consistency between the expression centile ranks and the previously known data on RAAS supports the robustness of our methodology and its possible use as a reference method in such large scale meta-analysis. The expression and coordination patterns allows for a better prediction of favored pathways of extRAAS and their interactions in each tissue. The reprocibility of the patterns of expression and coordination across datasets of a given tissue, and their tissue-specific features provides a better chance for finding the most specific and efficient RAAS-targeting drugs to treat a particular tissue pathophysiology, overcoming inter-individual variabilities. The coordination patterns may also provide the basis for developing new therapeutics that can modulate the expression of a subset of genes simultaneously, thus providing a more efficient way for the modulation of extRAAS activity. Nevertheless, further studies should be done on extRAAS in each particular tissue to validate the reproducibility of these results at the protein level to better understand how the system contributes to local tissue homeostasis and how alterations in the local organization of the system may contribute to tissue pathophysiology.

IV.2 SCIENTIFIC MANUSCRIPT I

The implication of the renin-angiotensin-aldosterone system (extRAAS) in atheroma development has been well described. However, a complete view of the extRAAS and its regulation in atheroma is still missing. Therefore, we use transcriptomic data analysis to map the transcriptional organization of the extended extRAAS (extRAAS), which includes 37 genes coding for classical and novel extRAAS participants. We also propose the potential transcriptional regulators of extRAAS genes in atheroma. Five microarray datasets containing a total of 590 human samples representing carotid and peripheral atheroma were downloaded from the GEO database. Correlation-based hierarchical clustering (R software) of extRAAS genes within each dataset allowed the identification of modules of co-expressed genes. Reproducible co-expression modules across datasets were then extracted. Transcription factors (TFs) having common binding sites (TFBSs) in the promoters of coordinated genes were identified using the Genomatix software and analyzed for their correlation with extRAAS genes in the microarray datasets. Expression data revealed the expressed extRAAS components and their relative abundance displaying the favored pathways in atheroma. Three co-expression modules with more than 80% reproducibility across datasets were extracted. Two of them (M1 and M2) contained genes coding for angiotensin metabolizing enzymes involved in different pathways: M1 included ACE, MME, RNPEP, and DPP3, in addition to 7 other genes; and M2 included CMA1, CTSG, and CPA3. The third module (M3) contained genes coding for receptors known to be implicated in atheroma (AGTR1, MR, GR, LNPEP, EGFR and GPER). M1 and M3 were negatively correlated in 3 of the 5 datasets. We identified 19 TFs that have enriched TFBSs in the promoters of M1 genes, two TFs for M3, but none was found for M2. Among the extracted TFs, IRF5, MAX and ETV5 showed significant positive correlations with peptidase-coding genes from M1 ($p<0.01$). In addition, ETS1 and SMAD1 were positively correlated to receptor coding genes from M3. In conclusion, the three co-expression modules display the transcriptional organization of local extRAAS in human carotid atheroma. The identification of several TFs potentially associated with extRAAS genes may provide a basis for the discovery of atheroma-specific modulators of extRAAS activity.

PROMOTER ANALYSIS OF COORDINATED GENES REVEALS POTENTIAL TRANSCRIPTION FACTORS ASSOCIATED WITH THE RENIN-ANGIOTENSIN-ALDOSTERONE SYSTEM IN HUMAN ATHEROMA

Ali Nehme[1,2], Catherine Cerutti[1], Kazem Zibara[2]*, Giampiero Bricca[1]*.

[1] EA4173, Functional genomics of arterial hypertension, Hôpital Nord-Ouest, Villefranche-sur-Saône; Université Lyon1, Lyon, France.

[2] ER045, Laboratory of stem cells, Department of Biology, Faculty of sciences, Lebanese University, Beirut, Lebanon.

* Co-last and corresponding authors

Address correspondence to:

⋆ Dr Giampiero BRICCA, EA4173, Functional genomics of arterial hypertension, Université Lyon1, Domaine Rockefeller, 8 avenue Rockefeller, France; email: giampiero.bricca@inserm. fr

*Dr Kazem ZIBARA, ER045, Laboratory of stem cells, Department of Biology, Faculty of Sciences, Lebanese University, Beirut – Lebanon; email: kzibara@ul. edu. lb

Short title: **Extended extRAAS tissue organization**

Word count:

Grey scale illustrations: 7 (Figures 1-4 and tables 1-3)

Colored Illustrations: 1 (Figure 4)

IV.2.1 Introduction

Atherosclerosis remains and continues to be the leading cause of death and disability in developed countries[22]. The importance of the renin-angiotensin-aldosterone system (RAAS) as a key player in both atherosclerotic risk factors development and local atherosclerotic remodeling has been experimentally and clinically documented[208,454,455]. In fact, systemic RAAS is a key factor in the non-specific amplification of atherosclerotic remodeling and its treatment plays a major role in reducing the risk factors of vascular remodeling[454]. In addition to systemic RAAS, local components of RAAS in the vessel wall act at the paracrine level to regulate vascular wall homeostasis[224,456].

Many studies have investigated the implication of RAAS in atherosclerosis. Studies have shown that angiotensin peptides and aldosterone play major roles in atherosclerotic lesion development by exerting local effects in the vessel wall that modulate local processes that drive lesion initiation and progression[208,454]. However, these studies remain scattered and provide no clear view of the global organization of system with its increasing complexity. Indeed, studies investigating the effects of RAAS in atherosclerosis usually target one pathway without testing the simultaneous impact of the other pathways. In fact, different RAAS pathways exert different, even opposite, effects and the final action of RAAS in a tissue depends on the final balance between the different components of the system, favoring certain pathways over the others[457]. This rule also apply in the vascular wall, where the local balance between the different pathways play a key role in maintaining vessel wall physiology, and a change in this balance may lead to a pathophysiological state, such as atherosclerosis[458]. Therefore, investigating RAAS at the tissue level should be done in a system biology approach that provide a global view of the local organization of the system, which will provide a more clear view of the various active pathways and their interaction in the tissue, and thus a better prediction of the final effects on the tissue.

We have been studying over the last decade the expression and activity of multiple RAAS components in the arterial wall and described their alteration in atherosclerosis in relation to T2D in human and animals[223–226]. We have recently defined, based on literature and results obtained in the laboratory, an extended extRAAS (extRAAS) which includes 38 participants. Using a meta-analysis on transcriptomic data we showed that this system possesses a tissue-specific organization characterized by specific patterns of expression and coordination[209].

In this study and using the same approach we constructed a map of the extRAAS in atheroma plaque, which shows extRAAS mRNA organization both at the expression and coordination levels. We further analyzed the promoters of coordinated extRAAS genes to identify candidate TFs that may regulate this organization.

IV.2.2 Methods

Patients and tissue samples: The investigation conforms to the principles outlined in the declaration of Helsinki[446]. All procedures were approved by the local ethical committee and the patients gave informed consent. Thirty two patients who underwent carotid endarterectomy at the university hospital of Lyon (Hôpital Edouard Herriot) were included in the study. The carotid endarterectomy samples were collected in the surgery room and immediately dissected in two fragments: the atheroma plaque (ATH) and the macroscopically intact tissue (MIT). Each fragment was further divided: one part was immediately frozen in liquid nitrogen for RNA analysis and the other was used for histological examination. To avoid the inherent problems of control tissue collection, we made intra-patient comparison of the transcript profiles.

Total RNA extraction: mRNA was extracted from tissues using Trizol (Invitrogen,USA) following the manufacturer's instructions, then treated with DNAse (Qiagen, FRANCE), and purified using the RNeasy MiniElute TM clean up kit (Qiagen, FRANCE) according to the manufacturer's instructions. Quantification and estimation of RNA purity was performed using NanoDrop (Nanodrop, USA). Finally, RNA integrity was assessed using Agilent 2100 Bioanalyzer (Agilent Technologies, USA) in order to measure RNA integrity number (RIN).

Constructing extRAAS: The genes involved in the RAAS system were taken from the renin-angiotensin human pathway (hsa04614) of the KEGG database (http://www.genome.jp/kegg/pathway.html). It included 25 genes potentially contributing to the activity of the system, including the precursor angiotensinogen (AGT), angiotensin metabolizing enzymes, and receptors. We added to this system 12 genes of the steroid hormones biosynthesis pathway (hsa00140) obtained from the KEGG database, including those coding for enzymes involved in de novo synthesis and degradation of corticoids, in addition to the gluco- and mineralo-corticoid receptors GR and MR and the G protein-coupled estrogen receptor 1

(GPER). Grouping together these two pathways resulted in the extended RAAS (extRAAS) constituting 37 genes (supplementary table 1).

Microarray experiments and statistical analysis: Samples of high quality were transferred to the platform of the Strasbourg Genopole for labeling and hybridization with Affymetrix Human GeneChip Gene 1.0 ST Arrays (Affymetrix, Santa Clara, CA, USA) according to the manufacturer's protocol. Each mRNA sample was hybridized to its own microarray resulting in 64 arrays from 32 patients). Data were normalized with Affymetrix Expression Console software using the robust multiarray average (RMA) method and were log2 transformed. The data were uploaded to the Gene Expression Omnibus database (http://www.ncbi. nlm.nih.gov.gate2. inist.fr/geo/query/acc.cgi?acc=GSE43292). No expression threshold was imposed, but expression of genes emerging from our computations was checked, bearing interest only at genes with mean expression higher than the first tertile of its distribution (MIT and ATH, log2 of expression > 5. 04). Comparison between MIT and ATH used paired tests corrected for multiple comparisons (Significance Analysis of Microarrays software). We considered only significant differences with q-value = 0. Among extRAAS genes, CYP21A2 was targeted by 3 probe sets on the array; the most expressed one was selected.

Clustering of extRAAS genes: Clustering: We first studied the internal organization of the extRAAS by means of a hierarchical clustering of the genes using their log2 expression values across the 32 patients. It was based on the Pearson correlation distance and the Ward agglomerative method (R software, package cluster). The resulted dendrogram was cut in order to identify 5 gene clusters, thus defining the cutting height (0.85 for both MIT and ATH). The 2 best clusters were selected for further analysis.

Downloading microarray datasets: Published microarray datasets containing expression data for human and mouse atheroma were downloaded from the GEO database. Age, gender,

and ethnicity were not taken into account in selecting the datasets. Expression data of atherosclerotic samples in each dataset were then extracted into a separate file for further analysis. Only datasets with more than 10 atheroma samples were retained for further analysis.

Extraction of expression levels of extRAAS genes: After filtering, the datasets were checked for the expression distribution of their individual samples and those that showed large variability between samples were eliminated. Datasets were normalized by their authors using different methods including the robust multichip average (RMA), GC-RMA or a global score method[442]; those lacking any transformation were log 2-transformed. Expression levels of genes were expressed using the centile rank in order to compare expression data between different datasets. The centile rank of a gene was calculated using the R-software by normalizing its mean expression level relative to the mean expression data distribution over the microarray. The ECR values were presented as (1) mean ± SD to show intra- and inter-tissue variation in gene expression and (2) mean ± SEM to describe specific gene expression.

Gene clustering and co-expression modules extraction: The R software was used for statistical description and clustering of extRAAS transcripts in each dataset using the "Cluster" R library. Gene transcripts were hierarchically clustered in each dataset using Pearson correlation distance and Ward's agglomeration method[459]. Each of the dendrograms obtained was then cut at a given level to identify gene clusters. The cut-off level was chosen on the basis of a balance between the level of clustering strength, assessed with the agglomerative coefficient and a minimum of 3 gene transcripts per cluster. Reproducible co-expression modules of clustered genes were then extracted. These were defined as sets of 2 or more genes coordinated across datasets. The average coordination rate (ACR) of genes within a module was calculated as the average percentage of coordinated genes, which were clustered together across the different datasets in a specific tissue. A threshold of >55% was

the criterion used to define representative gene modules. The average inter-cluster correlations were also calculated the correlation coefficients between individual genes. They were further visually checked with scatter plots.

Promoter analysis of coordinated genes: transcription start clusters (TSC) were identified using the SwissRegulon database[451]. Alternatively, the dbTSS database[452] was used to extract individual TSS in the region of active transcription for certain genes for which no TSC could be extracted. A TSC or TSS is considered active when the expression of downstream exons is >1.5 folds greater than the upstream exon. Exon expression levels were obtained from raw expression data of the GSE43292 dataset obtained in our lab. After defining active TSCs, promoter sequences were extracted using the Genomatix database[450] and the SwissRegulon human genome database. A Promoter was defined by the sum of promoter sequences obtained by Genomatix around a specific TSC obtained from SwissRegulon. If no Genomatix promoter sequence could be obtained for a specific active TSC, then the promoter is considered as the 100-500 bp downstream and 400-700 bp upstream of the TSC in SwissRegulon genome viewer. For TSS obtained from the dbTSS, a promoter region of 600 bp is extracted, with 500 bp upstream and 100 bp downstream the TSS using the NCBI genome viewer. Consecutive promoters for adjacent TSCs were joined in one promoter. Promoter sequences of coordinated extRAAS genes were then analyzed simultaneously using the commonTF tool from Genomatix using default options in order to identify enriched transcription factor binding sites (TFBSs) in the promoters of coordinated genes. All of the position-weight matrices (each one associated with one TFBS) having at least one match in the studied promoters were obtained with their enrichment p-value in the group of studied promoters. One TFBS was taken as significantly enriched if its adjusted p-value (p-value/total number of position-weight matrices having at least one match in the studied promoters) was less than 0.05. Extraction of ECR for transcription factors in the datasets was

done as previously mentioned. Gene clustering and co-expression modules expression of extRAAS genes with TFs was also done in order to identify gene coordination between TFs and extRAAS genes.

IV.2.3 Results

ExtRAAS genes expression levels and clusters from our lab data: Figure 1A shows the expression level of 35 extRAAS genes in ATH compared to MIT. There was significant increase in the expression of multiple genes coding for angiotensin metabolizing enzymes, including CTSA, CTSD, RNPEP, ANPEP, DPP3, CPA3, MME and ACE, in addition to that coding for the renin/prorenin receptor IGF2R. On the contrary, AGTR1, LNPEP, and NR3C2 transcripts showed a significant decrease in their expression levels. Figure 1B shows the dendrogram obtained in MIT and ATH samples. Two of the 5 clusters identified were very similar in both low grade and advanced atheroma lesions. The first cluster found in both stages of atheroma groups 10 strongly associated transcripts with mean correlations of 0.66 in MIT and 0.71 in ATH. It differs only by the replacement of the PREP transcript present in MIT by the THOP1 transcript in ATH. With the exception of IGF2R, this group contains only transcripts coding for angiotensin metabolizing peptidases whose expression increases in the atheromatous plaque compared to MIT. The second group, also isolated from both low grade and advanced atheroma, associates transcripts coding for the receptors MR, GR, AT1R and AT4R also shows strong correlation between its components (mean r = 0.49 in MIT and 0.42 in ATH). In ATH, this cluster included ENPEP and AGT, the AGTR1 transcript being less strongly correlated with the other receptor transcripts. These genes (except NR3C1) had significantly lower expression in ATH compared to MIT. In addition, strong negative correlations were detected between the genes of these 2 clusters in both conditions (mean r = -0.53 in MIT and -0.52 in ATH).

Downloaded Microarray datasets: In order to check for the reproducibility of our results in other datasets and other atheroma lesion types (coronary, peripheral), the expression and coordination of extRAAS genes was also analyzed in previously published datasets available on the GEO database. A total of 10 microarray datasets with 1111 samples were downloaded

from the GEO database, including our dataset (GSE43292). Table 1 shows the features of the downloaded datasets. The total number of samples per sub-dataset ranged between 18 and 290, whereas that per tissue ranged between 18 and 539. The maximum number of datasets was 4, corresponding to human atherosclerotic lesions. The datasets were obtained using Affymetrix (GEO accessions: GPL570, GPL571, GPL6244, GPL1261 and GPL8759) and Rosetta/Merck (GEO accessions: GPL4372, 10687) platforms. Due to the limited number of mice datasets, sub-datasets containing less than 10 samples were retained for analysis.

Expression of extRAAS transcripts in downloaded human datasets: The workflow for analysis of GEO datasets is present in Figure 2. Downloaded datasets were normalized as described in materials and methods. Expression levels of gene transcripts were calculated in each dataset using the expression centile rank (ECR) (figure 3 and supplementary table 2). Figure 3 shows extRAAS co-expression modules and the corresponding transcript ECR levels in both normal human vessels and human atheroma.

In normal human mammary vessels, ECR ranges between 1, for AKR1D1, and 97, for ATP6AP2, with a mean= 40 ± 28 (figure 3a). Interestingly, the main genes of the Ang (1-7) pathway possess low ECR. Indeed, the ECR of ACE2, AGTR2, and Mas1 are all below the first tertile, with ECR equals to 13, 29 and 18, respectively (figure 3a). Similarly, REN (ECR= 34) and ACE (ECR= 7) possess a low ECR. However, AGTR1 transcript (67) is more than two folds higher than that of AGTR2 (29) and Mas1 (18) (figure 3a). In addition, all receptors, except AGTR2 and MAS1, have relatively high expression levels with ECR ranging between 50 (EGFR) and 90 (GR) (figure 3a).

On the other hand, the mean ECR across the different datasets in human atheroma ranges between 12 ± 7 for AKR1D1, and 99 ± 2 for CTSD, with an average of 55 ± 23 (figure 3b). Interestingly, AGT is highly expressed across all datasets in both normal vessels and

atheroma, with an ECR= 85 (figure 3a) in normal vessels and mean ECR (MCR) of 85 ± 6 (figure 3b) across atheroma datasets. Compared to normal vessels, there is a strong increase in the ECR of both ANPEP and HSD11B2 with respective 7-folds and 5-folds increase (figure 3). In addition, the ECR of CMA1, LNPEP, MAS1, KLK1 and THOP1 nearly double in atheroma compared to normal vessels (figure 3). CTSD also doubles and become the highest expressed gene in atheroma. Both CYP11B1 and CYP11B2 increase by 1.6 folds in atheroma, although CYP11B1 still have its ECR below the first tertile. In contrast, both AGTR1 and MR decrease by 1.3- and 1.4-folds, respectively.

Clustering of ExtRAAS transcripts in downloaded human datasets: Hierarchical clustering of extRAAS genes in each dataset showed that all the 37 extRAAS genes could be strongly clustered with a mean agglomerative coefficient above 0.7 (not shown) across datasets (by definition between 0 and 1). This indicates that a strong correlation clearly exists within extRAAS. Since atheroma contained 6 datasets, local extRAAS modules of co-expressed genes were identified by calculating the ACR of gene sets across datasets. Gene clusters/modules with gene expression levels (ECR) are included present in supplementary table 4.

In normal human vessels, 3 large clusters with agglomeration coefficient equals to 86 were identified (Figure 3a). The first cluster contains 10 genes encoding both enzymes (CTSA, CTSD, RNPEP and ENPEP) and receptors (AGTR1, MR, GR, GPER, ATP6AP2 and IGF2R). Apart from ENPEP which possesses ECR= 2, all genes of this module have an ECR greater than 50, with mean ECR equals to 67 ± 16 (ENPEP excluded). The second cluster contains 11 genes (Figure 3a), including AGT, REN and the two receptors EGFR and LNPEP, in addition to other genes coding for enzymes involved in angiotensin metabolism and corticosteroids biosynthesis. The expression of genes within this cluster ranges considerably between 23 (CYP17A1) and 85 (AGT). The third cluster contains 15 genes with

low expression levels, the highest being CPA3 with ECR=49 (Figure 3a). Indeed the mean ECR for this module is equal to 19 ± 14. This module includes the two Ang (1-7) generating enzymes (ACE2 and MME) and receptors (AGTR2 and Mas1). Interestingly, it also includes ACE and CMA1. In addition, it includes the two key corticosteroid enzymes CYP11B1 and CYP11B2.

Interestingly, clustering of extRAAS genes in the downloaded atheroma datasets was very similar to that obtained in our lab. By joining the different clustering patterns from the different datasets, including our dataset, 5 modules could be extracted from the 6 atheroma datasets with ACR greater than 80, except for one module, which includes only two genes and possess an ACR of 67 (Figure 3b). The first atheroma module includes genes with high centile rank ranging between 47 ± 11 (MME) and 99 ± 2 (CTSD) with an average ECR equal to 76 ± 18 (Figure 3b). It contains 9 genes coding for angiotensin-metabolizing enzymes, including ACE, MME, CTSA and CTSD, in addition to the two R/PRs ATP6AP2 and IGF2R. The second module contains the receptor-coding genes, AGTR1, GR, MR, LNPEP, EGFR and GPER, in addition to AGT (Figure 3b). Interestingly, all the transcripts in this module possess a high expression level in atheroma, with an intra-cluster mean ECR equals to 59 ± 11. The third module includes only the three genes: CPA3, CTSG and CMA1 (Figure 3b). Interestingly, this module is 100% reproducible across the 6 datasets. The expression levels of the three genes are 65 ± 13, 49 ± 10 and 31 ± 7, for CPA3, CTSG and CMA1, respectively. The fourth module includes 11 genes with medial to low expressed genes, with ECR ranging between 22 (ACE2) and 61 (KLK1), and MCR= 38 ± 11 (Figure 3b). The fifth module only includes ENPEP and HSD11B1 with ECR of 29 ± 6 and 70 ± 9, respectively.

Interestingly, Inter-cluster correlations revealed a general negative correlation between the first and the second modules of atheroma in 5 of the 6 datasets, corresponding to 810 of 876 samples (data not shown). This is opposite to what is found in normal vessels where the

receptors are clustered and positively correlated to CTSA and CTSD and their companion enzymes (Figure 3a). In addition, ACE changes from being lowly expressed and coordinated with ACE2 and Ang (1-7) receptors in normal vessels to being highly expressed and coordinated with the first module in atheroma (Figure 3b).

ExtRAAS maps: extRAAS maps were built for each tissue using expression levels and co-expression modules (Supplementary Figures A-F). Degradation pathways leading to angiotensin peptides with no known activity, such as the angiotensin (5-10) and angiotensin (1-5) pathways, in addition to the angiotensin (1-12) pathway, were not included in the maps. As shown in figure 4, the substrate of the system, AGT, is highly expressed in both normal and atherosclerotic human vessels, and it can be metabolized into the three major bioactive peptides of the system, Ang-II, Ang-IV and Ang (1-7). However, it looks like the expression of angiotensin metabolizing enzymes in atheroma (figure 4b) is higher and more coordinated than in normal vessels (figure 4a). In addition, the corticosteroid system seems to be more expressed in atheroma compared to normal human vessels. Interestingly, there exist strong correlations between the receptors in both normal and atherosclerotic vessels. Indeed, 7 and 6 receptor transcripts are coordinated in normal human vessels (figure 4a) and in atheroma (figure 4b), respectively. On the same hand, cortisol production is favored over its degradation in both tissues, which is manifested by the high expression of HSD11B1 and the absence of HSD11B2 (figure 4a and 4b). An interesting feature that can be seen in both tissues is the absence of transcripts coding for ACE2, AGTR2 and MAS1, which are known to be the players in the Ang (1-7) pathway. In addition, the Ang-IV pathway much more active in atheroma compared to normal human vessels, manifested by the presence of both the receptor LNPEP and the enzyme ANPEP in high levels in atheroma (figure 4b), and their absence in normal vessels (figure 4a). Moreover, ACE, which is known to be the major Ang-II

producing enzyme is expressed at high levels and coordinated with other peptidases in atheroma (figure 4b), but surprisingly missing in normal vessels (figure 4a).

Mouse datasets: 3 datasets were retained from the downloaded mouse datasets. The larger dataset was GSE38120 containing expression data from 188 normal mouse aortas. The second dataset (GSE10000) contain 18 samples. This dataset was separated into two tissue-datasets from 9 wt normal aortas and 9 apoE-deficient "normal" aortas; although the two tissue-datasets obtained from GSE10000 possess a number of samples that was lower than our threshold (10 samples), these were kept to compare between normal and apoE-deficient aortas from the same experiment. The last dataset (GSE38574) contained 29 samples from atherosclerotic aortas. In the latter dataset there was high variability in the expression between samples, which can be separated into 3 sets: The first set included 2 samples with extremely high expression levels among all genes was eliminated. Another set included 9 genes with high, but not extreme, expression levels was also eliminated since the number of samples was lower than in the third dataset, which contained 18 samples with medial expression levels and was retained for further analysis. All mouse datasets were missing probe sets for Akr1C4, Cyp21A2, Gper, Ren, Slc2A4Rg and Znf76.

ExtRAAS expression and coordination in mouse: For normal mouse aortas, GSE38120 was missing 5 genes, Agtr1a, Agtr1b, Cyp11b1, Lnpep, Nr3c2, and thus it was analyzed for the rest of the extRAAS genes (Supplementary table 4 and supplementary figure D). Centile ranks of extRAAS and TF transcripts and their coordination are present in supplementary tables 3 and 6, respectively.

An interesting feature that can be seen when comparing between human and mouse atheroma (Figures 3b and 3c, see also Supplementary table 4) is the presence of a large modules that is very similar in atheroma from both species and containing mainly angiotensin metabolizing

enzymes. These modules comprising 11 transcripts in both species included CTSA, CTSD, ACE, PREP, RNPEP, ANPEP and DPP3. In addition to the angiotensin metabolizing enzymes, this module includes the renin/prorenin receptors ATP6AP2 and IGF2R, in addition to MME and NLN in human; whereas in mouse it includes and Cma1, Cpa3, Thop1 and the receptor Egfr. Another important feature is the presence of a module that constitutes mainly coordinated receptors in both human and mouse atheroma (Figures 3b and 3c, see also supplementary table 4). Indeed, the module contains the three receptors MR, GR and LNPEP in both species atheroma. In human these are also coordinated with AGTR1, EGFR and GPER and AGT. whereas in mouse atheroma, these are coordinated with the two R/PR receptors, Atp6ap2 and Igf2r, and the two enzymes Mme and Enpep. Interestingly, similar module is also present in apoE-deficient (Supplementary table 4) mouse aortas, but neither in wt mouse aortas or normal human vessels.

Promoter analysis: Promoters were extracted only for genes that belong to coordination modules obtained from human atheroma. The features of the extracted promoters are shown in supplementary table 5. A total of 38 promoters for 32 genes were extracted. The number of extracted TSCs per gene ranged between 1 and 19 (IGF2R), with a mean of 3 ± 4. For certain genes like KLK1, CYP11B2 and CPA3, no TSC could be extracted from SwissRegulon database, yet at least one TSS could be extracted from dbTSS database. On the same hand, two active promoters could be extracted for certain genes, such as CPA3, CYP11A1, EGFR, IGF2R, KLK1, LNPEP and PREP. Promoters' length ranged between 587 bp with one TSC for EGFR and IGF2R, and 2609 with 7 TSC for CTSA. The mean promoter length was 1162 ± 454 bp. The promoter GC content ranged between 29% with 635 bp and 1 TSC for LNPEP, and 75% with 1014 bp and 18 TSC for IGF2R, with a mean GC content of 55 ± 12%. After extracting promoter sequences, Common TFBSs that are enriched in the promoter of coordinated genes, were extracted using the CommonTF tool in Genomatix suite. A total of

21 TFBS were extracted; 19 were found to be enriched in the promoters of module 1 genes and 2 for module 2 genes. No TFBS could be extracted for modules 3 and 4. Interestingly, for each of modules 1 & 2, the extracted TFBS were found to be enriched in more than 80% of the promoters of corresponding genes. Indeed, for module one, the TFBSs were found to be enriched in the promoter of at least 9 genes of the 11 genes of this module (82%). On the same hand, both the TFBSs for IRF5 and IRF6 were found to be enriched in the promoters of 5 of the 6 genes of module 2 (83%). The extracted TFBSs with their corresponding TFs are shown in Table 2. Of the extracted TFs, EGR1 and IRF5 were previously described in atherosclerosis[453,460,461].

TFs expression levels: similarly to extRAAS genes, the ECR was also used to express the levels of TF transcripts (supplementary tables 2 and 3). Of the 22 TFs obtained using the commonTF Genomatix tool, CDF1 and ZBTB14 were excluded from further analysis since they were not represented by any probe set in most of the microarray platforms. Interestingly, all TFs have ECR higher than the first tertile in human atheroma except for SPIB (ECR= 32) (table 3 and supplementary table 2). However, in human normal vessels, genes with transcripts less than the first tertile include SMAD1, MAX, ETS1 and FOXN1. Indeed, the genes that seem to be positively regulated with a fold change greater than 1.5x in human atheroma compared to normal human vessels include SMAD1 (2 folds), MAX (4.4 folds), ETS1 (5 folds) and FOXN1 (3.5 folds), in addition to ETV5 (1.8 folds) and IRF5 (1.8 folds). On the other hand, genes with 1.5-fold decrease include SPIB (1.6 folds), IRF6 (1.5 folds) and SLC2A4RG (1.6 folds). Similarly in mouse, all TFs have ECR greater than the first tertile in mouse atheroma and both wt and apoE-deficient normal aortas except for Foxn1 and Pax9 (supplementary table 3). There was no important change in the expression of TFs between normal aorta from wt and apo-E-deficient mice. When comparing the expression level of TFs between normal (mean of GSE10000 and GSE38120) and atherosclerotic aortas

of mouse, only Etv5 showed a 2 fold greater expression in atherosclerotic aorta, with very low, if any, change in expression of the rest of TFs.

ExtRAAS and TF transcripts clustering: Clustering of extRAAS with TFs gave very similar results to those obtained when clustering extRAAS alone in both human and mouse. In human, the first module included the same set of enzymes and receptors as module 1, with HSD11B1 and the 4 TFs ELF1, ETV5, IRF5 and MAX (table 3). All the transcripts in this module possess expression levels higher than 50, except PREP, which had an ECR of 34 ± 3. In mouse similar module was obtained; however, it also includes Cpa3 and Cma1, with the three TFs Elk3, Egr1 and Egr3, which constitute a separate module (module 3) in human atheroma (Supplementary table 6). On the other hand, it excluded Elf1, Hsd11b1, Nln, Atp6ap2, Igf2r and Mme. The latter three were coordinated with the second module of receptors in mouse atheroma, which included the same set of receptors obtained when clustering extRAAS genes alone. In human atheroma, the same module of receptors (module 2) was obtained; however, without GPER; but with AGT and ENPEP (table 3). It also includes 6 TFs, which are CTCF, ELK4, ETS1, IRF6, PAX9 and SMAD1 (table 3). The ECR of these genes ranged between 25 ± 2 for ENPEP and 87 ± 2 for AGT, with a mean ECR= 57 ± 20. Similar module was obtained in mouse atheroma but without Pax9, Agt, and Egfr. The latter two being coordinated with the first module of peptidases. The fourth module in human atheroma contain 19 genes (table 3), which is similar to another one in mouse (Supplementary table 6); however, without Elk1, Thop1, Cyp11b2, Ren, Gper, Slc2a4rg, Cyp21a2 and Akr1c4. The latter 5 are missing in the GSE38574 dataset. Interestingly, the results obtained in both human and mouse atherosclerotic aortas were highly different to their normal counterparts, both at coordination within TFs or between TFs and extRAAS (Supplementary table 6). For example, the TFs ETV5, MAX, IRF5 and ELF1, which are coordinated with the module of peptidases in both human and mouse atheroma are distributed

over the different clusters in normal vessels, with only ELF1 coordinated with the peptidases (Supplementary table 6). In normal mouse aortas, only the Irf5 and Ets1 are coordinated with the large module of angiotensin metabolizing enzymes (Supplementary table 6).

Since modules 1, 2 and 3 of extRAAS obtained in human atheroma bear some similarities to those previously obtained in normal human kidney and omental adipose tissue[209], we obtained their coordination patterns of extRAAS and TF transcripts (Supplementary table 6) and compared it to atheroma. In both human kidney and adipose tissues, all TFs possess an ECR greater than the first tertile except Pax1 and SpIb (Supplementary table 6). The mean TF ECR of 65 ± 22 and 67 ± 22 was obtained for the kidney and adipose, respectively. Compared with the kidney, little, if any, similarities could be obtained in the coordination patterns (Supplementary table 6). On the other hand in omental adipose, 4 of the 6 TFs that were coordinated with the module 2 in human atheroma were also coordinated with the highly similar set of transcripts in normal omental adipose (Supplementary table 6). Indeed, both normal adipose and human atheroma include a module constituting AGTR1, LNPEP, NR3C1, NR3C2, ENPEP, SMAD1, CTCF, ETS1 and ELK4. In atheroma it also includes AGT, EGFR, PAX9 and IRF6, while in adipose it includes ELK1, IGF2R, MAX and ELF1; the latter three being coordinated with module 1 in human atheroma.

IV.2.4 Discussion

Although many studies were done to elucidate extRAAS's participation in local atheroma development, these remain disperse and give no clear global view of the different arms of the system in the disease. In this study we describe for the first time the local expression of 37 extRAAS genes in atheroma at the mRNA level. The results are presented in map that shows the favorable pathways of extRAAS in atheroma (figure 4, see also supplementary figures A-F). We also reveal potential transcription factors that play a role in the transcriptional regulation of extRAAS genes in atheroma.

Despite the fact that this study only showed the expression of extRAAS genes in atheroma at the mRNA level, the latter may provide stronger indication of the local expression of extRAAS components. Indeed, in contrast to proteins that could be imported from the circulation, mRNAs are mainly intracellular molecules that are almost totally generated by local cellular transcription.

The map of extRAAS shows that the substrate of the system, AGT, is expressed at high levels and could be metabolized to produce all the known bioactive angiotensin peptides in atheroma. The low levels of Agt in mouse compared to human atheroma suggest that angiotensin peptides production is driven by locally expressed AGT in human atheroma, whereas in mouse it could be driven by AGT imported from the circulation. The results in mouse were also in contrast to other studies detecting AGT mRNA in the media and adventitia of several mouse arterial beds[218,219,221]. Thus further investigations should be done to clarify these contradictions. Although renin transcript is very low in atheroma, its Ang-I generating activity could be compensated by the very high levels of CTSD, and the expression of other Ang-I generating enzyme such as cathepsin G and kallikrein-1, in addition to Ang-(1-12), which should be further investigated. It may also be imported from

the circulation by its highly expressed receptors, ATP6AP2 and IGF2R, which are both known to bind and activate prorenin and enhance renin activity[201,462].

The coordination of angiotensin metabolizing enzymes involved in generation of all angiotensin peptides indicate that angiotensin peptide generation is tightly regulated in atheroma thus leading to a balance in the antagonistic pathways. Thus, it seems that the local effects of the different bioactive pathways of the system are most probably differentiated at the response level by the differentially expressed receptors. Indeed, this can be clearly seen by the high coordination and medial expression of the pro-atherogenic receptor transcripts, AGTR1, MR, GPER and EGFR, and the very low levels of AGTR2 and Mas transcripts. The positive correlation between the pro-atherogenic receptors and AGT indicate that the system maintain a pro-atherogenic state by the substrate, which fuel the production of the different peptides that exert their effects on these receptors. Despite the very high levels of the cortisol receptor GR in both human and mouse atheroma, which is known for its athero-protective effects, the high 11β-HSD1/11β-HSD2 in both species' atheroma may support the pro-atherogenic effects of cortisol, which is known to bind MR at high levels and exert pro-atherogenic effects[414]. Although, cortisol binding to MR may reduce the binding capacity of aldosterone, the latter may still be able to bind to GPER, which is expressed at sufficient levels (MCR in human atheroma= 62 ± 2).

Extensive studies have been done on the effects of Ang-II, Ang-(1-7) and aldosterone in atheroma. However, our results suggest that the Ang-IV pathway could also play a major role in atheroma as suggested by the high expression of its enzymes and receptors. Thus further studies on the effects of this pathway on atherosclerosis and its differential expression between normal and atherosclerotic wall should be done.

Several studies investigated the common transcriptional regulation of multiple RAAS genes[463,464]. However, these studies focused on classical RAAS participants, mainly AGT,

REN, ACE and AGTR1. In this study we propose multiple TFs that could be candidates for the regulation of multiple extRAAS genes. In addition, the comparison of the extRAAS and TF modules between different tissues (atheroma, kidney and adipose) indicate that the global tissue-specific organization of extRAAS could be in part related to tissue-specific transcriptional mechanisms. One of the relevant receptors obtained by our analysis is IRF5, which is positively correlated to angiotensin metabolizing enzymes in atheroma (table 3) and negatively correlated to the coordinated receptors (Table 4, module 2 in human atheroma), which strongly support the role of this TF in the extRAAS organization obtained in human atheroma. Although IRF5 is known to be a pro-inflammatory TF and upregulated by inflammation[465], a recent study showed opposite effects of IRF5 deficiency which resulted in atheroma regression [453]. This could be indirectly related to its negative correlation to the receptors. However, this needs to be validated both in vitro and in vivo.

The correlation of TFs to extRAAS genes with no promoter-enriched TFBSs indicates that there could be a DNA-independent link between TFs and extRAAS genes. For example, no common TF could be extracted for module 3 in human atheroma, which includes the 3 genes CPA3 and CMA1 and CTSG. For the latter, only 1 TSC could be extracted, whereas no TSC could be extracted for CPA3 and CMA1. Thus it seems that the expression of these genes is most probably regulated by post-transcriptional mechanisms such as miRNA binding. The correlation of these genes with certain TFs that was reproducible in both human and mouse atheroma may indicate that these post-transcriptional mechanisms are under the control of these TFs. This could be similar to correlations obtained between the TFs associated with extRAAS receptors. Indeed, despite that only TFBS matrices for IRF5 and IRF6 were found to be enriched in the promoters of the receptor module genes, 6 TFs were coordinated with these receptors, including IRF6. However, one should keep in mind that these TFs may bind

to enhancer sequences that are several Kb away from the gene TSS[466] and thus may not be present in the promoter region we have analyzed.

ExtRAAS organization, and its correlation with specific TFs was very similar in human and mouse atheroma. Indeed, only minor changes could be observed. For example, module 3 in human atheroma that constitutes the 3 TFs EGR1, EGR3 and ELK3 and the 3 extRAAS CPA3, CMA1 and CTSG was totally joined into module 1 in mouse atheroma, indicating a stringent correlation between these genes that it could be atheroma related. Indeed, although we have previously CPA3, CMA1 and CTSG are highly coordinated in omental adipose[209], this study showed that they are coordinated with different TFs than those in atheroma (supplementary table 2). Therefore, it seems that organization of extRAAS obtained in atheroma and despite certain similarities with the organizations obtained in other tissues, it might be regulated by specific mechanisms than that in other tissues.

In summary, our results indicate that the organization of extRAAS in atheroma is beyond the arterial bed of the atherosclerotic lesion, but also beyond inter-individual variability. However, cellular distribution of extRAAS needs to be elucidated, as well as how they translate into enzymatic activity, peptide production and signaling. The high similarity in the organization of extRAAS between human and mouse atheroma suggests that mouse could be used as a model for studying extRAAS in atheroma. In addition, we have shown that the correlation of genes and TFs at the transcriptional level may be used as a way to predict potential TFs that regulate the expression of proteins involved in a certain pathway. Although these TFs are not validated in vivo or in vitro, we recently showed that the coordination between transcripts could be reproduced in cell culture as the result of common transcription factors activation[467]. Thus, in vitro and in vivo studies on these TFs should be done to investigate their pharmacological relevance. The specificity of the correlations between extRAAS organization and the extracted TFs may provide the basis for the development of

new pharmaceuticals that can target extRAAS in atheroma without affecting its organization in other tissue.

Funding

A.N. was awarded a scholarship from"La Nouvelle Société Francophone d'Athérosclérose" (NSFA). This work was supported by a Campus France grant from Coopération pour l'Évaluation et le Développement de la Recherche (CEDRE).

Author Contributions Statement

AN performed experiments, analyzed data and wrote the manuscript. CC provided the scripts on R-software and performed statistical analyses. GB and KZ designed the study, analyzed data and wrote the manuscript.

Conflict-of-interest disclosure: The authors declare that they have no conflict of interest.

IV.2.5 Tables and Figures Legends

Table 1: Downloaded datasets features.

Table 2: The transcription factor binding sites (TFBS) matrices obtained by Genomatix. TF, transcription factor. In the first column are the modules from which the TFBS was extracted. Matrix families are written as annotated by Genomatix. The corresponsing transcription factor and gene ID were extracted from the NCBI database. TFBS having at least one match in the studied promoters were obtained with their enrichment p-value in the group of studied promoters.

Table 3: ExtRAAS co-expression modules in human atheroma. The corresponding number of data sets, samples and modules is present in brackets under tissue name. At the top of each module the average coordination rates are expressed in percentage. The mRNA abundance of each gene is present next to the gene symbol and is expressed in centile rank. black = enzymes; blue = receptors; and red = transcription factors.

Figure 1: Expression and coordination of 35 extRAAS genes in macroscopically intact tissue (MIT) and atheroma plaque (ATH) of 32 patients. (A) log2 mRNA levels of extRAAS genes was calculated as mean ± SD. Genes having mean expression level higher than the median value over the microarray are present in the upper graph, whereas genes having mean expression level lower than the median value over the microarray are present in the lower graph. (B) Dendrograms of 35 extRAAS transcripts. Hierarchical clustering used the “Cluster” package of R. The agglomerative coefficients were 0.71 in MIT and 0.75 in ATH.

Figure 2: Experimental work flow for the analysis of extRAAS genes expression in the downloaded datasets. Microarrays were downloaded from the GEO database then filtered based on certain inclusion and exclusion criteria. Expression and coordination patterns of extRAAS genes were then extracted from each dataset. Results obtained from datasets of the same tissue were then joined and reproducible patterns of expression and coordination were identified. for each tissue, the identified reproducible patterns were then used to construct a map of extRAAS organization. Promoter sequences of coordinated extRAAS genes were extrated then analyzed for enriched common transcription factor binding sites (TFBSs). The corresponding TFs were then analyzed for their expression and coordination with extRAAS genes.

Figure 3: The level of expression of extRAAS genes and their coordination in normal human vessels (A), human atheroma (B) and mouse atheroma (C). Colores indicate coordinated genes. ECR, expression centile rank.

Figure 4: ExtRAAS maps in human normal human vessels (A) and atheroma (B). Below tissue name the number of data sets, samples and modules are represented between brackets (data sets, samples, modules). Gene transcripts are represented by the corresponding official symbols. The genes are represented based on their coordination (same color = same module) and mean centile expression rank (MCR, different font size). Non-clustered genes are represented in black color. Gene transcripts below the first tertile (MCR < 33.3) in each tissue were excluded for simplicity. Angiotensin peptides and corticosteroid metabolites are represented in gray italics.

IV.2.6 Tables

Species	Tissue	Datasets accession	Platform accession	Samples/ssub-dataset	Datasets/Tissue	Samples/Tissue
Human	Normal mammary artery	GSE13760	GPL571	37	1	37
	Carotid atheroma	GSE21545 GSE28829 GSE43292 GSE24495	GPL570 GPL570 GPL6244 GPL10687	126 29 32 113	4	300
	Peripheral atheroma	GSE24702 GSE37824	GPL10687 GPL4372	290 249	2	539
Mouse	Normal aorta	GSE10000 GSE10000 GSE38120	GPL1261 GPL1261 GPL8759	9 9 188	2	206
	Atherosclerotic aorta	GSE38574	GPL1261	29	1	18

Table 1: Downloaded datasets features.

Module	# enriched promoters	Matrix family	Matrix	TF	Gene ID	p-value
1	11	V$CTCF	V$CTCF.01	CTCF	10664	2.8018E-05
	11	V$EGRF	V$EGR1.01	EGR1	1958	2.819E-06
	11	V$ETSF	V$ETV5.01	ETV5	2119	4.1533E-05
	11	V$ETSF	V$CETS1P54.01	ETS1	2113	6.2052E-05
	11	V$ETSF	V$ELK4.01	ELK4	2005	7.7327E-05
	11	V$SMAD	V$GC_SBE.01	SMAD1	4086	4.579E-05
	11	V$WHNF	V$WHN.01	FOXN1	8456	2.039E-05
	10	V$CDEF	V$CDE.01	CDF1	832368	3.2529E-05
	10	V$CTCF	V$CTCF.02	CTCF	10664	9.4871E-05
	10	V$EBOX	V$MAX.03	MAX	4149	4.3658E-05
	10	V$EGRF	V$EGR3.01	EGR3	1960	7.283E-05
	10	V$ETSF	V$SPIB.01	SPIB	6689	1.9407E-05
	10	V$ETSF	V$ELK3.01	ELK3	2004	4.922E-05
	10	V$ETSF	V$ELF1.01	ELF1	1997	5.1331E-05
	10	V$PAX9	V$PAX9.01	PAX9	5083	1.3268E-05
	10	V$STAF	V$ZNF76_143.01	ZNF76	7629	2.5613E-05
	10	V$ZF5F	V$ZF5.03	ZBTB14	7541	2.1672E-05
	9	V$ETSF	V$ELK1.02	ELK1	2002	3.2004E-05
	9	V$HDBP	V$HDBP1_2.01	SLC2A4RG	56731	5.3282E-05
2	5	V$IRFF	V$IRF6.01	IRF6	3664	1.5376E-05
	5	V$IRFF	V$IRF5.01	IRF5	3663	3.0845E-05

Table 2: The transcription factor binding sites (TFBS) matrices obtained by Genomatix.

Tissues (datasets, samples)	Module 1		Module 2		Module 3		Module 4		Module 5
Human atheroma	91%		86%		89%		90%		
(7, 876, 4)	CTSD	98	AGT	88	EGR1	82	ELK1	74	
	CTSA	97	CTCF	83	ELK3	75	GPER	62	
	ATP6AP2	93	ETS1	83	CPA3	64	KLK1	56	
	ETV5	90	NR3C1	75	EGR3	64	THOP1	54	
	IGF2R	89	ELK4	69	CTSG	49	SLC2A4RG	53	
	MAX	89	LNPEP	69	CMA1	30	CYP11B2	46	
	RNPEP	89	EGFR	67			CYP21A2	46	
	ANPEP	86	SMAD1	66			CYP17A1	39	
	DPP3	81	IRF6	50			CYP11A1	37	
	ELF1	80	AGTR1	49			AGTR2	36	
	PREP	78	NR3C2	45			FOXN1	35	
	IRF5	75	PAX9	35			SPIB	32	
	HSD11B1	66	ENPEP	29			HSD11B2	30	
	MME	64					REN	27	
	NLN	59					CYP11B1	23	
	ACE	56					ACE2	22	
							AKR1C4	21	
							MAS1	20	
							AKR1D1	11	

Table 3: ExtRAAS co-expression modules in human atheroma.

IV.2.7 Figures

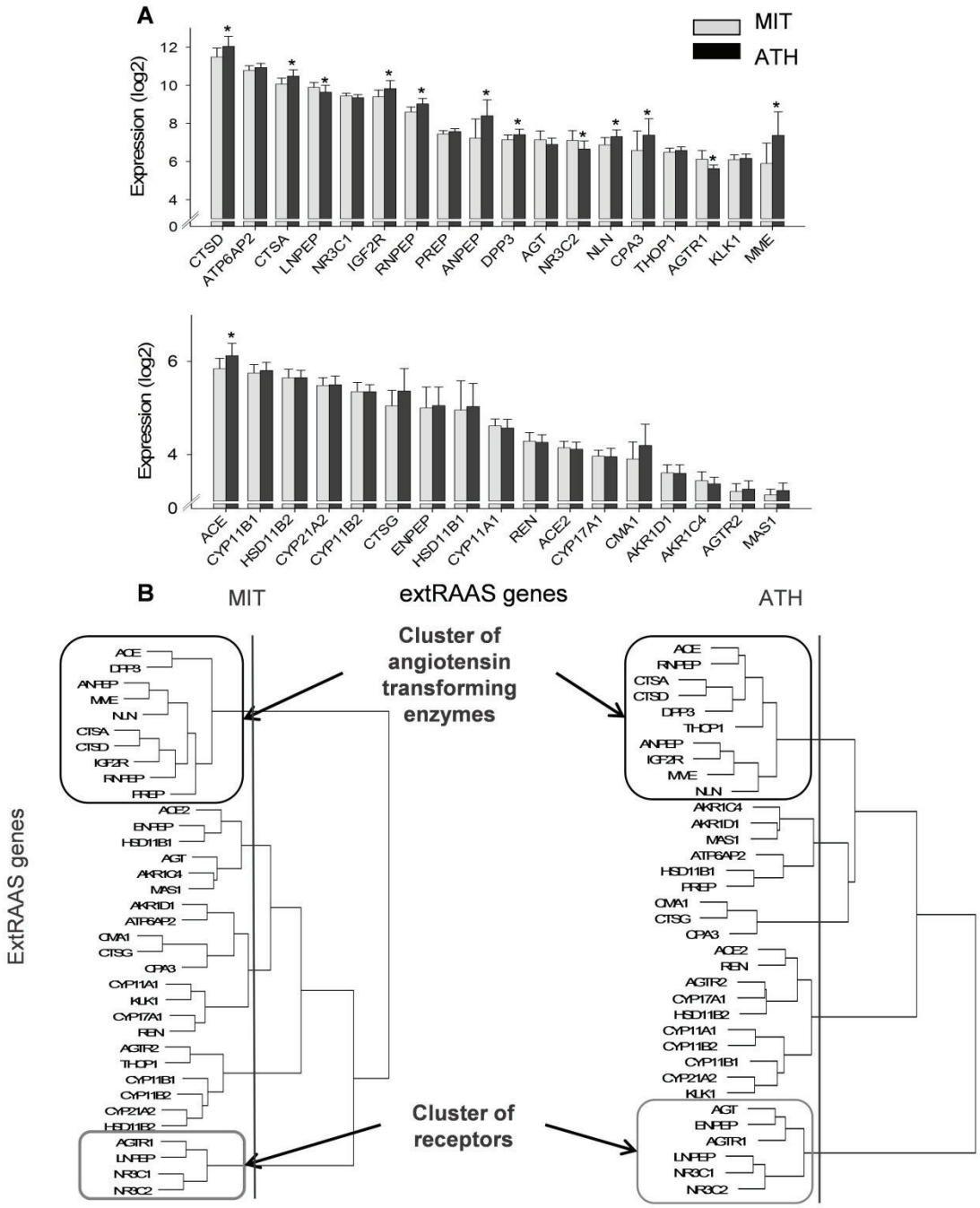

Figure 1: Expression and coordination of 35 extRAAS genes in macroscopically intact tissue (MIT) and atheroma plaque (ATH) of 32 patients.

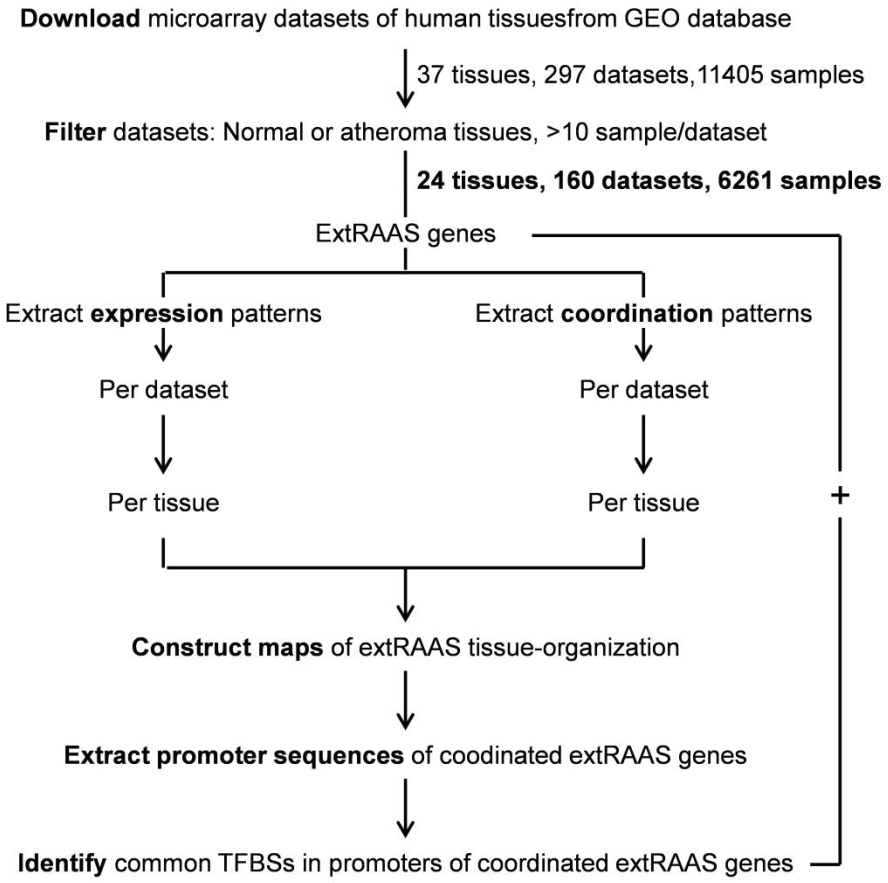

Figure 2: Experimental work flow for the analysis of extRAAS genes expression in the downloaded datasets.

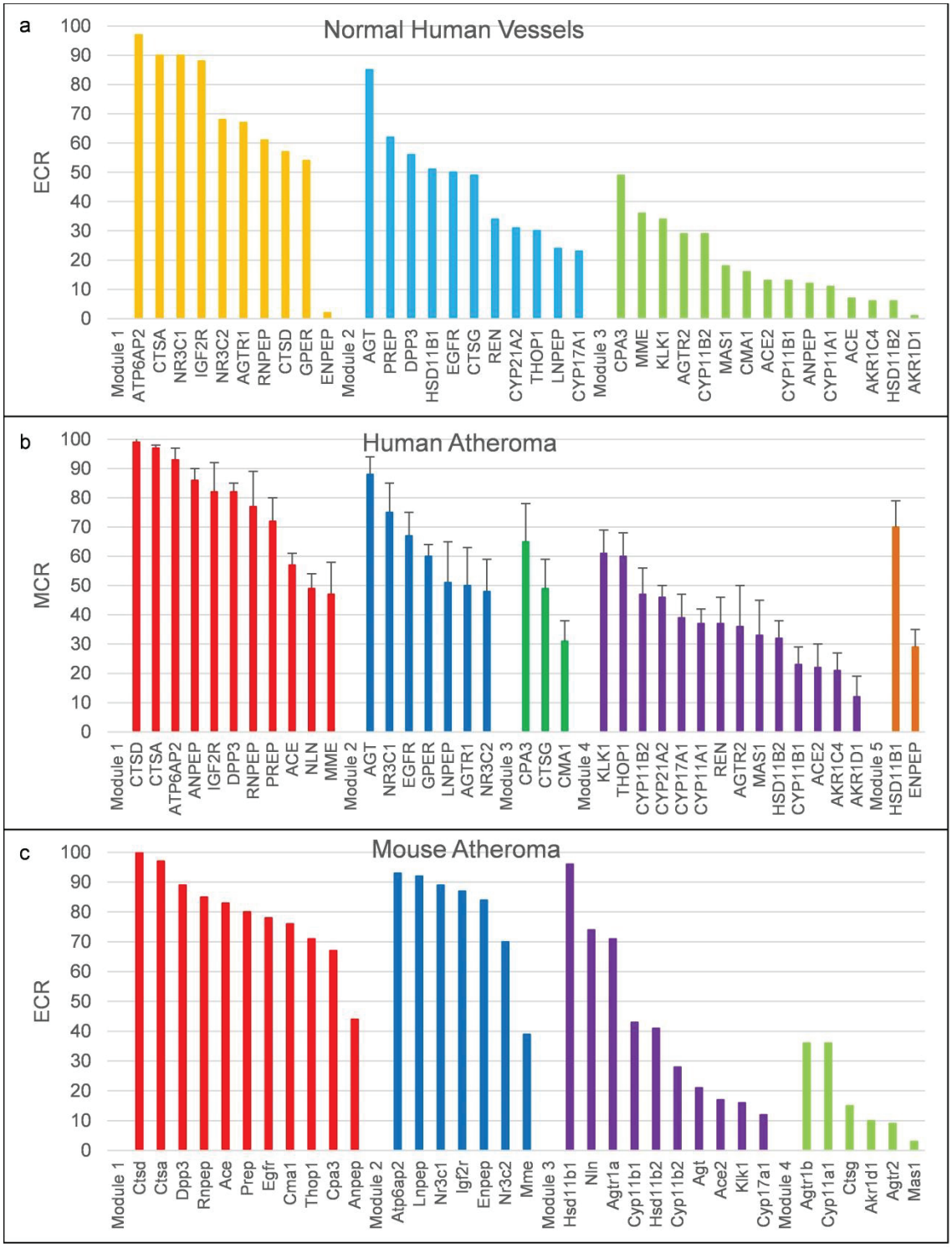

Figure 3: The level of expression of extRAAS genes and their coordination in normal human vessels (A), human atheroma (B) and mouse atheroma (C).

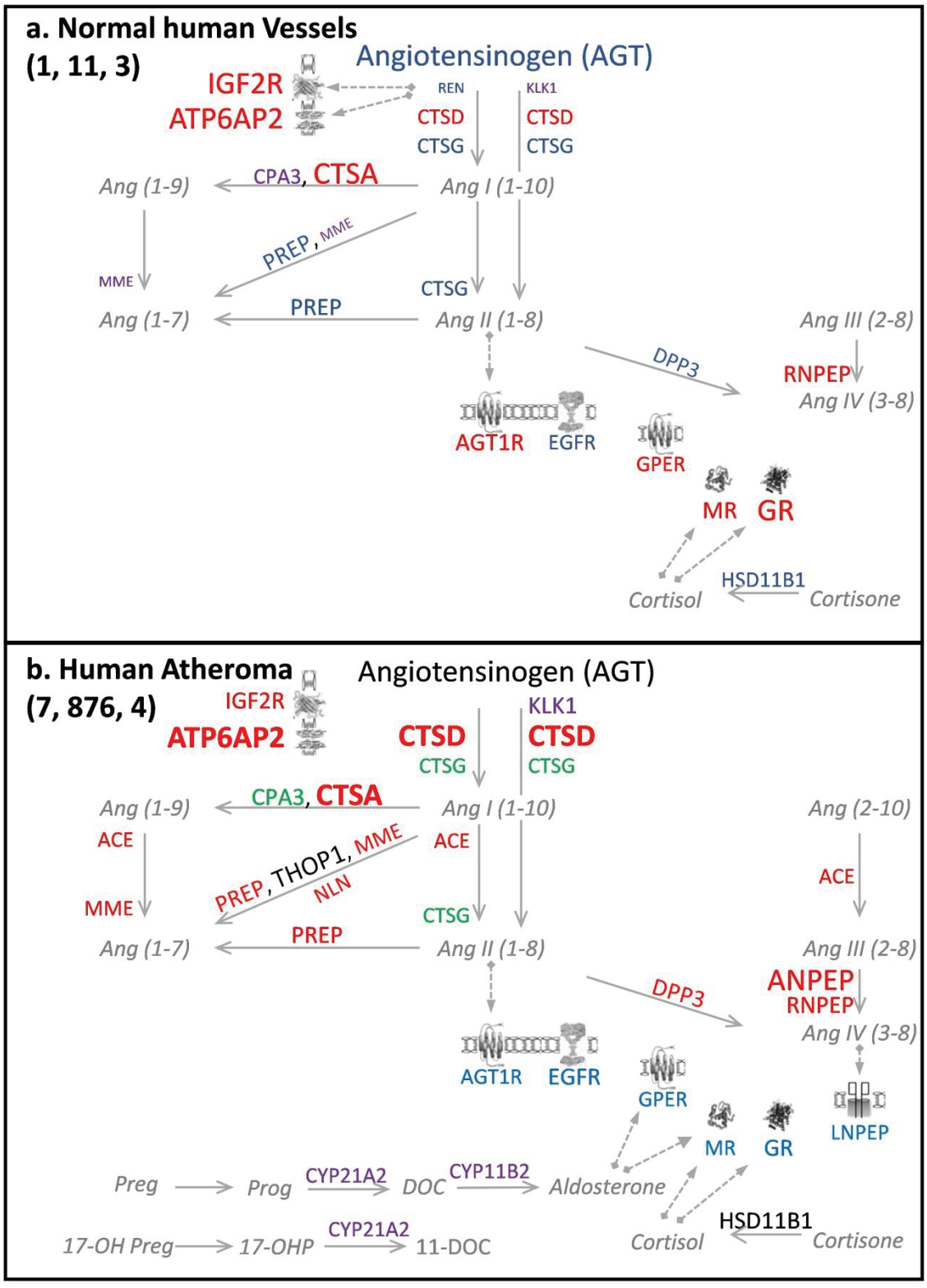

Figure 4: ExtRAAS maps in human normal human vessels (A) and atheroma (B).

Supplementary Table S1: Extended renin-angiotensin-aldosterone system (ExtRAAS) gene.

Supplementary Table S1: Extended renin-angiotensin-aldosterone system (ExtRAAS) gene. ExtRAAS constitute 37 genes; 25 encode for the renin-angiotensin system (RAS) components corresponding to angiotensinogen (AGT) 17 enzymes and 7 receptors; and 12 genes encode for corticosteroid system (COS) proteins corresponding to 9 enzymes and 3 receptors. Classical RAAS genes are annotated by an asterisk. RAS, renin-angiotensin system; COS, corticosteroid system; GeneID, gene refseq ID.

System	Gene Symbol	Gene Description	GeneID
RAS	ACE*	angiotensin I converting enzyme (peptidyl-dipeptidase A) 1	1636
RAS	ACE2	angiotensin I converting enzyme (peptidyl-dipeptidase A) 2	59272
RAS	AGT*	angiotensinogen (serpin peptidase inhibitor, clade A, member 8)	183
RAS	AGTR1*	angiotensin II receptor, type 1	185
RAS	AGTR2	angiotensin II receptor, type 2	186
RAS	ANPEP	alanyl (membrane) aminopeptidase	290
RAS	ATP6AP2	ATPase, H+ transporting, lysosomal accessory protein 2	10159
RAS	CMA1	chymase 1, mast cell	1215
RAS	CPA3	carboxypeptidase A3 (mast cell)	1359
RAS	CTSA	cathepsin A	5476
RAS	CTSD	cathepsin D	1509
RAS	CTSG	cathepsin G	1511
RAS	DPP3	dipeptidyl-peptidase 3	10072
RAS	EGFR	epidermal growth factor receptor	1956
RAS	ENPEP	glutamyl aminopeptidase (aminopeptidase A)	2028
RAS	IGF2R	insulin-like growth factor 2 receptor	3482
RAS	KLK1	kallikrein 1	3816
RAS	LNPEP	leucyl/cystinyl aminopeptidase	4012
RAS	MAS1	MAS1 oncogene	4142
RAS	MME	membrane metallo-endopeptidase	4311
RAS	NLN	neurolysin (metallopeptidase M3 family)	57486
RAS	PREP	prolyl endopeptidase	5550
RAS	REN*	renin	5972
RAS	RNPEP	arginyl aminopeptidase (aminopeptidase B)	6051
RAS	THOP1	thimet oligopeptidase 1	7064
COS	AKR1C4	aldo-keto reductase family 1, member C4	1109
COS	AKR1D1	aldo-keto reductase family 1, member D1	6718
COS	CYP11A1	cytochrome P450, family 11, subfamily A, polypeptide 1	1583
COS	CYP11B1	cytochrome P450, family 11, subfamily B, polypeptide 1	1584
COS	CYP11B2*	cytochrome P450, family 11, subfamily B, polypeptide 2	1585
COS	CYP17A1	cytochrome P450, family 17, subfamily A, polypeptide 1	1586
COS	CYP21A2	cytochrome P450, family 21, subfamily A, polypeptide 2	1589
COS	GPER	G protein-coupled estrogen receptor 1	2852
COS	HSD11B1	hydroxysteroid (11-beta) dehydrogenase 1	3290
COS	HSD11B2*	hydroxysteroid (11-beta) dehydrogenase 2	3291
COS	NR3C1	nuclear receptor subfamily 3, group C, member 1 (glucocorticoid receptor)	2908
COS	NR3C2*	nuclear receptor subfamily 3, group C, member 2	4306

Supplementary Table S2: Expression centile profiles of extRAAS genes in human

Supplementary Table S2: Expression centile profiles of extRAAS genes in human. MIT, macroscopically intact tissue.

Group	Gene	Normal	MIT	Atheroma
RAS	ACE	7	46	56 ± 2
Enzyme	ACE2	13	22	22 ± 3
Substrate	AGT	85	67	88 ± 2
Receptor	AGTR1	67	50	49 ± 5
Receptor	AGTR2	29	10	36 ± 8
COS	AKR1C4	6	13	21 ± 2
COS	AKR1D1	1	15	11 ± 3
RAS	ANPEP	12	69	86 ± 1
Receptor	ATP6AP2	97	98	93 ± 1
RAS	CMA1	16	19	30 ± 2
RAS	CPA3	49	58	64 ± 5
TF	CTCF	80	88	83 ± 4
RAS	CTSA	90	96	97 ± 0
RAS	CTSD	57	99	98 ± 0
RAS	CTSG	49	34	49 ± 4
COS	CYP11A1	11	28	37 ± 2
COS	CYP11B1	13	44	23 ± 2
COS	CYP11B2	29	38	46 ± 3
COS	CYP17A1	23	20	39 ± 3
COS	CYP21A2	31	37	46 ± 1
RAS	DPP3	56	67	81 ± 1
Receptor	EGFR	50	75	67 ± 3
TF	EGR1	93	92	82 ± 7
TF	EGR3	88	53	64 ± 6
TF	ELF1	75	95	80 ± 5
TF	ELK1	88	70	74 ± 3
TF	ELK3	53	78	75 ± 3
TF	ELK4	58	74	69 ± 3
RAS	ENPEP	2	33	29 ± 2
TF	ETS1	16	91	83 ± 4
TF	ETV5	50	80	90 ± 1
TF	FOXN1	10	33	35 ± 2
Receptor	GPER	54	49	62 ± 2
COS	HSD11B1	51	32	66 ± 4
COS	HSD11B2	6	43	30 ± 2
Receptor	IGF2R	88	93	89 ± 2
TF	IRF5	41	59	75 ± 2
TF	IRF6	75	45	50 ± 3
RAS	KLK1	34	50	56 ± 3
Receptor	LNPEP	24	95	69 ± 5
Receptor	MAS1	18	9	20 ± 2
TF	MAX	20	73	89 ± 2
RAS	MME	36	46	64 ± 4
RAS	NLN		63	59 ± 2
Receptor	NR3C1	90	93	75 ± 4
Receptor	NR3C2	68	67	45 ± 4
TF	PAX9	42	48	35 ± 1
RAS	PREP	62	72	78 ± 1
RAS	REN	34	24	27 ± 2
RAS	RNPEP	61	86	89 ± 1
TF	SLC2A4RG	86	62	53 ± 2
TF	SMAD1	33	66	66 ± 5
TF	SPIB	52	47	32 ± 2
RAS	THOP1	30	57	54 ± 2
TF	ZNF76	64	64	67 ± 4

Supplementary Table S3: Expression centile profiles of extRAAS genes in mouse

Supplementary Table S3: Expression centile profiles of extRAAS genes in mouse. Wt, wild type aortas in GSE10000; apoE, apoE-deficient aortas in GSE10000.

Group	Gene	Normal	wt	atheroma	apoE
RAS	Ace	64	96	83	96
Enzyme	Ace2	31	28	17	16
Substrate	Agt	48	9	21	10
Receptor	Agtr1a		71	71	69
Receptor	Agtr1b		63	36	63
Receptor	Agtr2	1	8	9	4
COS	Akr1d1	2	12	10	15
RAS	Anpep	44	56	44	71
Receptor	Atp6ap2	78	96	93	98
RAS	Cma1	61	72	76	71
RAS	Cpa3	61	74	67	71
TF	Ctcf	69	89	82	89
RAS	Ctsa	90	94	97	97
RAS	Ctsd	98	99	100	100
RAS	Ctsg	13	14	15	20
COS	Cyp11a1	8	34	36	34
COS	Cyp11b1		49	43	34
COS	Cyp11b2	23	48	28	44
COS	Cyp17a1	12	18	12	16
RAS	Dpp3	69	76	89	77
Receptor	Egfr	47	85	78	86
TF	Egr1	85	99	96	99
TF	Egr3	40	68	68	74
TF	Elf1	52	55	65	53
TF	Elk1	42	51	63	52
TF	Elk3	63	86	82	90
TF	Elk4	87	93	92	93
RAS	Enpep	69	91	84	89
TF	Ets1	75	92	88	93
TF	Etv5	15	65	77	71
TF	Foxn1	12	48	26	46
COS	Hsd11b1	98	92	96	92
COS	Hsd11b2	23	47	41	45
Receptor	Igf2r	85	90	87	91
TF	Irf5	39	57	69	70
TF	Irf6	30	77	67	76
RAS	Klk1	23	15	16	14
Receptor	Lnpep		94	92	94
Receptor	Mas1	1	7	3	4
TF	Max		70	69	72
RAS	Mme	59	50	39	44
RAS	Nln	62	60	74	64
Receptor	Nr3c1	88	96	89	96
Receptor	Nr3c2		71	70	67
TF	Pax9	22	29	31	30
RAS	Prep	73	79	80	79
RAS	Rnpep	75	75	85	79
TF	Smad1	72	94	92	93
TF	Spib	55	52	57	60
RAS	Thop1	51	31	71	36
COS	Akr1C4	missing	missing	missing	missing
COS	Cyp21A2	missing	missing	missing	missing
COS	Gper	missing	missing	missing	missing
RAS	Ren	missing	missing	missing	missing
TF	Slc2A4Rg	missing	missing	missing	missing
TF	Znf76	missing	missing	missing	missing

Supplementary Table S4: ExtRAAS co-expression modules

Supplementary Table S4: ExtRAAS co-expression modules. Below each tissue the number of datasets, samples and clusters/modules are represented as (datasets, samples, clusters/modules). At the top of each module of human atheroma the average the coordination rate is expressed in percentage (average percentage of genes within a module that are always coordinated across the different datasets of a specific tissue). Next to each gene symbol the abundance of the mRNA is expressed in centile rank. Black = enzymes; blue = receptors.

Tissues (datasets, samples)	Module 1		Module 2		Module 3		Module 4		Module 5		Non-clustered	
Normal Vessels												
(1, 11, 3)	ATP6AP2	97	AGT	85	CPA3	49						
	CTSA	90	PREP	62	MME	36						
	NR3C1	90	DPP3	56	KLK1	34						
	IGF2R	88	HSD11B1	51	AGTR2	29						
	NR3C2	68	EGFR	50	CYP11B2	29						
	AGTR1	67	CTSG	49	MAS1	18						
	RNPEP	61	REN	34	CMA1	16						
	CTSD	57	CYP21A2	31	ACE2	13						
	GPER	54	THOP1	30	CYP11B1	13						
	ENPEP	2	LNPEP	24	ANPEP	12						
			CYP17A1	23	CYP11A1	11						
					ACE	7						
					AKR1C4	6						
					HSD11B2	6						
					AKR1D1	1						
Macroscopically	CTSD	99	LNPEP	95	ATP6AP2	98	AGT	67	THOP1	57		
intact tissue	CTSA	96	NR3C1	93	CPA3	58	ENPEP	33	GPER	49		
(GSE 43292)	IGF2R	93	EGFR	75	KLK1	50	HSD11B1	32	CYP11B1	44		
(1, 32, 5)	RNPEP	86	NR3C2	67	CTSG	34	ACE2	22	HSD11B2	43		
	PREP	72	AGTR1	50	CYP11A1	28	AKR1C4	13	CYP11B2	38		
	ANPEP	69			REN	24	MAS1	9	CYP21A2	37		
	DPP3	67			CYP17A1	20			AGTR2	10		
	NLN	63			CMA1	19						
	ACE	46			AKR1D1	15						
	MME	46										
Human atheroma	88%		82%		100%		85%		67%			
(7, 876, 5)	**CTSD**	**98**	AGT	88	CPA3	64	KLK1	56	HSD11B1	66		
	CTSA	**97**	NR3C1	75	CTSG	49	THOP1	54	ENPEP	29		
	ATP6AP2	**93**	LNPEP	69	CMA1	30	CYP11B2	46				
	IGF2R	89	EGFR	67			CYP21A2	46				
	RNPEP	89	GPER	62			CYP17A1	39				
	ANPEP	86	AGTR1	49			CYP11A1	37				
	DPP3	81	NR3C2	45			AGTR2	36				
	PREP	78					HSD11B2	30				
	MME	64					REN	27				
	NLN	59					CYP11B1	23				
	ACE	56					ACE2	22				
							AKR1C4	21				
							MAS1	20				
							AKR1D1	11				
Mouse normal aorta	Ctsd	98	Nr3c1	88	Prep	73	Hsd11b1	98			Agtr1a	
(1, 188, 4)	Ctsa	90	Igf2r	85	Cma1	61	Cyp11b2	23			Agtr1b	
	Rnpep	75	Atp6ap2	78	Cpa3	61	Ctsg	13			Cyp11b1	
	Dpp3	69	Enpep	69	Thop1	51	Cyp17a1	12			Lnpep	
	Ace	64	Nln	62	Ace2	31	Cyp11a1	8			Nr3c2	
	Agt	48	Mme	59	Hsd11b2	23	Akr1d1	2				
	Egfr	47			Klk1	23	Agtr2	1				
	Anpep	44					Mas1	1				

Mouse atheroma (1, 18, 4)	Ctsd	100	Atp6ap2	93	Hsd11b1	96	Agtr1b	36				
	Ctsa	97	Lnpep	92	Nln	74	Cyp11a1	36				
	Dpp3	89	Nr3c1	89	Agtr1a	71	Ctsg	15				
	Rnpep	85	Igf2r	87	Cyp11b1	43	Akr1d1	10				
	Ace	83	Enpep	84	Hsd11b2	41	Agtr2	9				
	Prep	80	Nr3c2	70	Cyp11b2	28	Mas1	3				
	Egfr	78	Mme	39	Agt	21						
	Cma1	76			Ace2	17						
	Thop1	71			Klk1	16						
	Cpa3	67			Cyp17a1	12						
	Anpep	44										
ApoE-deficient aorta (1, 9, 4)	Ctsd	100	Nr3c1	96	Ace	96	Igf2r	91				
	Atp6ap2	98	Lnpep	94	Hsd11b2	45	Egfr	86				
	Ctsa	97	Enpep	89	Thop1	36	Cyp11b2	44				
	Hsd11b1	92	Prep	79	Ctsg	20	Cyp11a1	34				
	Rnpep	79	Agtr1a	69	Akr1d1	15	Cyp11b1	34				
	Dpp3	77	Nr3c2	67	Mas1	4	Ace2	16				
	Anpep	71	Agtr1b	63			Agtr2	4				
	Cma1	71	Mme	44								
	Cpa3	71										
	Nln	64										
	Cyp17a1	16										
	Klk1	14										
	Agt	10										
Mouse normal aorta (GSE10000) (1, 9, 4)												
	Ctsd	99	Ctsa	94	Atp6ap2	96	Nr3c1	96				
	Ace	96	Lnpep	94	Enpep	91	Agtr1b	63				
	Hsd11b1	92	Prep	79	Igf2r	90	Anpep	56				
	Dpp3	76	Rnpep	75	Egfr	85	Cyp11b1	49				
	Cpa3	74	Mme	50	Agtr1a	71	Ctsg	14				
	Cma1	72	Cyp11a1	34	Hsd11b2	47						
	Nr3c2	71	Mas1	7	Agtr2	8						
	Nln	60			Cyp11b2	48						
	Cyp17a1	18			Thop1	31						
	Klk1	15			Ace2	28						
	Akr1d1	12										
	Agt	9										

Supplementary Table S5: Extracted promoters feature

Supplementary Table S5: Extracted promoters feature. TSC, transcription start cluster; bp, base pairs.

Gene	Genomic location	origin	TSC	Length (bp)	GC content
ACE	chr17: 61553922 - 61555393	swissregulon (hg19)	4	1471	72%
ACE2	chrX: 15619037 - 15620922	swissregulon (hg19)	0	1885	39%
AGTR1	hr3: 148415071 - 148416062	swissregulon (hg19)	1	991	55%
AGTR2	chrX: 115301419 - 115302515	swissregulon (hg19)	1	1096	33%
ANPEP	chr15: 90348503 - 90349103	swissregulon (hg19)	3	600	64%
ATP6AP2	chrX: 40439340 - 40440770	swissregulon (hg19)	3	1430	56%
CMA1	chr14: 24976606 - 24978063	swissregulon (hg19)	0	1457	47%
CPA3	chr3: 148595651 - 148596378	swissregulon (hg19)	0	727	35%
CPA3	chr3: 148582445 - 148583580	swissregulon (hg19)	0	1135	42%
CTSA	chr20: 44519091 - 44521700	swissregulon (hg19)	7	2609	62%
CTSD	chr11: 1784627 - 1785999	swissregulon (hg19)	7	1372	68.50%
CTSG	chr14: 25045045 - 25046070	swissregulon (hg19)	1	1025	46%
CYP11A1	chr15: 74659443 - 74660581	swissregulon (hg19)	1	1138	52%
CYP11A1	chr15: 74658138 - 74659053	swissregulon (hg19)	1	915	60%
CYP11B1	chr8: 143960828 - 143961762	swissregulon (hg19)	0	934	54%
CYP11B2	chr8: 143998916 - 143999759	swissregulon (hg19)	0	843	57%
CYP17A1	chr10: 104596660 - 104597820	swissregulon (hg19)	1	1160	53%
CYP21A2	chr6: 32005542 - 32006628	swissregulon (hg19)	0	1086	55%
DPP3	chr11: 66246984 - 66248360	swissregulon (hg19)	4	1376	63.50%
EGFR	chr7: 55212393 - 55212980	swissregulon (hg19)	1	587	56%
EGFR	chr7: 55086215 - 55087472	swissregulon (hg19)	3	1257	72%
GPER	chr7: 1125943 - 1126989	swissregulon (hg19)	1	1046	56%
HSD11B2	chr16: 67464055 - 67465454	swissregulon (hg19)	8	1399	71%
IGF2R	chr6: 160463689 - 160464276	swissregulon (hg19)	1	587	45%
IGF2R	chr6: 160389631 - 160390645	swissregulon (hg19)	18	1014	75%
KLK1	chr19: 51326617 - 51327543	swissregulon (hg19)	0	926	61%
KLK1	chr19: 51324005 - 51324605	swissregulon (hg19)	0	600	63%
LNPEP	chr5: 97011700 - 97012335	NCBI (GRCh38)	1	635	29%
LNPEP	chr5: 96293655 - 96294582	swissregulon (hg19)	1	927	41%
MAS1	chr6: 160327481 - 160328500	swissregulon (hg19)	0	1019	45%
MME	chr3: 154860913 - 154862242	swissregulon (hg19)	2	1329	34%
NLN	chr5: 65017219 - 65018665	swissregulon (hg19)	2	1446	65%
NR3C1	chr5: 142782323 - 142784741	swissregulon (hg19)	11	2418	68%
NR3C2	chr4: 149362850 - 149364154	swissregulon (hg19)	4	1304	60%
PREP	chr6: 105285468 - 105286099	swissregulon (hg19)	1	631	45%
PREP	chr6: 105850259 - 105851499	swissregulon (hg19)	8	1240	68%
REN	chr1: 204134950 - 204135783	swissregulon (hg19)	0	833	55%
RNPEP	chr1: 201951000 - 201952699	swissregulon (hg19)	6	1699	63%

Supplementary Table S6: ExtRAAS and TFs co-expression modules

Supplementary Table S6: ExtRAAS and TFs co-expression modules. Below each tissue the number of datasets, samples and clusters/modules are represented as (datasets, samples, clusters/modules). At the top of each module of human atheroma the average the coordination rate is expressed in percentage (average percentage of genes within a module that are always coordinated across the different datasets of a specific tissue). Next to each gene symbol the abundance of the mRNA is expressed in centile rank. Black = enzymes; blue = receptors; and red = transcription factors.

Tissues (datasets, samples)	Module 1		Module 2		Module 3		Module 4		Module 5		Module 6		Non-clustered genes	
Normal Human Vessels (1, 11, 3)	ATP6AP2	97	ELK1	88	IRF5	41	ZNF76	64	EGR1	93				
	CTSA	90	IRF6	75	MME	36	PREP	62	EGR3	88				
	NR3C1	90	SPIB	52	KLK1	34	ELK4	58	AGT	85				
	IGF2R	88	EGFR	50	SMAD1	33	DPP3	56	ELK3	53				
	SLC2A4RG	86	CPA3	49	AGTR2	29	HSD11B1	51	ETV5	50				
	CTCF	80	CTSG	49	CYP11B2	29	REN	34						
	ELF1	75	PAX9	42	MAX	20	THOP1	30						
	NR3C2	68	CYP21A2	31	MAS1	18	LNPEP	24						
	AGTR1	67	CYP17A1	23	CMA1	16								
	RNPEP	61	ETS1	16	ACE2	13								
	CTSD	57	CYP11B1	13	ANPEP	12								
	GPER	54			CYP11A1	11								
	ENPEP	2			FOXN1	10								
					ACE	7								
					AKR1C4	6								
					HSD11B2	6								
					AKR1D1	1								
Human Macroscopically Intact Tissue (MIT) (GSE 43292) (1, 32, 5)	CTSD	99	LNPEP	95	ATP6AP2	98	ELK1	70	EGR1	92				
	CTSA	96	NR3C1	93	ETS1	91	KLK1	50	ZNF76	64				
	ELF1	95	CTCF	88	MAX	73	GPER	49	SLC2A4RG	62				
	IGF2R	93	EGFR	75	AGT	67	SPIB	47	THOP1	57				
	RNPEP	86	ELK4	74	SMAD1	66	CYP11B1	44	EGR3	53				
	ETV5	80	NR3C2	67	CPA3	58	HSD11B2	43	CYP11B2	38				
	ELK3	78	AGTR1	50	PAX9	48	CYP21A2	37	AGTR2	10				
	PREP	72	IRF6	45	CTSG	34	FOXN1	33						
	ANPEP	69			ENPEP	33	CYP11A1	28						
	DPP3	67			HSD11B1	32	REN	24						
	NLN	63			ACE2	22	CYP17A1	20						
	IRF5	59			CMA1	19								
	ACE	46			AKR1D1	15								
	MME	46			AKR1C4	13								
					MAS1	9								
Human Atheroma (7, 876, 4)	91%		86%		89%		90%							
	CTSD	98	AGT	87.5	EGR1	82	ELK1	74					ZNF76	67
	CTSA	97	CTCF	83	ELK3	75	GPER	62						
	ATP6AP2	93	ETS1	83	CPA3	64	KLK1	56						
	ETV5	90	NR3C1	75	EGR3	64	THOP1	54						
	IGF2R	89	ELK4	69	CTSG	49	SLC2A4RG	53						
	MAX	89	LNPEP	69	CMA1	30	CYP11B2	46						
	RNPEP	89	EGFR	67			CYP21A2	46						
	ANPEP	86	SMAD1	66			CYP17A1	39						
	DPP3	81	IRF6	50			CYP11A1	37						
	ELF1	80	AGTR1	49			AGTR2	36						
	PREP	78	NR3C2	45			FOXN1	35						
	IRF5	75	PAX9	35			SPIB	32						
	HSD11B1	66	ENPEP	29			HSD11B2	30						
	MME	64					REN	27						
	NLN	59					CYP11B1	23						
	ACE	56					ACE2	22						
							AKR1C4	21						
							MAS1	20						
							AKR1D1	11						

Normal Human Kidney (4, 84, 6)	90%		79%		85%		86%		75%		83%					
	ACE2		AGTR1		CTSG		CPA3		AGTR2		CMA1		ACE			
	AGT		ATP6AP2		EGR3		ELF1		CYP11A1		CTCF		EGFR			
	ANPEP		NR3C1		ETV5		ELK4		CYP11B1		CYP11B2		AKR1C4			
	CTSA		NR3C2		IRF5		ETS1		EGR1		CYP21A2		IRF6			
	CYP17A1		PREP		SPIB		HSD11B1		FOXN1		ELK3		ELK1			
	DPP3		ZNF76				LNPEP		HSD11B2		IGF2R		CTSD			
	ENPEP						SMAD1				MAS1		GPER			
	KLK1										PAX9		AKR1D1			
	MME										THOP1		MAX			
	REN															
	RNPEP															
	SLC2A4RG															
Normal Human Omental Adipose (4, 86, 6)	92%		90%		92%		92%		92%		100%					
	ANPEP		LNPEP		ACE2		AGT		RNPEP		EGR1					
	ATP6AP2		ELK4		ZNF76		AKR1D1		THOP1		EGR3					
	CMA1		AGTR1		EGFR		CYP11B2		AKR1C4							
	CPA3		CTCF		ELK3		CYP17A1									
	CTSG		ETS1		PREP		HSD11B2									
	HSD11B1		IGF2R		ACE		KLK1									
	CTSA		MAX		GPER		SPIB									
	CTSD		ELF1		SLC2A4RG		AGTR2									
	DPP3		ENPEP		MME		CYP11B1									
	ETV5		NR3C1				FOXN1									
	CYP11A1		SMAD1				REN									
	PAX9		ELK1				CYP21A2									
			NR3C2				IRF6									
							IRF5									
							MAS1									
Mouse normal aorta (1, 188, 3)	Ctsd	98	Nr3c1	88	Hsd11b1	98							Agtr1a			
	Ctsa	90	Elk4	87	Igf2r	85							Agtr1b			
	Egr1	85	Atp6ap2	78	Enpep	69							Cyp11b1			
	Rnpep	75	Ets1	75	Nln	62							Lnpep			
	Dpp3	69	Prep	73	Cma1	61							Max			
	Ace	64	Smad1	72	Cpa3	61							Nr3c2			
	Elk3	63	Ctcf	69	Mme	59							Akr1C4			
	Spib	55	Elf1	52	Ace2	31							Cyp21A2			
	Thop1	51			Irf6	30							Gper			
	Agt	48			Cyp11b2	23							Ren			
	Egfr	47			Pax9	22							Slc2A4Rg			
	Anpep	44			Cyp11a1	8							Znf76			
	Elk1	42			Agtr2	1										
	Egr3	40														
	Irf5	39														
	Hsd11b2	23														
	Klk1	23														
	Etv5	15														
	Ctsg	13														
	Cyp17a1	12														
	Foxn1	12														
	Akr1d1	2														
	Mas1	1														

Mouse atheroma (1, 18, 4)	Ctsd	100	Atp6ap2	93	Hsd11b1	96							Akr1C4	
	Ctsa	97	Elk4	92	Nln	74							Cyp21A2	
	Egr1	96	Lnpep	92	Elf1	65							Gper	
	Dpp3	89	Smad1	92	Spib	57							Ren	
	Rnpep	85	Nr3c1	89	Cyp11b1	43							Slc2A4Rg	
	Ace	83	Ets1	88	Hsd11b2	41							Znf76	
	Elk3	82	Igf2r	87	Agtr1b	36								
	Prep	80	Enpep	84	Cyp11a1	36								
	Egfr	78	Ctcf	82	Pax9	31								
	Etv5	77	Agtr1a	71	Foxn1	26								
	Cma1	76	Nr3c2	70	Ace2	17								
	Thop1	71	Irf6	67	Klk1	16								
	Irf5	69	Mme	39	Ctsg	15								
	Max	69	Cyp11b2	28	Cyp17a1	12								
	Egr3	68			Akr1d1	10								
	Cpa3	67			Agtr2	9								
	Elk1	63			Mas1	3								
	Anpep	44												
	Agt	21												
Mouse normal aorta (GSE10000) (1, 9, 5)	Ctsd	99	Ctsa	94	Atp6ap2	96	Enpep	91	Nr3c1	96			Akr1C4	
	Egr1	99	Lnpep	94	Smad1	94	Igf2r	90	Anpep	56			Cyp21A2	
	Ace	96	Prep	79	Elk4	93	Agtr1a	71	Elf1	55			Gper	
	Ets1	92	Rnpep	75	Ctcf	89	Foxn1	48	Cyp11b1	49			Ren	
	Hsd11b1	92	Max	70	Egfr	85	Thop1	31	Ctsg	14			Slc2A4Rg	
	Elk3	86	Elk1	51	Agtr1b	63	Ace2	28					Znf76	
	Irf6	77	Mme	50	Hsd11b2	47	Agtr2	8						
	Dpp3	76	Cyp11a1	34	Cyp17a1	18								
	Cpa3	74	Pax9	29	Klk1	15								
	Cma1	72	Mas1	7	Akr1d1	12								
	Nr3c2	71												
	Egr3	68												
	Etv5	65												
	Nln	60												
	Irf5	57												
	Spib	52												
	Cyp11b2	48												
	Agt	9												
ApoE aorta (GSE10000) (1, 9, 4)	Ctsd	100	Nr3c1	96	Smad1	93	Egr1	99					Akr1C4	
	Atp6ap2	98	Lnpep	94	Igf2r	91	Ace	96					Cyp21A2	
	Ctsa	97	Elk4	93	Egfr	86	Ctcf	89					Gper	
	Ets1	93	Enpep	89	Foxn1	46	Rnpep	79					Ren	
	Hsd11b1	92	Prep	79	Ace2	16	Cpa3	71					Slc2A4Rg	
	Elk3	90	Irf6	76	Agtr2	4	Cyp11b2	44					Znf76	
	Dpp3	77	Agtr1a	69			Thop1	36						
	Egr3	74	Nr3c2	67			Cyp11a1	34						
	Max	72	Agtr1b	63			Cyp11b1	34						
	Anpep	71	Elf1	53										
	Cma1	71	Elk1	52										
	Etv5	71	Hsd11b2	45										
	Irf5	70	Mme	44										
	Nln	64	Ctsg	20										
	Spib	60	Akr1d1	15										
	Pax9	30	Mas1	4										
	Cyp17a1	16												
	Klk1	14												
	Agt	10												

Supplementary Atlas S1: ExtRAAS maps in all studied tissues

Supplementary Atlas S1: ExtRAAS maps in all studied tissues. For each tissue, the number of datasets, samples and modules are represented as (datasets, samples, modules) below the tissue name. Gene transcripts are represented by the corresponding official symbols. The genes are represented in the map based on their coordination (same color = same cluster) and mean expression centile rank (MCR, 4 levels, larger font size= higher expression level). Genes below the first tertile (MCR ≤ 33) in each tissue were omitted for simplicity. Non-clustered genes are colored in black. Angiotensin peptides and corticosteroid metabolites are represented in gray italics. Expression profiles of ExtRAAS genes in each tissue are represented using their MCR in a bar graph. Colors in the bar graphs represent coordinated genes.

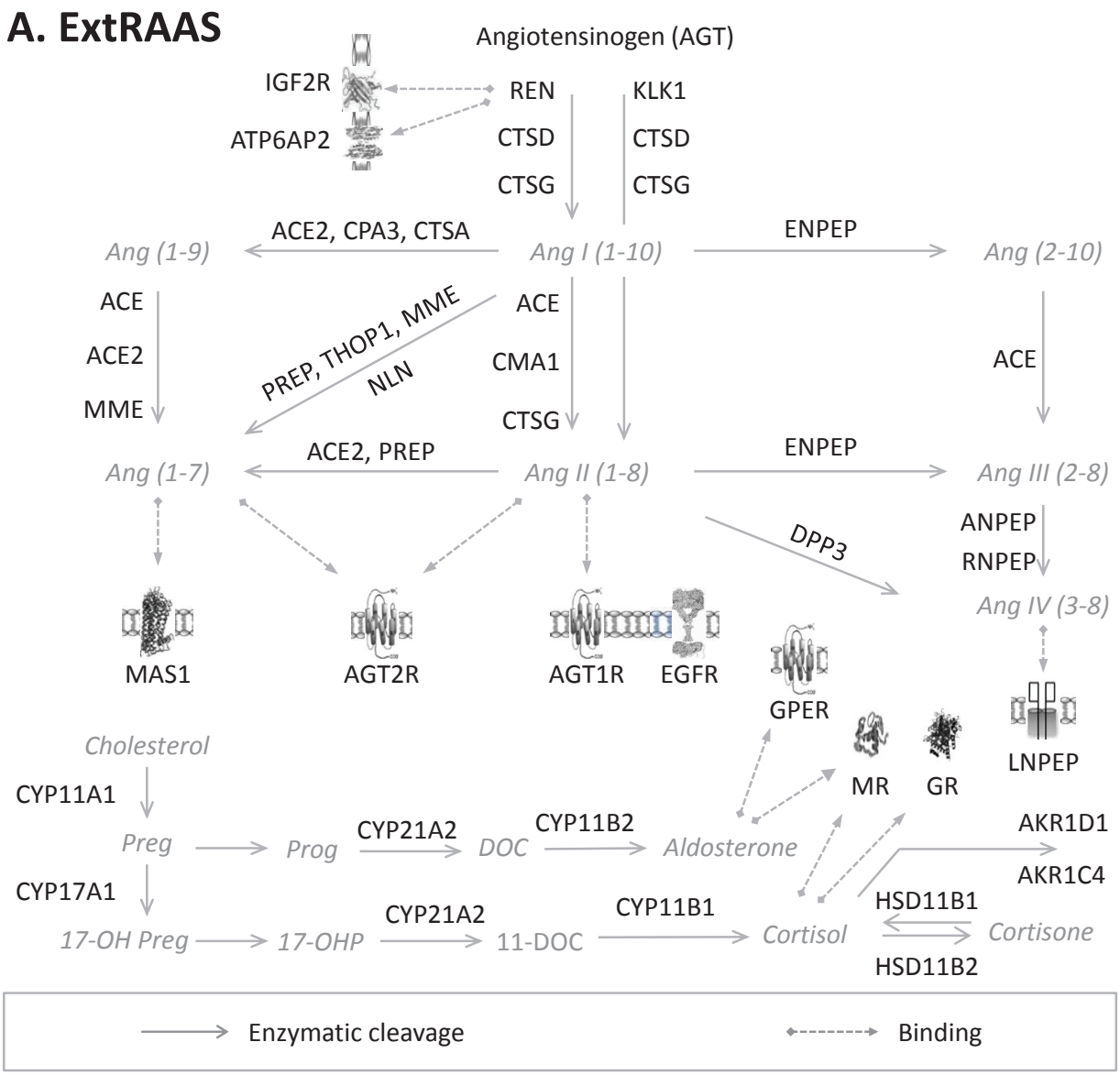

Figure font size

≤ 33 ➔ eleminated

34-40 ➔ 9

41-60 ➔ 11

61-80 ➔ 14

81-90 ➔ 18

91-100 ➔ 18

B. Normal human Vessels (1, 11, 3)

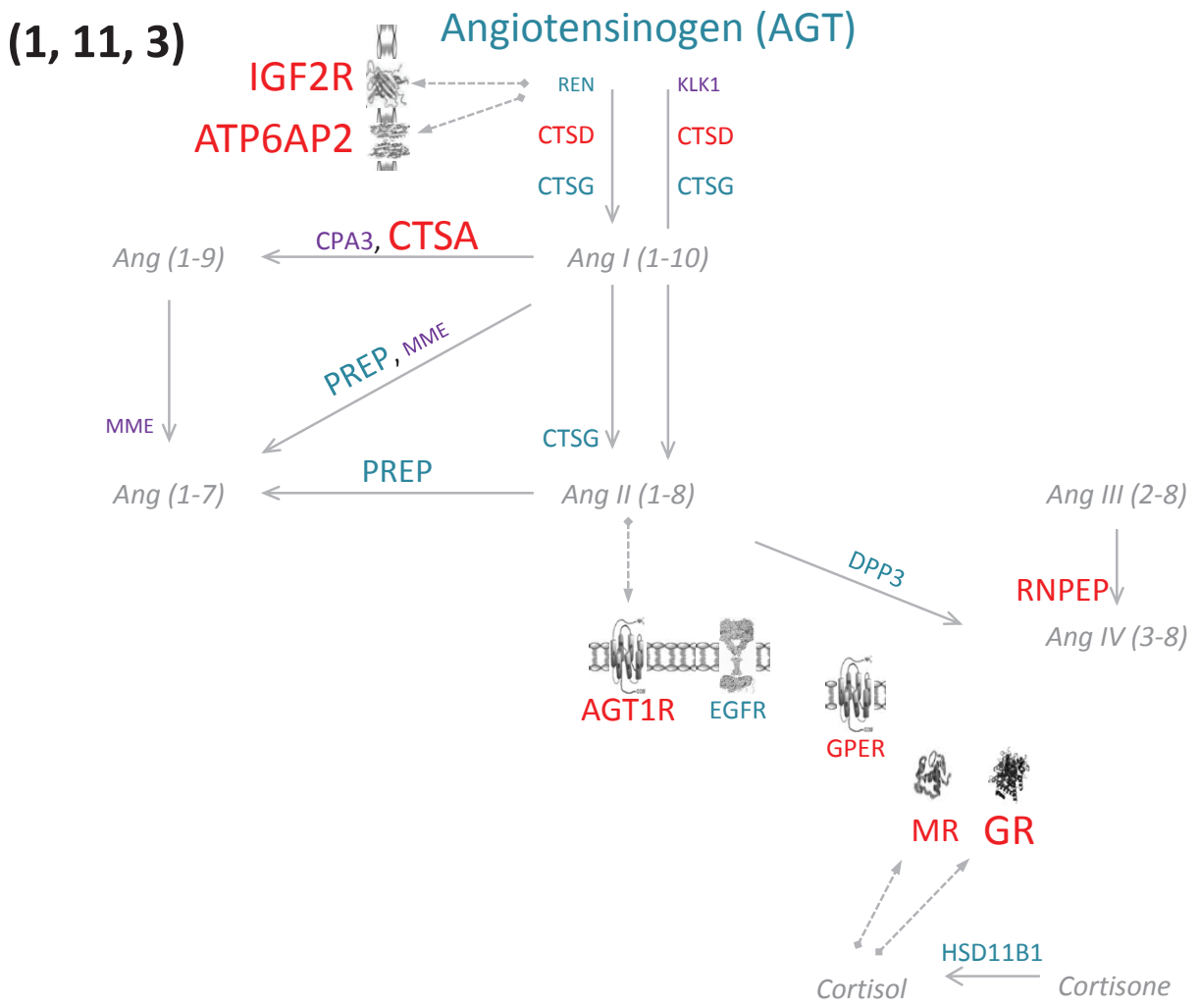

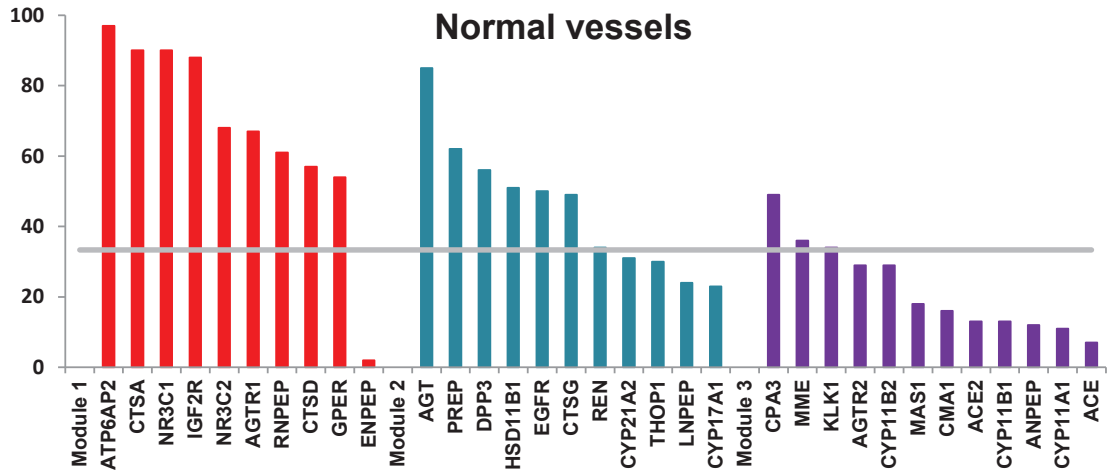

C. Human Atheroma (7, 876, 4)

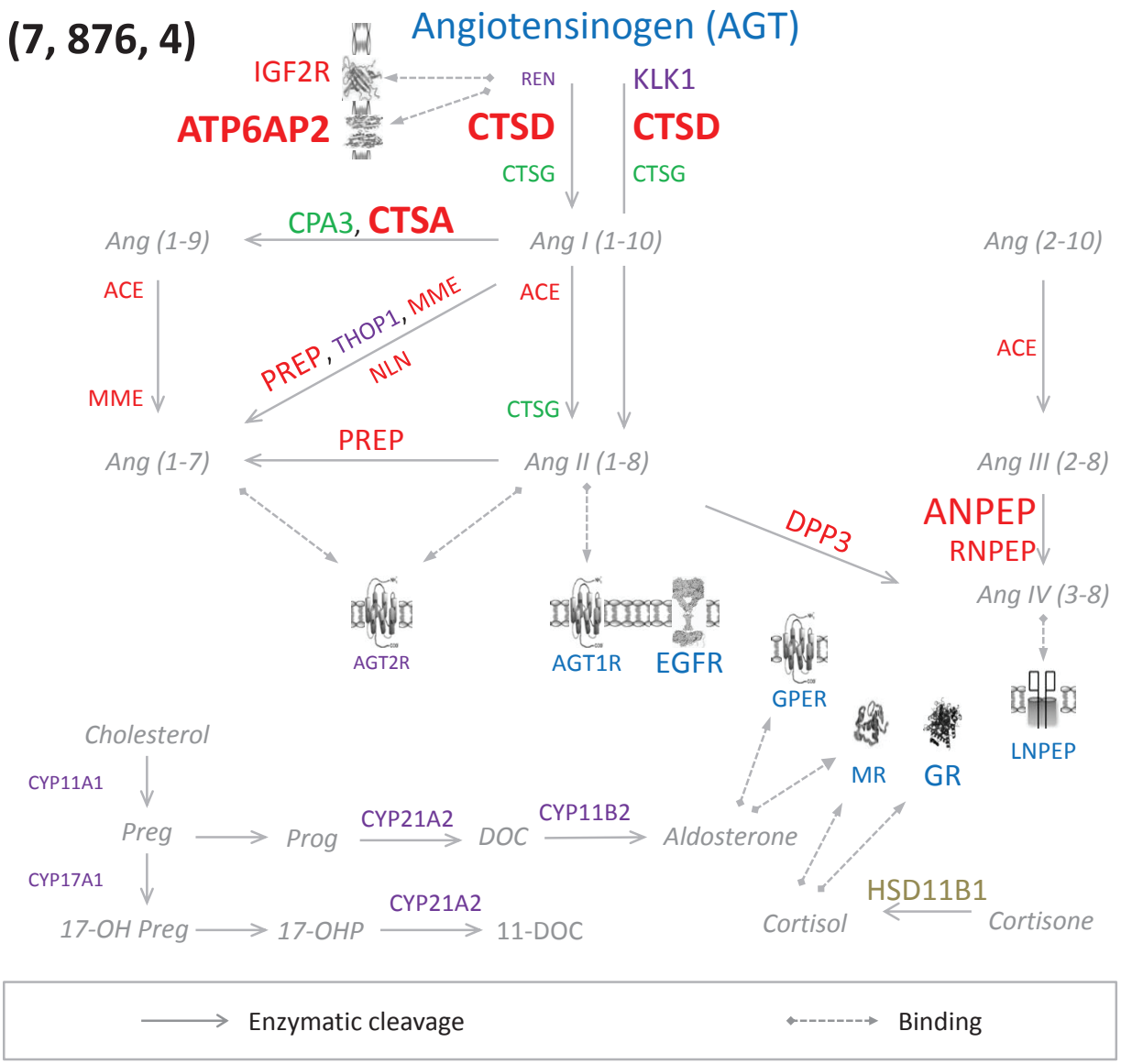

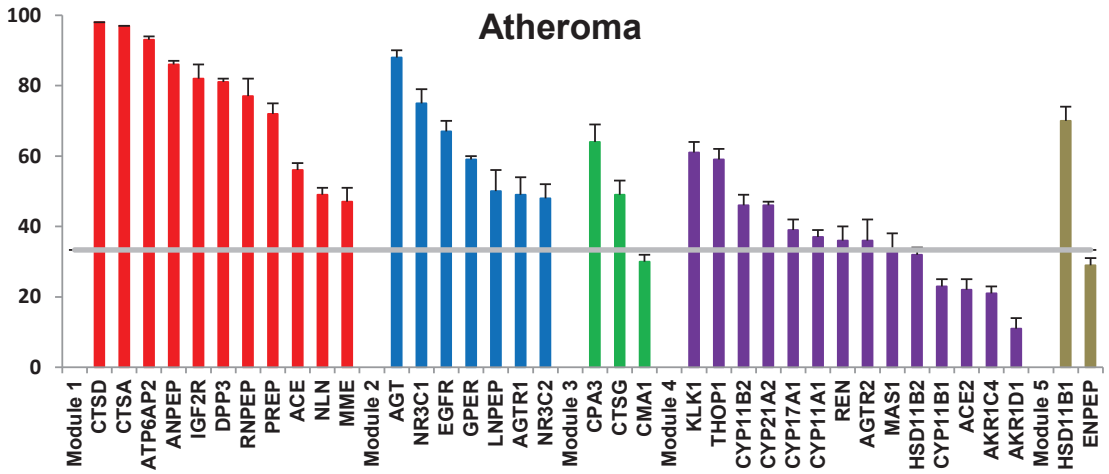

D. Mouse normal aortas (1, 188, 3)

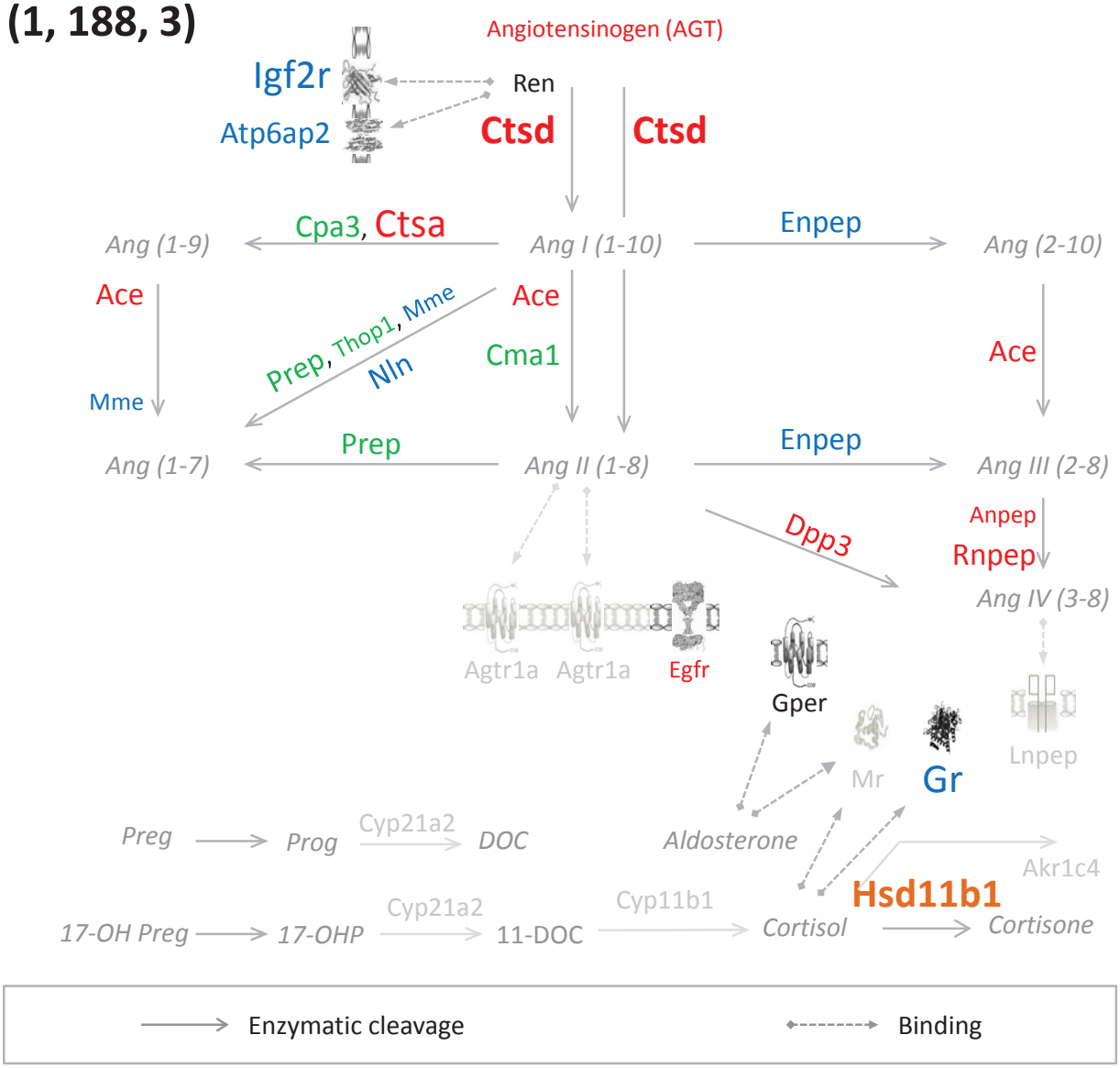

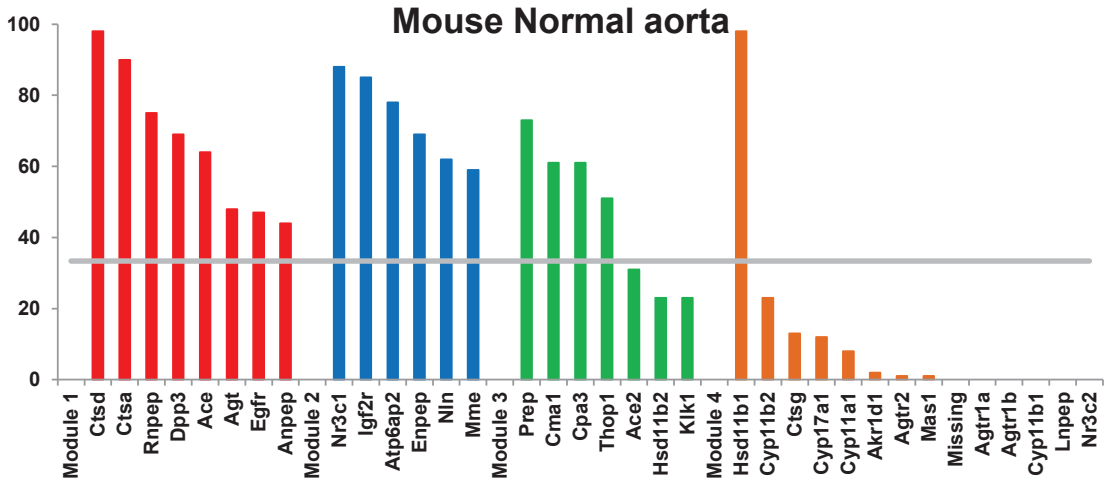

E. Mouse Atheroma (1, 18, 4)

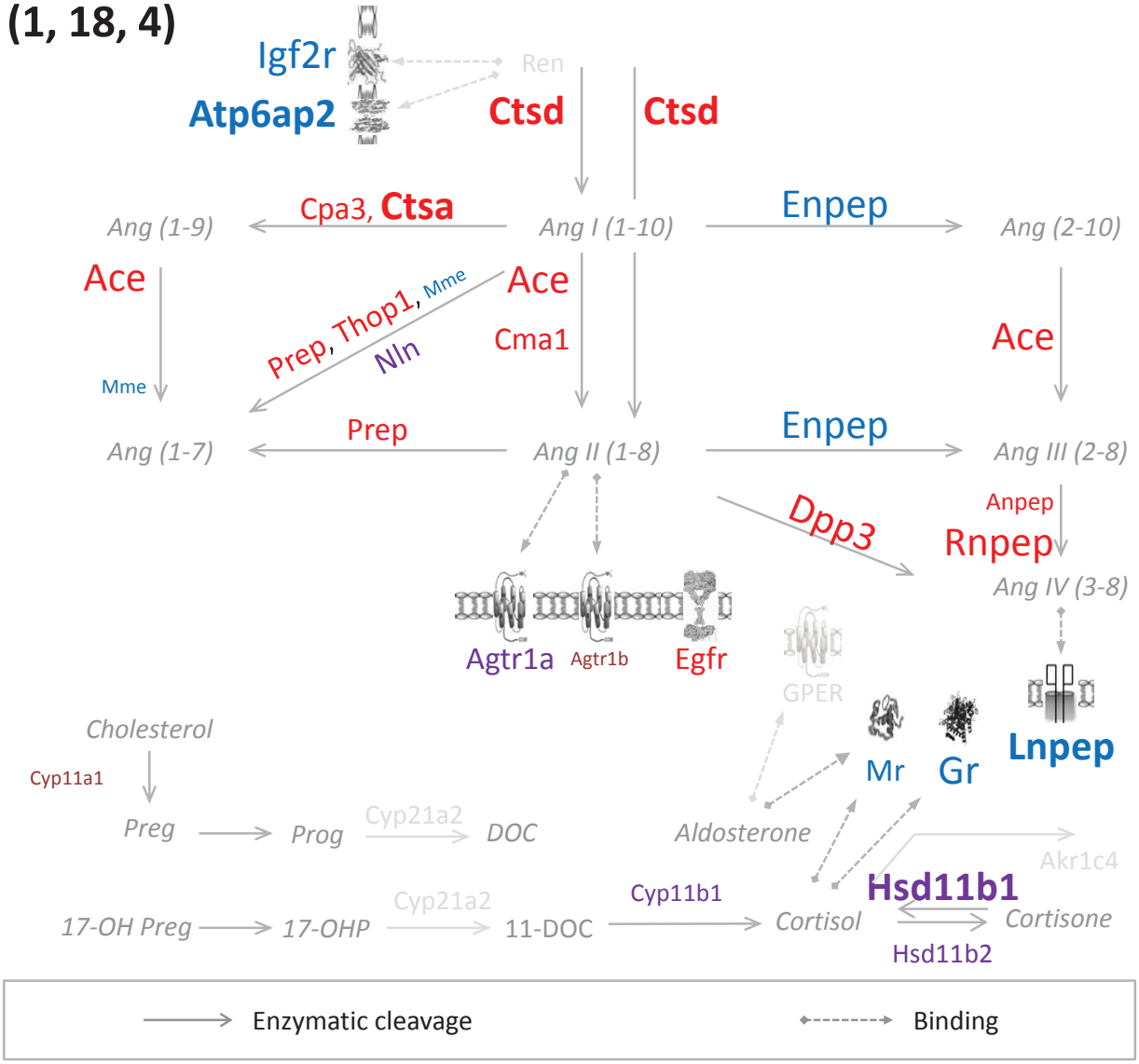

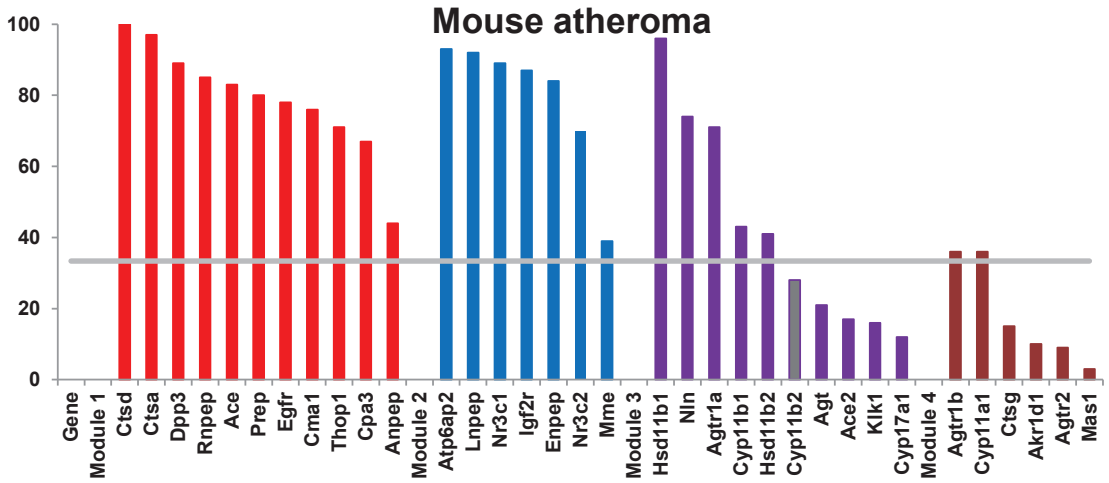

F. Mouse ApoE aorta (1, 9, 4)

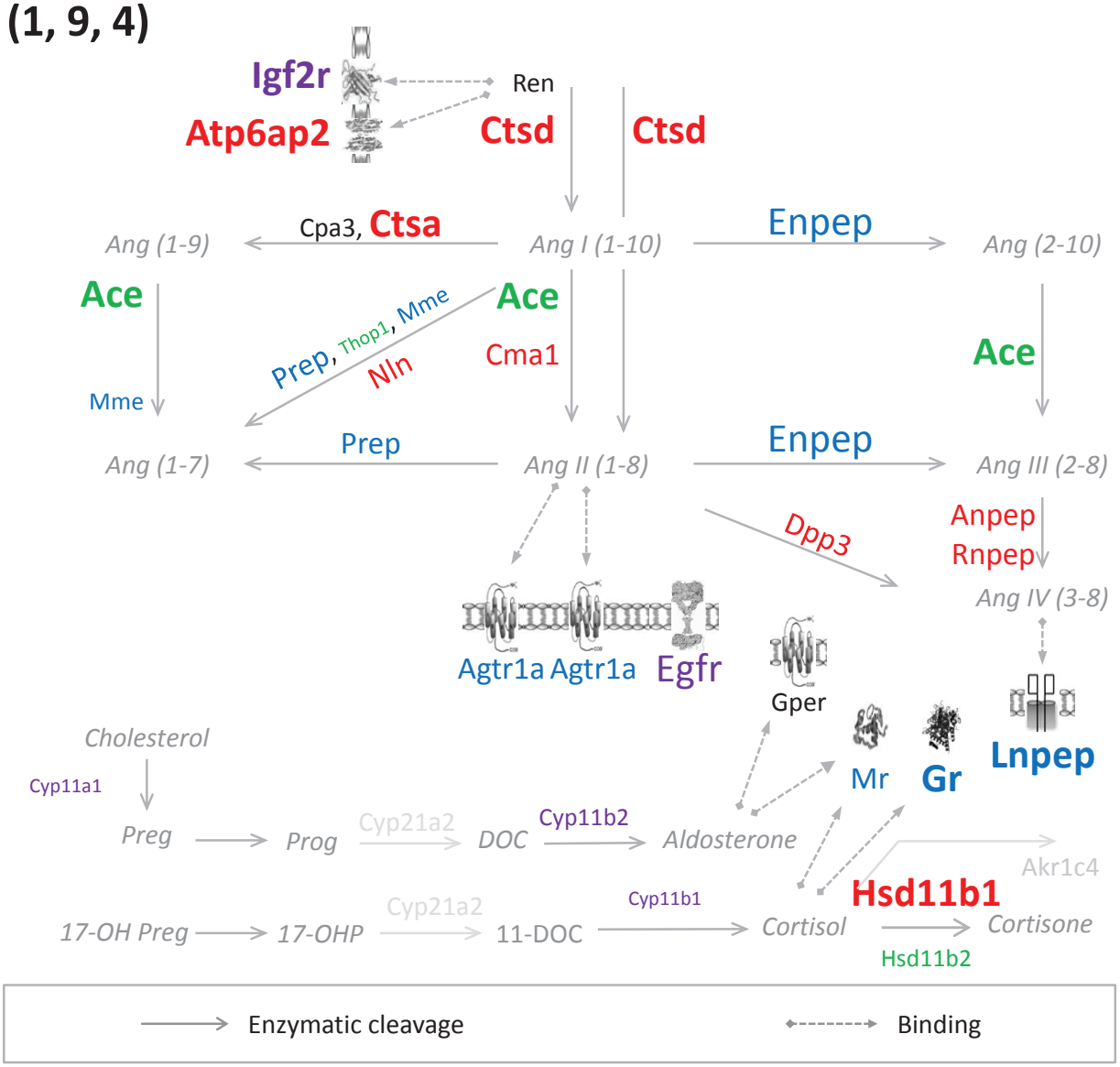

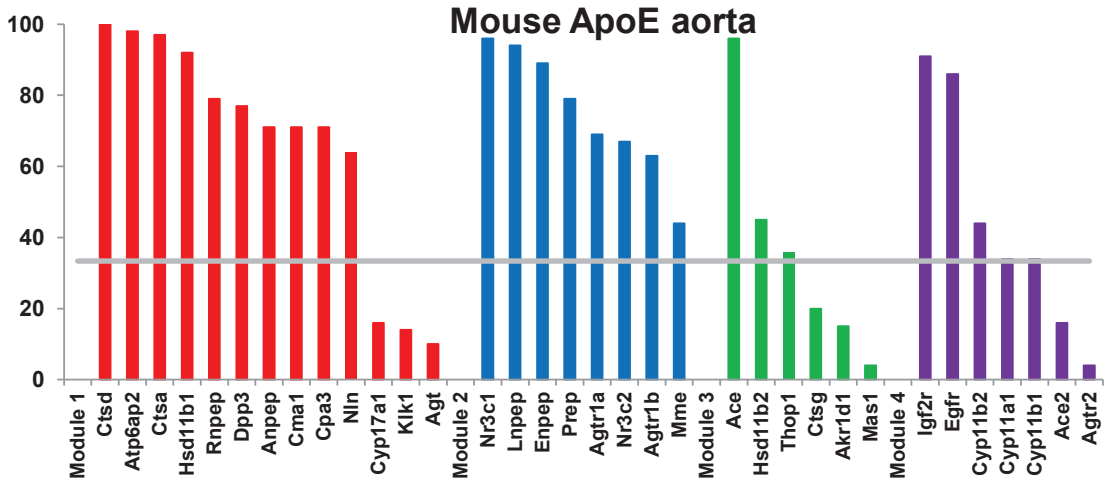

IV.2.9 Summary of scientific manuscript I

In this manuscript we established a model of extRAAS organization at the mRNA level in human atheroma. Using transcriptomic data obtained in our lab, we revealed the patterns of expression and coordination of extRAAS in human carotid atheroma. In atheroma, there is a general increase of coordinated angiotensin metabolizing enzyme-coding genes compared to nearby MIT, whereas at the same time, a decrease in highly coordinated receptor-coding genes, including AGTR1, MR and LNPEP. The similarity in the coordination patterns between atheroma lesions and MIT and its difference from that in normal vacscular tissue indicates that the system is altered during initial stages of atheroma development, which is[454] consistent with previously known roles of RAAS in atheroma initiation and progression. The patterns of extRAAS in atheroma lesions were validated in 5 other microarray datasets, including 807 carotid and peripheral atheroma samples. We further validated extRAAS organization in atheroma lesions of apoE-deficient mice, an animal models for the study of atherosclerosis *in vivo*. Indeed, the patterns of extRAAS were highly conserved in apoE-deficient mice atheroma lesions, but also similar to normal aortas from this animal model. Interestingly, they were different from the patterns of extRAAS in normal aortas of wild-type mice, which further supports that the patterns of extRAAS obtained in atheroma are related to atheroma initiation and development. After establishing the map of extRAAS in atheroma,we did further analysis in order to identify candidate TFs that could be involved in the regulation of the expression extRAASgenes in atheroma. By analyzing the promoters of extRAAS genes we identified 19 TFs that have common binding sites in the promoters of coordinated peptidases, and 2 TFs for the coordinated receptors ($p< 0.05$). By identifying the co-expression patterns we found that there are specific correlations between certain TFs and extRAAS co-expression modules, which were reproducible across human atheroma datasets and in mouse atherosclerotic aortas. However, these correlaions need further validation *in vitro* and *in vivo*using molecular biology techniques such as knocking down or overexpressing TFs and checking for the effects on extRAAS genes. The validation of these TFs may open the way for the development of new RAAS-targeting drugs that can modulate the global organization of extRAAS in atheroma.

IV.3 RNA SAMPLES FOR MICROARRAY HYBRIDIZATION

We started with 88 MIT samples obtained from 95 carotid samples obtained by carotid endarterectomy. Out of these 88 MIT, only 34 samples yielded VSMCSs. Each VSMCS sample was then splitted into 3 duplicates that were treated by the convenient differentiation medium: basal medium to retain contractile phenotype, ADM to obtain lipid-storing phenotype and ODM to obtain calcified phenotype. At the end of the differentiation protocol we obtained 21 contractile VSMCs samples, 20 with lipid storing phenotype and only 18 with the calcified phenotype. RNA was then extracted from each sample using TRIZOL reagent. After quality control (experimental approach for objective 2), only 41 samples met with the inclusion criteria. Table IV.1 shows the list of RNA samples with quality and quantity suitable for microarray analysis.

Table IV.1: list of RNA samples suitable for a future microarray analysis.

# patients	Phenotypes/patient	# samples
9	Control, Adipocytic and Osteoblastic	27
2	Control and Adipocytic	4
2	Control and Osteoblastic	4
1	Adipocytic and Osteoblastic	2
3	Control	3
0	Adipocytic	0
1	Osteoblastic	1
18	Total	41

IV.4 PHENOTYPIC VALIDATION OF VSMCS

The Shift from contractile to the other phenotypes can be seen on microscope. In the case of lipid storing phenotype there is a change in the shape of VSMCs from spindle shaped to a more rounded shape with extensions and the accumulation of lipid droplets in the cytoplasm. However, in the calcified phenotype cells become dense and form accumulations. RT-qPCR measurements showed 1.5-fold decrease in a-SMA expression in lipid storing phenotype compared to control phenotype. On the contrary, neither FABP4, nor FAT4 showed significant change in their expression levels between the two phenotypes (data not shown). On the other hand, significant calcification and mineralization was detected in calcified VSMCs using AP

assay (figure IV.1A) and alizarin red staining (figure IV.1B), respectively. Negative results were obtained using both assays in control phenotype (figure IV.1).

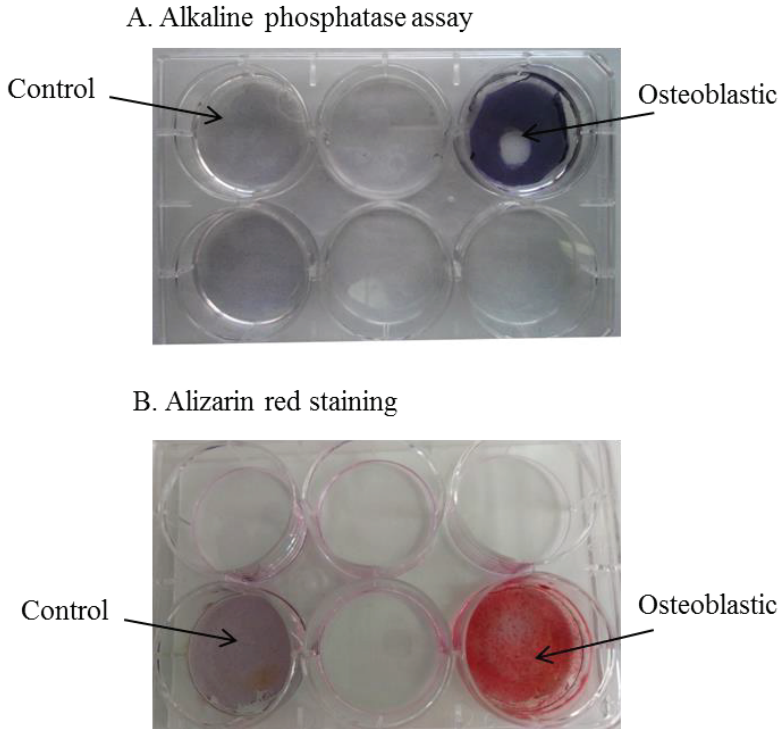

Figure IV.1: validation of VSMCs calcification and mineralization. Alkakline Phospahtase assay AP assay results in dark violet color in calcified VSMCs, whereas no staining in controls. On the other hand, alizarine satining result in red coloration of mineralized VSMCs, but faint blue color in control cells.

IV.5 FIRST SIRNA TRANSFECTION TRIAL

See Scientific manuscript I for the results concerning promoter analysis and relevant TFs identification. After identifying relevant TFs, their effects on target extRAAS genes should be validated (Figure 3.8). Inspired by the recent study showing an association between IRF5 expression and atherosclerotic lesions development[453] (Watkins AA et al. 2015), our first trial was on IRF5 knockdown.

As a first trial, IRF5 gene knockdown was done using two different combinations of siRNA concentration and transfection reagent volume. 5 nM and 10 nM of siRNA was transfected using 8µl and 12µl of transferrin, respectively. Control cells were transfected with scrambled random siRNA (CA) using the same conditions. RT-qPCR measurement was done for 18S, IRF5, GR,

MR, AGTR1, CTSA, ACE and MME 48 hours after transfection. The results of this trial are presented in Figure IV.1.

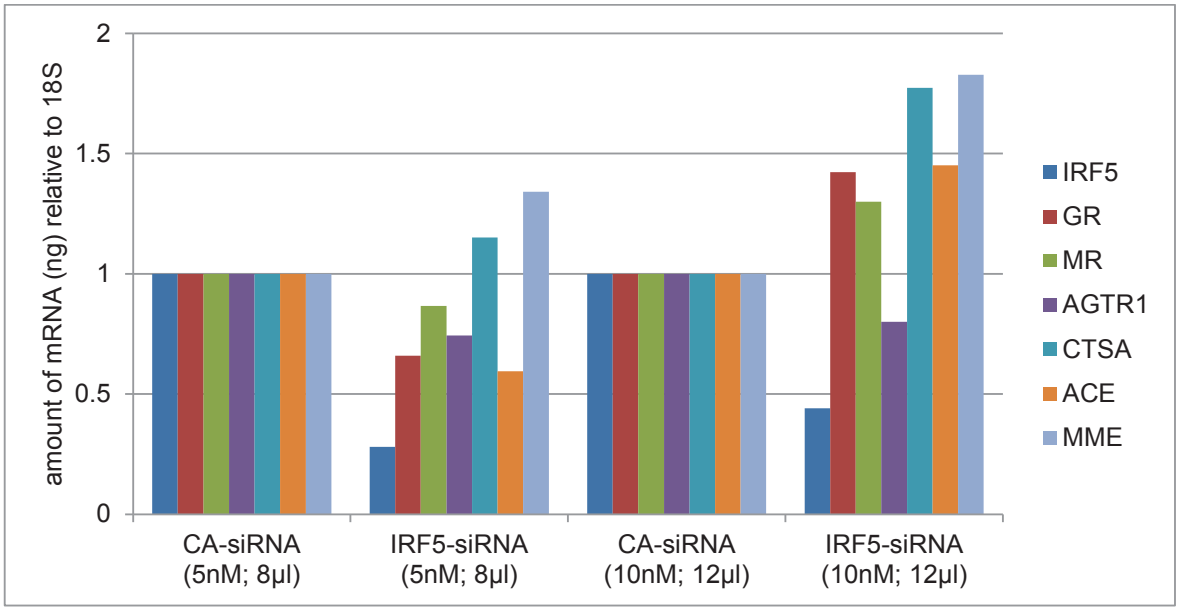

Figure IV.2: results of the first trial of IRF transfection. Transfection was done using 2 different combinations of siRNA concentration and transfection reagent volume (siRNA concentration, TRANSFERRin volume) using both control (CA) and IRF5 siRNA. 7 genes were measured after siRNA transfection.

IRF5 knockdown resulted in a 2-folds reduction in IRF5 transcript in both conditions, accompanied with a change in the expression of the other measured genes. However, the change in the measured extRAAS gave different results between the two conditions. CTSA and MME transcripts increased in both conditions; however, the fold change was greater for both transcripts in the 10nM IRF5-siRNA condition. In addition, there were certain contradictions between the results of the two conditions, which can be seen from the levels of MR, GR and AGTR1 transcripts. The levels of these genes decreased with 5 nM IRF5-siRNA transfection, whereas they increased decreased with 10 nM IRF5-siRNA transfection. This could be due to off target knockdown accompanied with the 10 nM transfected siRNA in the second condition. However, this is just a first trial and further validation and setting up should be done.

V. General Discussion

Most studies on tissue extRAAS focus on the local production of peptides in a specific tissue or the response to exogenous peptides treatment, with rare studies investigating both levels simultaneously. In both cases this will provide an inconclusive results on the actual effects of the system in a tissue as these results rely on a level that depends on the presence of the other one. For instance, the local production of a bioactive molecule in a tissue does not necessitate that this molecule will exert its effects in that tissue. Indeed, the favorable microenvironment should be available for a molecule to effectively exert its effects. This microenvironment could be characterized by the expression of the receptors of the molecule and the molecular pathways that can transduce the signal from the receptor to the final effectors, in addition to the absence of the antagonizing pathways that may inhibit the action of this molecule. In fact, this should be the basis for discussing the local effects of extRAAS at the tissue level. Indeed, all bioactive peptides and molecules of extRAAS rely on the presence their corresponding receptors as well as on the presence and levels of synergistic and antagonistic molecules to exert their effects in a specific tissue. Similarly, an expressed receptor cannot exert any effects without being bound and activated by its ligand. The issue is even more complex in extRAAS as each peptide or molecule may bind to different receptors and vice versa, thus leading to different, even opposite, effects. Moreover, seveal studies showed that certain effects induced by certain angiotensin peptides could be exerted by other downstream peptides. For example, the Ang-(1-7)-induced inhibitory effects on the energy-dependent solute transport in proximal tubules of the rat kidney were shown to be mediated by the metabolism of Ang-(1-7) into Ang (3-7), which binds to the AT4R, leading to a decrease in energy-dependent solute transport[468]. Such results may raise questions about the previously described “direct” effects of certain peptides. Therefore, studies investigating RAAS in a specific tissue should take into account the local expression and activity of both enzymes and receptors, which will provide a more clear view on the possible bioactive molecules produced locally in the tissue and their interaction with the corresponding receptors. Our lab has been studying extRAAS implication in atheroma during the last decade by measuring the expression of multiple extRAAS components. Based on our studies and on the literature we have joined the different pathways of extRAAS, with their component enzymes and receptors, into one system including classical and newly discovered enzymes and receptors. In this study, we aimed to identify the organization of extRAAS in the atherosclerotic lesion at the

mRNA level. To achieve this objective, we relied on transcriptomic data obtained in our lab, in addition to publicly available microarray datasets available on the GEO database.

V.1 EXTRAAS ORGANIZATION IN ATHEROMA

The presence of similar organization in MIT and advanced lesions, which was different from that in normal vascular tissue, indicates that the organization is established at early stages of atheroma and may be involved in lesion initiation and progression.

The extRAAS map in atheroma indicates that a highly expressed AGT could fuel the production of all angiotensin peptides by locally expressed angiotensin metabolizing enzymes. However, our results also suggest that only Ang-II and Ang-IV could exert their effects on their expressed receptors, whereas Ang-(1-7) despite its production may not be active due the very low expression levels of its receptor transcripts Mas1 and AGTR2. Despite the high levels of the corticosteroid receptors coding transcripts, their effects might be limited by the low production of their ligands, aldosterone and cortisol, as suggested by the very low levels of both aldosterone synthase (CYP11B2) and cortisol synthase (CYP11B1) transcripts. However, we can't exclude that aldosterone could be imported from the circulation, and at the same time it may exert its effects by binding to its receptor that is mainly present on epithelial cells facing the lumen of the vessel. On the same hand, it seems from the map that cortisol is mainly produced from cortisone by the action of 11b-HSD1. However, further investigations should be done in order to identify the source of cortisone in the vessel wall. Although there were modest correlations between the angiotensin and the corticosteroid system at the enzymatic level, there was strong correlation between both systems at the receptor levels. Thus, it seems that the signal generation in the two systems is regulated independently in atheroma, whereas they are tightly correlated at the signal response level, which will allow for a stronger synergy that will produce stronger effects as we have discussed in the introduction (See review manuscript I).

Despite the fact that mRNA expression does not provide any support for functional relevance of this organization, it may be an evidence for the local expression of the different components in the vessel wall and atheroma. Further support for these results at the protein and metabolic levels, will indicate if the system could be globally modulated at all levels by pharmacologically

targeting it at the transcriptional level. This will better allow targeting multiple pathways simultaneously by targeting their expression instead of using enzymatic or receptor inhibitors that target one enzyme or pathway, without affecting other alternative enzymes that can still support the production of the targeted peptide. An example of this issue is ACE inhibitors, which were shown to be not totally effective in certain cases where alternative Ang-II enzymes overcome its actions in inhibiting Ang-II generation[469].

V.2 TISSUE-SPECIFICITY OF EXTRAAS ORGANIZATION IN ATHEROMA

By comparing the organization of extRAAS obtained from atheroma and the other 23 normal human tissues, we can see that extRAAS possesses a tissue-specific organization that is characterized by a specific pattern expression and coordination. Expression pattern provide an indication on the locally favored extRAAS pathways in a specific tissue, whereas coordination pattern informs about the interaction of the different pathways and how the system is balanced at the tissue level. In addition, the correlations of the extracted TFs to extRAAS genes were also specific to atheroma when comparing it to that obtained from the kidney and adipose tissues. The importance of these findings in our study is that the tissue-specific organization of extRAAS in atheroma compared to other tissues indicates that atheroma possesses specific characteristics that could be manipulated in order to modulate the system's local organization in atheroma without affecting its organization in other normally functioning tissues. In addition, the reproducibility of this organization across multiple human datasets that include a total of more than 800 human atheroma samples from different arterial beds independent of inter-individual variability further support the role of correlation of this organization to atherosclerotic lesion processes. Thus, this will provide an easier way for future pharmacological approaches as it will not rely on personalized treatments. Moreover, the similarity of the organization between human and apoE-deficient mice atheroma suggest that we can use this animal model to further study the organization of this system in vivo. Since the organization of extRAAS in normal vascular tissue was obtained from only one dataset, the need for other datasets on normal vascular tissue is of importance to validate the reproducibility of the organization obtained and its difference from atheroma organization.

V.3 CANDIDATE TFs

We have extracted 21 candidate TFs that have enriched TFBSs in the "core" promoters of coordinated extRAAS genes. Interestingly, we found that these TFs were highly correlated to extRAAS organization at the mRNA level as was obtained by the analysis of transcriptomic data. Indeed, specific TFs were coordinated with co-expression modules in atheroma with reproducible results obtained from the 8 human atheroma datasets. The reproducibility of the correlations between TFs and extRAAS in mouse atheroma further support the role of these TFs in extRAAS regulation in atheroma. However, further support of these correlations need to be provided both in vitro and in vivo. This could be done through molecular biology techniques by modulating the levels of one or more TFs then checking for the effects on extRAAS genes expression. Indeed, we have started in setting up the knockdown experiments of IRF5 in primary VSMCs, which are major players in atheroma development and progression.

Interestingly, these TFs were found to be correlated to other genes than those which we extracted their TFBSs from. Thus, it seems that these TFs are regulating the expression of these genes by mechanisms not involving the promoter regions we have identified. TFs may act on a gene by binding to enhancer sequences outside the core promoter that could be several Kbs away from the TSS[470,471]. However, this may raise questions about other TFs that act from a distance that we couldn't extract from promoter sequences we analyzed. Thus further study of the correlation of extRAAS genes with all known TFs to check for other correlated ones should be done. Indeed, we recently established a new method that could extract external genes in the genome that are significantly correlated to multiple extRAAS genes in a microarray dataset based on their transcript levels. Thus we may use this method by doing targeted analysis on TF transcripts rather than analyzing the whole transcriptome. In addition, a TF may act indirectly on a gene through post-transcriptional mechanisms or by regulating other genes that have impact on the expression of coordinated extRAAS genes. Thus further investigations on the mechanisms by which these TFs may regulate extRAAS genes expression should be done.

V.4 RELEVANT TFs

From the extracted TFs we propose certain relevant TFs that could play a major role in extRAAS organization in atheroma and could be candidate for pharmacological studies. These relevant TFs

include those that are coordinated with modules 1, 2 and 3 of extRAAS co-expression modules in human atheroma, which we will call set1, set 2 and set 3 respectively. Set 1 includes the 3 TF-coding genes ELF1, ETV5, IRF5 and MAX. This set is interesting for two main reasons: (1) it is positively correlated to the largest module that includes 10 angiotensin peptidases that are involved in all angiotensin pathways, in addition to the two R/PR receptor-coding genes (ATP6AP2 and IGF2R), which are known to enhance renin activity in tissues[462]; and (2) it is negatively correlated to module 2, which comprises the major receptors of the system. Thus, by targeting this set of TFs we may alter gene expression of extRAAS in atheroma both at the signal generation and signal response levels. However, since it is oppositely correlated to the two modules, its modulation may exert no additional effects as the final change in the signal generation will be buffered by an opposite change in signal response. Since inhibition or downregulation is more likely achieved than stimulation or overexpression from the pharmacological point of view, set 2 of TFs seems to be a promising pharmacological target. Importantly, this set is positively correlated to the module of receptors in atheroma that contain AGTR1 and NR3C2 (MR-coding gene), which are known for their key role in enhancing atheroma development, in addition to EGFR and GPER. Thus, downregulation of these receptors may lead to a profound impact by "shutting down" the pro-atherogenic effects of locally produced peptides. In addition, downregulating this set of TFs may also drain the local source of the peptides by downregulating AGT expression, which is also correlated to this set of TFs. However, before moving forward in any pharmacological approach, we need to validate the impact of these TFs and investigate their mechanisms of action on extRAAS genes. The third set (set 3) of TFs is interesting since it is correlated to 3 genes that are coordinated in 80% of the tissues we analyzed in this study[209]. Further studying this set will provide an explanation on the possible mechanisms by which TFs are correlated to non-TFBSs containing genes. Indeed, 3 TF-coding genes were coordinated with module 3 genes despite that we couldn't extract any enriched TFBSs in the promoter of these genes.

In summary, the one pathway investigation lead to the huge knowledge we have today about the impact of extRAAS on atherosclerosis development. However, these data should be now connected to the global organization of extRAAS in atheroma by using systems biology approaches. This will provide more elaborate information on how the organization of the system is altered in atherosclerotic lesions and thus a more clear view on the actual actions of the system

in the lesion *in vivo*. Therefore, this will allow for a more specific and efficient targeting of extRAAS in the disease by using the most efficient combination of therapeutics that target specific enzymes and receptors, which gets the system back into its normal balanced state (figure V.1). In addition, understanding by which the organization is altered and maintained in pathological states will provide the basis for the discovery of new therapeutics that may modulate the global organization rather than targeting one enzyme or pathway. The TFs that we have extracted in this study could provide a relevant pharmacological target for the modulation of multiple extRAAS genes in atheroma, which will provide a way to manipulate multiple extRAAS arms in order to obtain a more balanced response to the system in the vascular wall. Therefore, our results provide the basis for further elaborate studies on the global organization of extRAAS in atherosclerosis and other tissues.

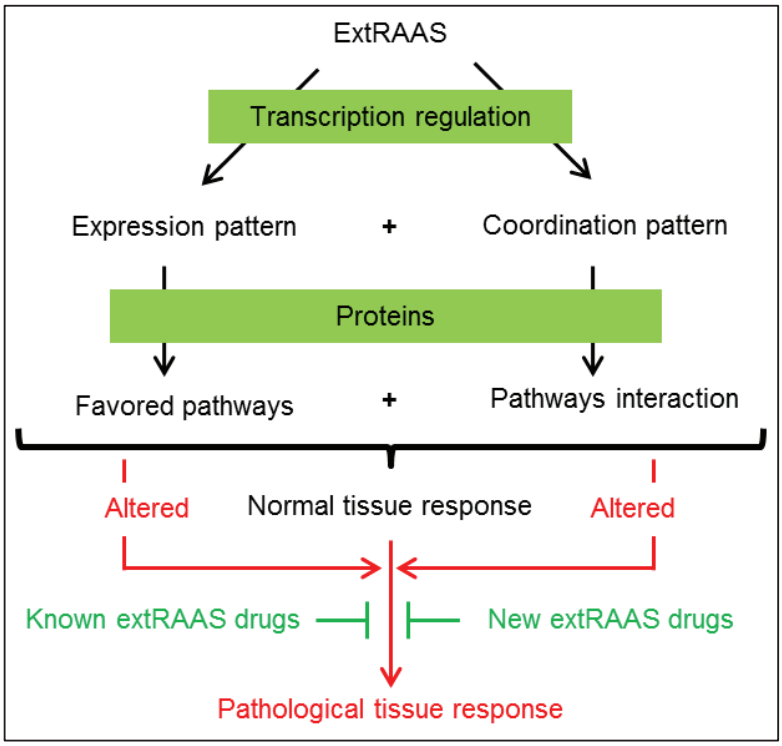

Figure V.1: conclusion and perspectives. ExtRAAS transcriptional regulation in a tissue leads to specific patterns of expression and coordination of extRAAS transcripts. These are then translated into proteins, which define the local favored pathways that will interact leading to final tissue response. An alteration in either transcriptional regulation or in the activity of translated proteins may lead to pathological tissue response. Understanding the mechanisms leading to this alteration may provide the opportunity for targeting the global organization of the system, thus getting it back to its normal balanced state.

VI. BIBLIOGRAPHY

1. Betts, J. G. *et al. Anatomy & physiology*. (2013). at <http://openstaxcollege.org/textbooks/anatomy-and-physiology>
2. Stary, H. C. *et al.* A definition of the intima of human arteries and of its atherosclerosis-prone regions. A report from the Committee on Vascular Lesions of the Council on Arteriosclerosis, American Heart Association. *Circulation* **85,** 391–405 (1992).
3. Dudley, A. C. Tumor Endothelial Cells. *Cold Spring Harb. Perspect. Med.* **2,** (2012).
4. Rudijanto, A. The role of vascular smooth muscle cells on the pathogenesis of atherosclerosis. *Acta Medica Indones.* **39,** 86–93 (2007).
5. Knipe, H. & D'Souza, D. Histology of blood vessels | Radiology Reference Article | Radiopaedia.org. *Radiopaedia* at <http://radiopaedia.org/articles/histology-of-blood-vessels>
6. Sumpio, B. E., Riley, J. T. & Dardik, A. Cells in focus: endothelial cell. *Int. J. Biochem. Cell Biol.* **34,** 1508–1512 (2002).
7. Yuan, S. Y. & Rigor, R. R. The Endothelial Barrier. (2010). at <http://www.ncbi.nlm.nih.gov.gate2.inist.fr/books/NBK54116/>
8. Cines, D. B. *et al.* Endothelial Cells in Physiology and in the Pathophysiology of Vascular Disorders. *Blood* **91,** 3527–3561 (1998).
9. Metz, R. P., Patterson, J. L. & Wilson, E. Vascular smooth muscle cells: isolation, culture, and characterization. *Methods Mol. Biol. Clifton NJ* **843,** 169–176 (2012).
10. Rensen, S. S. M., Doevendans, P. A. F. M. & van Eys, G. J. J. M. Regulation and characteristics of vascular smooth muscle cell phenotypic diversity. *Neth. Heart J.* **15,** 100–108 (2007).
11. Ponticos, M. & Smith, B. D. Extracellular matrix synthesis in vascular disease: hypertension, and atherosclerosis. *J. Biomed. Res.* **28,** 25–39 (2014).
12. Eble, J. A. & Niland, S. The extracellular matrix of blood vessels. *Curr. Pharm. Des.* **15,** 1385–1400 (2009).
13. Kelleher, C. M., McLean, S. E. & Mecham, R. P. Vascular extracellular matrix and aortic development. *Curr. Top. Dev. Biol.* **62,** 153–188 (2004).
14. Jacob, M. P. Extracellular matrix remodeling and matrix metalloproteinases in the vascular wall during aging and in pathological conditions. *Biomed. Pharmacother. Bioméd. Pharmacothérapie* **57,** 195–202 (2003).
15. *WHO_TRS_143.pdf*. 20 (1958). at <http://apps.who.int/iris/bitstream/10665/40402/1/WHO_TRS_143.pdf>
16. Atherosclerosis. at <http://www.heart.org/HEARTORG/Conditions/Cholesterol/WhyCholesterolMatters/Atherosclerosis_UCM_305564_Article.jsp>
17. Atherosclerosis - National Library of Medicine - PubMed Health. at <http://www.ncbi.nlm.nih.gov.gate2.inist.fr/pubmedhealth/PMH0062943/>
18. Stary, H. C. *et al.* A definition of advanced types of atherosclerotic lesions and a histological classification of atherosclerosis. A report from the Committee on Vascular

Lesions of the Council on Arteriosclerosis, American Heart Association. *Arterioscler. Thromb. Vasc. Biol.* **15,** 1512–1531 (1995).

19. Expert Dyslipidemia Panel of the International Atherosclerosis Society Panel members. An International Atherosclerosis Society Position Paper: global recommendations for the management of dyslipidemia--full report. *J. Clin. Lipidol.* **8,** 29–60 (2014).
20. Roger, V. L. *et al.* Executive summary: heart disease and stroke statistics--2012 update: a report from the American Heart Association. *Circulation* **125,** 188–197 (2012).
21. Vinereanu, D. Risk factors for atherosclerotic disease: present and future. *Herz* **31 Suppl 3,** 5–24 (2006).
22. WHO | The top 10 causes of death. *WHO* at <http://www.who.int/mediacentre/factsheets/fs310/en/index.html>
23. Fruchart, J.-C., Nierman, M. C., Stroes, E. S. G., Kastelein, J. J. P. & Duriez, P. New risk factors for atherosclerosis and patient risk assessment. *Circulation* **109,** III15–19 (2004).
24. Stary, H. C. *et al.* A definition of initial, fatty streak, and intermediate lesions of atherosclerosis. A report from the Committee on Vascular Lesions of the Council on Arteriosclerosis, American Heart Association. *Arterioscler. Thromb. J. Vasc. Biol. Am. Heart Assoc.* **14,** 840–856 (1994).
25. Whitman, S. C. A Practical Approach to Using Mice in Atherosclerosis Research. *Clin. Biochem. Rev.* **25,** 81–93 (2004).
26. Nakashima, Y., Wight, T. N. & Sueishi, K. Early atherosclerosis in humans: role of diffuse intimal thickening and extracellular matrix proteoglycans. *Cardiovasc. Res.* **79,** 14–23 (2008).
27. Witztum, J. L. The oxidation hypothesis of atherosclerosis. *Lancet Lond. Engl.* **344,** 793–795 (1994).
28. Steinberg, D. Thematic review series: the pathogenesis of atherosclerosis. An interpretive history of the cholesterol controversy: part I. *J. Lipid Res.* **45,** 1583–1593 (2004).
29. Libby, P., Ridker, P. M. & Maseri, A. Inflammation and Atherosclerosis. *Circulation* **105,** 1135–1143 (2002).
30. Williams, K. J. & Tabas, I. The response-to-retention hypothesis of early atherogenesis. *Arterioscler. Thromb. Vasc. Biol.* **15,** 551–561 (1995).
31. Nievelstein, P. F., Fogelman, A. M., Mottino, G. & Frank, J. S. Lipid accumulation in rabbit aortic intima 2 hours after bolus infusion of low density lipoprotein. A deep-etch and immunolocalization study of ultrarapidly frozen tissue. *Arterioscler. Thromb. J. Vasc. Biol. Am. Heart Assoc.* **11,** 1795–1805 (1991).
32. Schwenke, D. C. Selective increase in cholesterol at atherosclerosis-susceptible aortic sites after short-term cholesterol feeding. *Arterioscler. Thromb. Vasc. Biol.* **15,** 1928–1937 (1995).
33. Schwenke, D. C. & Carew, T. E. Initiation of atherosclerotic lesions in cholesterol-fed rabbits. II. Selective retention of LDL vs. selective increases in LDL permeability in susceptible sites of arteries. *Arterioscler. Dallas Tex* **9,** 908–918 (1989).

34. Schwenke, D. C. & Carew, T. E. Initiation of atherosclerotic lesions in cholesterol-fed rabbits. I. Focal increases in arterial LDL concentration precede development of fatty streak lesions. *Arterioscler. Dallas Tex* **9,** 895–907 (1989).
35. Napoli, C. *et al.* Fatty streak formation occurs in human fetal aortas and is greatly enhanced by maternal hypercholesterolemia. Intimal accumulation of low density lipoprotein and its oxidation precede monocyte recruitment into early atherosclerotic lesions. *J. Clin. Invest.* **100,** 2680–2690 (1997).
36. Nakashima, Y., Fujii, H., Sumiyoshi, S., Wight, T. N. & Sueishi, K. Early human atherosclerosis: accumulation of lipid and proteoglycans in intimal thickenings followed by macrophage infiltration. *Arterioscler. Thromb. Vasc. Biol.* **27,** 1159–1165 (2007).
37. Libby, P., Ridker, P. M. & Hansson, G. K. Inflammation in Atherosclerosis: From Pathophysiology to Practice. *J. Am. Coll. Cardiol.* **54,** 2129–2138 (2009).
38. Libby, P. Inflammation and cardiovascular disease mechanisms. *Am. J. Clin. Nutr.* **83,** 456S–460S (2006).
39. Sakakura, K. *et al.* Pathophysiology of atherosclerosis plaque progression. *Heart Lung Circ.* **22,** 399–411 (2013).
40. Chait, A. & Bornfeldt, K. E. Diabetes and atherosclerosis: is there a role for hyperglycemia? *J. Lipid Res.* **50,** S335–S339 (2009).
41. Steiner, G. Diabetes and atherosclerosis: an overview. *Diabetes* **30,** 1–7 (1981).
42. Ram, C. V. Hypertension and atherosclerosis. *Prim. Care* **18,** 559–575 (1991).
43. Parthasarathy, S., Quinn, M. T., Schwenke, D. C., Carew, T. E. & Steinberg, D. Oxidative modification of beta-very low density lipoprotein. Potential role in monocyte recruitment and foam cell formation. *Arterioscler. Dallas Tex* **9,** 398–404 (1989).
44. Simionescu, M. & Sima, A. V. in *Inflammation and Atherosclerosis* (eds. Wick, G. & Grundtman, C.) 19–37 (Springer Vienna, 2012). at <http://link.springer.com/chapter/10.1007/978-3-7091-0338-8_2>
45. Endres, M., Laufs, U., Merz, H. & Kaps, M. Focal expression of intercellular adhesion molecule-1 in the human carotid bifurcation. *Stroke J. Cereb. Circ.* **28,** 77–82 (1997).
46. Orekhov, A. N., Andreeva, E. R., Mikhailova, I. A. & Gordon, D. Cell proliferation in normal and atherosclerotic human aorta: proliferative splash in lipid-rich lesions. *Atherosclerosis* **139,** 41–48 (1998).
47. Hillebrands, J.-L., Klatter, F. A. & Rozing, J. Origin of vascular smooth muscle cells and the role of circulating stem cells in transplant arteriosclerosis. *Arterioscler. Thromb. Vasc. Biol.* **23,** 380–387 (2003).
48. Lacolley, P., Regnault, V., Nicoletti, A., Li, Z. & Michel, J.-B. The vascular smooth muscle cell in arterial pathology: a cell that can take on multiple roles. *Cardiovasc. Res.* **95,** 194–204 (2012).
49. Nakashima, Y., Chen, Y.-X., Kinukawa, N. & Sueishi, K. Distributions of diffuse intimal thickening in human arteries: preferential expression in atherosclerosis-prone arteries from an early age. *Virchows Arch. Int. J. Pathol.* **441,** 279–288 (2002).

50. Rajendran, P. *et al.* The Vascular Endothelium and Human Diseases. *Int. J. Biol. Sci.* **9,** 1057–1069 (2013).
51. Ribeiro-Oliveira, A. *et al.* The renin–angiotensin system and diabetes: An update. *Vasc. Health Risk Manag.* **4,** 787–803 (2008).
52. Reynolds, M. M. & Annich, G. M. The artificial endothelium. *Organogenesis* **7,** 42–49 (2011).
53. van Hinsbergh, V. W. M. Endothelium—role in regulation of coagulation and inflammation. *Semin. Immunopathol.* **34,** 93–106 (2012).
54. Simionescu, M. Implications of early structural-functional changes in the endothelium for vascular disease. *Arterioscler. Thromb. Vasc. Biol.* **27,** 266–274 (2007).
55. He, P. Leucocyte/endothelium interactions and microvessel permeability: coupled or uncoupled? *Cardiovasc. Res.* **87,** 281–290 (2010).
56. Davì, G. & Patrono, C. Platelet activation and atherothrombosis. *N. Engl. J. Med.* **357,** 2482–2494 (2007).
57. Ross, R. Atherosclerosis is an inflammatory disease. *Am. Heart J.* **138,** S419–420 (1999).
58. Li, D. & Mehta, J. L. Antisense to LOX-1 inhibits oxidized LDL-mediated upregulation of monocyte chemoattractant protein-1 and monocyte adhesion to human coronary artery endothelial cells. *Circulation* **101,** 2889–2895 (2000).
59. Cushing, S. D. *et al.* Minimally modified low density lipoprotein induces monocyte chemotactic protein 1 in human endothelial cells and smooth muscle cells. *Proc. Natl. Acad. Sci. U. S. A.* **87,** 5134–5138 (1990).
60. Kita, T. *et al.* Role of oxidized LDL in atherosclerosis. *Ann. N. Y. Acad. Sci.* **947,** 199–205; discussion 205–206 (2001).
61. Quinn, M. T., Parthasarathy, S., Fong, L. G. & Steinberg, D. Oxidatively modified low density lipoproteins: a potential role in recruitment and retention of monocyte/macrophages during atherogenesis. *Proc. Natl. Acad. Sci. U. S. A.* **84,** 2995–2998 (1987).
62. Autio, I., Jaakkola, O., Solakivi, T. & Nikkari, T. Oxidized low-density lipoprotein is chemotactic for arterial smooth muscle cells in culture. *FEBS Lett.* **277,** 247–249 (1990).
63. McMurray, H. F., Parthasarathy, S. & Steinberg, D. Oxidatively modified low density lipoprotein is a chemoattractant for human T lymphocytes. *J. Clin. Invest.* **92,** 1004–1008 (1993).
64. Weis, M., Schlichting, C. L., Engleman, E. G. & Cooke, J. P. Endothelial determinants of dendritic cell adhesion and migration: new implications for vascular diseases. *Arterioscler. Thromb. Vasc. Biol.* **22,** 1817–1823 (2002).
65. Marshall, D. & Haskard, D. O. Clinical overview of leukocyte adhesion and migration: where are we now? *Semin. Immunol.* **14,** 133–140 (2002).
66. Davies, P. F. Spatial hemodynamics, the endothelium, and focal atherogenesis: a cell cycle link? *Circ. Res.* **86,** 114–116 (2000).

67. Boisvert, W. A., Santiago, R., Curtiss, L. K. & Terkeltaub, R. A. A leukocyte homologue of the IL-8 receptor CXCR-2 mediates the accumulation of macrophages in atherosclerotic lesions of LDL receptor-deficient mice. *J. Clin. Invest.* **101,** 353–363 (1998).
68. Haley, K. J. *et al.* Overexpression of eotaxin and the CCR3 receptor in human atherosclerosis: using genomic technology to identify a potential novel pathway of vascular inflammation. *Circulation* **102,** 2185–2189 (2000).
69. Collins, R. G. *et al.* P-Selectin or intercellular adhesion molecule (ICAM)-1 deficiency substantially protects against atherosclerosis in apolipoprotein E-deficient mice. *J. Exp. Med.* **191,** 189–194 (2000).
70. Johnson, J. L. & Newby, A. C. Macrophage heterogeneity in atherosclerotic plaques. *Curr. Opin. Lipidol.* **20,** 370–378 (2009).
71. Boyle, J. J. Macrophage activation in atherosclerosis: pathogenesis and pharmacology of plaque rupture. *Curr. Vasc. Pharmacol.* **3,** 63–68 (2005).
72. Fadini, G. P. & Ciciliot, S. Vascular smooth muscle cells and monocyte-macrophages accomplice in the accelerated atherosclerosis of insulin resistance states. *Cardiovasc. Res.* **103,** 194–195 (2014).
73. Mantovani, A., Sica, A. & Locati, M. Macrophage polarization comes of age. *Immunity* **23,** 344–346 (2005).
74. Morisaki, N. *et al.* Human macrophages modulate the phenotype of cultured rabbit aortic smooth muscle cells through secretion of platelet-derived growth factor. *Eur. J. Clin. Invest.* **22,** 461–468 (1992).
75. Zhu, Y., Hojo, Y., Ikeda, U., Takahashi, M. & Shimada, K. Interaction between monocytes and vascular smooth muscle cells enhances matrix metalloproteinase-1 production. *J. Cardiovasc. Pharmacol.* **36,** 152–161 (2000).
76. Boyle, J. J., Weissberg, P. L. & Bennett, M. R. Tumor necrosis factor-alpha promotes macrophage-induced vascular smooth muscle cell apoptosis by direct and autocrine mechanisms. *Arterioscler. Thromb. Vasc. Biol.* **23,** 1553–1558 (2003).
77. Al-Sadi, H. in *Current Basic and Pathological Approaches to the Function of Muscle Cells and Tissues - From Molecules to Humans* (ed. Sugi, H.) (InTech, 2012). at <http://www.intechopen.com/books/current-basic-and-pathological-approaches-to-the-function-of-muscle-cells-and-tissues-from-molecules-to-humans/vascular-smooth-muscle-cells-and-the-comparative-pathology-of-atherosclerosis>
78. Braun, M., Pietsch, P., Schrör, K., Baumann, G. & Felix, S. B. Cellular adhesion molecules on vascular smooth muscle cells. *Cardiovasc. Res.* **41,** 395–401 (1999).
79. Doran, A. C., Meller, N. & McNamara, C. A. The Role of Smooth Muscle Cells in the Initiation and Early Progression of Atherosclerosis. *Arterioscler. Thromb. Vasc. Biol.* **28,** 812–819 (2008).
80. Ley, K. & Huo, Y. VCAM-1 is critical in atherosclerosis. *J. Clin. Invest.* **107,** 1209–1210 (2001).

81. Chistiakov, D. A., Orekhov, A. N. & Bobryshev, Y. V. Vascular smooth muscle cell in atherosclerosis. *Acta Physiol. Oxf. Engl.* **214,** 33–50 (2015).
82. Hedin, U., Bottger, B. A., Luthman, J., Johansson, S. & Thyberg, J. A substrate of the cell-attachment sequence of fibronectin (Arg-Gly-Asp-Ser) is sufficient to promote transition of arterial smooth muscle cells from a contractile to a synthetic phenotype. *Dev. Biol.* **133,** 489–501 (1989).
83. Thyberg, J. & Hultgårdh-Nilsson, A. Fibronectin and the basement membrane components laminin and collagen type IV influence the phenotypic properties of subcultured rat aortic smooth muscle cells differently. *Cell Tissue Res.* **276,** 263–271 (1994).
84. Corjay, M. H., Thompson, M. M., Lynch, K. R. & Owens, G. K. Differential effect of platelet-derived growth factor- versus serum-induced growth on smooth muscle alpha-actin and nonmuscle beta-actin mRNA expression in cultured rat aortic smooth muscle cells. *J. Biol. Chem.* **264,** 10501–10506 (1989).
85. Hautmann, M. B., Madsen, C. S. & Owens, G. K. A transforming growth factor beta (TGFbeta) control element drives TGFbeta-induced stimulation of smooth muscle alpha-actin gene expression in concert with two CArG elements. *J. Biol. Chem.* **272,** 10948–10956 (1997).
86. Li, X. *et al.* Suppression of smooth-muscle alpha-actin expression by platelet-derived growth factor in vascular smooth-muscle cells involves Ras and cytosolic phospholipase A2. *Biochem. J.* **327 (Pt 3),** 709–716 (1997).
87. Su, B. *et al.* Redox regulation of vascular smooth muscle cell differentiation. *Circ. Res.* **89,** 39–46 (2001).
88. Pidkovka, N. A. *et al.* Oxidized phospholipids induce phenotypic switching of vascular smooth muscle cells in vivo and in vitro. *Circ. Res.* **101,** 792–801 (2007).
89. Gomez, D. & Owens, G. K. Smooth muscle cell phenotypic switching in atherosclerosis. *Cardiovasc. Res.* **95,** 156–164 (2012).
90. Gittenberger-de Groot, A. C., DeRuiter, M. C., Bergwerff, M. & Poelmann, R. E. Smooth muscle cell origin and its relation to heterogeneity in development and disease. *Arterioscler. Thromb. Vasc. Biol.* **19,** 1589–1594 (1999).
91. Rong, J. X., Shapiro, M., Trogan, E. & Fisher, E. A. Transdifferentiation of mouse aortic smooth muscle cells to a macrophage-like state after cholesterol loading. *Proc. Natl. Acad. Sci. U. S. A.* **100,** 13531–13536 (2003).
92. Allahverdian, S., Chehroudi, A. C., McManus, B. M., Abraham, T. & Francis, G. A. Contribution of intimal smooth muscle cells to cholesterol accumulation and macrophage-like cells in human atherosclerosis. *Circulation* **129,** 1551–1559 (2014).
93. Sugiyama, S. *et al.* Characterization of smooth muscle-like cells in circulating human peripheral blood. *Atherosclerosis* **187,** 351–362 (2006).
94. Mooney, J. E. *et al.* Cellular plasticity of inflammatory myeloid cells in the peritoneal foreign body response. *Am. J. Pathol.* **176,** 369–380 (2010).

95. Iwata, H. *et al.* Bone marrow-derived cells contribute to vascular inflammation but do not differentiate into smooth muscle cell lineages. *Circulation* **122,** 2048–2057 (2010).
96. Bentzon, J. F., Sondergaard, C. S., Kassem, M. & Falk, E. Smooth muscle cells healing atherosclerotic plaque disruptions are of local, not blood, origin in apolipoprotein E knockout mice. *Circulation* **116,** 2053–2061 (2007).
97. Caplice, N. M. *et al.* Smooth muscle cells in human coronary atherosclerosis can originate from cells administered at marrow transplantation. *Proc. Natl. Acad. Sci. U. S. A.* **100,** 4754–4759 (2003).
98. Fuster, V., Topol, E. J. & Nabel, E. G. *Atherothrombosis and Coronary Artery Disease*. (Lippincott Williams & Wilkins, 2005).
99. Linton, M. F. & Fazio, S. Macrophages, inflammation, and atherosclerosis. *Int. J. Obes. Relat. Metab. Disord. J. Int. Assoc. Study Obes.* **27 Suppl 3,** S35–40 (2003).
100. Owens, G. K., Kumar, M. S. & Wamhoff, B. R. Molecular regulation of vascular smooth muscle cell differentiation in development and disease. *Physiol. Rev.* **84,** 767–801 (2004).
101. Campbell, J. H. & Campbell, G. R. The role of smooth muscle cells in atherosclerosis. *Curr. Opin. Lipidol.* **5,** 323–330 (1994).
102. Barry-Lane, P. A. *et al.* p47phox is required for atherosclerotic lesion progression in ApoE(-/-) mice. *J. Clin. Invest.* **108,** 1513–1522 (2001).
103. Zalba, G. *et al.* Vascular oxidant stress: molecular mechanisms and pathophysiological implications. *J. Physiol. Biochem.* **56,** 57–64 (2000).
104. Beckman, J. S., Beckman, T. W., Chen, J., Marshall, P. A. & Freeman, B. A. Apparent hydroxyl radical production by peroxynitrite: implications for endothelial injury from nitric oxide and superoxide. *Proc. Natl. Acad. Sci. U. S. A.* **87,** 1620–1624 (1990).
105. Packard, R. R. S., Lichtman, A. H. & Libby, P. Innate and adaptive immunity in atherosclerosis. *Semin. Immunopathol.* **31,** 5–22 (2009).
106. Stemme, S. *et al.* T lymphocytes from human atherosclerotic plaques recognize oxidized low density lipoprotein. *Proc. Natl. Acad. Sci. U. S. A.* **92,** 3893–3897 (1995).
107. Bobryshev, Y. V. Dendritic cells in atherosclerosis: current status of the problem and clinical relevance. *Eur. Heart J.* **26,** 1700–1704 (2005).
108. Paulson, K. E. *et al.* Resident intimal dendritic cells accumulate lipid and contribute to the initiation of atherosclerosis. *Circ. Res.* **106,** 383–390 (2010).
109. Baetta, R. & Corsini, A. Role of polymorphonuclear neutrophils in atherosclerosis: current state and future perspectives. *Atherosclerosis* **210,** 1–13 (2010).
110. Mehta, J. L., Rasouli, N., Sinha, A. K. & Molavi, B. Oxidative stress in diabetes: a mechanistic overview of its effects on atherogenesis and myocardial dysfunction. *Int. J. Biochem. Cell Biol.* **38,** 794–803 (2006).
111. Sun, Y. *et al.* Free cholesterol accumulation in macrophage membranes activates Toll-like receptors and p38 mitogen-activated protein kinase and induces cathepsin K. *Circ. Res.* **104,** 455–465 (2009).

112. Gui, T., Shimokado, A., Sun, Y., Akasaka, T. & Muragaki, Y. Diverse roles of macrophages in atherosclerosis: from inflammatory biology to biomarker discovery. *Mediators Inflamm.* **2012,** 693083 (2012).
113. Bickel, P. E. & Freeman, M. W. Rabbit aortic smooth muscle cells express inducible macrophage scavenger receptor messenger RNA that is absent from endothelial cells. *J. Clin. Invest.* **90,** 1450–1457 (1992).
114. Ruan, X. Z. *et al.* Mechanisms of dysregulation of low-density lipoprotein receptor expression in vascular smooth muscle cells by inflammatory cytokines. *Arterioscler. Thromb. Vasc. Biol.* **26,** 1150–1155 (2006).
115. Takahashi, M. *et al.* Interleukin-1beta attenuates beta-very low-density lipoprotein uptake and its receptor expression in vascular smooth muscle cells. *J. Mol. Cell. Cardiol.* **38,** 637–646 (2005).
116. Lim, H.-J. *et al.* PPARgamma activation induces CD36 expression and stimulates foam cell like changes in rVSMCs. *Prostaglandins Other Lipid Mediat.* **80,** 165–174 (2006).
117. Wågsäter, D., Olofsson, P. S., Norgren, L., Stenberg, B. & Sirsjö, A. The chemokine and scavenger receptor CXCL16/SR-PSOX is expressed in human vascular smooth muscle cells and is induced by interferon gamma. *Biochem. Biophys. Res. Commun.* **325,** 1187–1193 (2004).
118. Li, Q. & Yokoyama, S. Independent regulation of cholesterol incorporation into free apolipoprotein-mediated cellular lipid efflux in rat vascular smooth muscle cells. *J. Biol. Chem.* **270,** 26216–26223 (1995).
119. Pitas, R. E. Expression of the acetyl low density lipoprotein receptor by rabbit fibroblasts and smooth muscle cells. Up-regulation by phorbol esters. *J. Biol. Chem.* **265,** 12722–12727 (1990).
120. Sawamura, T. *et al.* An endothelial receptor for oxidized low-density lipoprotein. *Nature* **386,** 73–77 (1997).
121. Devries-Seimon, T. *et al.* Cholesterol-induced macrophage apoptosis requires ER stress pathways and engagement of the type A scavenger receptor. *J. Cell Biol.* **171,** 61–73 (2005).
122. Tabas, I. Macrophage death and defective inflammation resolution in atherosclerosis. *Nat. Rev. Immunol.* **10,** 36–46 (2010).
123. Moore, K. J. & Tabas, I. Macrophages in the pathogenesis of atherosclerosis. *Cell* **145,** 341–355 (2011).
124. Cai, Q., Lanting, L. & Natarajan, R. Interaction of monocytes with vascular smooth muscle cells regulates monocyte survival and differentiation through distinct pathways. *Arterioscler. Thromb. Vasc. Biol.* **24,** 2263–2270 (2004).
125. Chen, L. *et al.* Interaction of vascular smooth muscle cells and monocytes by soluble factors synergistically enhances IL-6 and MCP-1 production. *Am. J. Physiol. Heart Circ. Physiol.* **296,** H987–996 (2009).

126. Sternlicht, M. D. & Werb, Z. How matrix metalloproteinases regulate cell behavior. *Annu. Rev. Cell Dev. Biol.* **17,** 463–516 (2001).
127. Chait, A. & Wight, T. N. Interaction of native and modified low-density lipoproteins with extracellular matrix. *Curr. Opin. Lipidol.* **11,** 457–463 (2000).
128. Camejo, G., Hurt, E., Thubrikar, M. & Bondjers, G. Modification of low density lipoprotein association with the arterial intima. A possible environment for the antiatherogenic action of beta-blockers. *Circulation* **84,** VI17–22 (1991).
129. Kaplan, M. & Aviram, M. Retention of oxidized LDL by extracellular matrix proteoglycans leads to its uptake by macrophages: an alternative approach to study lipoproteins cellular uptake. *Arterioscler. Thromb. Vasc. Biol.* **21,** 386–393 (2001).
130. Kostner, G. [Recent pathophysiologic aspects of atherogenesis]. *Wien. Med. Wochenschr. 1946* **140,** 101–109 (1990).
131. Chang, M. Y., Potter-Perigo, S., Tsoi, C., Chait, A. & Wight, T. N. Oxidized low density lipoproteins regulate synthesis of monkey aortic smooth muscle cell proteoglycans that have enhanced native low density lipoprotein binding properties. *J. Biol. Chem.* **275,** 4766–4773 (2000).
132. Iverius, P. H. The interaction between human plasma lipoproteins and connective tissue glycosaminoglycans. *J. Biol. Chem.* **247,** 2607–2613 (1972).
133. Galis, Z. S. *et al.* Targeted disruption of the matrix metalloproteinase-9 gene impairs smooth muscle cell migration and geometrical arterial remodeling. *Circ. Res.* **91,** 852–859 (2002).
134. Moiseeva, E. P. Adhesion receptors of vascular smooth muscle cells and their functions. *Cardiovasc. Res.* **52,** 372–386 (2001).
135. Yin, B. L., Hao, H., Wang, Y. Y., Jiang, Y. J. & Xue, S. Downregulating osteopontin reduces angiotensin II-induced inflammatory activation in vascular smooth muscle cells. *Inflamm. Res. Off. J. Eur. Histamine Res. Soc. Al* **58,** 67–73 (2009).
136. Molossi, S., Clausell, N. & Rabinovitch, M. Reciprocal induction of tumor necrosis factor-alpha and interleukin-1 beta activity mediates fibronectin synthesis in coronary artery smooth muscle cells. *J. Cell. Physiol.* **163,** 19–29 (1995).
137. Koyama, H., Raines, E. W., Bornfeldt, K. E., Roberts, J. M. & Ross, R. Fibrillar collagen inhibits arterial smooth muscle proliferation through regulation of Cdk2 inhibitors. *Cell* **87,** 1069–1078 (1996).
138. Barnes, M. J. & Farndale, R. W. Collagens and atherosclerosis. *Exp. Gerontol.* **34,** 513–525 (1999).
139. Orr, A. W. *et al.* Molecular mechanisms of collagen isotype-specific modulation of smooth muscle cell phenotype. *Arterioscler. Thromb. Vasc. Biol.* **29,** 225–231 (2009).
140. Franco, C. *et al.* Doxycycline alters vascular smooth muscle cell adhesion, migration, and reorganization of fibrillar collagen matrices. *Am. J. Pathol.* **168,** 1697–1709 (2006).
141. Stary, H. C. Natural history of calcium deposits in atherosclerosis progression and regression. *Z. Für Kardiologie* **89 Suppl 2,** 28–35 (2000).

142. Bobryshev, Y. V. Transdifferentiation of smooth muscle cells into chondrocytes in atherosclerotic arteries in situ: implications for diffuse intimal calcification. *J. Pathol.* **205,** 641–650 (2005).
143. Fitzpatrick, L. A., Severson, A., Edwards, W. D. & Ingram, R. T. Diffuse calcification in human coronary arteries. Association of osteopontin with atherosclerosis. *J. Clin. Invest.* **94,** 1597–1604 (1994).
144. Nakano-Kurimoto, R. *et al.* Replicative senescence of vascular smooth muscle cells enhances the calcification through initiating the osteoblastic transition. *Am. J. Physiol. Heart Circ. Physiol.* **297,** H1673–1684 (2009).
145. Bear, M., Butcher, M. & Shaughnessy, S. G. Oxidized low-density lipoprotein acts synergistically with beta-glycerophosphate to induce osteoblast differentiation in primary cultures of vascular smooth muscle cells. *J. Cell. Biochem.* **105,** 185–193 (2008).
146. Byon, C. H. *et al.* Oxidative stress induces vascular calcification through modulation of the osteogenic transcription factor Runx2 by AKT signaling. *J. Biol. Chem.* **283,** 15319–15327 (2008).
147. Nakahara, R. *et al.* Fluorophotometric determination of hydrogen peroxide and other reactive oxygen species with fluorescein hydrazide (FH) and its crystal structure. *Chem. Pharm. Bull. (Tokyo)* **56,** 977–981 (2008).
148. Li, X., Yang, H.-Y. & Giachelli, C. M. BMP-2 promotes phosphate uptake, phenotypic modulation, and calcification of human vascular smooth muscle cells. *Atherosclerosis* **199,** 271–277 (2008).
149. Aikawa, E. *et al.* Osteogenesis associates with inflammation in early-stage atherosclerosis evaluated by molecular imaging in vivo. *Circulation* **116,** 2841–2850 (2007).
150. Newby, A. C., Libby, P. & van der Wal, A. C. Plaque instability--the real challenge for atherosclerosis research in the next decade? *Cardiovasc. Res.* **41,** 321–322 (1999).
151. Lee, R. T. & Libby, P. The Unstable Atheroma. *Arterioscler. Thromb. Vasc. Biol.* **17,** 1859–1867 (1997).
152. Boyle, J. J. Association of coronary plaque rupture and atherosclerotic inflammation. *J. Pathol.* **181,** 93–99 (1997).
153. Bennett, M. R. Apoptosis of vascular smooth muscle cells in vascular remodelling and atherosclerotic plaque rupture. *Cardiovasc. Res.* **41,** 361–368 (1999).
154. Clarke, M. C. H., Talib, S., Figg, N. L. & Bennett, M. R. Vascular smooth muscle cell apoptosis induces interleukin-1-directed inflammation: effects of hyperlipidemia-mediated inhibition of phagocytosis. *Circ. Res.* **106,** 363–372 (2010).
155. Clarke, M. C. H. *et al.* Chronic apoptosis of vascular smooth muscle cells accelerates atherosclerosis and promotes calcification and medial degeneration. *Circ. Res.* **102,** 1529–1538 (2008).
156. Geng, Y.-J. & Libby, P. Progression of atheroma: a struggle between death and procreation. *Arterioscler. Thromb. Vasc. Biol.* **22,** 1370–1380 (2002).

157. Clarke, M. & Bennett, M. The emerging role of vascular smooth muscle cell apoptosis in atherosclerosis and plaque stability. *Am. J. Nephrol.* **26,** 531–535 (2006).
158. Virmani, R. *et al.* Atherosclerotic plaque progression and vulnerability to rupture: angiogenesis as a source of intraplaque hemorrhage. *Arterioscler. Thromb. Vasc. Biol.* **25,** 2054–2061 (2005).
159. Vengrenyuk, Y., Cardoso, L. & Weinbaum, S. Micro-CT based analysis of a new paradigm for vulnerable plaque rupture: cellular microcalcifications in fibrous caps. *Mol. Cell. Biomech. MCB* **5,** 37–47 (2008).
160. Ku, D. N., Giddens, D. P., Zarins, C. K. & Glagov, S. Pulsatile flow and atherosclerosis in the human carotid bifurcation. Positive correlation between plaque location and low oscillating shear stress. *Arterioscler. Dallas Tex* **5,** 293–302 (1985).
161. Vaughan, D. E. Fibrinolytic balance, the renin-angiotensin system and atherosclerotic disease. *Eur. Heart J.* **19 Suppl G,** G9–12 (1998).
162. Atlas, S. A. The renin-angiotensin aldosterone system: pathophysiological role and pharmacologic inhibition. *J. Manag. Care Pharm. JMCP* **13,** 9–20 (2007).
163. Piepho, R. W. & Beal, J. An overview of antihypertensive therapy in the 20th century. *J. Clin. Pharmacol.* **40,** 967–977 (2000).
164. Reid, I. A., Morris, B. J. & Ganong, W. F. The renin-angiotensin system. *Annu. Rev. Physiol.* **40,** 377–410 (1978).
165. Dzau, V. J. & Herrmann, H. C. Hormonal control of angiotensinogen production. *Life Sci.* **30,** 577–584 (1982).
166. Hsueh, W. A. Potential effects of renin activation on the regulation of renin production. *Am. J. Physiol.* **247,** F205–212 (1984).
167. Skeggs, L. T., Kahn, J. R. & Shumway, N. P. The preparation and function of the hypertensin-converting enzyme. *J. Exp. Med.* **103,** 295–299 (1956).
168. Woodrow, D. Endothelial cells 3 volumes. Una S. Ryan, (Ed.). CRC Press. Inc: Florida U.S.A., Vol. 1, 191 pages; Vol. 2, 282 pages., Vol. 3, 251 pages, £296.50 (1988). *Cell Biochem. Funct.* **8,** 138–138 (1990).
169. Kohlstedt, K., Busse, R. & Fleming, I. Signaling via the angiotensin-converting enzyme enhances the expression of cyclooxygenase-2 in endothelial cells. *Hypertension* **45,** 126–132 (2005).
170. Gasparo, M. de, Catt, K. J., Inagami, T., Wright, J. W. & Unger, T. International Union of Pharmacology. XXIII. The Angiotensin II Receptors. *Pharmacol. Rev.* **52,** 415–472 (2000).
171. Murphy, T. J., Nakamura, Y., Takeuchi, K. & Alexander, R. W. A cloned angiotensin receptor isoform from the turkey adrenal gland is pharmacologically distinct from mammalian angiotensin receptors. *Mol. Pharmacol.* **44,** 1–7 (1993).
172. Kim, S. & Iwao, H. Molecular and Cellular Mechanisms of Angiotensin II-Mediated Cardiovascular and Renal Diseases. *Pharmacol. Rev.* **52,** 11–34 (2000).
173. Touyz, R. M. & Berry, C. Recent advances in angiotensin II signaling. *Braz. J. Med. Biol. Res.* **35,** 1001–1015 (2002).

174. Nouet, S. & Nahmias, C. Signal transduction from the angiotensin II AT2 receptor. *Trends Endocrinol. Metab. TEM* **11,** 1–6 (2000).
175. Jaffe, I. Z. & Mendelsohn, M. E. Angiotensin II and aldosterone regulate gene transcription via functional mineralocortocoid receptors in human coronary artery smooth muscle cells. *Circ. Res.* **96,** 643–650 (2005).
176. Bhargava, A., Wang, J. & Pearce, D. Regulation of epithelial ion transport by aldosterone through changes in gene expression. *Mol. Cell. Endocrinol.* **217,** 189–196 (2004).
177. Willenberg, H. S., Schinner, S. & Ansurudeen, I. New mechanisms to control aldosterone synthesis. *Horm. Metab. Res. Horm. Stoffwechselforschung Horm. Métabolisme* **40,** 435–441 (2008).
178. Verhovez, A. *et al.* Aldosterone does not modify gene expression in human endothelial cells. *Horm. Metab. Res. Horm. Stoffwechselforschung Horm. Métabolisme* **44,** 234–238 (2012).
179. Ferrario, C. M. *et al.* An evolving story of angiotensin-II-forming pathways in rodents and humans. *Clin. Sci. Lond. Engl. 1979* **126,** 461–469 (2014).
180. Gros, R., Ding, Q., Liu, B., Chorazyczewski, J. & Feldman, R. D. Aldosterone mediates its rapid effects in vascular endothelial cells through GPER activation. *Am. J. Physiol. Cell Physiol.* **304,** C532–540 (2013).
181. Naseem, R. H. *et al.* Plasma cathepsin D isoforms and their active metabolites increase after myocardial infarction and contribute to plasma renin activity. *Basic Res. Cardiol.* **100,** 139–146 (2005).
182. Batenburg, W. W. & Danser, A. H. J. (Pro)renin and its receptors: pathophysiological implications. *Clin. Sci. Lond. Engl. 1979* **123,** 121–133 (2012).
183. Ideishi, M., Sasaguri, M., Ikeda, M. & Arakawa, K. Angiotensin-converting activity of tissue kallikrein. *Nephron* **55 Suppl 1,** 62–64 (1990).
184. Okada, H. A Look at Transactivation of the EGF Receptor by Angiotensin II. *J. Am. Soc. Nephrol. JASN* **23,** 183–185 (2012).
185. Dhanda, S., Singh, J. & Singh, H. Hydrolysis of various bioactive peptides by goat brain dipeptidylpeptidase-III homologue. *Cell Biochem. Funct.* **26,** 339–345 (2008).
186. Carrera, M. P. *et al.* Renin-angiotensin system-regulating aminopeptidase activities are modified in the pineal gland of rats with breast cancer induced by N-methyl-nitrosourea. *Cancer Invest.* **24,** 149–153 (2006).
187. Li, X. C., Campbell, D. J., Ohishi, M., Yuan, S. & Zhuo, J. L. AT1 receptor-activated signaling mediates angiotensin IV-induced renal cortical vasoconstriction in rats. *Am. J. Physiol. Renal Physiol.* **290,** F1024–1033 (2006).
188. Montezano, A. C. *et al.* Aldosterone and Angiotensin II Synergistically Stimulate Migration in Vascular Smooth Muscle Cells Through c-Src-Regulated Redox-Sensitive RhoA Pathways. *Arterioscler. Thromb. Vasc. Biol.* **28,** 1511–1518 (2008).
189. Huang, B. S., Ahmadi, S., Ahmad, M., White, R. A. & Leenen, F. H. H. Central neuronal activation and pressor responses induced by circulating ANG II: role of the brain

aldosterone-‘ouabain’ pathway. *Am. J. Physiol. Heart Circ. Physiol.* **299,** H422–430 (2010).

190. Min, L.-J. *et al.* Aldosterone and Angiotensin II Synergistically Induce Mitogenic Response in Vascular Smooth Muscle Cells. *Circ. Res.* **97,** 434–442 (2005).
191. Lemarié, C. A. *et al.* Aldosterone-Induced Activation of Signaling Pathways Requires Activity of Angiotensin Type 1a Receptors. *Circ. Res.* **105,** 852–859 (2009).
192. Aguilera, G. & Catt, K. J. Regulation of aldosterone secretion during altered sodium intake. *J. Steroid Biochem.* **19,** 525–530 (1983).
193. Mulrow, P. J. Adrenal renin: a possible local regulator of aldosterone production. *Yale J. Biol. Med.* **62,** 503–510 (1989).
194. MacKenzie, S. M., Fraser, R., Connell, J. M. C. & Davies, E. Local renin-angiotensin systems and their interactions with extra-adrenal corticosteroid production. *J. Renin-Angiotensin-Aldosterone Syst. JRAAS* **3,** 214–221 (2002).
195. Schiffrin, E. L., Franks, D. J. & Gutkowska, J. Effect of aldosterone on vascular angiotensin II receptors in the rat. *Can. J. Physiol. Pharmacol.* **63,** 1522–1527 (1985).
196. Shelat, S. G., Flanagan-Cato, L. M. & Fluharty, S. J. Glucocorticoid and mineralocorticoid regulation of angiotensin II type 1 receptor binding and inositol triphosphate formation in WB cells. *J. Endocrinol.* **162,** 381–391 (1999).
197. Harada, E. *et al.* Aldosterone Induces Angiotensin-Converting-Enzyme Gene Expression in Cultured Neonatal Rat Cardiocytes. *Circulation* **104,** 137–139 (2001).
198. Ayari, H. *et al.* Auto-amplification of cortisol actions in human carotid atheroma is linked to arterial remodeling and stroke. *Fundam. Clin. Pharmacol.* **28,** 53–64 (2014).
199. Ganten, D. *et al.* Angiotensin-forming enzyme in brain tissue. *Science* **173,** 64–65 (1971).
200. Husain, A. *et al.* Evidence for the existence of a family of biologically active angiotensin I-like peptides in the dog central nervous system. *Circ. Res.* **52,** 460–464 (1983).
201. Nguyen, G. *et al.* Pivotal role of the renin/prorenin receptor in angiotensin II production and cellular responses to renin. *J. Clin. Invest.* **109,** 1417–1427 (2002).
202. Paul, M., Mehr, A. P. & Kreutz, R. Physiology of Local Renin-Angiotensin Systems. *Physiol. Rev.* **86,** 747–803 (2006).
203. Slight, S. H., Joseph, J., Ganjam, V. K. & Weber, K. T. Extra-adrenal mineralocorticoids and cardiovascular tissue. *J. Mol. Cell. Cardiol.* **31,** 1175–1184 (1999).
204. Harrison-Bernard, L. M. The renal renin-angiotensin system. *Adv. Physiol. Educ.* **33,** 270–274 (2009).
205. Lusis, A. J. Atherosclerosis. *Nature* **407,** 233–241 (2000).
206. Soufi, M., Sattler, A. M., Maisch, B. & Schaefer, J. R. Molecular mechanisms involved in atherosclerosis. *Herz* **27,** 637–648 (2002).
207. Bader, M. Tissue renin-angiotensin-aldosterone systems: Targets for pharmacological therapy. *Annu. Rev. Pharmacol. Toxicol.* **50,** 439–465 (2010).

208. Pacurari, M., Kafoury, R., Tchounwou, P. B. & Ndebele, K. The Renin-Angiotensin-aldosterone system in vascular inflammation and remodeling. *Int. J. Inflamm.* **2014,** 689360 (2014).
209. Nehme, A. *et al.* Atlas of tissue renin-angiotensin-aldosterone system in human: A transcriptomic meta-analysis. *Sci Rep* **5,** (2015).
210. Jia, E.-Z. *et al.* Renin-angiotensin-aldosterone system gene polymorphisms and coronary artery disease: detection of gene-gene and gene-environment interactions. *Cell. Physiol. Biochem. Int. J. Exp. Cell. Physiol. Biochem. Pharmacol.* **29,** 443–452 (2012).
211. Pávková Goldbergová, M. *et al.* Difference in angiotensinogen haplotype frequencies between chronic heart failure and advanced atherosclerosis patients - new prognostic factor? *Physiol. Res. Acad. Sci. Bohemoslov.* **60,** 55–64 (2011).
212. Niemiec, P., Zak, I. & Wita, K. The M235T polymorphism of the AGT gene modifies the risk of coronary artery disease associated with the presence of hypercholesterolemia. *Eur. J. Epidemiol.* **23,** 349–354 (2008).
213. Al-Najai, M. *et al.* Association of the angiotensinogen gene polymorphism with atherosclerosis and its risk traits in the Saudi population. *BMC Cardiovasc. Disord.* **13,** 17 (2013).
214. Tsai, C.-T. *et al.* Interaction of gender, hypertension, and the angiotensinogen gene haplotypes on the risk of coronary artery disease in a large angiographic cohort. *Atherosclerosis* **203,** 249–256 (2009).
215. van Rijn, M. J. E. *et al.* Polymorphisms of the renin-angiotensin system are associated with blood pressure, atherosclerosis and cerebral white matter pathology. *J. Neurol. Neurosurg. Psychiatry* **78,** 1083–1087 (2007).
216. Burdon, K. P. *et al.* Association analysis of genes in the renin-angiotensin system with subclinical cardiovascular disease in families with Type 2 diabetes mellitus: the Diabetes Heart Study. *Diabet. Med. J. Br. Diabet. Assoc.* **23,** 228–234 (2006).
217. Desjardins-Giasson, S., Gutkowska, J., Garcia, R. & Genest, J. Renin substrate in rat mesenteric artery. *Can. J. Physiol. Pharmacol.* **59,** 528–532 (1981).
218. Naftilan, A. J. *et al.* Localization and differential regulation of angiotensinogen mRNA expression in the vessel wall. *J. Clin. Invest.* **87,** 1300–1311 (1991).
219. Rakugi, H., Jacob, H. J., Krieger, J. E., Ingelfinger, J. R. & Pratt, R. E. Vascular injury induces angiotensinogen gene expression in the media and neointima. *Circulation* **87,** 283–290 (1993).
220. Hellmann, W. *et al.* Angiotensinogen gene expression in extrahepatic rat tissues: application of a solution hybridization assay. *Naunyn. Schmiedebergs Arch. Pharmacol.* **338,** 327–331 (1988).
221. Campbell, D. J. & Habener, J. F. Cellular localization of angiotensinogen gene expression in brown adipose tissue and mesentery: quantification of messenger ribonucleic acid abundance using hybridization in situ. *Endocrinology* **121,** 1616–1626 (1987).

222. Cassis, L. A., Lynch, K. R. & Peach, M. J. Localization of angiotensinogen messenger RNA in rat aorta. *Circ. Res.* **62,** 1259–1262 (1988).
223. Legedz, L. *et al.* Cathepsin G is associated with atheroma formation in human carotid artery. *J. Hypertens.* **22,** 157–166 (2004).
224. Bricca, G. *et al.* Local Angiotensin Pathways in Human Carotid Atheroma: Towards a Systems Biology Approach, Local Angiotensin Pathways in Human Carotid Atheroma: Towards a Systems Biology Approach. *Conf. Pap. Sci. Conf. Pap. Sci.* **2015, 2015,** e593086 (2015).
225. Hodroj, W. *et al.* Increased Insulin-Stimulated Expression of Arterial Angiotensinogen and Angiotensin Type 1 Receptor in Patients With Type 2 Diabetes Mellitus and Atheroma. *Arterioscler. Thromb. Vasc. Biol.* **27,** 525–531 (2007).
226. Ayari, H. *et al.* Mutual amplification of corticosteroids and angiotensin systems in human vascular smooth muscle cells and carotid atheroma. *J. Mol. Med. Berl. Ger.* (2014). doi:10.1007/s00109-014-1193-7
227. Lu, H., Rateri, D. L., Cassis, L. A. & Daugherty, A. The role of the renin-angiotensin system in aortic aneurysmal diseases. *Curr. Hypertens. Rep.* **10,** 99–106 (2008).
228. Re, R., Fallon, J. T., Dzau, V., Ouay, S. C. & Haber, E. Renin synthesis by canine aortic smooth muscle cells in culture. *Life Sci.* **30,** 99–106 (1982).
229. Iwai, N., Izumi, M., Inagami, T. & Kinoshita, M. Induction of renin in medial smooth muscle cells by balloon injury. *Hypertension* **29,** 1044–1050 (1997).
230. Lilly, L. S. *et al.* Renin expression by vascular endothelial cells in culture. *Circ. Res.* **57,** 312–318 (1985).
231. Campbell, D. J. & Valentijn, A. J. Identification of vascular renin-binding proteins by chemical cross-linking: inhibition of binding of renin by renin inhibitors. *J. Hypertens.* **12,** 879–890 (1994).
232. Danser, A. H. Local renin-angiotensin systems. *Mol. Cell. Biochem.* **157,** 211–216 (1996).
233. Liu, F. Y., Liu, X. Y., Zhang, L. J., Cheng, Y. P. & Jiang, Y. N. Binding of prorenin to (pro)renin receptor induces the proliferation of human umbilical artery smooth muscle cells via ROS generation and ERK1/2 activation. *J. Renin-Angiotensin-Aldosterone Syst. JRAAS* **15,** 99–108 (2014).
234. Brasier, A. R., Recinos, A. & Eledrisi, M. S. Vascular Inflammation and the Renin-Angiotensin System. *Arterioscler. Thromb. Vasc. Biol.* **22,** 1257–1266 (2002).
235. Kaschina, E. *et al.* Transition from atherosclerosis to aortic aneurysm in humans coincides with an increased expression of RAS components. *Atherosclerosis* **205,** 396–403 (2009).
236. Jessup, J. A. *et al.* Localization of the novel angiotensin peptide, angiotensin-(1-12), in heart and kidney of hypertensive and normotensive rats. *Am. J. Physiol. Heart Circ. Physiol.* **294,** H2614–2618 (2008).
237. Nagata, S. *et al.* Isolation and identification of proangiotensin-12, a possible component of the renin-angiotensin system. *Biochem. Biophys. Res. Commun.* **350,** 1026–1031 (2006).

238. Westwood, B. M. & Chappell, M. C. Divergent pathways for the angiotensin-(1-12) metabolism in the rat circulation and kidney. *Peptides* **35,** 190–195 (2012).
239. Moniwa, N. *et al.* Primacy of angiotensin converting enzyme in angiotensin-(1-12) metabolism. *Am. J. Physiol. Heart Circ. Physiol.* **305,** H644–650 (2013).
240. Prosser, H. C., Richards, A. M., Forster, M. E. & Pemberton, C. J. Regional vascular response to ProAngiotensin-12 (PA12) through the rat arterial system. *Peptides* **31,** 1540–1545 (2010).
241. Diet, F. *et al.* Increased accumulation of tissue ACE in human atherosclerotic coronary artery disease. *Circulation* **94,** 2756–2767 (1996).
242. Ruiz-Ortega, M. *et al.* Role of the renin-angiotensin system in vascular diseases: expanding the field. *Hypertension* **38,** 1382–1387 (2001).
243. Ruiz-Ortega, M., Lorenzo, O., Suzuki, Y., Rupérez, M. & Egido, J. Proinflammatory actions of angiotensins. *Curr. Opin. Nephrol. Hypertens.* **10,** 321–329 (2001).
244. Weiss, D., Sorescu, D. & Taylor, W. R. Angiotensin II and atherosclerosis. *Am. J. Cardiol.* **87,** 25C–32C (2001).
245. Daugherty, A., Manning, M. W. & Cassis, L. A. Angiotensin II promotes atherosclerotic lesions and aneurysms in apolipoprotein E-deficient mice. *J. Clin. Invest.* **105,** 1605–1612 (2000).
246. Griffin, S. A. *et al.* Angiotensin II causes vascular hypertrophy in part by a non-pressor mechanism. *Hypertension* **17,** 626–635 (1991).
247. Rajagopalan, S. *et al.* Angiotensin II-mediated hypertension in the rat increases vascular superoxide production via membrane NADH/NADPH oxidase activation. Contribution to alterations of vasomotor tone. *J. Clin. Invest.* **97,** 1916–1923 (1996).
248. Chua, C. C., Hamdy, R. C. & Chua, B. H. Upregulation of vascular endothelial growth factor by angiotensin II in rat heart endothelial cells. *Biochim. Biophys. Acta* **1401,** 187–194 (1998).
249. Dimmeler, S., Rippmann, V., Weiland, U., Haendeler, J. & Zeiher, A. M. Angiotensin II induces apoptosis of human endothelial cells. Protective effect of nitric oxide. *Circ. Res.* **81,** 970–976 (1997).
250. Alvarez, A. *et al.* Direct evidence of leukocyte adhesion in arterioles by angiotensin II. *Blood* **104,** 402–408 (2004).
251. Piqueras, L. *et al.* Angiotensin II induces leukocyte-endothelial cell interactions in vivo via AT(1) and AT(2) receptor-mediated P-selectin upregulation. *Circulation* **102,** 2118–2123 (2000).
252. Gräfe, M. *et al.* Angiotensin II-induced leukocyte adhesion on human coronary endothelial cells is mediated by E-selectin. *Circ. Res.* **81,** 804–811 (1997).
253. Tummala, P. E. *et al.* Angiotensin II induces vascular cell adhesion molecule-1 expression in rat vasculature: A potential link between the renin-angiotensin system and atherosclerosis. *Circulation* **100,** 1223–1229 (1999).

254. Pastore, L. *et al.* Angiotensin II stimulates intercellular adhesion molecule-1 (ICAM-1) expression by human vascular endothelial cells and increases soluble ICAM-1 release in vivo. *Circulation* **100,** 1646–1652 (1999).
255. Hernández-Presa, M. *et al.* Angiotensin-converting enzyme inhibition prevents arterial nuclear factor-kappa B activation, monocyte chemoattractant protein-1 expression, and macrophage infiltration in a rabbit model of early accelerated atherosclerosis. *Circulation* **95,** 1532–1541 (1997).
256. Griendling, K. K., Ushio-Fukai, M., Lassègue, B. & Alexander, R. W. Angiotensin II signaling in vascular smooth muscle. New concepts. *Hypertension* **29,** 366–373 (1997).
257. Kranzhöfer, R. *et al.* Angiotensin induces inflammatory activation of human vascular smooth muscle cells. *Arterioscler. Thromb. Vasc. Biol.* **19,** 1623–1629 (1999).
258. Geisterfer, A. A., Peach, M. J. & Owens, G. K. Angiotensin II induces hypertrophy, not hyperplasia, of cultured rat aortic smooth muscle cells. *Circ. Res.* **62,** 749–756 (1988).
259. Xi, X. P. *et al.* Central role of the MAPK pathway in ang II-mediated DNA synthesis and migration in rat vascular smooth muscle cells. *Arterioscler. Thromb. Vasc. Biol.* **19,** 73–82 (1999).
260. Ling, S. *et al.* Matrix-dependent gene expression of egr-1 and PDGF A regulate angiotensin II-induced proliferation in human vascular smooth muscle cells. *Hypertension* **34,** 1141–1146 (1999).
261. Cheng, J.-F. *et al.* Involvement of profilin-1 in angiotensin II-induced vascular smooth muscle cell proliferation. *Vascul. Pharmacol.* **55,** 34–41 (2011).
262. Pollman, M. J., Yamada, T., Horiuchi, M. & Gibbons, G. H. Vasoactive substances regulate vascular smooth muscle cell apoptosis. Countervailing influences of nitric oxide and angiotensin II. *Circ. Res.* **79,** 748–756 (1996).
263. Wolf, G. & Wenzel, U. O. Angiotensin II and cell cycle regulation. *Hypertension* **43,** 693–698 (2004).
264. Hayek, T., Attias, J., Smith, J., Breslow, J. L. & Keidar, S. Antiatherosclerotic and antioxidative effects of captopril in apolipoprotein E-deficient mice. *J. Cardiovasc. Pharmacol.* **31,** 540–544 (1998).
265. Keidar, S., Attias, J., Smith, J., Breslow, J. L. & Hayek, T. The angiotensin-II receptor antagonist, losartan, inhibits LDL lipid peroxidation and atherosclerosis in apolipoprotein E-deficient mice. *Biochem. Biophys. Res. Commun.* **236,** 622–625 (1997).
266. Keidar, S., Kaplan, M., Hoffman, A. & Aviram, M. Angiotensin II stimulates macrophage-mediated oxidation of low density lipoproteins. *Atherosclerosis* **115,** 201–215 (1995).
267. Keidar, S., Heinrich, R., Kaplan, M., Hayek, T. & Aviram, M. Angiotensin II administration to atherosclerotic mice increases macrophage uptake of oxidized ldl: a possible role for interleukin-6. *Arterioscler. Thromb. Vasc. Biol.* **21,** 1464–1469 (2001).
268. Keidar, S. & Attias, J. Angiotensin II injection into mice increases the uptake of oxidized LDL by their macrophages via a proteoglycan-mediated pathway. *Biochem. Biophys. Res. Commun.* **239,** 63–67 (1997).

269. Hayek, T., Aviram, M., Heinrich, R., Sakhnini, E. & Keidar, S. Losartan inhibits cellular uptake of oxidized LDL by monocyte-macrophages from hypercholesterolemic patients. *Biochem. Biophys. Res. Commun.* **273,** 417–420 (2000).
270. Li, D. Y., Zhang, Y. C., Philips, M. I., Sawamura, T. & Mehta, J. L. Upregulation of endothelial receptor for oxidized low-density lipoprotein (LOX-1) in cultured human coronary artery endothelial cells by angiotensin II type 1 receptor activation. *Circ. Res.* **84,** 1043–1049 (1999).
271. Morawietz, H. *et al.* Angiotensin II induces LOX-1, the human endothelial receptor for oxidized low-density lipoprotein. *Circulation* **100,** 899–902 (1999).
272. Cheng, Z. J., Vapaatalo, H. & Mervaala, E. Angiotensin II and vascular inflammation. *Med. Sci. Monit. Int. Med. J. Exp. Clin. Res.* **11,** RA194–205 (2005).
273. Mollnau, H. *et al.* Effects of angiotensin II infusion on the expression and function of NAD(P)H oxidase and components of nitric oxide/cGMP signaling. *Circ. Res.* **90,** E58–65 (2002).
274. Warnholtz, A. *et al.* Increased NADH-oxidase-mediated superoxide production in the early stages of atherosclerosis: evidence for involvement of the renin-angiotensin system. *Circulation* **99,** 2027–2033 (1999).
275. Dandona, P. *et al.* Angiotensin II receptor blocker valsartan suppresses reactive oxygen species generation in leukocytes, nuclear factor-kappa B, in mononuclear cells of normal subjects: evidence of an antiinflammatory action. *J. Clin. Endocrinol. Metab.* **88,** 4496–4501 (2003).
276. Griendling, K. K. & Ushio-Fukai, M. Reactive oxygen species as mediators of angiotensin II signaling. *Regul. Pept.* **91,** 21–27 (2000).
277. Han, Y., Runge, M. S. & Brasier, A. R. Angiotensin II induces interleukin-6 transcription in vascular smooth muscle cells through pleiotropic activation of nuclear factor-kappa B transcription factors. *Circ. Res.* **84,** 695–703 (1999).
278. Schieffer, B. *et al.* Expression of angiotensin II and interleukin 6 in human coronary atherosclerotic plaques: potential implications for inflammation and plaque instability. *Circulation* **101,** 1372–1378 (2000).
279. Chen, X. L., Tummala, P. E., Olbrych, M. T., Alexander, R. W. & Medford, R. M. Angiotensin II induces monocyte chemoattractant protein-1 gene expression in rat vascular smooth muscle cells. *Circ. Res.* **83,** 952–959 (1998).
280. Pueyo, M. E. *et al.* Angiotensin II stimulates endothelial vascular cell adhesion molecule-1 via nuclear factor-kappaB activation induced by intracellular oxidative stress. *Arterioscler. Thromb. Vasc. Biol.* **20,** 645–651 (2000).
281. Tham, D. M. *et al.* Angiotensin II is associated with activation of NF-kappaB-mediated genes and downregulation of PPARs. *Physiol. Genomics* **11,** 21–30 (2002).
282. Takagishi, T., Murahashi, N., Azagami, S., Morimatsu, M. & Sasaguri, Y. Effect of angiotensin II and thromboxane A2 on the production of matrix metalloproteinase by human aortic smooth muscle cells. *Biochem. Mol. Biol. Int.* **35,** 265–273 (1995).

283. Tamura, K. *et al.* Mechanism of angiotensin II-mediated regulation of fibronectin gene in rat vascular smooth muscle cells. *J. Biol. Chem.* **273,** 26487–26496 (1998).
284. Kato, H. *et al.* Angiotensin II stimulates collagen synthesis in cultured vascular smooth muscle cells. *J. Hypertens.* **9,** 17–22 (1991).
285. Regenass, S., Resink, T. J., Kern, F., Bühler, F. R. & Hahn, A. W. Angiotensin-II-induced expression of laminin complex and laminin A-chain-related transcripts in vascular smooth muscle cells. *J. Vasc. Res.* **31,** 163–172 (1994).
286. Tokimitsu, I., Kato, H., Wachi, H. & Tajima, S. Elastin synthesis is inhibited by angiotensin II but not by platelet-derived growth factor in arterial smooth muscle cells. *Biochim. Biophys. Acta* **1207,** 68–73 (1994).
287. Finckenberg, P. *et al.* Angiotensin II induces connective tissue growth factor gene expression via calcineurin-dependent pathways. *Am. J. Pathol.* **163,** 355–366 (2003).
288. Bailey, W. L., LaFleur, D. W., Forrester, J. S., Fagin, J. A. & Sharifi, B. G. Stimulation of rat vascular smooth muscle cell glycosaminoglycan production by angiotensin II. *Atherosclerosis* **111,** 55–64 (1994).
289. Diep, Q. N., Li, J. S. & Schiffrin, E. L. In vivo study of AT(1) and AT(2) angiotensin receptors in apoptosis in rat blood vessels. *Hypertension* **34,** 617–624 (1999).
290. deBlois, D. *et al.* Angiotensin II induction of osteopontin expression and DNA replication in rat arteries. *Hypertension* **28,** 1055–1063 (1996).
291. Dechend, R. *et al.* AT(1) receptor agonistic antibodies from preeclamptic patients cause vascular cells to express tissue factor. *Circulation* **101,** 2382–2387 (2000).
292. Napoleone, E., Di Santo, A., Camera, M., Tremoli, E. & Lorenzet, R. Angiotensin-converting enzyme inhibitors downregulate tissue factor synthesis in monocytes. *Circ. Res.* **86,** 139–143 (2000).
293. Feener, E. P., Northrup, J. M., Aiello, L. P. & King, G. L. Angiotensin II induces plasminogen activator inhibitor-1 and -2 expression in vascular endothelial and smooth muscle cells. *J. Clin. Invest.* **95,** 1353–1362 (1995).
294. Ihara, M. *et al.* Increased chymase-dependent angiotensin II formation in human atherosclerotic aorta. *Hypertension* **33,** 1399–1405 (1999).
295. Miyazaki, M. & Takai, S. Tissue angiotensin II generating system by angiotensin-converting enzyme and chymase. *J. Pharmacol. Sci.* **100,** 391–397 (2006).
296. Ohishi, M. *et al.* Relative localization of angiotensin-converting enzyme, chymase and angiotensin II in human coronary atherosclerotic lesions. *J. Hypertens.* **17,** 547–553 (1999).
297. Fukuhara, M. *et al.* Angiotensin-converting enzyme expression in human carotid artery atherosclerosis. *Hypertension* **35,** 353–359 (2000).
298. Okamura, A. *et al.* Upregulation of renin-angiotensin system during differentiation of monocytes to macrophages. *J. Hypertens.* **17,** 537–545 (1999).
299. Padmanabhan, N., Jardine, A. G., McGrath, J. C. & Connell, J. M. Angiotensin-converting enzyme-independent contraction to angiotensin I in human resistance arteries. *Circulation* **99,** 2914–2920 (1999).

300. Hollenberg, N. K., Fisher, N. D. L. & Price, D. A. Pathways for Angiotensin II Generation in Intact Human Tissue Evidence From Comparative Pharmacological Interruption of the Renin System. *Hypertension* **32,** 387–392 (1998).
301. Arakawa, K. & Urata, H. Hypothesis regarding the pathophysiological role of alternative pathways of angiotensin II formation in atherosclerosis. *Hypertension* **36,** 638–641 (2000).
302. Snyder, R. A., Kaempfer, C. E. & Wintroub, B. U. Chemistry of a human monocyte-derived cell line (U937): identification of the angiotensin I-converting activity as leukocyte cathepsin G. *Blood* **65,** 176–182 (1985).
303. Touyz, R. M. & Schiffrin, E. L. Signal Transduction Mechanisms Mediating the Physiological and Pathophysiological Actions of Angiotensin II in Vascular Smooth Muscle Cells. *Pharmacol. Rev.* **52,** 639–672 (2000).
304. Kljajic, S. T. *et al.* Direct AT_2 receptor stimulation is athero-protective and stabilizes plaque in apolipoprotein E-deficient mice. *Int. J. Cardiol.* **169,** 281–287 (2013).
305. Siragy, H. M. The potential role of the angiotensin subtype 2 receptor in cardiovascular protection. *Curr. Hypertens. Rep.* **11,** 260–262 (2009).
306. Newton, C. R., Curran, B. & Victorino, G. P. Angiotensin II type 2 receptor effect on microvascular hydraulic permeability. *J. Surg. Res.* **120,** 83–88 (2004).
307. Chong, T. J. & Victorino, G. P. Angiotensin II subtype AT1 and AT2 receptors regulate microvascular hydraulic permeability via cAMP and cGMP. *J. Surg. Res.* **131,** 105–110 (2006).
308. Tsutsumi, Y. *et al.* Angiotensin II type 2 receptor overexpression activates the vascular kinin system and causes vasodilation. *J. Clin. Invest.* **104,** 925–935 (1999).
309. Wu, L. *et al.* Roles of angiotensin II type 2 receptor stimulation associated with selective angiotensin II type 1 receptor blockade with valsartan in the improvement of inflammation-induced vascular injury. *Circulation* **104,** 2716–2721 (2001).
310. Widdop, R. E., Jones, E. S., Hannan, R. E. & Gaspari, T. A. Angiotensin AT2 receptors: cardiovascular hope or hype? *Br. J. Pharmacol.* **140,** 809–824 (2003).
311. Viswanathan, M., Tsutsumi, K., Correa, F. M. & Saavedra, J. M. Changes in expression of angiotensin receptor subtypes in the rat aorta during development. *Biochem. Biophys. Res. Commun.* **179,** 1361–1367 (1991).
312. Sales, V. L. *et al.* Angiotensin type 2 receptor is expressed in murine atherosclerotic lesions and modulates lesion evolution. *Circulation* **112,** 3328–3336 (2005).
313. Akishita, M. *et al.* Inflammation influences vascular remodeling through AT2 receptor expression and signaling. *Physiol. Genomics* **2,** 13–20 (2000).
314. Purushothaman, K.-R. *et al.* Expression of angiotensin-converting enzyme 2 and its end product angiotensin 1-7 is increased in diabetic atheroma: implications for inflammation and neovascularization. *Cardiovasc. Pathol.* **22,** 42–48 (2013).
315. Nickenig, G., Sachinidis, A., Seewald, S., Böhm, M. & Vetter, H. Influence of oxidized low-density lipoprotein on vascular angiotensin II receptor expression. *J. Hypertens. Suppl. Off. J. Int. Soc. Hypertens.* **15,** S27–30 (1997).

316. Nickenig, G. *et al.* Hypercholesterolemia is associated with enhanced angiotensin AT1-receptor expression. *Am. J. Physiol.* **272,** H2701–2707 (1997).
317. Potter, D. D., Sobey, C. G., Tompkins, P. K., Rossen, J. D. & Heistad, D. D. Evidence that macrophages in atherosclerotic lesions contain angiotensin II. *Circulation* **98,** 800–807 (1998).
318. López-Farré, A. *et al.* Angiotensin II AT(1) receptor antagonists and platelet activation. *Nephrol. Dial. Transplant. Off. Publ. Eur. Dial. Transpl. Assoc. - Eur. Ren. Assoc.* **16 Suppl 1,** 45–49 (2001).
319. Ardaillou, R. & Chansel, D. Synthesis and effects of active fragments of angiotensin II. *Kidney Int.* **52,** 1458–1468 (1997).
320. Sampaio, W. O., Henrique de Castro, C., Santos, R. A. S., Schiffrin, E. L. & Touyz, R. M. Angiotensin-(1-7) counterregulates angiotensin II signaling in human endothelial cells. *Hypertension* **50,** 1093–1098 (2007).
321. Xiao, X. *et al.* Angiotensin-(1-7) counteracts angiotensin II-induced dysfunction in cerebral endothelial cells via modulating Nox2/ROS and PI3K/NO pathways. *Exp. Cell Res.* **336,** 58–65 (2015).
322. Lovren, F. *et al.* Angiotensin converting enzyme-2 confers endothelial protection and attenuates atherosclerosis. *Am. J. Physiol. Heart Circ. Physiol.* **295,** H1377–1384 (2008).
323. Yang, J. *et al.* Endogenous activated angiotensin-(1-7) plays a protective effect against atherosclerotic plaques unstability in high fat diet fed ApoE knockout mice. *Int. J. Cardiol.* **184,** 645–652 (2015).
324. Sahara, M. *et al.* Deletion of angiotensin-converting enzyme 2 promotes the development of atherosclerosis and arterial neointima formation. *Cardiovasc. Res.* **101,** 236–246 (2014).
325. Dong, B. *et al.* Overexpression of ACE2 enhances plaque stability in a rabbit model of atherosclerosis. *Arterioscler. Thromb. Vasc. Biol.* **28,** 1270–1276 (2008).
326. Zhang, C. *et al.* Angiotensin-converting enzyme 2 attenuates atherosclerotic lesions by targeting vascular cells. *Proc. Natl. Acad. Sci. U. S. A.* **107,** 15886–15891 (2010).
327. Zhang, Z., Chen, L., Zhong, J., Gao, P. & Oudit, G. Y. ACE2/Ang-(1-7) signaling and vascular remodeling. *Sci. China Life Sci.* **57,** 802–808 (2014).
328. Guo, Y.-J., Li, W.-H., Wu, R., Xie, Q. & Cui, L.-Q. ACE2 overexpression inhibits angiotensin II-induced monocyte chemoattractant protein-1 expression in macrophages. *Arch. Med. Res.* **39,** 149–154 (2008).
329. Hayashi, N. *et al.* The counterregulating role of ACE2 and ACE2-mediated angiotensin 1-7 signaling against angiotensin II stimulation in vascular cells. *Hypertens. Res. Off. J. Jpn. Soc. Hypertens.* **33,** 1182–1185 (2010).
330. Liang, B. *et al.* Angiotensin-(1-7) Attenuates Angiotensin II-Induced ICAM-1, VCAM-1, and MCP-1 Expression via the MAS Receptor Through Suppression of P38 and NF-κB Pathways in HUVECs. *Cell. Physiol. Biochem. Int. J. Exp. Cell. Physiol. Biochem. Pharmacol.* **35,** 2472–2482 (2015).

331. Zhang, F., Ren, J., Chan, K. & Chen, H. Angiotensin-(1-7) regulates Angiotensin II-induced VCAM-1 expression on vascular endothelial cells. *Biochem. Biophys. Res. Commun.* **430,** 642–646 (2013).
332. Yang, J. M. *et al.* Angiotensin-(1-7) dose-dependently inhibits atherosclerotic lesion formation and enhances plaque stability by targeting vascular cells. *Arterioscler. Thromb. Vasc. Biol.* **33,** 1978–1985 (2013).
333. Zhang, F., Hu, Y., Xu, Q. & Ye, S. Different effects of angiotensin II and angiotensin-(1-7) on vascular smooth muscle cell proliferation and migration. *PloS One* **5,** e12323 (2010).
334. Strawn, W. B., Ferrario, C. M. & Tallant, E. A. Angiotensin-(1-7) reduces smooth muscle growth after vascular injury. *Hypertension* **33,** 207–211 (1999).
335. Song, B. *et al.* Angiotensin-converting enzyme 2 attenuates oxidative stress and VSMC proliferation via the JAK2/STAT3/SOCS3 and profilin-1/MAPK signaling pathways. *Regul. Pept.* **185,** 44–51 (2013).
336. Yang, H.-Y. *et al.* Angiotensin-(1-7) stimulates cholesterol efflux from angiotensin II-treated cholesterol-loaded THP-1 macrophages through the suppression of p38 and c-Jun N-terminal kinase signaling. *Mol. Med. Rep.* **12,** 1387–1392 (2015).
337. Liang, B. *et al.* Angiotensin-(1-7) upregulates (ATP-binding cassette transporter A1) ABCA1 expression through cyclic AMP signaling pathway in RAW 264.7 macrophages. *Eur. Rev. Med. Pharmacol. Sci.* **18,** 985–991 (2014).
338. Simões e Silva, A. C., Silveira, K. D., Ferreira, A. J. & Teixeira, M. M. ACE2, angiotensin-(1-7) and Mas receptor axis in inflammation and fibrosis. *Br. J. Pharmacol.* **169,** 477–492 (2013).
339. Grobe, J. L. *et al.* Prevention of angiotensin II-induced cardiac remodeling by angiotensin-(1-7). *Am. J. Physiol. Heart Circ. Physiol.* **292,** H736–742 (2007).
340. Alsaadon, H. *et al.* Increased aortic intimal proliferation due to MasR deletion in vitro. *Int. J. Exp. Pathol.* **96,** 183–187 (2015).
341. Fressatto de Godoy, M. A., Pernomian, L., de Oliveira, A. M. & Rattan, S. Biosynthetic pathways and the role of the MAS receptor in the effects of Angiotensin-(1-7) in smooth muscles. *Int. J. Hypertens.* **2012,** 121740 (2012).
342. Sluimer, J. C. *et al.* Angiotensin-converting enzyme 2 (ACE2) expression and activity in human carotid atherosclerotic lesions. *J. Pathol.* **215,** 273–279 (2008).
343. Zulli, A. *et al.* Immunolocalization of ACE2 and AT2 receptors in rabbit atherosclerotic plaques. *J. Histochem. Cytochem. Off. J. Histochem. Soc.* **54,** 147–150 (2006).
344. Schwacke, J. H. *et al.* Network Modeling Reveals Steps in Angiotensin Peptide Processing. *Hypertension* **61,** 690–700 (2013).
345. Kovarik, J. J. *et al.* 8D.03: EVIDENCE FOR AN ACE-INDEPENDENT TISSUE-SPECIFIC RAS REGULATION AFTER KIDNEY TRANSPLANTATION. *J. Hypertens.* **33 Suppl 1,** e113–114 (2015).

346. Wilson, B. A. *et al.* An angiotensin-(1-7) peptidase in the kidney cortex, proximal tubules, and human HK-2 epithelial cells that is distinct from insulin-degrading enzyme. *Am. J. Physiol. Renal Physiol.* **308,** F594–601 (2015).
347. Grobe, N., Leiva, O., Morris, M. & Elased, K. M. Loss of prolyl carboxypeptidase in two-kidney, one-clip goldblatt hypertensive mice. *PloS One* **10,** e0117899 (2015).
348. Marshall, A. C., Pirro, N. T., Rose, J. C., Diz, D. I. & Chappell, M. C. Evidence for an angiotensin-(1-7) neuropeptidase expressed in the brain medulla and CSF of sheep. *J. Neurochem.* **130,** 313–323 (2014).
349. Pereira, H. J. V., Souza, L. L., Salgado, M. C. O. & Oliveira, E. B. Angiotensin processing is partially carried out by carboxypeptidases in the rat mesenteric arterial bed perfusate. *Regul. Pept.* **151,** 135–138 (2008).
350. Metsärinne, K. P. *et al.* Activated mast cells increase the level of endothelin-1 mRNA in cocultured endothelial cells and degrade the secreted Peptide. *Arterioscler. Thromb. Vasc. Biol.* **22,** 268–273 (2002).
351. Raffai, G., Durand, M. J. & Lombard, J. H. Acute and chronic angiotensin-(1-7) restores vasodilation and reduces oxidative stress in mesenteric arteries of salt-fed rats. *Am. J. Physiol. Heart Circ. Physiol.* **301,** H1341–1352 (2011).
352. Sampaio, W. O. *et al.* Angiotensin-(1-7) through receptor Mas mediates endothelial nitric oxide synthase activation via Akt-dependent pathways. *Hypertension* **49,** 185–192 (2007).
353. Jawien, J. *et al.* Angiotensin-(1-7) receptor Mas agonist ameliorates progress of atherosclerosis in apoE-knockout mice. *J. Physiol. Pharmacol. Off. J. Pol. Physiol. Soc.* **63,** 77–85 (2012).
354. Fraga-Silva, R. A. *et al.* Treatment with Angiotensin-(1-7) reduces inflammation in carotid atherosclerotic plaques. *Thromb. Haemost.* **111,** 736–747 (2014).
355. Baños, M. *et al.* Relationship between angiotensin II receptor expression and cardiovascular risk factors in Mexican patients with coronary occlusive disease. *Exp. Mol. Pathol.* **91,** 478–483 (2011).
356. Matrougui, K., Loufrani, L., Heymes, C., Lévy, B. I. & Henrion, D. Activation of AT(2) receptors by endogenous angiotensin II is involved in flow-induced dilation in rat resistance arteries. *Hypertension* **34,** 659–665 (1999).
357. Touyz, R. M., Endemann, D., He, G., Li, J. S. & Schiffrin, E. L. Role of AT2 receptors in angiotensin II-stimulated contraction of small mesenteric arteries in young SHR. *Hypertension* **33,** 366–372 (1999).
358. Burrell, J. H. & Lumbers, E. R. Angiotensin receptor subtypes in the uterine artery during ovine pregnancy. *Eur. J. Pharmacol.* **330,** 257–267 (1997).
359. McMullen, J. R., Gibson, K. J., Lumbers, E. R., Burrell, J. H. & Wu, J. Interactions between AT1 and AT2 receptors in uterine arteries from pregnant ewes. *Eur. J. Pharmacol.* **378,** 195–202 (1999).

360. Ruiz-Ortega, M., Lorenzo, O. & Egido, J. Angiotensin III increases MCP-1 and activates NF-kappaB and AP-1 in cultured mesangial and mononuclear cells. *Kidney Int.* **57,** 2285–2298 (2000).
361. Yamamoto, Y., Yamamguchi, T., Shimamura, M. & Hazato, T. Angiotensin III is a new chemoattractant for polymorphonuclear leukocytes. *Biochem. Biophys. Res. Commun.* **193,** 1038–1043 (1993).
362. Kerins, D. M., Hao, Q. & Vaughan, D. E. Angiotensin induction of PAI-1 expression in endothelial cells is mediated by the hexapeptide angiotensin IV. *J. Clin. Invest.* **96,** 2515–2520 (1995).
363. Esteban, V. *et al.* Angiotensin IV Activates the Nuclear Transcription Factor-κB and Related Proinflammatory Genes in Vascular Smooth Muscle Cells. *Circ. Res.* **96,** 965–973 (2005).
364. Chen, S., Patel, J. M. & Block, E. R. Angiotensin IV-mediated pulmonary artery vasorelaxation is due to endothelial intracellular calcium release. *Am. J. Physiol. Lung Cell. Mol. Physiol.* **279,** L849–856 (2000).
365. Vinh, A., Widdop, R. E., Chai, S. Y. & Gaspari, T. A. Angiotensin IV-evoked vasoprotection is conserved in advanced atheroma. *Atherosclerosis* **200,** 37–44 (2008).
366. Patel, J. M. *et al.* Angiotensin IV receptor-mediated activation of lung endothelial NOS is associated with vasorelaxation. *Am. J. Physiol.* **275,** L1061–1068 (1998).
367. Moeller, I. *et al.* Up regulation of AT4 receptor levels in carotid arteries following balloon injury. *Regul. Pept.* **83,** 25–30 (1999).
368. Newfell, B. G. *et al.* Aldosterone regulates vascular gene transcription via oxidative stress-dependent and -independent pathways. *Arterioscler. Thromb. Vasc. Biol.* **31,** 1871–1880 (2011).
369. Milliez, P. *et al.* Evidence for an increased rate of cardiovascular events in patients with primary aldosteronism. *J. Am. Coll. Cardiol.* **45,** 1243–1248 (2005).
370. Strauch, B. *et al.* Increased arterial wall stiffness in primary aldosteronism in comparison with essential hypertension. *Am. J. Hypertens.* **19,** 909–914 (2006).
371. Rosa, J. *et al.* Peripheral arterial stiffness in primary aldosteronism. *Physiol. Res. Acad. Sci. Bohemoslov.* **61,** 461–468 (2012).
372. de Rita, O., Hackam, D. G. & Spence, J. D. Effects of aldosterone on human atherosclerosis: plasma aldosterone and progression of carotid plaque. *Can. J. Cardiol.* **28,** 706–711 (2012).
373. Ivanes, F. *et al.* Aldosterone, mortality, and acute ischaemic events in coronary artery disease patients outside the setting of acute myocardial infarction or heart failure. *Eur. Heart J.* **33,** 191–202 (2012).
374. Pitt, B. *et al.* The effect of spironolactone on morbidity and mortality in patients with severe heart failure. Randomized Aldactone Evaluation Study Investigators. *N. Engl. J. Med.* **341,** 709–717 (1999).

375. Pitt, B. Do diuretics and aldosterone receptor antagonists improve ventricular remodeling? *J. Card. Fail.* **8,** S491–493 (2002).
376. Jaffe, I. Z. *et al.* Placental growth factor mediates aldosterone-dependent vascular injury in mice. *J. Clin. Invest.* **120,** 3891–3900 (2010).
377. McGraw, A. P., McCurley, A., Preston, I. R. & Jaffe, I. Z. Mineralocorticoid receptors in vascular disease: connecting molecular pathways to clinical implications. *Curr. Atheroscler. Rep.* **15,** 340 (2013).
378. Sun, Y. The renin-angiotensin-aldosterone system and vascular remodeling. *Congest. Heart Fail. Greenwich Conn* **8,** 11–16 (2002).
379. Maron, B. A. *et al.* Aldosterone increases oxidant stress to impair guanylyl cyclase activity by cysteinyl thiol oxidation in vascular smooth muscle cells. *J. Biol. Chem.* **284,** 7665–7672 (2009).
380. Caprio, M. *et al.* Functional mineralocorticoid receptors in human vascular endothelial cells regulate intercellular adhesion molecule-1 expression and promote leukocyte adhesion. *Circ. Res.* **102,** 1359–1367 (2008).
381. Ishizawa, K. *et al.* Aldosterone stimulates vascular smooth muscle cell proliferation via big mitogen-activated protein kinase 1 activation. *Hypertension* **46,** 1046–1052 (2005).
382. Xiao, F., Puddefoot, J. R. & Vinson, G. P. Aldosterone mediates angiotensin II-stimulated rat vascular smooth muscle cell proliferation. *J. Endocrinol.* **165,** 533–536 (2000).
383. Hatakeyama, H. *et al.* Vascular aldosterone. Biosynthesis and a link to angiotensin II-induced hypertrophy of vascular smooth muscle cells. *J. Biol. Chem.* **269,** 24316–24320 (1994).
384. Michea, L. *et al.* Eplerenone blocks nongenomic effects of aldosterone on the Na+/H+ exchanger, intracellular Ca2+ levels, and vasoconstriction in mesenteric resistance vessels. *Endocrinology* **146,** 973–980 (2005).
385. McCurley, A. *et al.* Direct regulation of blood pressure by smooth muscle cell mineralocorticoid receptors. *Nat. Med.* **18,** 1429–1433 (2012).
386. Rocha, R. *et al.* Aldosterone induces a vascular inflammatory phenotype in the rat heart. *Am. J. Physiol. Heart Circ. Physiol.* **283,** H1802–1810 (2002).
387. Rocha, R. *et al.* Selective aldosterone blockade prevents angiotensin II/salt-induced vascular inflammation in the rat heart. *Endocrinology* **143,** 4828–4836 (2002).
388. Sanz-Rosa, D. *et al.* Participation of aldosterone in the vascular inflammatory response of spontaneously hypertensive rats: role of the NFkappaB/IkappaB system. *J. Hypertens.* **23,** 1167–1172 (2005).
389. Keidar, S. *et al.* Aldosterone administration to mice stimulates macrophage NADPH oxidase and increases atherosclerosis development: a possible role for angiotensin-converting enzyme and the receptors for angiotensin II and aldosterone. *Circulation* **109,** 2213–2220 (2004).
390. Nagata, D. *et al.* Molecular mechanism of the inhibitory effect of aldosterone on endothelial NO synthase activity. *Hypertension* **48,** 165–171 (2006).

391. Jaffe, I. Z., Tintut, Y., Newfell, B. G., Demer, L. L. & Mendelsohn, M. E. Mineralocorticoid receptor activation promotes vascular cell calcification. *Arterioscler. Thromb. Vasc. Biol.* **27,** 799–805 (2007).
392. Wu, S.-Y. *et al.* Endogenous aldosterone is involved in vascular calcification in rat. *Exp. Biol. Med. Maywood NJ* **237,** 31–37 (2012).
393. Ward, M. R., Kanellakis, P., Ramsey, D., Funder, J. & Bobik, A. Eplerenone suppresses constrictive remodeling and collagen accumulation after angioplasty in porcine coronary arteries. *Circulation* **104,** 467–472 (2001).
394. Wakabayashi, K. *et al.* Eplerenone suppresses neointimal formation after coronary stent implantation in swine. *Int. J. Cardiol.* **107,** 260–266 (2006).
395. Rajagopalan, S., Duquaine, D., King, S., Pitt, B. & Patel, P. Mineralocorticoid receptor antagonism in experimental atherosclerosis. *Circulation* **105,** 2212–2216 (2002).
396. Keidar, S. *et al.* Effect of eplerenone, a selective aldosterone blocker, on blood pressure, serum and macrophage oxidative stress, and atherosclerosis in apolipoprotein E-deficient mice. *J. Cardiovasc. Pharmacol.* **41,** 955–963 (2003).
397. Lombès, M. *et al.* Immunohistochemical and biochemical evidence for a cardiovascular mineralocorticoid receptor. *Circ. Res.* **71,** 503–510 (1992).
398. Christy, C. *et al.* 11beta-hydroxysteroid dehydrogenase type 2 in mouse aorta: localization and influence on response to glucocorticoids. *Hypertension* **42,** 580–587 (2003).
399. Bene, N. C., Alcaide, P., Wortis, H. H. & Jaffe, I. Z. Mineralocorticoid receptors in immune cells: emerging role in cardiovascular disease. *Steroids* **91,** 38–45 (2014).
400. Brem, A. S., Bina, R. B., King, T. C. & Morris, D. J. Localization of 2 11beta-OH steroid dehydrogenase isoforms in aortic endothelial cells. *Hypertension* **31,** 459–462 (1998).
401. Kornel, L. Colocalization of 11 beta-hydroxysteroid dehydrogenase and mineralocorticoid receptors in cultured vascular smooth muscle cells. *Am. J. Hypertens.* **7,** 100–103 (1994).
402. Hadoke, P. W. *et al.* Endothelial cell dysfunction in mice after transgenic knockout of type 2, but not type 1, 11beta-hydroxysteroid dehydrogenase. *Circulation* **104,** 2832–2837 (2001).
403. Takeda, Y. *et al.* Regulation of aldosterone synthase in human vascular endothelial cells by angiotensin II and adrenocorticotropin. *J. Clin. Endocrinol. Metab.* **81,** 2797–2800 (1996).
404. Gros, R. *et al.* Delineating the receptor mechanisms underlying the rapid vascular contractile effects of aldosterone and estradiol. *Can. J. Physiol. Pharmacol.* **89,** 655–663 (2011).
405. Li, F. *et al.* Activation of GPER Induces Differentiation and Inhibition of Coronary Artery Smooth Muscle Cell Proliferation. *PloS One* **8,** e64771 (2013).
406. Meyer, M. R. *et al.* G protein-coupled estrogen receptor protects from atherosclerosis. *Sci. Rep.* **4,** 7564 (2014).
407. Hadoke, P. W. F., Kipari, T., Seckl, J. R. & Chapman, K. E. Modulation of 11β-hydroxysteroid dehydrogenase as a strategy to reduce vascular inflammation. *Curr. Atheroscler. Rep.* **15,** 320 (2013).

408. Atalar, F. *et al.* 11β-hydroxysteroid dehydrogenase type 1 gene expression is increased in ascending aorta tissue of metabolic syndrome patients with coronary artery disease. *Genet. Mol. Res. GMR* **11,** 3122–3132 (2012).
409. Thieringer, R. *et al.* 11 Beta-hydroxysteroid dehydrogenase type 1 is induced in human monocytes upon differentiation to macrophages. *J. Immunol. Baltim. Md 1950* **167,** 30–35 (2001).
410. Cai, T. Q. *et al.* Induction of 11beta-hydroxysteroid dehydrogenase type 1 but not -2 in human aortic smooth muscle cells by inflammatory stimuli. *J. Steroid Biochem. Mol. Biol.* **77,** 117–122 (2001).
411. Gilmour, J. S. *et al.* Local amplification of glucocorticoids by 11 beta-hydroxysteroid dehydrogenase type 1 promotes macrophage phagocytosis of apoptotic leukocytes. *J. Immunol. Baltim. Md 1950* **176,** 7605–7611 (2006).
412. Hermanowski-Vosatka, A. *et al.* 11beta-HSD1 inhibition ameliorates metabolic syndrome and prevents progression of atherosclerosis in mice. *J. Exp. Med.* **202,** 517–527 (2005).
413. Luo, M. J. *et al.* 11β-HSD1 inhibition reduces atherosclerosis in mice by altering proinflammatory gene expression in the vasculature. *Physiol. Genomics* **45,** 47–57 (2013).
414. Chai, W. & Danser, A. H. J. Why are mineralocorticoid receptor antagonists cardioprotective? *Naunyn. Schmiedebergs Arch. Pharmacol.* **374,** 153–162 (2006).
415. Iqbal, J. *et al.* Contribution of endogenous glucocorticoids and their intravascular metabolism by 11β-HSDs to postangioplasty neointimal proliferation in mice. *Endocrinology* **153,** 5896–5905 (2012).
416. Lloyd, D. J. *et al.* Antidiabetic effects of 11beta-HSD1 inhibition in a mouse model of combined diabetes, dyslipidaemia and atherosclerosis. *Diabetes Obes. Metab.* **11,** 688–699 (2009).
417. Poon, M. *et al.* Dexamethasone inhibits macrophage accumulation after balloon arterial injury in cholesterol fed rabbits. *Atherosclerosis* **155,** 371–380 (2001).
418. Bray, P. J. *et al.* Glucocorticoid resistance caused by reduced expression of the glucocorticoid receptor in cells from human vascular lesions. *Arterioscler. Thromb. Vasc. Biol.* **19,** 1180–1189 (1999).
419. Goodwin, J. E. *et al.* Endothelial glucocorticoid receptor suppresses atherogenesis--brief report. *Arterioscler. Thromb. Vasc. Biol.* **35,** 779–782 (2015).
420. Preusch, M. R. *et al.* Critical role of macrophages in glucocorticoid driven vascular calcification in a mouse-model of atherosclerosis. *Arterioscler. Thromb. Vasc. Biol.* **28,** 2158–2164 (2008).
421. Dhawan, L., Liu, B., Blaxall, B. C. & Taubman, M. B. A novel role for the glucocorticoid receptor in the regulation of monocyte chemoattractant protein-1 mRNA stability. *J. Biol. Chem.* **282,** 10146–10152 (2007).
422. Berk, B. C., Gordon, J. B. & Alexander, R. W. Pharmacologic roles of heparin and glucocorticoids to prevent restenosis after coronary angioplasty. *J. Am. Coll. Cardiol.* **17,** 111B–117B (1991).

423. Sato, A., Sheppard, K. E., Fullerton, M. J., Sviridov, D. D. & Funder, J. W. Glucocorticoid receptor expression is down-regulated by Lp(a) lipoprotein in vascular smooth muscle cells. *Endocrinology* **136,** 3707–3713 (1995).
424. Sakai, M. *et al.* Glucocorticoid inhibits oxidized LDL-induced macrophage growth by suppressing the expression of granulocyte/macrophage colony-stimulating factor. *Arterioscler. Thromb. Vasc. Biol.* **19,** 1726–1733 (1999).
425. Henze, K., Chait, A., Albers, J. J. & Bierman, E. L. Hydrocortisone decreases the internalization of low density lipoprotein in cultured human fibroblasts and arterial smooth muscle cells. *Eur. J. Clin. Invest.* **13,** 171–177 (1983).
426. Deuchar, G. A. *et al.* 11β-hydroxysteroid dehydrogenase type 2 deficiency accelerates atherogenesis and causes proinflammatory changes in the endothelium in apoe-/- mice. *Endocrinology* **152,** 236–246 (2011).
427. Bodiga, S. *et al.* Enhanced susceptibility to biomechanical stress in ACE2 null mice is prevented by loss of the p47(phox) NADPH oxidase subunit. *Cardiovasc. Res.* **91,** 151–161 (2011).
428. Sukumaran, V. *et al.* Cardioprotective effects of telmisartan against heart failure in rats induced by experimental autoimmune myocarditis through the modulation of angiotensin-converting enzyme-2/angiotensin 1-7/mas receptor axis. *Int. J. Biol. Sci.* **7,** 1077–1092 (2011).
429. Sukumaran, V. *et al.* Olmesartan attenuates the development of heart failure after experimental autoimmune myocarditis in rats through the modulation of ANG 1-7 mas receptor. *Mol. Cell. Endocrinol.* **351,** 208–219 (2012).
430. Igase, M., Strawn, W. B., Gallagher, P. E., Geary, R. L. & Ferrario, C. M. Angiotensin II AT1 receptors regulate ACE2 and angiotensin-(1-7) expression in the aorta of spontaneously hypertensive rats. *Am. J. Physiol. Heart Circ. Physiol.* **289,** H1013–1019 (2005).
431. Ohshima, K. *et al.* Possible role of angiotensin-converting enzyme 2 and activation of angiotensin II type 2 receptor by angiotensin-(1-7) in improvement of vascular remodeling by angiotensin II type 1 receptor blockade. *Hypertension* **63,** e53–59 (2014).
432. Zhong, J.-C. *et al.* Telmisartan attenuates aortic hypertrophy in hypertensive rats by the modulation of ACE2 and profilin-1 expression. *Regul. Pept.* **166,** 90–97 (2011).
433. Zhang, Y. H. *et al.* ACE2 activity was increased in atherosclerotic plaque by losartan: Possible relation to anti-atherosclerosis. *J. Renin-Angiotensin-Aldosterone Syst. JRAAS* **16,** 292–300 (2015).
434. Pernomian, L. *et al.* MAS receptors mediate vasoprotective and atheroprotective effects of candesartan upon the recovery of vascular angiotensin-converting enzyme 2-angiotensin-(1-7)-MAS axis functionality. *Eur. J. Pharmacol.* **764,** 173–188 (2015).
435. Kostenis, E. *et al.* G-protein-coupled receptor Mas is a physiological antagonist of the angiotensin II type 1 receptor. *Circulation* **111,** 1806–1813 (2005).

436. Rautureau, Y., Paradis, P. & Schiffrin, E. L. Cross-talk between aldosterone and angiotensin signaling in vascular smooth muscle cells. *Steroids* **76,** 834–839 (2011).
437. Fan, Y.-Y. *et al.* Augmentation of intrarenal angiotensin II levels in uninephrectomized aldosterone/salt-treated hypertensive rats; renoprotective effects of an ultrahigh dose of olmesartan. *Hypertens. Res. Off. J. Jpn. Soc. Hypertens.* **29,** 169–178 (2006).
438. Virdis, A. *et al.* Spironolactone improves angiotensin-induced vascular changes and oxidative stress. *Hypertension* **40,** 504–510 (2002).
439. Batenburg, W. W., Jansen, P. M., van den Bogaerdt, A. J. & J Danser, A. H. Angiotensin II-aldosterone interaction in human coronary microarteries involves GPR30, EGFR, and endothelial NO synthase. *Cardiovasc. Res.* **94,** 136–143 (2012).
440. Cassis, L. A., Helton, M. J., Howatt, D. A., King, V. L. & Daugherty, A. Aldosterone does not mediate angiotensin II-induced atherosclerosis and abdominal aortic aneurysms. *Br. J. Pharmacol.* **144,** 443–448 (2005).
441. Michel, F. *et al.* Aldosterone enhances ischemia-induced neovascularization through angiotensin II-dependent pathway. *Circulation* **109,** 1933–1937 (2004).
442. Irizarry, R. A. *et al.* Exploration, normalization, and summaries of high density oligonucleotide array probe level data. *Biostat. Oxf. Engl.* **4,** 249–264 (2003).
443. Kaufman, L. & Rousseeuw, P. J. in *Finding Groups in Data* 1–67 (John Wiley & Sons, Inc., 1990). at <http://onlinelibrary.wiley.com.gate2.inist.fr/doi/10.1002/9780470316801.ch1/summary>
444. Open source Clustering software. at <http://bonsai.hgc.jp/~mdehoon/software/cluster/>
445. Java TreeView Homepage. at <http://jtreeview.sourceforge.net/>
446. World Medical Association declaration of Helsinki. Recommendations guiding physicians in biomedical research involving human subjects. *JAMA* **277,** 925–926 (1997).
447. Ross, R. The smooth muscle cell. II. Growth of smooth muscle in culture and formation of elastic fibers. *J. Cell Biol.* **50,** 172–186 (1971).
448. Davies, J. D. *et al.* Adipocytic differentiation and liver x receptor pathways regulate the accumulation of triacylglycerols in human vascular smooth muscle cells. *J. Biol. Chem.* **280,** 3911–3919 (2005).
449. Shioi, A. *et al.* β-Glycerophosphate Accelerates Calcification in Cultured Bovine Vascular Smooth Muscle Cells. *Arterioscler. Thromb. Vasc. Biol.* **15,** 2003–2009 (1995).
450. Cartharius, K. *et al.* MatInspector and beyond: promoter analysis based on transcription factor binding sites. *Bioinforma. Oxf. Engl.* **21,** 2933–2942 (2005).
451. Pachkov, M., Balwierz, P. J., Arnold, P., Ozonov, E. & van Nimwegen, E. SwissRegulon, a database of genome-wide annotations of regulatory sites: recent updates. *Nucleic Acids Res.* **41,** D214–220 (2013).
452. Suzuki, A. *et al.* DBTSS as an integrative platform for transcriptome, epigenome and genome sequence variation data. *Nucleic Acids Res.* **43,** D87–91 (2015).

453. Watkins, A. A. *et al.* IRF5 deficiency ameliorates lupus but promotes atherosclerosis and metabolic dysfunction in a mouse model of lupus-associated atherosclerosis. *J. Immunol. Baltim. Md 1950* **194,** 1467–1479 (2015).
454. Durante, A. *et al.* Role of the renin-angiotensin-aldosterone system in the pathogenesis of atherosclerosis. *Curr. Pharm. Des.* **18,** 981–1004 (2012).
455. Athyros, V. G., Katsiki, N., Karagiannis, A. & Mikhailidis, D. P. Combination of statin plus renin angiotensin system inhibition for the prevention or the treatment of atherosclerotic cardiovascular disease. *Curr. Pharm. Des.* **20,** 6299–6305 (2014).
456. Nguyen Dinh Cat, A. & Touyz, R. M. A new look at the renin–angiotensin system—Focusing on the vascular system. *Peptides* **32,** 2141–2150 (2011).
457. Ferreira, A. J. *et al.* Therapeutic implications of the vasoprotective axis of the renin-angiotensin system in cardiovascular diseases. *Hypertension* **55,** 207–213 (2010).
458. Mendoza-Torres, E. *et al.* ACE2 and vasoactive peptides: novel players in cardiovascular/renal remodeling and hypertension. *Ther. Adv. Cardiovasc. Dis.* **9,** 217–237 (2015).
459. Eisen, M. B., Spellman, P. T., Brown, P. O. & Botstein, D. Cluster analysis and display of genome-wide expression patterns. *Proc. Natl. Acad. Sci.* **95,** 14863–14868 (1998).
460. Blaschke, F., Bruemmer, D. & Law, R. E. Egr-1 is a major vascular pathogenic transcription factor in atherosclerosis and restenosis. *Rev. Endocr. Metab. Disord.* **5,** 249–254 (2004).
461. Rokosh, G. Heme Egr-1: new partners in atherosclerotic progression? *Circ. Res.* **102,** 6–8 (2008).
462. Nguyen, G. Renin/prorenin receptors. *Kidney Int.* **69,** 1503–1506 (2006).
463. Araujo, F. C. *et al.* Similarities and differences of X and Y chromosome homologous genes, SRY and SOX3, in regulating the renin-angiotensin system promoters. *Physiol. Genomics* **47,** 177–186 (2015).
464. Zhou, L. *et al.* Multiple Genes of the Renin-Angiotensin System Are Novel Targets of Wnt/β-Catenin Signaling. *J. Am. Soc. Nephrol. JASN* (2014). doi:10.1681/ASN.2014010085
465. Eames, H. L., Corbin, A. L. & Udalova, I. A. Interferon regulatory factor 5 in human autoimmunity and murine models of autoimmune disease. *Transl. Res. J. Lab. Clin. Med.* (2015). doi:10.1016/j.trsl.2015.06.018
466. Spitz, F. & Furlong, E. E. M. Transcription factors: from enhancer binding to developmental control. *Nat. Rev. Genet.* **13,** 613–626 (2012).
467. Dhaouadi, N. *et al.* Computational identification of potential transcriptional regulators of TGF-ß1 in human atherosclerotic arteries. *Genomics* **103,** 357–370 (2014).
468. Handa, R. K. Binding and signaling of angiotensin-(1-7) in bovine kidney epithelial cells involves the AT(4) receptor. *Peptides* **21,** 729–736 (2000).
469. Barreras, A. & Gurk-Turner, C. Angiotensin II receptor blockers. *Proc. Bayl. Univ. Med. Cent.* **16,** 123–126 (2003).

470. van Heyningen, V. & Bickmore, W. Regulation from a distance: long-range control of gene expression in development and disease. *Philos. Trans. R. Soc. Lond. B. Biol. Sci.* **368,** 20120372 (2013).
471. Dillon, N. & Sabbattini, P. Functional gene expression domains: defining the functional unit of eukaryotic gene regulation. *BioEssays News Rev. Mol. Cell. Dev. Biol.* **22,** 657–665 (2000).